Environment-Sensitive Base-Modified Fluorescent Ribonucleoside Analogue Probes: Synthesis, Incorporation and Applications

A thesis

Submitted in partial fulfillment of the requirements

of the degree of

Doctor of Philosophy

By

Maroti G. Pawar

ID: 20093027

INDIAN INSTITUTE OF SCIENCE EDUCATION AND RESEARCH, PUNE

2014

Dedicated to

My family whose support and encouragement make all things seems possible

भारतीय विज्ञान शिक्षा एवं अनुसंधान संस्थान, पुणे
INDIAN INSTITUTE OF SCIENCE EDUCATION AND RESEARCH (IISER), PUNE
(An Autonomous Institution, Ministry of Human Resource Development, Govt. of India)
900 NCL Innovation Park, Dr. Homi Bhabha Road, Pune 411008

Dr. Seergazhi G. Srivatsan
Assistant Professor
Department of Chemistry,
IISER Pune

CERTIFICATE

Certified that the work incorporated in the thesis entitled ***"Environment-Sensitive Base-Modified Fluorescent Ribonucleoside Analogue Probes: Synthesis, Incorporation and Applications"*** submitted by **Mr. Maroti G. Pawar** was carried out by the candidate, under my supervision. The work presented here or any part of it has not been included in any other thesis submitted previously for the award of any degree or diploma from any other university or institution.

Date: 18th September 2014, Pune

Dr. Seergazhi G. Srivatsan
Assistant Professor
(Research Supervisor)

Email: srivatsan@iiserpune.ac.in ● Ph: +91-20-25908021 ● Fax: +91-20-25908186

DECLARATION

I declare that, this written submission represents my ideas in my own words and where others' ideas have been included; I have adequately cited and referenced the original sources. I also declare that I have adhered to all principles of academic honesty and integrity and have not misrepresented or fabricated or falsified any idea / data / fact/ source in my submission. I understand that violation of the above will be cause for disciplinary action by the Institute and can also evoke penal action from the sources which have thus not been properly cited or from whom proper permission has not been taken when needed.

Date: 18th September 2014, Pune

Mr. Maroti G. Pawar

ID: 20093027

Acknowledgements

It gives me a great pleasure to express my deep sense of gratitude to my research supervisor Dr. ***Seergazhi G. Srivatsan*** *for all his advice, guidance, support and encouragement. His tireless enthusiasm was always a source of inspiration. I admire his lessons on independent thinking, perfection soft skills and many more in shaping up the researcher in me. I am also thankful to for his valuable suggestions and advice at the time of difficulty on personal matters.*

I am grateful to the Director, Dr. Krishna N. Ganesh, IISER Pune for all world class infrastructural and administrative support and facilities that have been provided during my research period. The financial support from CSIR in the form of research-fellowship for 5 years is also acknowledged.

I am very grateful to my research advisory committee members Dr. K. N. Ganesh, Dr. Girish Ratnaparkhi and Dr. H. V. Thulasiram for their fruitful suggestions, comments and encouragement through RAC meetings. I would like to specially thank Dr. L. S. Shashidhara for providing space in biology lab during our initial working days to carry out biological experiments. I am also very thankful to Dr. Sanjeev Galande for allowing us to carry out radiolabeling experiments in his lab at NCCS, Pune. I must acknowledge his student Dr. Ranveer, Dr. Kama, and Rahul for their help in radiolabeling experiments. I would like to thank Dr. Jayakannan, Dr. Partha Hazra and their students for helping me to carryout fluorescence and micelles experiments. I would also like to acknowledge Dr. S. K. Asha from NCL, Pune for allowing me to perform fluorescence experiments in her lab. I thank Mayura and Swati for MALDI-TOF and Pooja for NMR analysis.

I admire the co-operation of my labmates Rohini for introducing me to BOSS and helping me to setup lab from nothing, Anupam (Sawata), Arun, Shweta, Pramod (Khabarilal) for fruitful discussions and suggestions. I would like to thanks my juniors cum colleagues Ashok, Sudeshna (Pochis), Anurag (AAG), Jerrin (Bro), Sangmesh for keeping healthy and cheerful atmosphere in lab. I would like to thanks my friends Vijay (Potya), Dnyaneshwar (Gangan), Sharad (Kelya), Nitin (Dadya), and Balu (Bhaparya) for sharing their life experiences on tea time. I would like to thanks Deepak, Sachin, Sandeep, Prakash, Satish Malwal, Satish Ellipilli, Sushil, Dinesh, Rohan, Bapu, Prabhakar, Trimbak, Anantraj, Dharma, Kundan, Tushar, Arvind, Gopal, Santosh. I am very grateful to my entire cricket teammates from THE ALCHEMIST, WARRIORS and

RADICALS for allowing me to participate in IPL with them. I would like to acknowledge my JETTING group members Nagesh, Anil, Samadhan, Dhiraj, Majidbhai, Mujahid, Sainath, Avinash, Sai, Sharad, Chandrasekhar, Manik, Vaibhav, Papan from D-1/11 for their constant encouragement and support.

I shall always remain obliged to my parents and my entire family, for their unconditional love, blessings, sacrifices, patience and support. My research career would have not been possible without the active support. I thank my mother, father and brother for their love, support and encouragement all the time. Most importantly I would like express my sincere thank to my beloved wife Swati for her encouragement, support and patience during the last days of my PhD.

Maroti G. Pawar

Chapter 2 is a reprint of: Pawar, M. G.; Srivatsan, S. G. “Synthesis, Photophysical Characterization, and Enzymatic Incorporation of a Microenvironment-Sensitive Fluorescent Uridine Analog”. *Org. Lett.*, *13*, **2011**, 1114–1117.
The dissertation author is the main author and researcher for this work.

Chapter 3 is a reprint of: Pawar, M. G.; Srivatsan, S. G. “Environment-Responsive Fluorescent Nucleoside Analogue Probe for Studying Oligonucleotide Dynamics in a Model Cell-like Compartment.” *J. Phys. Chem. B 117*, **2013**, 14273−14282.
The dissertation author is the main author and researcher for this work.

Chapter 4 is a reprint of: Pawar, M. G.; Nuthanakanti, A., Srivatsan, S. G. “Heavy Atom Containing Fluorescent Ribonucleoside Analog Probe for the Fluorescence Detection of RNA-Ligand Binding.” *Bioconjugate Chem.*, *24*, **2013**, 1367−1377.
The dissertation author is the main author and researcher for this work.

Table of Contents

Chapter 2: Synthesis, Photophysical Characterization, and Enzymatic Incorporation of 5-Benzothiophene-Conjugated Fluorescent Uridine Analogue

Chapter 3: 5-Benzothiophene-Modified Uridine Analogue as a Fluorescence Probe for Studying Oligonucleotide Dynamics in a Model Cell-Like Compartment

Abbreviations

ε	absorption coefficient
εA	etheno A
$(MeO)_3PO$	trimethyl phosphate
µL	microliter
µM	micro molar
2-AP	2-aminopurine
A	adenine
ACE	bis (2-Acetoxyethoxy) methyl
ACN	acetonitrile
AMP	adenosine monophosphate
BODIPY	boron-dipyrromethene
C	cytosine
CD	circular dichroism
CMP	cytidine monophosphate
cP	centipoise
DAPI	4', 6-diamidino-2-phenylindole
DEAE	diethylaminoethyl
DLS	dynamic light scattering
DMSO	N, N-dimethyl sulfoxide
DMT	dimethoxytrityl
ds	double stranded
EDTA	ethylenediaminetetraacetic acid
em	emission
EPR	electron paramagnetic resonance
G	guanine
GFP	green fluorescent protein
GMP	guanosine monophosphate
HPA	hydroxylpiccolinic acid
HPLC	high performance liquid chromatography
in vitro	outside living organism
in vivo	inside living organism
LED	light emitting diode

MAD	multiwavelength anomalous dispersion
MALDI-TOF	matrix assisted laser desorption ionisation-time of flight
max	maximum
mg	milligram
MHz	megahertz
mM	milimolar
nm	nanometer
nmol	nanomolar
NMPs	nucleoside monophosphate
NMR	nuclear magnetic resonance
NTPs	nucleoside triphosphates
PAGE	polyacrylamide gel electrophoresis
PAH	polycyclic aromatic hydrocarbon
pC	pyrroloC
Pd	palladium
$POCl_3$	phosphorus oxychloride
ppm	parts per million
rel	relative
R*f*	retention factor
SAD	single-wavelength anomalous dispersion
SNP	single nucleotide polymorphism
ss	single stranded
T	thymine
TAR	trans-activation responsive region
TBDMS	tert-butyldimethylsilyl
TCSPC	time correlated single photon counting
TEAB	triethylammonium bicarbonate buffer
Tm	thermal melting
TOM	triisopropylsilyloxymethy
Tris	tris (hydroxymethyl) amino methane
U	uridine
UMP	uridine monophosphate
WC	watson-crick

Synopsis

Environment-Sensitive Base-Modified Fluorescent Ribonucleoside Analogue Probes: Synthesis, Incorporation and Applications

Background: Several biophysical tools have been developed to uncover the fundamentals of nucleic acid folding and recognition processes.[1-5] In particular, fluorescent nucleoside analogues that report changes in their conformation and surrounding environment in the form of changes in the fluorescence properties such as quantum yield, emission maximum, lifetime and anisotropy have found wide applications in developing tools to investigate the structure, dynamics and function of nucleic acids.[6-9] However, the majority of nucleoside analogues either have excitation and emission maximum in UV region and or exhibit progressive fluorescence quenching upon incorporation into single stranded and double stranded oligonucleotides, which preclude their implementation in certain fluorescence methods (*e.g.*, single-molecule spectroscopy and cell microscopy).[10]

The overall aim of this thesis is to develop nucleoside probes that (i) are structurally minimally invasive, (ii) have emission maximum in the visible region, (iii) retain appreciable fluorescence efficiency when incorporated into oligonucleotides and (iv) importantly, report changes in microenvironment via changes in the photophysical properties. This thesis illustrates the design strategy, synthetic methodology, photophysical characterizations, enzymatic incorporation into RNA oligonucleotides and applications of two new base-modified fluorescent nucleoside analogues derived by conjugating benzothiophene and selenophene moieties at the 5-position of uracil.

The thesis is organized as follows:

Chapter 1: Fluorescent Nucleoside Analogues as Probes for Studying Nucleic Acid Structure and Function

In this chapter a concise historical background on the development and applications of fluorescent nucleoside analogues is provided. In particular, emphasis is laid on the design and applications of base-modified fluorescent ribonucleoside analogues used as probes incorporated into RNA oligonucleotides. The limitations of presently available nucleoside analogues and inspiration for the present research work are also detailed in this chapter.

Chapter 2: Synthesis, Photophysical Characterization, and Enzymatic Incorporation of 5-Benzothiophene-Conjugated Fluorescent Uridine Analogue

The design of 5-benzothiophene-conjugated uridine analogue (**UTh**) is based on the heterobicyclic chromophore present in the naturally occurring fluorescent aromatic amino acid, tryptophan, which is moderately emissive and importantly, its fluorescence properties are highly responsive to its local environment. The nucleoside was synthesized by employing palladium-catalyzed cross-coupling reactions. Preliminary photophysical studies indicated that the nucleoside was reasonably emissive with emission maximum in the visible region.[17] Quantum yield, lifetime and anisotropy of the nucleoside were found to be highly sensitive to changes in solvent polarity and viscosity imparting probe-like attributes to the nucleoside (Figure 1).[18]

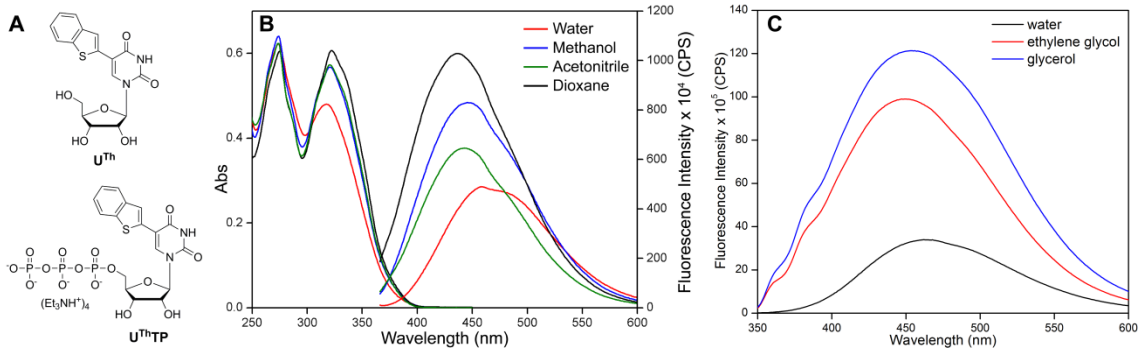

Figure 1. (**A**) Chemical structure of fluorescent nucleoside **UTh** and corresponding triphosphate **UThTP**. (**B** and **C**) Absorption and emission studies illustrating the responsiveness of **UTh** to changes in solvent polarity and viscosity, respectively.

Although, solid-phase chemical synthesis is the method of choice for synthesizing modified oligoribonucleotides, enzymatic incorporation by transcription reaction in the presence of T7 RNA polymerase was used to incorporate the modification into RNA oligonucleotides. The efficacy of T7 RNA polymerase in incorporating the modified ribonucleoside triphosphate (**UThTP)** into RNA transcripts was investigated by performing *in vitro* transcription reactions in the presence of various templates (Figure 2). The modified transcripts were purified by PAGE, and further characterized by mass analysis and by enzymatic digestion followed by HPLC analysis of the ribonucleoside products. Collectively, these experiments demonstrated the usefulness of *in vitro* transcription reactions in generating singly- and doubly-modified fluorescent oligoribonucleotides.[17] Furthermore, UV-thermal melting analysis indicated that the benzothiophene modification had little impact on the hybridization efficiency of the modified transcripts as compared to the control unmodified transcripts.

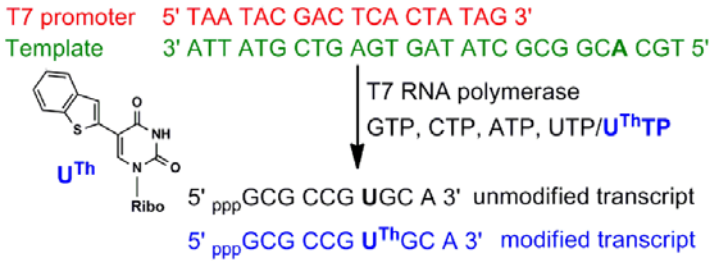

Figure 2. Enzymatic incorporation of **UThTP** by *in vitro* transcription reactions.

Fluorescence properties of emissive nucleoside analogues when incorporated into oligonucleotides are known to be influenced by a variety of mechanisms involving neighbouring bases.[11-14] Therefore, the effect of base pair substitution was studied by assembling a series of oligonucleotide duplexes in which the modified uridine was placed opposite to matched and mismatched bases. When the modification was placed opposite to complementary base in DNA and RNA oligonucleotides, the nucleoside showed slight enhancement into fluorescence intensity as compared to the single stranded oligonucleotide. This observation is noteworthy because most of the nucleoside analogues (*e.g.* 2-aminopurine, pyrroloC) show fluorescence quenching upon incorporation into double stranded oligonucleotides due stacking interaction and or electron transfer process between the fluorescent analogue and neighbouring bases.[15,16] Interestingly, when the modified nucleoside was placed opposite to pyrimidine bases it showed enhancement in fluorescence intensity as compared to when it was placed opposite to purines bases (Figure 3). Taken together, easy synthesis, amicability to enzymatic incorporation and sensitivity to changes in neighbouring base environment highlight the potential of ribonucleoside analogue **UTh** as an efficient fluorescent probe to investigate nucleic acid structure and recognition.[17]

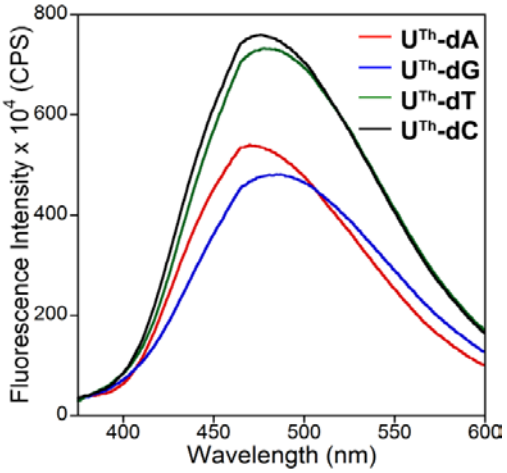

Figure 3. Emission spectra of duplexes containing **UTh** opposite to purines and pyrimidine residues.

Chapter 3: 5-Benzothiophene-Modified Uridine Analogue as a Fluorescence Probe for Studying Oligonucleotide Dynamics in a Model Cell-Like Compartment

The majority of fluorescent nucleoside analogue probes that have been used in the *in vitro* study of nucleic acids are not suitable for cell-based biophysical assays as they exhibit excitation maximum in the UV-region and low quantum yield within oligonucleotides.[18] Therefore, it was hypothesized that the photophysical characterization of oligonucleotides labeled with a fluorescent nucleoside analog in reverse micelles (RM), which are good biological membrane models and UV transparent,[19,20] would provide an alternative approach to study the properties of nucleic acids in a cell-like confined environment. In this chapter, the photophysical properties of 5-benzothiophene-conjugated uridine analogue $\mathbf{U^{Th}}$ in micelles and RM are described. The emissive nucleoside, which is polarity- and viscosity-sensitive, reports the environment of the surfactant assemblies via changes in its fluorescence properties.

Fluorescent properties of $\mathbf{U^{Th}}$ as a function of increasing concentrations of anionic (*e.g.* sodium dodecyl sulphate) and cationic (*e.g.* cetyl trimethyl ammonium bromide) surfactants were measured. As the concentration of surfactants was increased the fluorescence intensity increased with a small bathochromic shift, which saturated at higher concentrations of micelles (Figure 4). The critical micellar concentration (CMC) determined for anionic and cationic surfactants were in good agreement with the literature reports.[21]

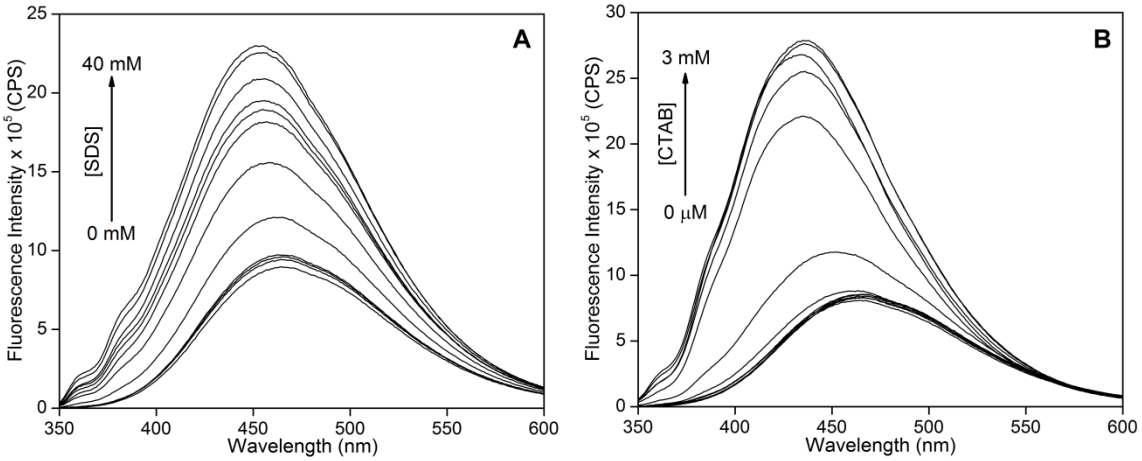

Figure 4. Emission spectra of aqueous solutions of ribonucleoside $\mathbf{U^{Th}}$ containing increasing concentration of SDS (**A**) and CTAB (**B**).

It has been shown that the size of the aqueous micellar core in RM increases linearly with w_0 (w_0 = [water]/[AOT]) resulting in variations in physical properties of the

entrapped water such as dynamics, polarity and viscosity.[22] As water content was increased the emissive nucleoside displayed changes in fluorescence properties such as fluorescence intensity, emission maximum, lifetime and anisotropy, which was consistent with the environment of RM. The ability of nucleoside to report the RM environment allowed us to investigate the effect of confinement on the oligonucleotide dynamics. The nucleoside analogue incorporated into a model RNA oligonucleotide and hybridized to its complementary DNA and RNA oligonucleotides, exhibited a significantly higher fluorescence intensity, lifetime and anisotropy in RM than in aqueous buffer (Figure 5). These results indicate that the motion of oligonucleotides is considerably retarded in RM as compared to in aqueous buffer, which is in agreement with the environment of the encapsulated water pool in RM.[21] Collectively these observations demonstrate that nucleoside $\mathbf{U^{Th}}$ could be utilized as a fluorescent label to study the function of nucleic acids in a model cellular setting.

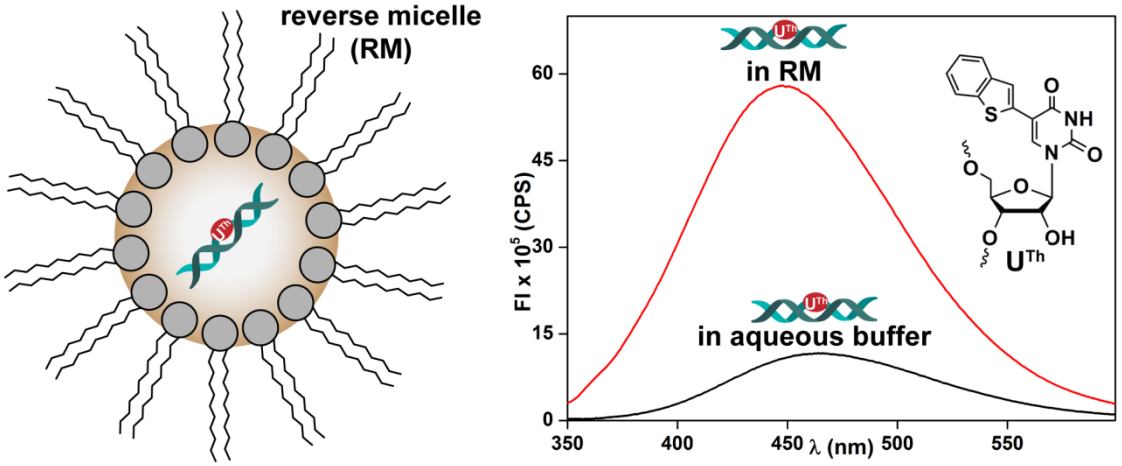

Figure 5. Encapsulation of $\mathbf{U^{Th}}$ containing oligonucleotide duplex in RM. Emission profile of $\mathbf{U^{Th}}$ containing oligonucleotide duplex in AOT RM and aqueous buffer.

Chapter 4: A Double Duty Ribonucleoside Analogue Probe Based on a 5-(selenophen-2-yl)pyrimidine Core for the Fluorescence Detection of RNA-Ligand Binding

The rate at which new functional RNAs are being discovered, and since the current knowledge on the structure-function relationship of RNA is limited, it is essential to develop robust tools to understand how RNA structure complements its function. Towards this endeavour, it is highly desirable to develop a label compatible with two complementing biophysical techniques, one that would provide information on the dynamics and recognition properties in real time and the other on the 3D structure of nucleic acids. In this chapter, the development of a new “double duty” ribonucleoside

analogue probe ($\mathbf{U}^{Se}$), based on a 5-(selenophen-2-yl)pyrimidine core, which could serve as a fluorescence probe as well as an anomalous scattering label (selenium atom) for the phase determination in X-ray crystallography is described (Figure 6). Notably, the superior anomalous scattering property of selenium atom that has been extensively used in protein X-ray crystallography has also been extended to nucleic acid X-ray crystallography.[23,24]

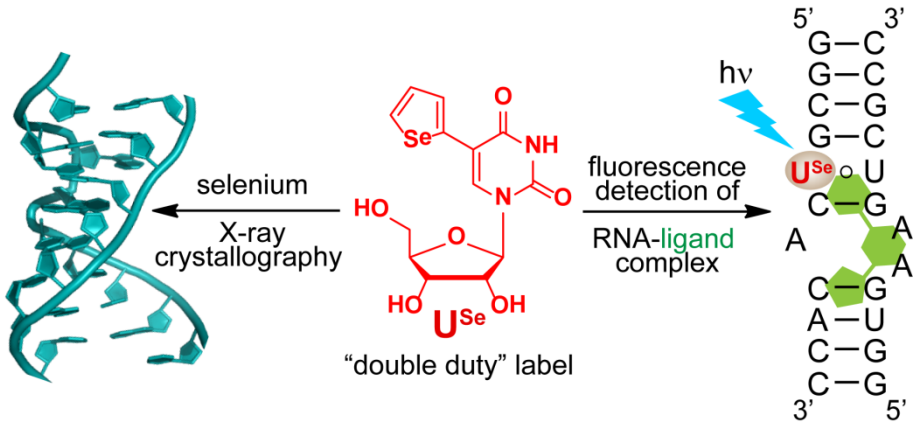

Figure 6. Selenophene-modified uridine ($\mathbf{U}^{Se}$) analogue as a double duty probe.

The selenophene-modified uridine analogue synthesized by performing a palladium-catalyzed cross-coupling reaction between 5-iodouridine and 2-(tri-*n*-butylstannyl)selenophene displayed emission in the visible region and a very good fluorescence solvatochromism. The corresponding triphosphate was amicable to enzymatic incorporation into RNA oligonucleotides, which allowed the easy synthesis of selenophene-labeled RNA oligonucleotides.[25] Although, the selenophene moiety attached at the 5 position of uracil is relatively small, its introduction can potentially affect the native structure of oligoribonucleotides and their ability to form stable duplexes. Small differences in T_m values between control unmodified and modified duplexes indicated that the modification had only a minor impact on the duplex stability.

Preliminary photophysical characterization of single stranded and duplexes of selenophene-modified oligonucleotides revealed that the fluorescence of emissive nucleoside was sensitive to base pair substitutions. Furthermore, as a proof of responsiveness of the nucleoside to RNA conformational changes, a therapeutically important RNA motif, bacterial ribosomal decoding site (A-site) RNA, was labeled with the emissive nucleoside, and a fluorescence binding assay was developed to effectively monitor the binding of aminoglycoside antibiotics to the bacterial A-site (Figure 7).[25] Taken together, this heavy-atom containing fluorescent label is a unique and useful combination wherein its dual properties can be utilized to study the dynamics, structure

and recognition properties of nucleic acids by two mutually exclusive but complementing techniques, namely, fluorescence and X-ray crystallography. Efforts to incorporate and crystallize selenophene-modified DNA and RNA motifs of biological relevance are currently being pursued in our group.

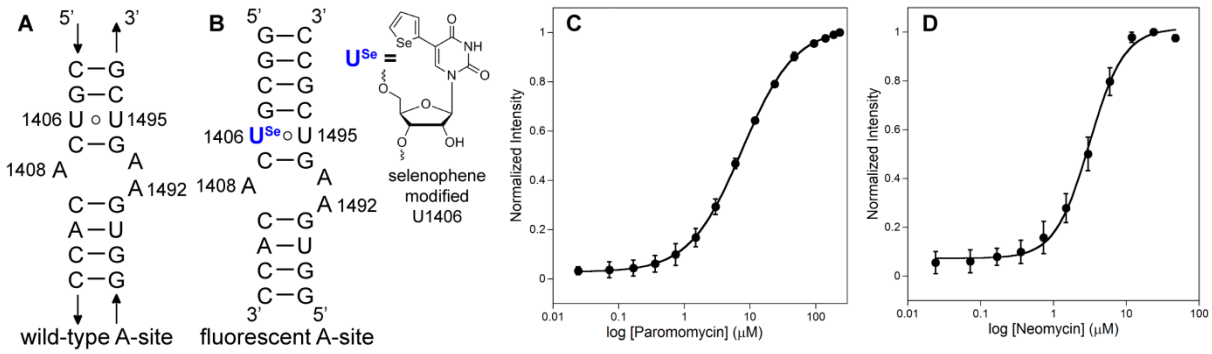

Figure 7. (**A**) Secondary structure of the bacterial A-site motif that binds to aminoglycoside antibiotics. (**B**) $\mathbf{U^{Se}}$-modified fluorescent A-site RNA model construct. (**C** and **D**) Curve fits for the titration of A-site with paromomycin and neomycin, respectively.

References:

1. DeRose, V. J. *Curr. Opin. Struct. Biol*. **2003**, *13*, 317–324.
2. Ranasinghe R. T.; Brown, T. *Chem. Commun.* **2005**, 5487–5502**.**
3. Hall, K. B. *Curr. Opin. Chem. Biol*. **2008**, *12*, 612–618.
4. Al-Hashimi, H. M.; Walter, N. G. *Curr. Opin. Struct. Biol.* **2008**, *18*, 321–329.
5. Aitken, C. E.; Petrov, A.; Puglisi, J. D. *Annu. Rev. Biophys.* **2010**, *39*, 491–513.
6. Wilson, J. N.; Kool, E. T. *Org. Biomol. Chem.* **2006**, *4*, 4265–4274.
7. Wilhelmsson, L. M. *Quart. Rev. Biophy*. **2010**, *43*, 159–183.
8. Sawant, A. A.; Srivatsan, S. G. *Pure Appl. Chem*. **2011**, *83*, 213–232.
9. Phelps, K.; Morris, A.; Beal, P. A. *ACS Chem. Biol.* **2012**, *7*, 100–109.
10. Sinkeldam, R. W.; Greco, N. J.; Tor, Y. *Chem. Rev*. **2010**, *110*, 2579–2619.
11. Rachofsky, E. L.; Osman, R.; Ross, J. B. A. *Biochemistry* **2001**, *40*, 946–956.
12. Jean, J. M.; Hall, K. B. *Proc. Natl. Acad. Sci. USA* **2001**, *98*, 37–41.
13. Doose, S.; Neuweiler, H.; Sauer, M. *ChemPhysChem* **2009**, *10*, 1389–1398.
14. Sinkeldam, R. W.; Wheat, A. J.; Boyaci, H.; Tor, Y. *ChemPhysChem* **2011**, *12*, 567–570.
15. Ward, D. C.; Reich, E.; Stryer, L. *J. Biol. Chem*. **1969**, *244*, 1228–1237.
16. Tinsley, R. A.; Walter, N. G. *RNA* **2006**, *12*, 522–529.
17. Pawar, M. G.; Srivatsan, S. G. *Org. Lett.* **2011**, *13*, 1114–1117.

18. Tanpure, A. A.; Pawar, M. G.; Srivatsan, S. G. *Isr. J. Chem*. **2013**, *53*, 366–378.
19. Luisi, P. L.; Giomini, M.; Pileni, M. P.; Robinson, B. H. *Biochim. Biophys. Acta* **1988**, *947*, 209–246.
20. Levinger, N. E. *Science* **2002**, *298*, 1722–1723.
21. Pawar, M. G.; Srivatsan, S. G. *J. Phy. Chem. B.* **2013**, *117*, 14273–14282.
22. Fletcher, P. D. I.; Howe, A. M.; Robinson, B. H. *J. Chem. Soc., Faraday Trans. 1* **1987**, *83*, 985–1006.
23. Egli, M.; Pallan, P. S. *Annu. Rev. Biophys. Biomol. Struct*. **2007**, *36*, 281–305.
24. Sheng, J.; Huang, Z. *Chem. Biodiversity* **2010**, *7*, 753–785.
25. Pawar, M. G.; Nuthanakanti, A.; Srivatsan, S. G. *Bioconjugate Chem.* **2013**, *24*, 1367–1377.

List of Publications

1. **Maroti G Pawar**, and Seergazhi G Srivatsan. Synthesis, Photophysical Characterization and Enzymatic Incorporation of a Microenvironment-Sensitive Fluorescent Uridine Analog. *Org. Lett.*, **2011**, *13* (5), 1114–1117.

2. **Maroti G Pawar** and Seergazhi G Srivatsan. Environment-Responsive Fluorescent Nucleoside Analogue Probe for Studying Oligonucleotide Dynamics in a Model Cell-like Compartment. *J. Phy. Chem. B.*, **2013**, 117 (46), 14273–14282.

3. **Maroti G Pawar**, Ashok Nuthanakanti, and Seergazhi G Srivatsan Heavy Atom Containing Fluorescent Ribonucleoside Analog Probe for the Fluorescence Detection of RNA-Ligand Binding. *Bioconjugate Chem.*, **2013**, *24* (8), 1367–1377.

4. Arun A Tanpure, **Maroti G Pawar**, and Seergazhi G Srivatsan Fluorescent Nucleoside Analogs: Probes for Investigating Nucleic Acid Structure and Function. *Isr. J. Chem.*, **2013**, *53* (6-7), 366–378.

CHAPTER-1

Fluorescent Nucleoside Analogues as Probes for Studying Nucleic Acid Structure and Function

1.1 Introduction

Nucleic acids participate in a wide variety of cellular processes, which are necessary for the flourishing and propagation of life. DNA acts as a genetic material in all living organism except some viruses (e.g., retrovirus). DNA undergoes self-replication in the presence of DNA polymerase to give its own copies. Further, DNA undergoes transcription in the presence of RNA polymerases to produce mRNA, which then acts as the template for the synthesis of corresponding protein by a process called translation. The translation process takes place in ribosomal machinery, which is composed of rRNA, tRNA and protein factors.[1]

RNA, for a long time, was considered to just serve as an information conduit between DNA and ribosomal machinery for the protein synthesis process. However, several seminal discoveries over the last four decades have expanded our understating on the functional role of RNA in contemporary biology.[2,3] Now RNA is considered as a functionally sophisticated biopolymer as it can (i) store and transfer genetic information, (ii) catalyze biological reactions, (iii) play a vital role in translation process, and (iv) act as a gene regulatory motif. RNA essentially performs its function by binding to protein, nucleic acid or small molecule metabolites. Although chemically less diverse as compared to proteins, RNA expands its functional repertoire by using its inherent conformational dynamics and by adopting diverse 3-dimensional structures that rapidly interconvert between different functional states.[4–9] As a result, several biophysical and theoretical tools have been developed to uncover the fundamentals of nucleic acid folding and recognition processes.[10]

The majority of biophysical investigations greatly rely on techniques, namely, fluorescence, electrophoresis, circular dichroism, calorimetry, nuclear magnetic resonance (NMR), electron paramagnetic resonance (EPR), X-ray crystallography and microscopy.[11–21] Among these, fluorescence spectroscopy is by far the most attractive technique as it is easily accessible, versatile and provides information in real time with great sensitivity. Consequently, fluorescence spectroscopy has been extensively used in investigating pathways and kinetics of conformational transformations of nucleic acids, nucleic acid-protein and nucleic acid-small molecule complexes.[11–14] Importantly, advances in ultrafast and single-molecule fluorescence spectroscopy techniques have allowed the investigation of conformational dynamics and processing of nucleic acids *in vitro* as well as in cells in a wide range of time scales.[22–24]

Unlike many proteins, which exhibit intrinsic fluorescence due to the presence of aromatic amino acids, natural nucleobases are practically non-emissive.[25,26] Hence, in order to study nucleic acids by fluorescence spectroscopy, it is imperative that a fluorescent reporter be introduced into nucleic acids either covalently or noncovalently. In this context, environment-sensitive fluorescent nucleoside analogues, which closely maintain the structural and functional integrity of natural nucleosides, have to provide effective tools to study the conformation dynamics and recognition properties of nucleic acids.[27,28] Several fluorescent nucleoside analogues have been developed by either extending the π-conjugation of the purine and pyrimidine core or by using naturally occurring fluorescent heterocycles and polycyclic aromatic hydrocarbons as nucleobase surrogates.[29,30] A significant number of these analogues that display useful photophysical properties have been implemented in several DNA-based, and to a relatively lesser extent in RNA-based biophysical assays. However, the majority of fluorescent nucleosides have excitation and emission maximum in the UV region and importantly, show drastic reduction in fluorescence quantum yield upon incorporation into single stranded and double stranded oligonucleotides due to interactions with neighbouring bases.[31–33] These drawbacks have essentially precluded their implementation in certain fluorescence methods (e.g., anisotropy, single-molecule spectroscopy and cell microscopy). Hence, most of the recent efforts in the development of new generation nucleoside analogue probes are focused toward the design and synthesis of probes with photophysical properties suitable for nucleic acid analysis *in vitro* and in cells.

In this chapter a brief discussion on the basic structure and function of nucleic acids, especially that of RNA, is provided. Further, a concise background on the development and applications of various biophysical techniques used in the study of nucleic acids is discussed. In particular, emphasis is laid on the design and applications of base-modified fluorescent ribonucleoside analogues used as probes incorporated into RNA oligonucleotides. The limitations of currently available nucleoside analogues and inspiration for the present research problem are also detailed in this chapter.

1.2 Components of Nucleic Acids

Nucleic acids are made of repeating units of nucleosides, which are connected to each other by a phosphodiester linkage. There are five nitrogen rich heterocyclic nucleobases found in nucleic acids. They are divided into monocyclic heterocycles, called pyrimidines (thymine, uracil, and cytosine) and bicyclic heterocycles, called purines (adenine and

guanine). In DNA guanine, adenine, cytosine and thymine bases are present, while in RNA thymine is substituted by uracil base. The heterocyclic bases are connected to the furanose, a pentose sugar, via a β-glycosidic bond, and are commonly referred to as nucleosides (Figure 1). The pentose sugar found in DNA is 2'-deoxy-D-ribose whereas in RNA it is D-ribose. The furanose sugar in DNA and RNA exist in a "puckered" conformation. This type of puckering is distinguished by denoting the carbon, normally C2' or C3', that is out of the plane with respect to a set of atoms, namely C1'-O4'-C4' (Figure 2).[34]

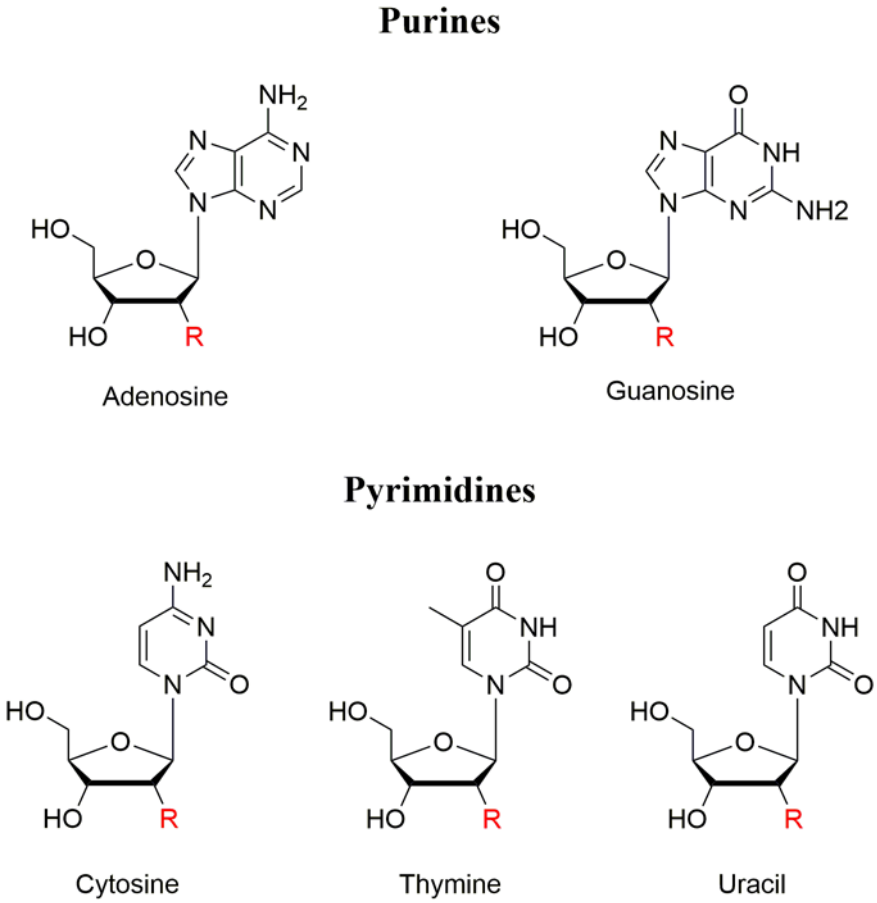

Figure 1. Chemical structure of nucleosides in DNA (R = H) and RNA (R = OH).

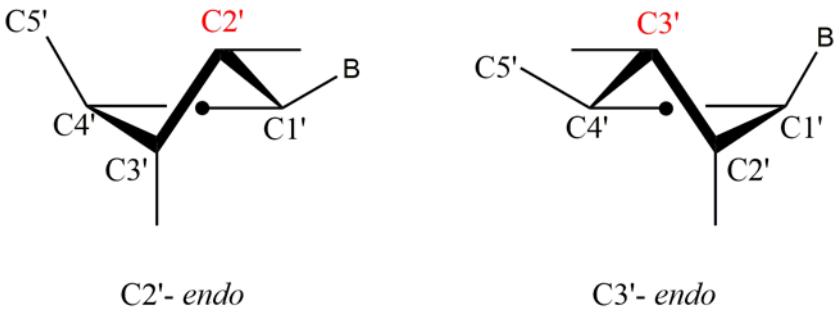

Figure 2. Puckered sugars conformations present in nucleosides.

Nucleosides are connected to each other via a phosphodiester bond from the 5'-hydroxyl of one nucleoside to the 3'-hydroxyl of the next nucleoside (Figure 3). The phosphate group connects nucleosides in a polymer-like chain where the termination of the chain ends in either the 5'-OH or 3'-OH of the nucleoside, thus distinguishing the direction of the chain.[34]

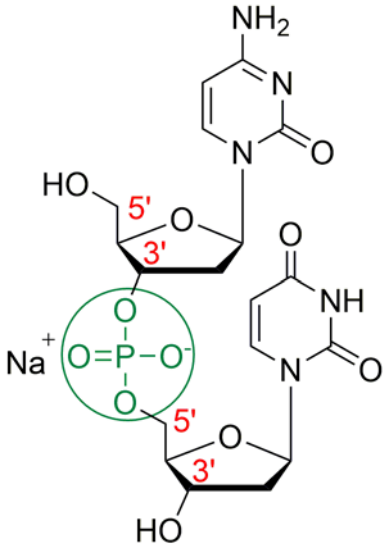

Figure 3. Phosphodiester linkage present in a dinucleotide.

1.3 Base Pairing

The nucleobases of nucleic acids can hydrogen bond (H-bond) with one another on the basis of size/shape and H-bonding complementarities to form base pairs. Typically, base pairing takes place between two cognate purines and pyrimidines based on the H-bonding complementarity. For example, cytosine and guanine form a stable base pair assisted by three hydrogen bonds, whereas adenine forms two stable hydrogen bonds with thymine in DNA or with uracil in RNA (Figure 4). The canonical A-T and G-C base pairs in nucleic acids are commonly known as Watson-Crick base pairs. Two complementary strands of DNA or RNA can form duplex, which is stabilized by base pairing and stacking interaction between the adjacent base pairs. In particular, a long chain of RNA can adopt multiple structures ranging from stem-loop, hair-pin, bulge and pseudoknot, to name a few.[34] In addition, nucleic acids can also form triplexes and other tertiary structures such as G-quadruplexes by Watson-Crick and Hoogsteen H-bonding.[35] Because hydrogen bonds are relatively weak, it is easy to unwind nucleic acid strands, for example during replication and transcription.

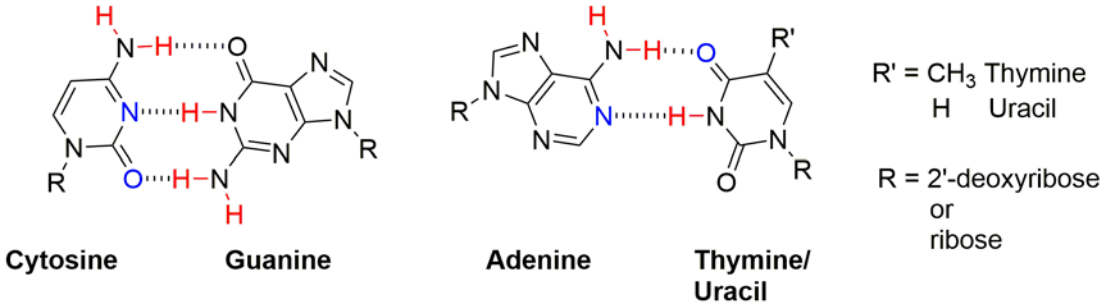

Figure 4. Purine-pyrimidine base pairs in nucleic acids. H-bond donors and acceptors are coloured in red and blue, respectively.

From hydrogen bonding and X-ray diffraction patterns, Watson and Crick discovered the antiparallel double helical structure of DNA. In their proposed structure nucleobase are found in anti confirmation, where the hydrogen bonding faces are opposite to furanose sugar. This results in negatively charged phosphate groups pointing outward toward the aqueous media, while the aromatic nucleobase bases point inwards toward each other creating a hydrophobic cavity. The anti-parallel helix generates two grooves that run along the helical axis, named the major and minor grooves. Depending upon the condition in which nucleic acids are placed and base sequences of pairing strands, nucleic acids can adopt mostly three forms A, B and Z. The B-form is most stable configuration at physiological conditions and it is the predominant form.

B-form is an alpha (right handed) helix. This helix makes turn every 3.4 nm, and the distance between two neighboring base pairs is 0.34 nm. B-DNA possesses 10.5 base pairs per turn.[34,36] A-form is also a right handed helix and exist at higher salt concentration. This form makes turn per 2.3 nm and has 11 base pairs per turn. This form is mainly formed by DNA-RNA and RNA-RNA duplexes.[34,36] Z-from is a left handed helix. The length of one turn of helix is 4.6 nm involving 12 base pairs. Z-from is observed in low salt concentration and containing alternate G-C rich nucleosides in nucleic acid.[34,36]

1.4 Functions of Nucleic Acids

DNA acts as a genetic material in all living organism except some viruses. DNA stores and transfers the genetic information from one generation to the next generation by replication process (Figure 5). During cell division DNA self-replicates in the presence of DNA-dependent DNA polymerase to give its own copies, which are faithfully integrated into two daughter nuclei. Further, DNA transfers the code for the protein synthesis to

RNA by a process called transcription. The mRNA containing the information, acts as the template for the synthesis of corresponding protein by a process called translation.

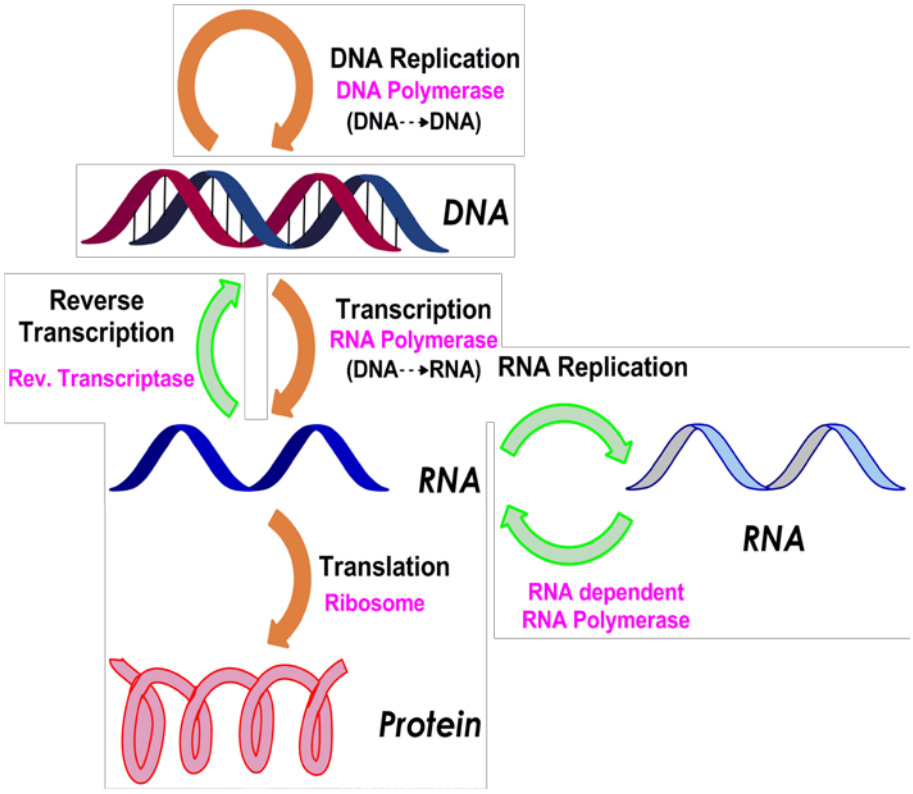

Figure 5. Information flow in biology. In some of the viruses, where DNA is absent as genetic material RNA acts as genetic material and in presence of RNA dependent RNA polymerase it gives its own copies.

In addition to facilitating the transfer of information from DNA to ribosomal machinery, several seminal discoveries have expanded the functional repertoire of RNA in biology. RNA can store and transfer genetic information, catalyze reactions necessary for the maturation of RNA, and can also act as gene regulatory motif. The discovery of regulation of protein expression by RNA interference (RNAi) is considered phenomenal as protein expressions where thought to be mostly regulated by proteins and small molecule metabolites.[37,38] RNAi is an evolutionarily conserved pathway for regulating gene expression in most eukaryotes, wherein small RNA oligonucleotides, either endogenously generated microRNA (miRNA) or exogenously administered small interfering RNA (siRNA), bind to a specific mRNA target and either increase or decrease protein expression.[39,40] Recent studies have shown that RNAi can be utilized in silencing oncogens and other genes implicated in cell proliferation, differentiation, and apoptosis.[41,42]

Another class of RNA gene control element that have been recently discovered is riboswitches. Riboswitches are structured RNA domains present in the noncoding regions

of mRNA of bacteria, and certain plants and fungi.[4,43] These RNA motifs bind to a specific small molecule metabolite in a concentration dependent manner and undergo structural reorganization.[37] This conformation change in mRNA is translated into a signal that modulates the expression of the protein it codes, which in turn is responsible for the biosynthesis of metabolite itself. Recent studies on the mechanism of action of certain antibacterial drugs suggest that these drugs function at least in part by targeting riboswitch RNA motifs.[44] Currently, riboswitches are being investigated as potential antibacterial drug targets.

Several bacterial- and viral-specific RNA molecules have been and are being rigorously evaluated as potential therapeutic targets. In this context, bacterial ribosomal decoding site RNA (A-site) is one of the oldest and well studied RNA motifs, which is a target for a class of antibiotic drugs called aminoglycosides. These aminoglycosides bind to A-site of 16S rRNA inducing a conformational change, which leads to codon-anticodon misreading, resulting in mistranslation.[45] Certain viral specific protein-RNA interactions like HIV-1 Tat-TAR (trans-activating (Tat) response element) and Rev-RRE (Rev response element), which are crucial recognition events in the HIV replication process are competitively inhibited by aminoglycoside antibiotics.[46] These are some of the representative examples of RNA function and RNA motifs of therapeutic importance (Figure 6). Detailed account on RNA structure and function are available in literature.[47–50]

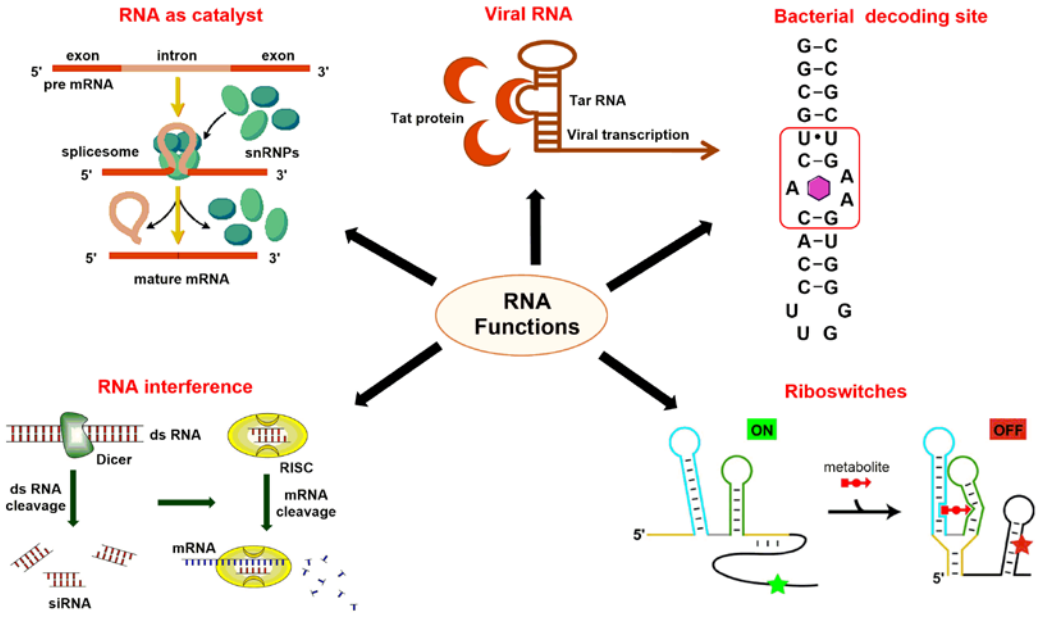

Figure 6. Functions of RNAs. RNA performs several functions like it acts as catalyst in RNA maturation process, it acts as genetic material in retroviruses, it react with drug molecules at bacterial decoding site. It also takes part in gene regulation process by interacting with small metabolite molecules in riboswitches or by reacting with nucleic acids in interference phenomenon.

1.5 Biophysical Techniques to Study Nucleic Acids

RNA performs its function by binding to protein, nucleic acid and small molecule metabolite targets, and doing so undergo conformation changes at both global as well as nucleotide levels. Hence, it is not surprising that several biophysical methods have been and are being developed to advance our fundamental understanding of RNA-protein, RNA-nucleic acid and RNA-small molecule interactions. Biophysical techniques that are commonly used in nucleic acid analysis are fluorescence, nuclear magnetic resonance (NMR), electron paramagnetic resonance (EPR), X-ray crystallography. Needless to say, many of these techniques depend upon the accessibility of RNA oligonucleotides labeled with appropriate reporters.

1.5.1 Nuclear Magnetic Resonance (NMR) Spectroscopy in Nucleic Acid Analysis

NMR spectroscopy has become a powerful tool to study RNA structure and dynamics because of the advances in instrumentation and developments in isotope labeling techniques (Figure 7).[51,52] RNA structure determination using NMR is not straight forward due to spectral crowding of sugar protons in ^{1}H and ^{2}H spectra and appearance of ^{13}C, ^{15}N and ^{31}P chemical shifts in a narrow region. This technique greatly relies on the selective labeling of nucleosides with stable isotopes such as ^{13}C, ^{15}N, ^{2}H and ^{19}F. Williamson and co-workers used isotopically labeled adenine and guanine nucleotides (**1**-**4**) to study the *de novo* purine synthesis pathways.[53] Pitsch and co-worker synthesized phosphoramidite substrates of 2'-TOM-protected ^{15}N-pyrimidine and ^{15}N-purine (**5**-**8**) nucleosides and used them in the solid-phase synthesis of RNA oligonucleotides, which undergo a topologically favoured conformational exchange between different hairpin folds. Using these isotope labeled RNA oligonucleotides they studied the kinetics of RNA folding process.[54,55]

Similarly, site-specific incorporation of fluorine atoms into RNA has been used in the investigation of RNA conformations. Strobel and Suydam synthesized ^{19}F-substituted adenosine and 7-deaza-adenosine analogues (**9**-**11**). They have used these fluorinated analogues to study nucleobase protonation by nucleotide analogue interference mapping (NAIM) in Varkud Satellite (VS) ribozyme.[56] Recently, Micura and co-workers synthesized 2′-trifluoromethylthio-modified pyrimidine nucleosides and studied their structure and base pairing properties in oligonucleotide sequences. 2′-Trifluoromethylthio-modified ribonucleosides (**12** and **13**) show small impact on thermodynamic stability, when incorporated into single-stranded oligonucleotides. However, when positioned in double helical regions, causes high extent of destabilization.[57]

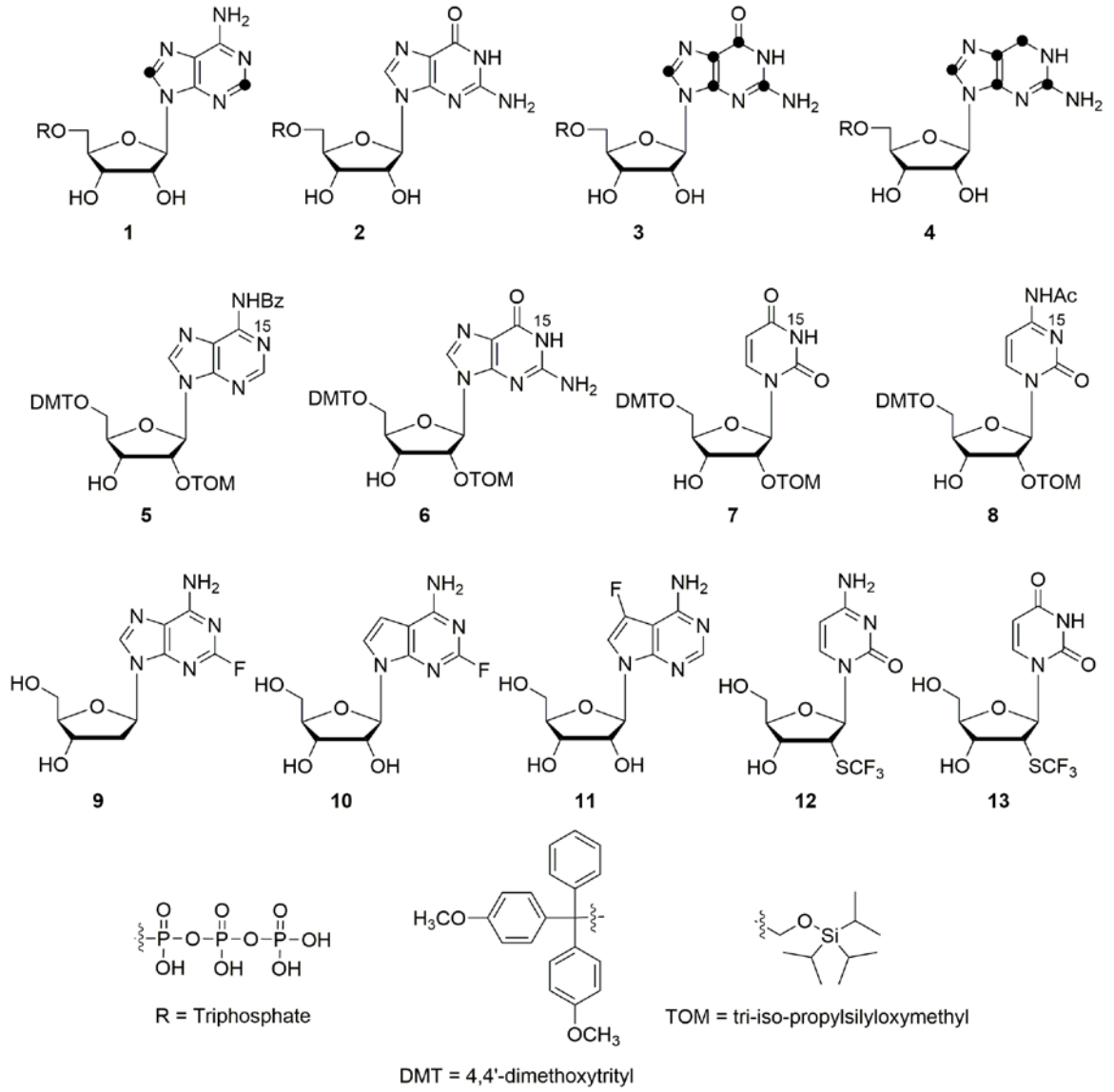

Figure 7. Representative examples of isotope-labeled nucleoside probes used in NMR spectroscopy. Carbon isotopes are shown in black solid dots.

1.5.2 Electron Paramagnetic Resonance (EPR) Spectroscopy in Nucleic Acid Analysis

The use of EPR in the study of DNA and RNA oligonucleotides has been gaining interest over the last few years. EPR studies mainly depend on the derivatization of nucleosides with paramagnetic species (Figure 8). As natural nucleosides are EPR-inactive, unnatural spin labels are chemically incorporated into nucleosides to make them paramagnetic. The commonly used spin label is nitroxide radical, which is site-specifically incorporated into RNA by an approach termed as site-directed spin labeling (SDSL).[58] Engels and co-workers site specifically introduced spin label 2,2,5,5-tetra-methyl-pyrrolin-1-yloxyl-3-acetylene (TPA) on to uridine, cytidine, adenosine and used these nucleoside for measurement of intramolecular distances in solvated RNA systems (**14-16**).[59] Sigrurdsson

and co-workers derivatized the ribose sugar of uridine (**17**) with 2,2,6,6-tetramethylpiperidine-1-oxyl-4-isocyanate (TEMPO) and placed it into four different positions of a well-characterized trans-activation responsive region (TAR) of HIV-1 RNA. They studied the interaction of spin labelled TAR-RNA with Tat protein.[60] Recently, Sigrurdsson group reported a new cytidine-based spin label probe (**18**) in which nitroxide containing ring was joined to a tricyclic nucleobase moiety. This label is highly useful as it can be used in EPR spectroscopy as well as can be used in fluorescence spectroscopy.[61]

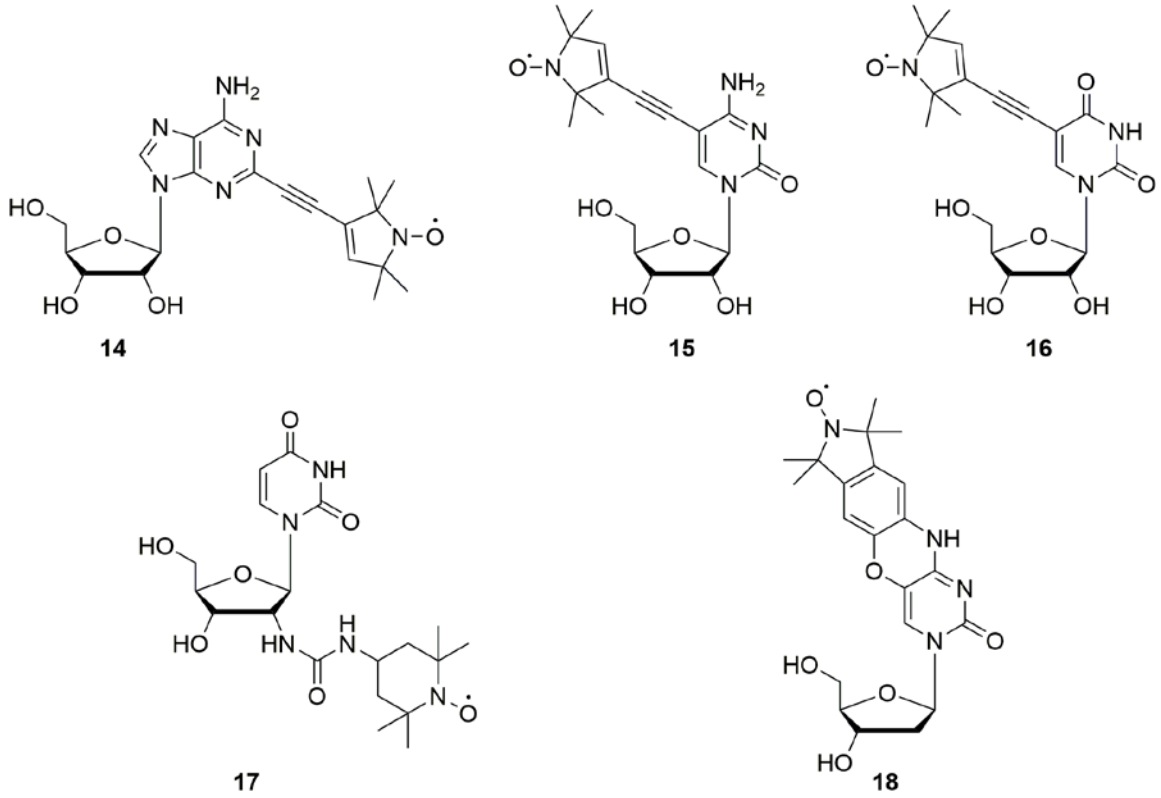

Figure 8. Representative examples of spin-labeled nucleoside probes used in EPR spectroscopy.

1.5.3 X-ray Crystallography in Nucleic Acid Analysis

High-resolution X-ray structures of a number of RNA molecules and complexes with proteins and small molecules have provided immense information on the relationship between RNA structure and function at the molecular level. 3-D structure determination of nucleic acids by X-ray crystallography most often requires heavy atom derivatization of nucleic acids for phase determination (Figure 9). Usually heavy atom labels are introduced into RNA by either soaking or co-crystallizing in salt solutions of heavy atoms.[62] Alternatively, incorporation of brominated or iodinated nucleoside analogues into RNA can also be used to introduce heavy atom as phasing agents. However, halogenated nucleosides are light-sensitive and are also known to undergo dehalogenation during X-ray crystallography analysis.[63] More recently, the anomalous scattering property of selenium

atom, which has been extensively used in the protein X-ray crystallography by multi-wavelength anomalous dispersion (MAD) phasing technique, has also been extended to 3-D structure determination of nucleic acids.[64] Egli, Huang and co-workers for the first time incorporated a selenium-modified nucleoside, 2'-methylselenouridine (**19**), into DNA and RNA, and successfully showed the utility of selenium atom in MAD phasing.[65] Based on this labeling strategy, Micura and co-workers reported site-specific incorporation of nucleosides containing 2'-methylseleno group (**20**) into relatively long RNAs (~100 nt).[66,67] 2'-methylseleno-modified RNA has been utilized in the structure determination of a ribozyme that catalyzes Diels–Alder reaction and HIV-1 genomic RNA dimerization initiation site (DIS) bound to aminoglycoside antibiotics.

Recently, Huang and co-workers have developed base-modified Se^4T (**21**) and Se^6G (**22**) nucleosides that can be incorporated into DNA oligonucleotides by conventional solid-phase synthesis protocol. Notably, crystal structure of a self-complementary octamer containing Se^4T and a ternary complex of DNA, RNA and RNase H containing Se^6G revealed no structural perturbation as compared to the crystal structure of native oligonucleotides.[68,69] Future advances in incorporation techniques and proven usefulness of selenium atom as a structurally benign MAD phasing label are likely to pave way for the regular use of selenium-modified nucleic acids in X-ray crystallography-based structural analysis of DNA and RNA.

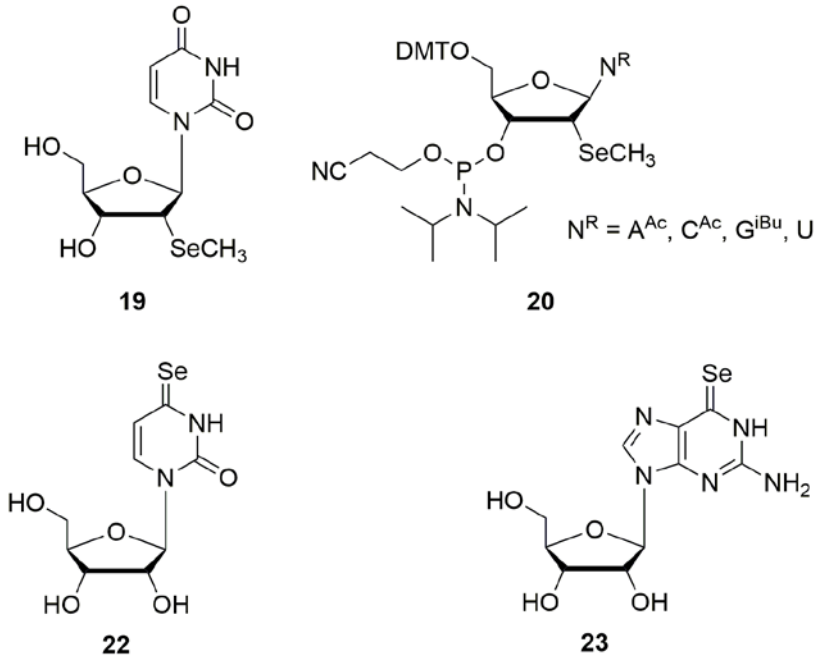

Figure 9. Representative examples of selenium-labeled nucleoside probes used in X-ray crystallography.

1.5.4 Fluorescence Spectroscopy in Nucleic Acid Analysis

Among the techniques described above on the study of nucleic acids fluorescence spectroscopy is by far the most widely used as it is easily accessible, versatile, and provides information in real time with exceptional sensitivity. Fluorescence-based methods, which use properties such as fluorescence intensity (FI), fluorescence lifetime (FLT), and fluorescence polarization (FP), and phenomenon like fluorescence resonance energy transfer (FRET), have been extensively used in the investigation of structure, dynamics and function of nucleic acids *in vitro* and in cells.[70–73]

(A) Steady-state fluorescence (SSF): Steady-state fluorescence is a straight forward and regularly employed technique. In this method, the fluorophore is excited with a constant flow of photon at an appropriate wavelength depending upon the absorption spectrum and the emission profile is recorded. The emission profile essentially gives information regarding the emission maximum and quantum yield of the fluorophore in a given solvent system. The ground-state and excited-state energy levels can be affected by several factors such as solvent polarity, collisional interactions, temperature, pH and ionic strength, which can potentially alter the emission maximum and/or the quantum yield.[74] Hence, nucleic acid probes, which report changes in these properties have been implemented in assays to study nucleic acids. For example, photophysical properties of 2-aminopurine (2-AP) incorporated into DNA and RNA oligonucleotides depend on the equilibrium between stacked and destacked states. 2-AP in the stacked state exhibits very low fluorescence quantum yield but in unstacked and solvent exposed environment it shows remarkable enhancement in florescence quantum yield.[33,75] Since this equilibrium can be altered by temperature, solvent, adjacent bases and bound protein or small molecule, 2-AP is one of the most extensively used nucleoside probes in the investigation of RNA folding and recognition processes.[29,76,77]

(B) Fluorescence resonance energy transfer (FRET): Fluorescence resonance energy transfer is a photophysical phenomenon in which energy transfer takes place between two distinct chromophores, commonly known as donor and acceptor (Figure 10).[74] The efficiency of energy-transfer between a donor and acceptor pair depends on extent of overlap between donor emission band and acceptor absorption band, distance between the donor–acceptor pair and also on orientation between donor and acceptor transition dipole moments. Most FRET-based studies use steady-state measurements in which changes in

fluorescence intensity of the donor or acceptor are measured. Most FRET-based systems have been designed using typically large donor-acceptor pairs to investigate RNA folding dynamics and binding events. However, only a few donor-acceptor pairs made of non-perturbing nucleoside surrogates have been designed and applied in the RNA studies (discussed in section 1.6).

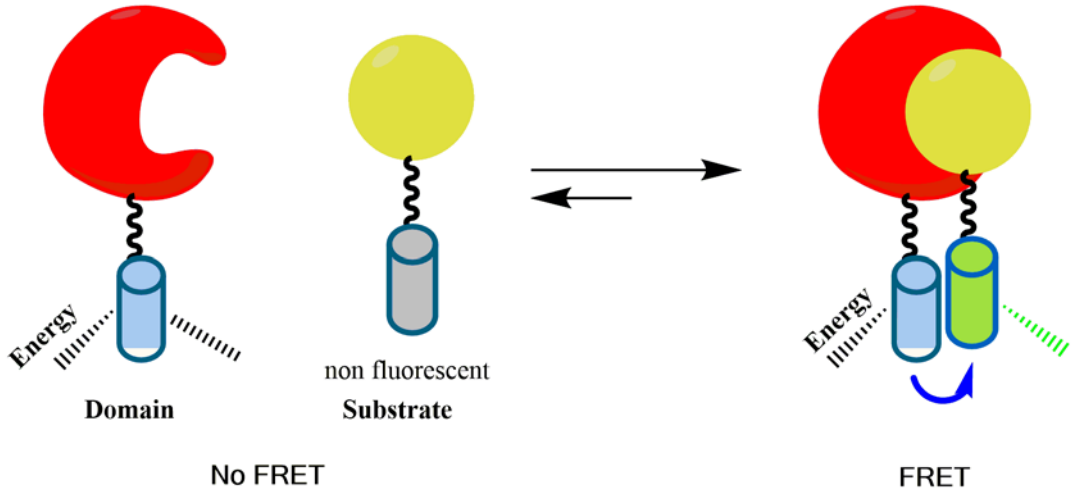

Figure 10. Schematic diagram of FRET process.

(C) Fluorescence polarization (FP): When a fluorescent molecule is excited with plane polarized light, fluorescence emission occurs from S_1 to S_0 energy level. This transition is parallel to the absorption transition (S_0-S_1). Therefore, the emission from a molecule upon excitation with polarized excitation light in the lowest energy absorption band (S_0-S_1) will usually be co-linear, if it were not that a molecule in solution can reorient during the time of excitation. In this way, the emission will be depolarized depending on the time the molecule spends in the excited state as well as on its size, shape and environment. If the molecule rotates and tumbles out of this plane during the excited state, light is emitted in a different plane compared to the plane of excitation light. The intensity of the emitted light can be monitored in vertical and horizontal planes. If a molecule is very large, little tumbling occurs and the emitted light remains highly polarized. If a molecule is small, rotation and tumbling is faster and the emitted light is less polarized. Fluorescence polarization values depend on viscosity of the solvent, the size and shape, and the inherent flexibility of the tumbling molecule.[79] Small molecules rotate faster during the excited state, and upon emission have low polarization values, whereas larger molecules or complexes, rotate slowly during the excited state, and therefore have high polarization values (Figure 11). Similarly, when a fluorescent probe is microenvironment sensitive

(e.g. viscosity sensitive), then in high viscous solvent its rate of tumbling decreases resulting in a higher FP value. However, in a low viscous solvent the same probe will show low values of FP.[74] It is important to mention here that the extent of FP depends on the rate of rotational diffusion of the probe and its excited-state lifetime. For accurate measurement of anisotropy, the fluorophore once incorporated into oligoribonucleotides should exhibit reasonable quantum yield and lifetime comparable to the rotational correlation times of the oligoribonucleotides.[80,81]

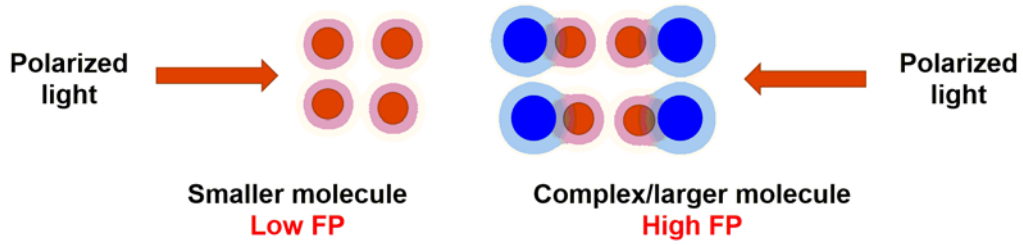

Figure 11. Schematic diagram of fluorescence polarization.

(D) Time-resolved Fluorescence Spectroscopy (TRFS): Time-resolved fluorescence spectroscopy is a powerful technique that can be used to study intensity decay profiles and determine excited-state lifetimes of fluorophores. Unlike steady-state measurements, time-resolved measurements can be used to indentify individual species present in a heterogeneous population on the basis of their lifetime. The heterogeneity can arise due to the presence of different conformational states of a given fluorophore. For example, intensity decay kinetics of 2-AP in aqueous buffer is monoexponential corresponding to a lifetime of ~10 ns.[75] However, upon incorporation into oligonucleotides it exhibits four distinct lifetimes ranging from 50 ps to 8 ns.[82,83] The longest lifetime has been assigned to the unstacked 2-AP base, which is also responsible for high fluorescence efficiency. The shortest lifetime component is assigned to the completely stacked state, which also represents the highly quenched state of 2-AP. The relative population of these components have been used in understanding the conformation dynamics of RNA during folding and binding events. Therefore, fluorescent ribonucleoside analogues that report subtle changes in conformation or environment via changes in their fluorescence properties such as emission maximum, quantum yield, lifetime and anisotropy are highly useful in studying the conformational dynamics and function of RNA.

1.6 Fluorescent Nucleoside Analogues

Natural nucleobases, the building blocks of nucleic acids, are practically non-fluorescent ($\Phi \sim 10^{-4}$, $\tau < 1$ ps in aqueous solution at room temperature).[25,26] As a result, nucleic acid needs to be labelled with a fluorescent reporter in order to study its properties by fluorescence spectroscopy. Different strategies have been used to make nucleic acid fluorescent depending upon the aim of study and property of the fluorophore. Fluorescent reporters are introduced into nucleic acids either noncovalently or covalently.

Non-covalent labelling can be achieved by using small-molecule dyes such as ethidium bromide (**23**), DAPI (**24**), SYBR Green (**25**), and Hoechst dyes (**26**), which bind nucleic acids noncovalently by intercalation or along the grooves.[84–88] Although these dyes have been extensively used for detecting nucleic acids they are not convenient for studying nucleic acid-ligand binding due to their bulkiness (can perturb the structure of nucleic acids) and constant binding and unbinding of the probes to DNA and RNA (can cause background fluorescence). These dyes are frequently used to visualize nucleic acids in gel electrophoresis and cell microscopy. Covalent modifications of nucleic acids are often achieved by attaching commercially available fluorescent derivatives (fluorescein **27**, rhodamine **28**, and cyanine dyes **29**) to the phosphate backbone, sugar, or base (Figure 12).[89,90] The advantages of these fluorescent probes are that they possess very high molar absorptivities, high fluorescence quantum yields and are significantly photo-stable. However, the major drawback of most of these fluorescent probes is that upon binding or incorporation they significantly perturb the native structure of nucleic acids. Hence, in order to minimize structural perturbations the probe molecule is attached to the oligonucleotide via a long linker.

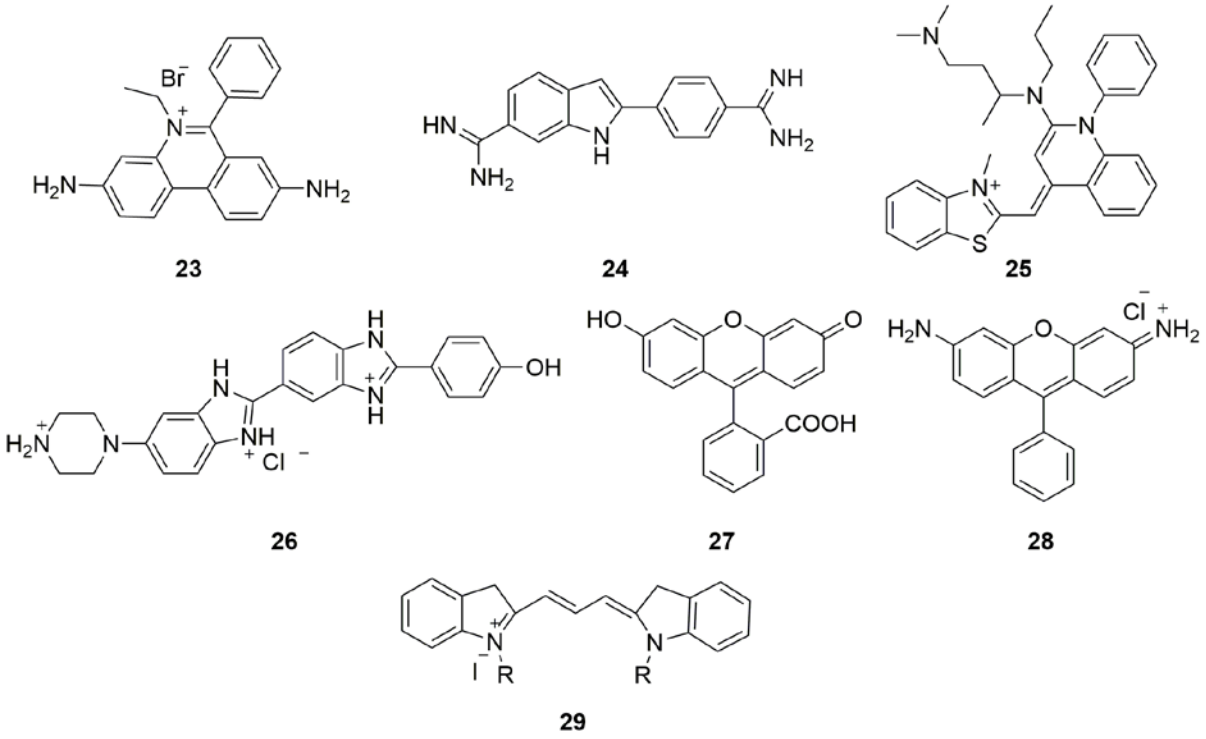

Figure 12. Non-covalent modifications used in nucleic acid analysis.

The conformational changes, which take place during a nucleic acid folding and recognition events occur at both global and nucleotide levels.[4–8] Changes in the conformation of nucleotides (e.g., near the binding site) most often alter their surrounding physical properties due to the interactions with neighbouring bases. Hence, introducing an environment-sensitive reporter molecule near the site of interest and surveying the local conformational changes by fluorescence has been shown to provide a better picture of the interaction under study.[27,28] An important requirement for such probes is that they should minimally perturb the native structure and function of the target nucleic acid. In this regard, base-modified fluorescent nucleoside analogues that are capable of reporting changes in their conformation and surrounding environment in the form of changes in the fluorescence properties such as quantum yield, emission maximum, lifetime, and anisotropy have found wide applications in developing tools to investigate the dynamics, structure, and function of nucleic acids.[29,30] An obvious advantage of several of these analogues is that they closely match the size and Watson-Crick (WC) H-bonding complementarity of the native bases and, hence, can be site-specifically incorporated into target oligonucleotides with minimal structural perturbations.

1.7 Design Strategy and Classification

In literature, several design strategies have been adopted to generate fluorescent nucleoside probes. Fluorescent probes are generated by extending the π conjugation of nucleobase ring system or by using naturally occurring fluorescent heterocycles as base surrogates. Based on the modification and hydrogen-bonding complementarities in comparison to natural nucleobases, base-modified nucleobase analogues are broadly classified into the following categories: (a) size-expanded bases, (b) extended bases, (c) pteridines, (d) polycyclic aromatic hydrocarbon (PAH) base analogues, and (e) isomorphic bases.

(A) ***Size-expanded base analogues:*** Size-expanded base analogues are synthesized by either fusing or inserting aromatic and heterocylic rings to pyrimidine and purine nucleobases. These modifications yield highly fluorescent nucleosides and they mostly maintain H-bonding complementarity of the native bases. In the early 1970's Leonard and co-workers first synthesized etheno-A (εA, **30**) followed by benzo-A.[91,92] Most of the size expanded nucleobases maintain H-bonding complementarity and show better photophysical properties. Later Seela and co-workers synthesized 7-deaza analogue of εA (**31**), which shows better photophysical properties and are stable over wide pH range. Using these probes they studied oligonucleotide denaturation by monitoring the fluorescence emission spectrum.[93] Moreau and co-workers developed naptho-expanded fluorescent nucleosides, BgQ (**32**) and Cf (**33**), which are pH sensitive. Due to their desirable photophysical properties and large surface area, these fluorescent probes were used in the study of double- and triple-stranded oligonucleotides.[94,95] Saito and co-workers have developed a large number of size expanded nucleobase analogues, which photophysically distinguish between the types of base opposite to emissive base. Saito named these analogues as base-discriminating fluorescent (BDF) nucleobases (**34, 35**). He used these emissive nucleobases in the detection of single nucleotide polymorphism (SNPs).[96,97] Matteucci and co-workers synthesized tricyclic cytidine nucleoside analogues phenothiazine (tC, **36**) and phenoxazine (tC^o, **37**), and incorporated them into oligonucleotides to maximize the stacking interaction and hence, the stability of the duplex for antisense applications.[98] Later, Wilhelmsson and co-workers thoroughly characterized the photophysical properties of tC and a phenoxazine-based cytidine analog tC^o in the free nucleoside form and also within oligonucleotides.[99,100] Unlike the majority of nucleoside probes, the quantum efficiencies of these fluorophores upon incorporation into

oligonucleotides are not dramatically reduced. Utilizing this property they could assemble a useful FRET pair using (tC) as the donor and its nitro analog, 7-nitro-1,3-diaza-2-oxophenothiazine (tC_{nitro}), as the acceptor.[101] Subsequently, Sigurdsson group performed a detailed study on the effects of flanking residues on the mismatch-detection abilities of a series of expanded cytidine analogues, tC^o, tC and $Ç^f$ (**38**).[61] They found $Ç^f$ to be superior in identifying all mismatches uniquely, suggesting that it could be utilized in the detection of SNPs. Sasaki and co-workers synthesized tricyclic cytosine derivative, G-clamp (Figure 13, **39**), composed of phenoxazine with an aminoethoxy unit at the end. These G-clamps were utilized in the detection of 8-oxoguanosine.[102] Sekine and co-workers have developed cyclized dC analogues, which maintain the H-bonding face of the parent nucleoside but extend the heterocycle surface by linking the 4 and 5 positions of pyrimidine core. They synthesized dChpp (**40**), dChpd (**41**), and dCmpp (**42**) derivatives, which display good fluorescence solvatochromism.[103]

Pyrrolo-C (pC, **43**), a side product in the Pd-mediated Sonogashira coupling reactions between terminal alkynes and 5-iodo-U, is a moderately emissive isoster of cytidine displaying emission maximum in the visible.[104,105] Initially pC was studied for its antimicrobial activity. Like most other fluorescent nucleoside analogues the quantum efficiency of pC drops significantly upon incorporation into oligonucleotide duplexes. Nevertheless, its non-perturbing nature and sensitivity to changes in its surrounding environment have been appropriately utilized in studying RNA secondary structure, conformational dynamics of 3'-end region of tRNA and thermodynamics of drug-DNA complexes.[106–108] Recently, few pC derivatives with improved fluorescence properties have been reported.[109,110] In particular, phenylpyrrolocytidine (PhpC, **44**) displays high quantum yield (0.31) and a red-shifted excitation and emission maximum (370 nm and 465 nm, respectively) compared to most other nucleoside analogues. [111,112] Hudson and co-workers incorporated PhpC into RNA oligonucleotides and studied the activity of HIV-1 RT ribonuclease H enzyme. A RNA-DNA heteroduplex containing a PhpC residue served as a very good substrate and reported the cleavage activity of RNase H enzyme with a remarkable enhancement in fluorescence intensity.[113] In a similar approach, a siRNA labeled with multiple PhpC residues was used to monitor the trafficking and silencing activity of siRNA inside living cells using fluorescence microscopy.[114] Since PhpC displayed reduction in fluorescence upon incorporation into oligonucleotides, the authors had to use siRNA labeled with at least three PhpC residues for effective fluorescence

monitoring inside the cells. However, the silencing activity by modified siRNA was reduced probably due to structural perturbation caused by multiple modifications.

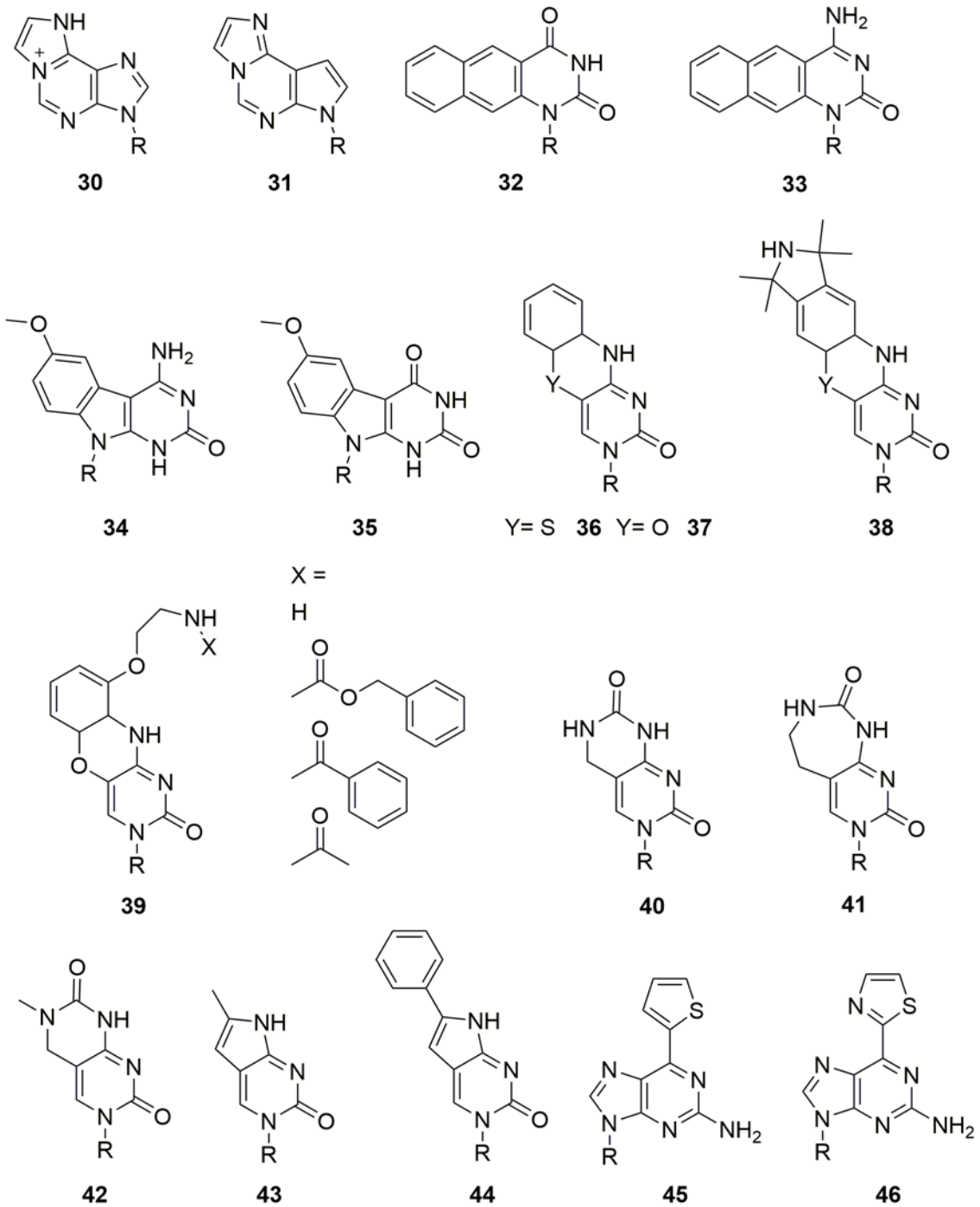

Figure 13. Representative examples of size-expanded fluorescent nucleoside analogues. R = ribose or 2'-deoxyribose.

(B) ***Extended nucleobase analogues:*** Extended fluorescent nucleobase analogues are synthesized by tethering known fluorophores to the nucleobases via a rigid or flexible linker (Figure 14). A number of extended analogues have been developed by attaching fluorescent aromatic systems, such as pyrene (**47**), perylene (**48**), BODIPY (**49**), prodan,

phenanthroline, anthracene, bipyridine, terpyridine, and thiazole orange.[28,115] Oligonucleotides containing such fluorescent tags have been used by numerous groups for variety applications, including detection of SNPs, nucleic acid lesions, and electron transfer process in nucleic acids.[116–120] Netzel and co-workers have attached pyrene at the 5-position of 2′-deoxyuridine directly via amide or ketone linkages and used in studying electron transfer processes in nucleic acids.[121,122] Engels and Zhou's groups have synthesized several 5-benzimidazolyl-2'-deoxyuridine derivatives (**50**), which show emission in the visible region and moderate antibacterial activity.[123,124] Recently, Hocek and co-workers constructed solvatochromic nucleoside analogues by conjugating aminophthalimide (**51**) and GFP-like (**52**) chromophores via an alkyne linker. They enzymatically incorporated the corresponding triphosphates into oligonucleotide reporters, and established fluorescence assays to detect the binding of DNA to p53, an important tumour suppressor protein.[125,126] Kim and co-workers have incorporated piperazinephenyl- (**53**) and pyrene-modified (**54**) pyrimidine and purine nucleosides into DNA oligonucleotides, and have studied their cellular uptake and i-motif formation by fluorescence spectroscopy.[127–129]

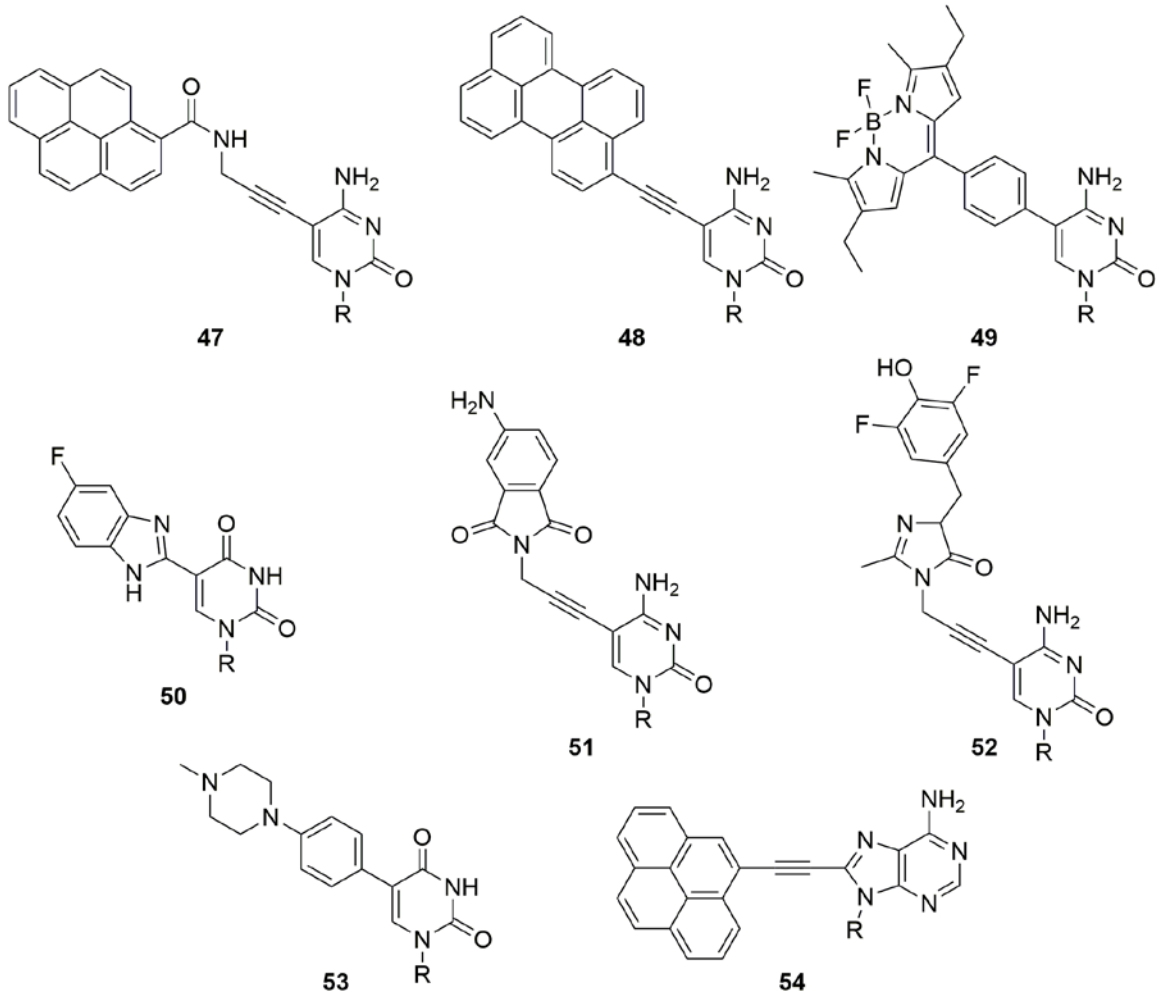

Figure 14. Representative examples of extended fluorescent nucleoside analogues. R = ribose or 2'-deoxyribose.

(C) ***Pteridines:*** Pteridines are naturally occurring planar heterobicyclic aromatic compounds bearing structural resemblance to the natural purines (Figure 15). Hawkins and co-workers were the first to study the usefulness of pteridines as nucleoside surrogates. Her group has developed four pteridines nucleoside analogues, two G analogues (3-MI **55** and 6-MI **56**) and two A-analogues (DMAP **57** and 6-MAP **58**).[130–134] Hermann and co-workers have used fluorescent pteridine analogues 3MI and 6MI, which display higher quantum efficiencies and red-shifted emission maxima, as alternatives to 2-AP to investigate the conformational changes in the bacterial ribosomal decoding site triggered by ligand binding.[135]

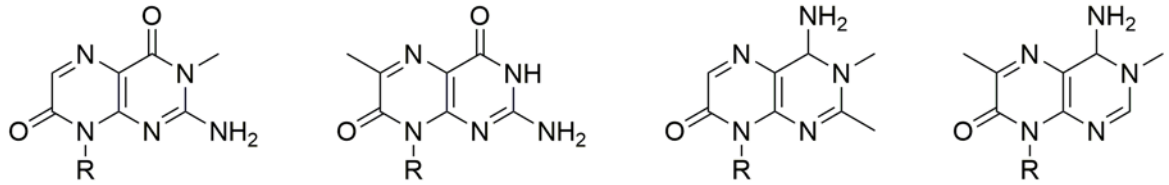

55 56 57 58

Figure 15. Examples of pteridines fluorescent nucleoside analogues. R = ribose or 2'-deoxyribose.

(D) ***Polycyclic aromatic hydrocarbon (PAH) base analogues:*** Kool and co-workers developed a new class of nucleoside analogues in which the bases were replaced with fluorescent PAHs that are highly non-polar and lack WC hydrogen bonding face (Figure 16). These analogues exhibit moderate (Φ = ~0.12) to very high fluorescence quantum efficiency, sometimes approaching unity. While free nucleosides of PAHs such as naphthalene, phenanthrene and pyrene show photophysical properties similar to that of parent fluorophores, incorporation into DNA results in fluorescence quenching due interactions with adjacent bases.[104] Kool and co-workers have used these fluorescent analogues as surrogates to investigate the steric requirement for specific enzyme-substrate interactions. In particular, they demonstrated that a non-hydrogen-bonding pyrene nucleoside triphosphate (dPTP, **59**), having the size and shape of a nucleobase pair could be efficiently and selectively incorporated by DNA polymerases opposite to an abasic site. These experiments ascertained the importance of steric complementarity in maintaining the fidelity of DNA synthesis.[136] Recently, Kool and co-workers have used combinatorial approach to assemble a library of "oligodeoxyfluorosides" containing different PAH fluorophores in a DNA-like chain (**60**-**62**). These polychromophoric oligomers display large Stokes shifts and a broad array of quantum yields and emission wavelengths encompassing the whole visible region.[28,137] These DNA polyfluorophores have been elegantly implemented in diagnostic assays to detect toxic gases and metal ions, and in multiplexed imaging of live cells.[138–140] A PAH base analogue modified with coumarin 102 (**63**) was utilized in pairing with abasic site in DNA.[141] Phenanthrenyl modified PAH analogue (**64**) were used to study electron transfer processes in DNA.[142]

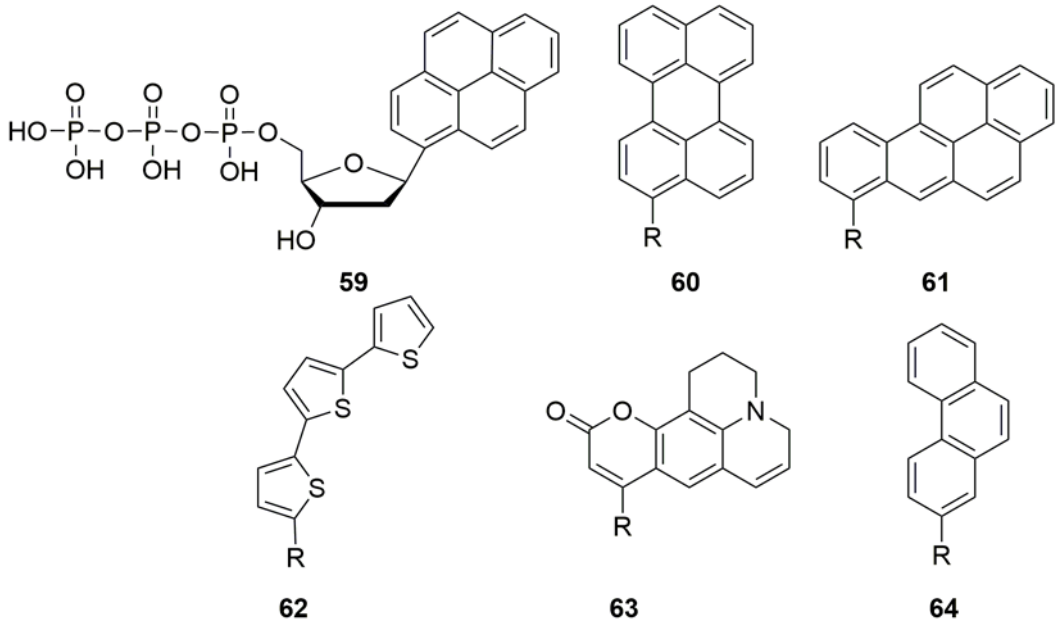

Figure 16. Representative examples of polycyclic aromatic hydrocarbon fluorescent nucleoside analogues. R = ribose or 2'-deoxyribose.

(E) ***Isomorphic bases analogues:*** Most of the above discussed nucleoside analogues structurally deviate from the natural nucleobases significantly, and therefore, isomorphic base analogues have been developed. These base analogues closely resemble natural nucleobases with respect to their overall dimensions, hydrogen bonding patterns, and ability to form isostructural W-C base pairs. Such analogues can be site-specifically incorporated near the point of investigation in a target nucleic acid with minimum structural perturbations and hence, are ideally suited for studying subtle alterations in conformation and dynamics that happen around the site of interest during a folding or recognition process.[29]

2-Aminopurine (2-AP, **65**), a constitutional isomer of adenine, was developed by Stryer and co-workers.[75] It base pairs strongly with thymine and uracil and serves as an adenine analogue in several enzymatic reactions. Because of its nonperturbing nature and exquisite sensitivity to conformational changes, 2-AP is the most widely utilized nucleoside analogues in the study of structure, dynamics and binding properties of nucleic acids.[27–29] Despite 2-AP's wide utility, excitation and emission maxima in the UV region and drastically reduced fluorescence efficiency within oligonucleotides significantly limits its applications, particularly in cell microscopy.[28,143]

Tor group initiated a program to develop structurally minimally perturbing nucleoside analogues with probe-like properties. They synthesized a series of nucleoside analogues by either conjugating or fusing aromatic five-membered heterocycles to

pyrimidine and purine cores (Figure 17).[28] Heterocycles such as furan, thiophene, oxazole, and thiazole were conjugated to purine and pyrimidine bases. Among these furan-conjugated pyrimidines showed favourable fluorescence properties, i.e., emission maxima in the visible region with a reasonable quantum yield and sensitivity to polarity changes.[144] Furan-modified uridine (**66**) and cytidine (**67**) analogues were site-specifically incorporated into model DNA and RNA oligonucleotide, without affecting the native structure. These fluorescent oligonucleotide reporters were effectively employed in the detection of abasic sites and the mutagenic oxidation product of guanosine (8-oxoG), and in the monitoring of RNA-aminoglycoside antibiotics and RNA-protein interactions.[145,146] Despite possessing high quantum yields, furan-conjugated purines were not evaluated further, as they displayed emission maxima in the UV region, and were found to be less sensitive to microenvironment changes as compared to corresponding pyrimidine analogues. They have also synthesized a fused thiophene derivative of uridine (**68**), which displays high quantum yield and excellent fluorescence solvatochromism. It was incorporated into RNA oligonucleotides by both solid phase chemical and enzymatic methods, and was utilized in devising fluorescence hybridization assays to detect mismatches in duplexes and to monitor the formation of RNA abasic sites by the depurination activity of ribosome inactivating protein (RIP) toxins.[147]

Recently, Tor and co-workers assembled new FRET pairs using fluorescent uridine analogues based on 5-methoxyquinazoline-2,4(1*H*,3*H*)-dione (**69**) and 5-aminoquinazoline-2,4(1*H*,3*H*)-dione (**70**), which served as an effective donor for coumarin and acceptor for tryptophan, respectively.[148] Using these FRET systems, fluorescence assays were developed to study the binding of aminoglycoside antibiotics to a model bacterial ribosomal decoding site (A-site) RNA motif and HIV-1 Rev peptide to its cognate RNA target, Rev Responsive Element (RRE). Other recent examples of isomorphic nucleoside analogues from this group include a complete set of highly emissive RNA alphabet derived from thieno[3,4-*d*]-pyrimidine as the heterocyclic core, and pH and polarity-sensitive 6-aza-uridine derivatives.[149,150] The suitability of these analogues in biophysical probing of nucleic acid-related processes is yet to be explored. Wagner and co-workers have recently developed an emissive 5-substituted UDP glucose analogue (**71**), which was designed based on 5-furan-modified uridine developed Tor and co-workers.[151] The fluorescent properties of UDP glucose analogue has been used in monitoring the activity of glycosyltransferase enzyme.

8-vinyl-deoxyadenosine (**72**), an alternative fluorescent probe to 2-AP, prompted Diederichsen and co-workers to develop an isomorphic guanosine analogue (**73)** by tethering a vinyl group at the 8 position of guanine.[152-154] The ability of this emissive and environment-sensitive nucleoside analogue to adopt both *syn* and *anti* conformation was appropriately utilized for studying the different topologies of G-quadruplexes.[153,154]

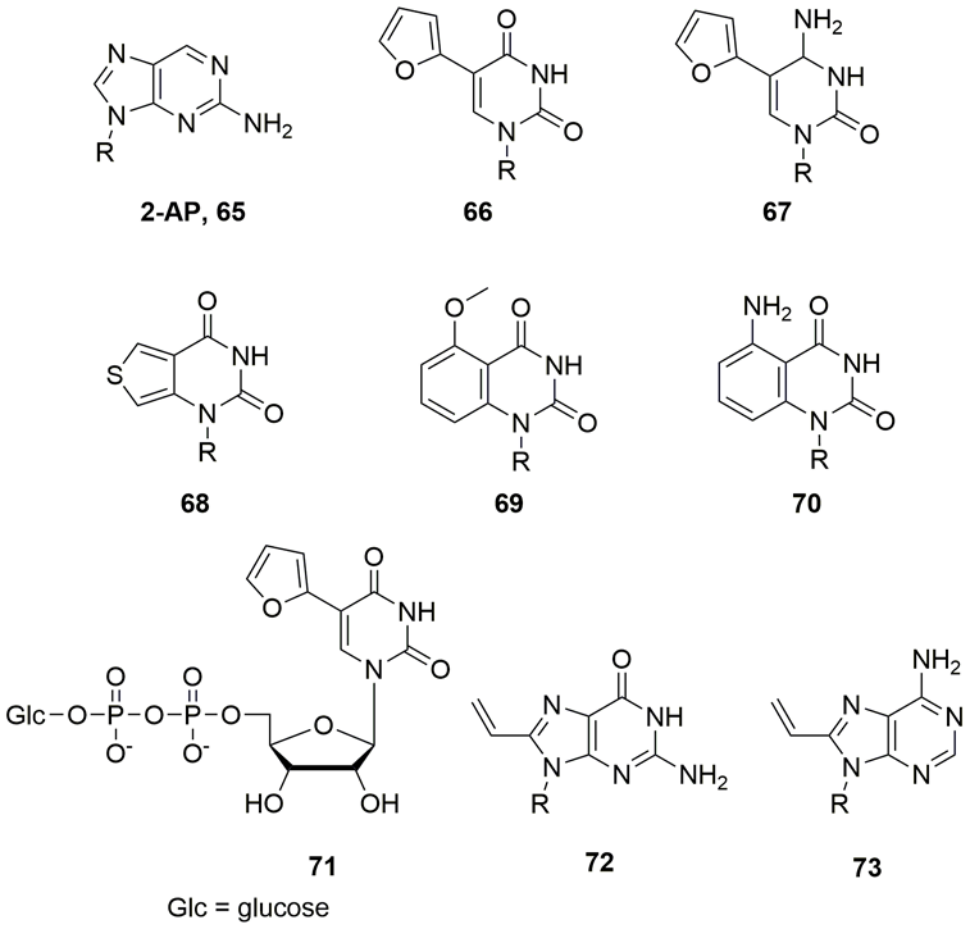

Figure 17. Representative examples of isomorphic fluorescent nucleoside analogues. R = ribose or 2'-deoxyribose.

1.8 Methods to Incorporate Ribonucleoside Analogues into RNA

Fluorescently modified nucleoside can be incorporated into RNA oligonucleotides by using chemical and enzymatic methods.[155,156] Solid-phase oligonucleotide synthesis is the most preferred and versatile method to incorporate modified nucleosides into oligonucleotides. The most significant advantage of this method is that it allows the site-specific labelling of nucleic acids with a variety of functionalities. Solid-phase RNA oligonucleotide synthesis is essentially performed by using the steps developed for solid-phase DNA synthesis. However, RNA synthesis requires additional orthogonal protection

of the 2'-OH group (Figure 18). Currently, there are three commonly used methods, which are being commercially employed to synthesize oligoribonucleotides. Two methods use fluoride-labile *tert*-butyldimethylsilyl (TBDMS) or triisopropylsilyloxymethyl (TOM) protecting group at the 2'-OH position while an acid labile dimethoxytrityl (DMT) is used at the 5'-position.[157–159] The third method uses a cyclododecyloxy-*bis*(trimethylsiloxy)silyl (SIL) protecting group at the 5'-OH position and the 2'-OH is protected with an acid-labile orthoester (ACE) group developed by Scaringe and Caruthers.[160,161] These methods are now being regularly used in synthesizing labeled oligoribonucleotides for bioanalytical and therapeutic applications.[162] However, there are several instances in which the synthesis of modified phosphoramidite substrates is tedious and also many modified phosphoramidite substrates undergo degradation under the chemical conditions employed in the solid-phase synthesis protocols.

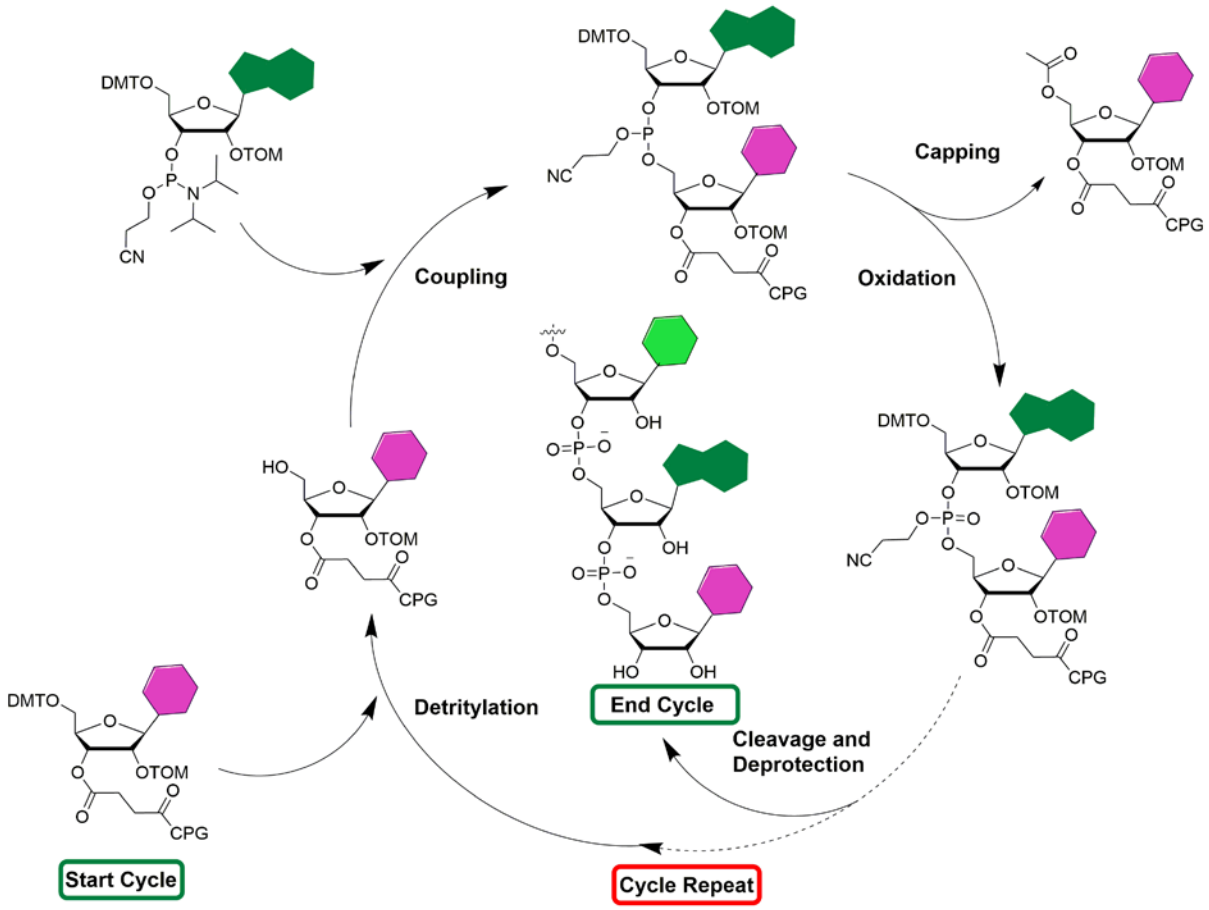

Figure 18. Solid-phase oligoribonucleotide synthesis using phosphoramidite approach.

Alternatively, emissive ribonucleoside can also be incorporated into RNA oligonucleotides by enzymatic methods using RNA polymerases and ligases. Since these methods operate under very mild conditions the modifications can be stably incorporated

into RNA oligonucleotides. The modified triphosphate substrates necessary for *in vitro* transcription reactions can be synthesized from corresponding ribonucleosides by performing a one-pot-two-step reaction in the presence of $POCl_3$ developed by Ludwig.[163] *In vitro* transcription reaction typically requires a promoter-template DNA duplex, RNA polymerase (e.g., T7 RNA polymerase) and NTPs (Figure 19). The promoter-template DNA duplex is assembled by annealing a T7 RNA polymerase consensus DNA promoter sequence to a template DNA sequence, which contains the coding region for the synthesis of complementary RNA. The synthesis of fluorescently modified RNA oligonucleotides by transcription reaction depends on the ability of the enzyme to accept and incorporate the modified triphosphate into growing RNA chain during the transcription reaction. Transcription reactions can be used to produce reasonably large quantities of modified RNA by using small amounts of the triphosphate substrate. Moreover, by simply using different template sequences corresponding modified RNA transcripts can be synthesized. However, the major drawback of this method is that it is difficult to control the site of incorporation and also not all modified triphosphates are effectively incorporated by the enzyme. In this context, Hirao and co-workers have demonstrated site-specific fluorescent labeling of RNA by using an unnatural base pair. The two purine analogues, 2-amino-6-(2-thienyl)purine and 2-amino-6-(2-thiazolyl)purine, are isomorphic fluorescent nucleosides that can be viewed as 2-AP derivatives. **(45** and **46)**[164,165]

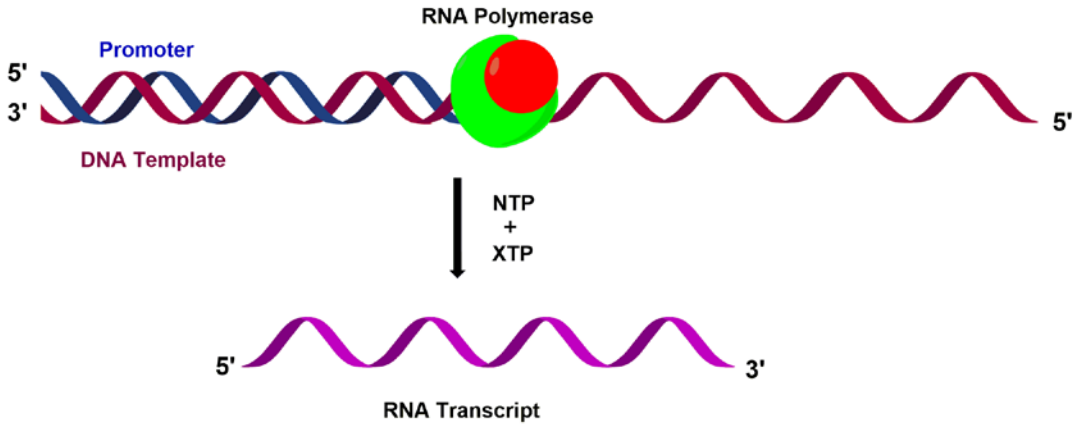

Figure 19. Enzymatic synthesis of modified oligoribonucleotide using DNA template, RNA polymerase modified ribonucleotide triphosphate and natural ribonucleotide triphosphates.

In another method, Micura and co-workers have used both the aspects i.e. chemical synthesis as well as enzymatic synthesis for incorporation of modified nucleosides into riboswitch domain. In order to study the ligand-induced folding of a riboswitch by fluorescence, they site-specifically incorporated 2-AP into the aptamer domain of

adenosine deaminase (*add*) mRNA from *Vibrio vulnificus*. Here, they chemically synthesized 2-AP modified oligonucleotide sequence and ligated it with another oligonucleotide sequence by using T4 RNA or T4 DNA to generate the fluorescent riboswitch construct.[166]

Postsynthetic modification by using chemoselective reactions is emerging as a useful alternative approach for labeling nucleic acids for a variety of applications. In this strategy, a nucleoside analogue containing a small reactive group is introduced into nucleic acid and further modification is achieved by performing a chemoselective reaction on the labeled reactive group.[167,168] Generally, postsynthetic modifications of nucleic acids are performed by using Cu(I) catalysed azide–alkyne cycloaddition (CuAAC), copper-free strain-promoted azide–alkyne cycloaddition (SPAAC) and Staudinger ligation reactions (Figure 20).[169-175] Recently, Luedtke and co-workers used Inverse electron demand Diels-Alder (invDA) for imaging of cellular DNA. For this purpose, they have treated the vinyl substituted deoxy uridine analogue to HeLa cells and stained with a tetramethylrhodamine–tetrazine conjugate.[176] Although these reactions have been used in the labeling of nucleic acids with variety of functionalities, postsynthetic modification to introduce non-perturbing and environment-sensitive fluorescent nucleoside analogues has not been well explored.

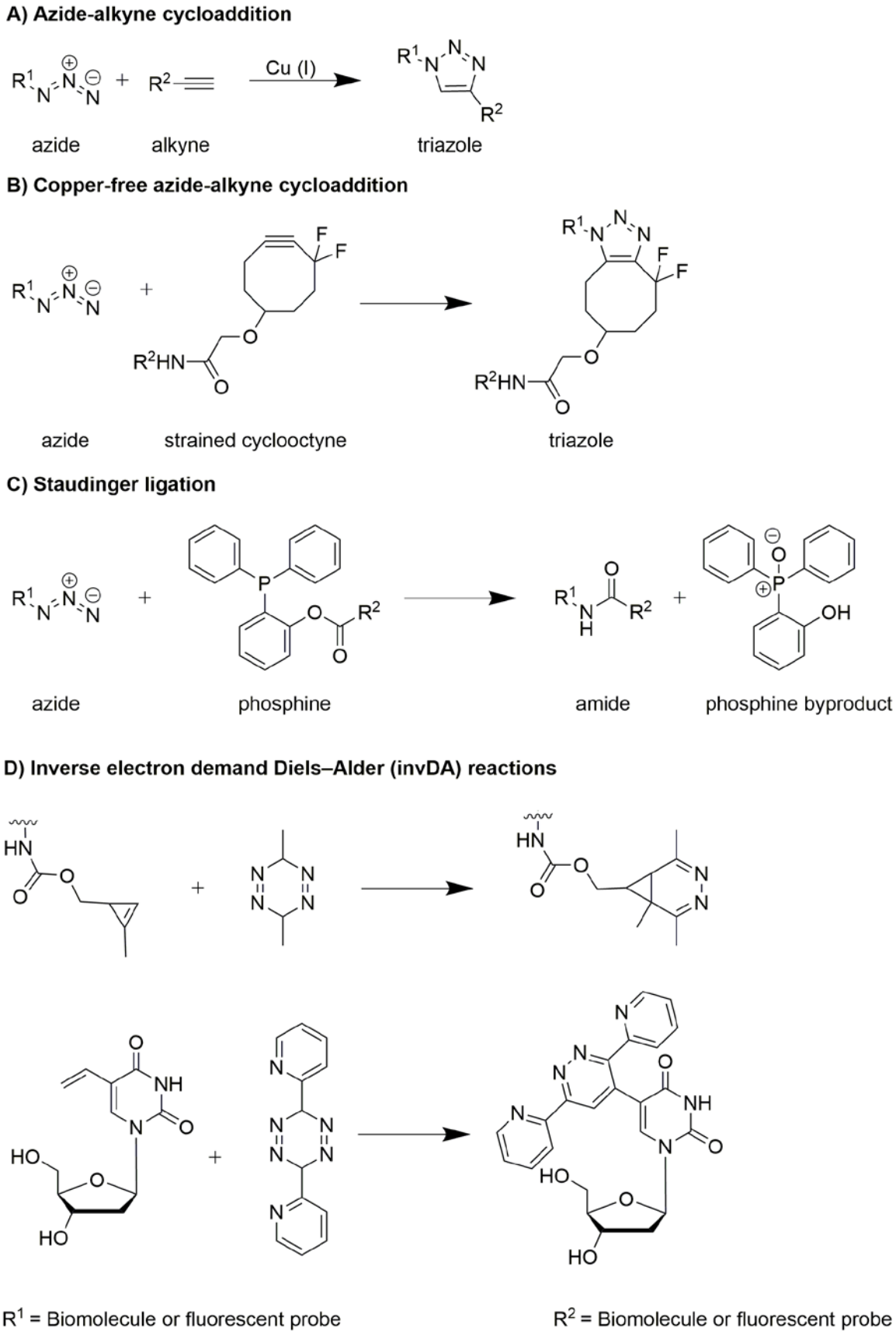

Figure 20. Chemoselective reactions commonly employed in the postsynthetic modifications of nucleic acids.

1.9 Statement of Research Problem

Innumerable examples of fluorescence nucleoside analogues probes with diverse structures and photophysical properties have been developed and implemented in nucleic acid-based diagnosis and in investigating nucleic acid structure, dynamics and function. However, the majority of nucleosides have excitation maximum in the UV region and also exhibit drastically reduced quantum yields when incorporated into oligonucleotides. These shortcomings have essentially precluded their use in certain fluorescence-based methods, for example anisotropy, single-molecule spectroscopy and cell microscopy. With chemists becoming increasing interested in biology and medicine, development of new generation nucleoside analogues with fluorescence properties suitable for nucleic acid analysis *in vitro* and in cells is highly desirable.

Aim: The aim of the research problem was to design and synthesize base-modified nucleoside analogue probes that (i) retain Watson-Crick base pairing ability, (ii) have excitation and emission maximum in the visible region, (iii) have reasonable quantum yield when incorporated into oligonucleotides, and (iv) importantly, report changes in conformation/environment during a nucleic acid folding or recognition process via changes in its photophysical properties such as emission maximum, quantum yield, lifetime and anisotropy.

Based on these criteria and by drawing inspiration from naturally occurring environment-sensitive fluorescent amino acid, tryptophan, two new base-modified fluorescent nucleoside analogues have been developed by conjugating benzothiophene and selenophene moieties at the 5-position of uracil (Figure 21).

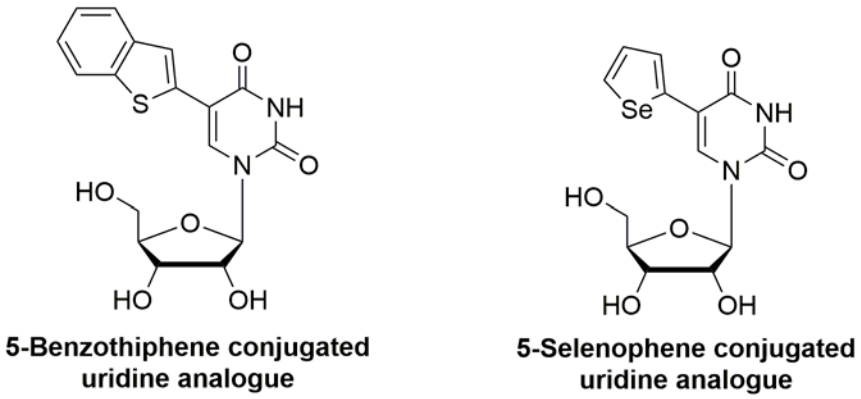

Figure 21. Benzothiophene and selenophene conjugated fluorescent uridine analogues.

Thorough photophysical characterization of 5-benzothiophene conjugated uridine in solvents of different polarity and viscosity adequately bestowed probe-like attributes to the nucleoside. This fluorescent nucleoside was incorporated by *in vitro* transcription reaction in the presence of corresponding triphosphate to generate fluorescently labeled RNA oligonucleotides. Interestingly, incorporation of benzothiophene-modified uridine into RNA oligonucleotide had little impact on the hybridization efficiency. In addition to retaining appreciable fluorescence efficiency within oligonucleotides, the probe, when placed opposite to complementary and mismatched bases, was able to photophysically distinguish between purine and pyrimidine bases. Furthermore, the ability of this nucleoside to sense and report different domains of micelle was utilized in studying oligonucleotide dynamics in a cell-like confined environment using reverse micelle as a membrane model.

The 5-selenophene-modified uridine analogue represents a new class of nucleoside analogues, which has been termed as "double-duty" probe. This analogue could serve as a fluorescence probe as well as an anomalous scattering label (selenium atom) for the phase determination in X-ray crystallography. Hence, could be utilized in studying the properties nucleic acid in solution and in real-time by fluorescence and in solid-state by X-ray crystallography. Such a probe is expected to provide better understanding of the structure-function relationship of nucleic acids. As a proof of responsiveness of this nucleoside, we have developed a fluorescence binding assay to effectively monitor the binding of aminoglycoside antibiotics to the bacterial ribosomal decoding site RNA (A-site). Efforts to incorporate and crystallize selenophene-modified DNA and RNA motifs of biological relevance are currently being pursued in Srivatsan group.

Taken together, easy synthesis, amicability to enzymatic incorporation and sensitivity to changes in neighbouring base environment highlight the potential of these ribonucleoside analogue**s** as efficient fluorescent probes to investigate nucleic acid structure and function.

1.10 References

(1) Nelson, D. L., and Cox, M. M. (2000) *Lehninger Principles of Biochemistry.* 3rd edition. Worth Publishers: New York.

(2) Werstuck, G., and Green, M. R. (1998) Controlling gene expression in living cells through small molecule–RNA interactions. *Science* 296–298.

(3) Tor, Y. (1999) RNA and the small molecule world. *Angew. Chem. Int. Ed. 38*, 1579–1582.

(4) Mandal, M., Breaker. R. R. (2004) Gene regulation by riboswitches. *Nat. Rev. Mol. Cell Biol. 5*, 451−463.

(5) Hermann, T., and Patel, D. J. (2000) RNA bulges as architectural and recognition motifs. *Structure 8*, R47−R54.

(6) Leulliot, N., and Varani, G. (2001) Current topics in RNA Protein recognition: control of specificity and biological function through induced fit and conformational capture. *Biochemistry 40*, 7947−7956.

(7) Hall, K.B. (2008) RNA in motion. *Curr Opin Chem. Biol.*, *12*,612–618.

(8) Al-Hashimi, H. M., and Walter, N. G. (2008) RNA dynamics: it is about time. *Curr. Opin. Struct. Biol. 18*, 321−329.

(9) Walter, N.G. (2009) The blessing and curse of RNA dynamics: past, present, and future. *Methods 49*, 85−86.

(10) Wachowius, F., and Höbartner, C. (2010) Chemical RNA modifications for studies of RNA structure and dynamics. *ChemBioChem 11*, 469–480.

(11) Asseline, U. (2006), Development and applications of fluorescent oligonucleotides. *Curr. Org. Chem. 10*, 491–518.

(12) Srivatsan, S. G., and Famulok, M. (2007) Functional nucleic acids in high throughput screening and drug discovery. *Comb. Chem. High Throughput Screening*, *10*, 698–705.

(13) Shi, X., Herschlag, D. (2009) Fluorescence polarization anisotropy to measure RNA dynamics. *Methods Enzymol. 469*, 287–302.

(14) Juskowiak, B. (2011) Nucleic acid-based fluorescent probes and their analytical potential. *Anal. Bioanal. Chem.*, *399*, 3157–3176.

(15) DeRose, V. J. (2003) Metal ion binding to catalytic RNA molecules. *Curr. Opin. Struct. Biol.* 2003, 13, 317–324.

(16) Piton, N., Mu, Y., Stock, G., Prisner, T.F., Schiemann, O. and Engels, J.W. (2007), Base-specific spin labeling of RNA for structure determination. *Nucl. Acids Res.*, 35, 3128–3143.

(17) Aitken, C. E., Petrov, A., and Puglisi, J. D. (2010) Single ribosome dynamics and the mechanism of translation. *Annu. Rev. Biophys. 39*, 491–513.

(18) Bardaro, M. F., Jr., and Varani, G. (2012) Examining the relationship between RNA function and motion using nuclear magnetic resonance. *WIREs RNA 3*, 122−132.

(19) Nguyen, P., and Qin, P. Z. (2012) RNA dynamics: perspectives from spin labels. *WIREs RNA 3*, 62−72.

(20) Holbrook, S. R. (2008) Structural principles from large RNAs. *Annu. Rev. Biophys. 37*, 445−464.

(21) Serganov, A., and Patel, D. J. (2012) Molecular recognition and function of riboswitches. *Curr. Opin. Struct. Biol. 22*, 279−286.

(22) Xia, T. (2008)Taking femtosecond snapshots of RNA conformational dynamics and complexity. *Curr. Opin. Chem. Biol. 12*, 604–611.

(23) Ha, T. (2004) Structural Dynamics and Processing of Nucleic Acids Revealed by Single-Molecule Spectroscopy. *Biochemistry, 43*, 4055–4063.

(24) Zhao, R., and Rueda, D. (2009) RNA folding dynamics by single-molecule fluorescence resonance energy transfer. *Methods 49*:112–117.

(25) Stimson, S. M. M., and Reuter, S. M. A. (1941) The fluorescence of some purines and pyrimidines. *J. Am. Chem. Soc., 63*,697–699.

(26) Peon, J., and Zewail, A. H. (2001) DNA/RNA nucleotides and nucleosides: direct measurement of excited – state lifetimes by femtosecond fluorescence up-conversion. *Chem. Phys. Lett., 348*, 255–262.

(27) Rist, M. J., and Marino, J. P. (2002) Fluorescent nucleotide base analogues as probes of nucleic acid structure, dynamics and interactions. *Curr. Org. Chem., 6*, 775–793.

(28) Sinkeldam, R. W., Greco, N. J., and Tor, Y (2010) Fluorescent analogs of biomolecular building blocks: Design, properties, and applications. *Chem. Rev., 110*, 2579–2619.

(29) Srivatsan, S. G., and Sawant, A. A. (2011) Fluorescent ribonucleoside analogues as probes for investigating RNA structure and function. *Pure Appl. Chem. 83*, 213–232.

(30) Phelps, K., Morris, A., and Beal, P. A. (2012) Novel modifications in RNA. *ACS Chem. Biol. 7*, 100−109.

(31) Seidel, C. A. M., Schulz, A., and Sauer, M. H. M. (1996) Fluorescence Quenching by Proximal G-bases *J. Phys. Chem., 100*, 5541–5553.

(32) Kawai, M., Lee, M. J., Evans, K. O., and Nordlund, T. M. (2001) Temperature and base sequence dependence of 2-aminopurine fluorescence bands in single- and double-stranded oligodeoxynucleotides. *J. Fluoresc., 11*, 23–32.

(33) Rachofsky, E. L., Osman, R., and Ross, J. B. A. (2001) Probing structure and dynamics of DNA with 2-Aminopurine: Effects of local environment on fluorescence. *Biochemistry, 40*, 946–956.

(34) Blackburn, G. M., and Gait, M. J. (1996) *Nucleic acids in chemistry and biology*; 2nd ed.; Oxford University Press: Oxford, England; New York.

(35) Hoogsteen, K. (1963). The crystal and molecular structure of a hydrogen-bonded complex between 1-methylthymine and 9-methyladenine. *Acta Cryst.16*, 907–916.

(36) Dickerson, R. E., Drew, H. R., Conner, B. N., Wing, R. M., Fratini, A. V., and Kopka, M. L.(1982)The anatomy of A-, B-, and Z-DNA. Science 1982, 215, 475–485

(37) Fire, A., Xu, S., Montgomery, M. K., Kostas, S. A., Driver, S. E., and Mello, C. C. (1998) Potent and specific genetic interference by double-stranded RNA in *Caenorhabditis elegans*. *Nature 391*, 806–811.

(38) Baulcombe, D. (2004) RNA silencing in plants. *Nature 431*, 356–363.

(39) Bartel, D. P. (2009) MicroRNAs: target recognition and regulatory functions**.** *Cell 136*, 215–233.

(40) Carthew, R. W., and Sontheimer, E. J. (2009) Origins and Mechanisms of miRNAs and siRNAs. *Cell* 136, 642–655.

(41) Mocellin, S., Costa, R., and Nitti, D. (2006) RNA interference: ready to silence cancer? *J. Mol. Med.* 84, 4–15.

(42) Aagaard, L., Rossi, J. J. (2007) RNAi therapeutics: principles, prospects and challenges. *Adv. Drug Delivery Rev*. *59*, 75–86.

(43) Mironov, A. S., Gusarov, I., Rafikov, R., Lopez, L. E., Shatalin, K., Kreneva, R. A., Perumov, D. A., and Nudler, E. (2002) Sensing small molecules by nascent RNA: a mechanism to control transcription in bacteria. *Cell 111*, 747–756.

(44) Blount, K. F., and Breaker, R. R. (2006) Riboswitches as antibacterial drug targets. *Nat. Biotechnol. 24*, 1558–1564.

(45) Moazed, D., and Noller, H. F. (1987) Interaction of antibiotics with functional sites in 16S ribosomal RNA. *Nature 327*, 389–394.

(46) Zapp, M. L., Stern, S., Green, M. R. (1993) Small molecules that selectively block RNA binding of HIV-1 rev protein inhibit rev function and viral production. *Cell 74*, 969–978.

(47) Serganov, A., and Patel, D. J. (2007) Ribozymes, riboswitches and beyond: regulation of gene expression without proteins. *Nat. Rev. Genet. 8*, 776–790.

(48) Serganov, A. (2009) The long and the short of riboswitches. *Curr. Opin. Struct. Biol. 19*, 251–259.

(49) Schmeing, T. M., and Ramakrishnan, V. (2009). What recent ribosome structures have revealed about the mechanism of translation. *Nature 461*, 1234–1242.

(50) Ponting, C. P., Oliver, P. L., and Reik, W. (2009) Evolution and functions of long noncoding RNAs. *Cell*, *136*, 629–641.

(51) Qin, P. Z., Dieckmann, T. (2004) Application of NMR and EPR methods to the study of RNA. *Curr. Opin. Struct. Biol.*, *14*, 350–359.

(52) Fürtig, B, Richter, C, Wöhnert, J, and Schwalbe, H. (2003) NMR spectroscopy of RNA. *Chembiochem*. *4*, 936–962.

(53) Schultheisz, H. L., Szymczyna B. R., Scott, L. G. and Williamson, J. R. (2008) Pathway engineered enzymatic *de Novo* purine nucleotide synthesis , *ACS Chem. Biol*. *3*, 499–511.

(54) Wenter, P., and Pitsch, S. (2003) Synthesis of selectively ^{15}N-labeled 2'-O-{[(Triisopropylsilyl)oxy]methyl}(tom)-protected ribonucleoside phosphoramidites and their incorporation into a bistable 32Mer RNA sequence. *Helv. Chim. Acta*, *86*, 3955–3974.

(55) Wenter, P., Bodenhausen, G., Dittmer, J., and Pitsch, S. Kinetics of RNA refolding in dynamic equilibrium by ^{1}H-detected ^{15}N exchange NMR spectroscopy *J. Am. Chem. Soc.*, *128*, 7579–7587.

(56) Suydam, I. T., and. Strobel, S. A (2008) Fluorine substituted adenosines as probes of nucleobase protonation in functional RNAs. *J. Am. Chem. Soc*. *130*, 13639–13648.

(57) Kosutic, M., Jud, L., DaVeiga, C., Frener, M., Fauster, K., Kreutz, C., Ennifar, E., and Micura; R. (2014) Surprising base pairing and structural properties of 2'-Trifluoromethylthio-Modified RNA. *J. Am. Chem. Soc. 136*, 6656–6663.

(58) Sowa, G. Z., and Qin, P. Z. (2008) Site-directed spin labeling studies on nucleic acid structure and dynamics. *Prog. Nucleic Acid Res. Mol. Biol*. 82, 147–197.

(59) Piton, N., Mu, Y., Stock, G., Prisner, T. F., Schiemann, O., and Engels, J. W. (2007) Base-specific spin-labeling of RNA for structure determination. *Nucleic Acids Res.*, *35*, 3128–3143.

(60) Edwards, T. E., Okonogi, T. M., Robinson, B. H., and Sigurdsson, S. T. (2001) Site-specific incorporation of nitroxide spin-labels into internal sites of the TAR RNA; Structure-dependent dynamics of RNA by EPR Spectroscopy. *J. Am. Chem. Soc*, *123*, 1527–1528.

(61) Cekan, P., and Sigurdsson, S. T. (2008) Single base interrogation by a fluorescent nucleotide: each of the four DNA bases identified by fluorescence spectroscopy. *Chem. Commun*. 2008, 3393–3395.

(62) Mooers, B. H. Crystallographic studies of DNA and RNA. (2009) *Methods*, 47, 168–176.

(63) Ennifar, E., Carpentier, P., Ferrer, J.-L., Waltera, P. and Dumas, P. (2002) X-ray-induced debromination of nucleic acids at the Br K absorption edge and implications for MAD phasing. *Acta Cryst. D58*, 1262–1268.

(64) Olieric, V., Rieder, U., Lang, K., Serganov, A., Schulze-Briese, C., Micura, R., Dumas, P., and Ennifar, E. (2009) A fast selenium derivatization strategy for crystallization and phasing of RNA structures. *RNA*, *15*, 707–715.

(65) Du, Q., Carrasco, N., Teplova, M., Wilds, C. J., Egli, M., and Huang, Z. (2002) Internal derivatization of oligonucleotides with selenium for X-ray crystallography using MAD. *J. Am. Chem. Soc*, *124*. 24–25.

(66) Höbartner, C., Rieder, R., Kreutz, C., Puffer, B., Lang, K., Polonskaia, A., Serganov, A., and Micura, R. (2005) Syntheses of RNAs with up to 100 nucleotides containing site-specific 2′-methylseleno labels for use in X-ray crystallography. *J. Am. Chem. Soc.*, *127*, 12035–12045.

(67) Höbartner, C., and Micura, R. (2004).Chemical synthesis of selenium-modified oligoribonucleotides and their enzymatic ligation leading to an U6 SnRNA Stem-Loop segment. *J. Am. Chem. Soc*., *126*, 1141–1149.

(68) Salon, J., Sheng, J., Jiang, J., Chen, G., Caton-Williams, J., and Huang, Z. (2007) Oxygen replacement with selenium at the thymidine 4-Position for the Se base pairing and crystal structure studies. *J. Am. Chem. Soc. 129*, 4862–4863.

(69) Salon, J., Jiang, J., Sheng, J., Gerlits, O. O., and Huang, Z. (2008) Derivatization of DNAs with selenium at 6-position of guanine for function and crystal structure studies. *Nucleic Acids Res*., *36*, 7009–7018.

(70) Bevilacqua, P. C., and Turner, D. H. (2002) Use of fluorescence spectroscopy to elucidate RNA folding pathways. *Curr. Protoc. Nucleic Acid Chem*.,Unit 11.8.

(71) Walter, N. G. (2003) Probing RNA structural dynamics and function by fluorescence resonance energy transfer (FRET*). Curr. Protoc. Nucleic Acid Chem*., Unit 11.10

(72) Zhao, R., and Rueda, D. (2009) RNA folding dynamics by single-molecule fluorescence resonance energy transfer. *Methods 49*:112–117.

(73) Zhao, L., and Xia, T. (2009) Probing RNA conformational dynamics and heterogeneity using femtosecond time-resolved fluorescence spectroscopy. *Methods, 49*, 128–135.

(74) Lakowicz. J. R. (2006) *Principles of Fluorescence Spectroscopy*, 3rd ed., Springer, New York.

(75) Ward, D. C., Reich, E., and Stryer, L. (1969) Fluorescence studies of nucleotides and polynucleotides: Formycin, 2-aminopurine riboside, 2, 6-diaminopurine riboside, and their derivatives. *J. Biol. Chem. 244*, 1228–1237.

(76) Rist, M. J., and Marino, J. P. (2002) Fluorescent nucleotide base analogs as probes of nucleic acid structure, dynamics and interactions. *Curr. Org. Chem. 6*, 775–793.

(77) Hawkins, M. E. (2003) *In Topics in Fluorescence Spectroscopy, DNA Technology, 7*, J. R. Lakowicz (Ed.), Kluwer Academic/Plenum Publishers, New York.

(78) Li, P. T. X., Vieregg, J., and Tinoco, I. (2008) How RNA Unfolds and Refolds *Annu. Rev. Biochem.*, *77*, 77–100.

(79) Jameson, D. M., and Ross, J. A. (2010) Fluorescence Polarization/Anisotropy in Diagnostics and Imaging. *Chem. Rev., 110*, 2685–2708.

(80) Xu, H. Q., Zhang, A. H., Auclair, C. and Xi, X. G. (2003) Simultaneously monitoring DNA binding and helicase-catalyzed DNA unwinding by fluorescence polarization. *Nucl. Acids Res., 14*, e70.

(81) Zhu, Z., Ravelet, C., Perrier, S., Guieu, V., Fiore, E., and Peyrin, E. (2012)Single-stranded DNA binding protein-assisted fluorescence polarization aptamer assay for detection of small molecules. *Anal. Chem*. *84*, 7203−7211.

(82) Guest, C. R., Hochstrasser, R. A., Sowers, L. C. and Millar, D. P. (1991) Dynamics of Mismatched Base Pairs in DNA. *Biochemistry 30*, 3271−3279.

(83) Nordlund, T. M., Andersson, S., Nilsson, L., Rigler, R., Gräslund, A., and McLaughlin, L. W. (1989) Structure and dynamics of a fluorescent DNA oligomer containing the EcoRI recognition sequence: fluorescence, molecular dynamics, and NMR studies. *Biochemistry 28*, 9095−9103.

(84) Angerer, L. M., Georghiou, S., and Moudrianakis, E. N. (1974) Studies on the structure of deoxyribonucleoproteins. Spectroscopic characterization of the ethidium bromide binding sites. *Biochemistry*, *13*, 1075–1082.

(85) Lawrence, J. J., Louis. M. (1974) Ethidium bromide as a probe of chromatin structure**.** *FEBS Lett.*, *40*, 9–12.

(86) Russell, W. C., Newman, C., and Williamson, D. H. (1975) A simple cytochemical technique for demonstration of DNA in cells infected with mycoplasmas and viruses. *Nature 253*, 461–462.

(87) Zipper, H., Brunner, H., Bernhagen, J., and Vitzthum, F. (2004). Investigations on DNA intercalation and surface binding by SYBR Green I, its structure determination and methodological implications. *Nucleic Acids Research 32*, e103.

(88) Latt, S. A., Stetten, G., Juergens, L. A.; Willard, H. F., and Scher, C. D. (1975) Recent developments in the detection of deoxyribonucleic acid synthesis by 33258 Hoechst fluorescence. *The journal of histochemistry and cytochemistry: official journal of the Histochemistry Society 23*, 493–505.

(89) Ranasinghe, R. T. and Brown, T. (2005) Fluorescence based strategies for genetic analysis. *Chem. Commun.* (Cambridge, U.K.) 5487–5502.

(90) Marti, A. A., Jockusch, S., Stevens, N., Ju, J., and Turro, N. J. (2007) Fluorescent hybridization probes for sensitive and selective DNA and RNA detection. *Acc. Chem. Res*., *40*, 402 –409.

(91) Secrist III, J. A., Barrio, J. R., Leonard, N. J., and Weber, G. (1972) Fluorescent modification of adenosine-containing coenzymes. Biological activities and spectroscopic properties. *Biochemistry 11*, 3499–3506.

(92) Scopes, D. I. C.; Barrio, J. R.; and Leonard, N. J. (1977) Defined dimensional changes in enzyme cofactors: fluorescent "stretched-out" analogs of adenine nucleotides. *Science*, *195*, 296–298.

(93) Seela, F., Schweinberger, E., Xu, K. Y., Sirivolu, V. R., Rosemeyer, H., and Becker, E. M. (2007) 1,N^6-Etheno-2'-deoxytubercidin and pyrrolo-C: synthesis, base pairing, and fluorescence properties of 7-deazapurine nucleosides and oligonucleotides. *Tetrahedron 63*, 3471–3482.

(94) Godde, F.; Toulmé, J. J., and Moreau, S. (1998) Benzoquinazoline derivatives as substitutes for thymine in nucleic acid complexes. Use of fluorescence emission of

benzo[g]quinazoline-2,4-(1H,3H)-dione in probing duplex and triplex formation. *Biochemistry 37*, 13765–13775.

(95) Godde, F., Toulmé, J. J., and Moreau, S. (2000) 4-amino-1 H-benzo[g] quninazoline-2-one: a fluorescent analog of cytosine to probe protonation sites in triplex forming oligonucleotides. *Nucleic Acids Res. 28*, 2977–2985.

(96) Okamoto, A., Tainaka, K., Fukuta, T., and Saito, I. (2003) Clear distinction of purine bases on the complementary strand by a fluorescence change of a novel fluorescent nucleoside. *J. Am. Chem. Soc. 125*, 9296–9297.

(97) Okamoto, A., Saito, Y., and Saito, J. (2005) Design of base-discriminating fluorescent nucleosides. *Photochem. Photobiol., C, 6*, 108–122.

(98) Lin, K. Y., Jones, R. J., and Matteucci, M. (1995) Tricyclic 2'-deoxycytidine analogs: syntheses and incorporation into oligodeoxynucleotides which have enhanced binding to complementary RNA. *J. Am. Chem. Soc. 117*, 3873–3874.

(99) Wilhelmsson, L. M., Holmen, A., Lincoln, P., Nielsen, P. E., and Norden, B. (2001) A Highly Fluorescent DNA Base Analogue that Forms Watson−Crick Base Pairs with Guanine. *J. Am. Chem. Soc. 123*, 2434–2435.

(100) Sandin, P., Borjesson, K., Li, H., Martensson, J., Brown, T., Wilhelmsson, L. M., Albinsson, B. (2008) Characterization and use of an unprecedentedly bright and structurally non-perturbing fluorescent DNA base analogue. *Nucleic Acids Res. 36*, 157–167.

(101) Borjesson, K., Preus, S., El-Sagheer, A. H., Brown, T., Albinsson, B., and Wilhelmsson, L. M. (2009) Nucleic acid base analog FRET-pair facilitating detailed structural measurements in nucleic acid containing systems. *J. Am. Chem. Soc.*, 131, 4288–4293.

(102) Nakagawa, O., Ono, S., Li, Z., Tsujimoto, A., and Sasaki, S. (2007) Specific fluorescent probe for 8-oxoguanosine. *Angew.Chem., Int. Ed. 46*, 4500–4503.

(103) Miyata, K., Mineo, R., Tamamushi, R., Mizuta, M., Ohkubo, A., Taguchi, H., Seio, K., Santa, T., and Sekine, M. (2007) Synthesis and fluorescent properties of Bi- and Tricyclic 4-N-carbamoyldeoxycytidine derivatives. *J. Org. Chem. 72*, 102−108.

(104) Crisp, G. T., and Flynn, B. L. (1993) Palladium-catalyzed coupling of terminal alkynes with 5-(trifluoromethanesu1fonyloxy)pyrimidine nucleosides. *J. Org. Chem., 58*, 6614–6619.

(105) Robins, M. J., and Barr, P. J. (1983) Nucleic acid related compounds. 39. Efficient conversion of 5-Iodo to 5-alkynyl and derived 5-substituted uracil bases and nucleosides. *J. Org. Chem. 48*, 1854–1862.

(106) Tinsley, R. A., and Walter, N. G. (2006) Pyrrolo-C as a fluorescent probe for monitoring RNA secondary structure formation.*RNA 12*, 522–529.

(107) Zhang, C.-M., Liu, C., Christian, T., Gamper, H., Rozenski, J., Pan, D., Randolph, J. B., Wickstrom, E., Cooperman, B. S., and Hou, Y.-M. (2008) 2253Pyrrolo-C as a molecular probe for monitoring conformations of the tRNA 3′ end. *RNA, 14*, 2245–2253.

(108) Zhang, X., and Wadkins, R. M. (2009) DNA hairpins containing the cytidine analog Pyrrolo-dC: Structural, thermodynamic, and spectroscopic studies. *Biophys. J., 96*, 1884–1891.

(109) Hudson, R. H. E., and Choghamarani, A. G. (2007) An improved 6-substituted pyrrolocytosine for selective fluorimetric detection of guanosine-containing sequences. *Nucleosides, Nucleotides, Nucleic Acids, 26*, 533–537.

(110) Noe, M. S., Rios, A.C., and Tor, Y. (2012) Design, synthesis, and spectroscopic properties of extended and fused pyrrolo-dC and pyrrolo-C analogs. *Org. Lett.14*, 3150–3153.

(111) Ming, X., and Seela, F. (2012) A nucleobase-discriminating pyrrolo-dC click adduct designed for DNA fluorescence mismatch sensing. *Chem. Eur. J., 18*, 9590–9600.

(112) Ming, X., Ding, P., Leonard, P., Budow, S., and Seela, F. (2012) Parallel-stranded DNA: enhancing duplex stability by the ‘G-clamp’ and a pyrrolo-dC derivative. *Org. Biomol. Chem. 10*, 1861–1869.

(113) Wahba, A. S., Esmaeili, A., Damha, M. J., and Hudson, R. H. E., (2010) A single-label phenylpyrrolocytidine provides a molecular beacon-like response reporting HIV-1 RT RNase H activity. *Nucleic Acids Res. 38*, 1048–1056.

(114) Wahba, A. S., Azizi, F., Deleavey, G. F., Brown, C., Robert, F., Carrier, M., Kalota, A., Gewirtz, A. M., Pelletier, J., Hudson, R. H. E., and Damha, M. J. (2011) Phenylpyrrolocytosine as an Unobtrusive Base Modification for Monitoring Activity and Cellular Trafficking of siRNA. *ACS Chem. Biol. 6*, 912–919.

(115) Wilson, J. N., and Kool, E. T. (2006) Fluorescent DNA base replacements: reporters and sensors for biological systems. *Org. Biomol. Chem. 4*, 4265–4274.

(116) Tainaka, K., Tanaka, K., Ikeda, S., Nishiza, K.-I., Unzai, T., Fujiwara, Y., Saito, I., and Okamoto, A. (2007) PRODAN-Conjugated DNA: Synthesis and Photochemical Properties. *J. Am. Chem. Soc. 129*, 4776–4784.

(117) Saito, Y., Motegi, K., Bag, S. S., and Saito, I. (2008) Anthracene based base-discriminating fluorescent oligonucleotide probes for SNPs typing: Synthesis and photophysical properties. *Bioorg. Med. Chem. 16*, 107–113.

(118) Grigorenko, N. A., and Leumann, C. J. (2008) Electron transfer through a stable phenanthrenyl pair in DNA. *Chem. Commun*. (Cambridge, U.K.) 5417–5419.

(119) Ehrenschwender, T., and Wagenknecht, H.-A. (2011) 4,4-Difluoro-4-bora-3a,4a-diaza-s-indacene as a bright fluorescent label for DNA. *J. Org. Chem*., 76, 2301–2304.

(120) Okamoto, A., Sugizaki, K., Yuki, M., Yanagisawa, H., Ikeda, S., Sueoka, T., Hayashi, G., and Wang, D. O. (2013) A nucleic acid probe labeled with desmethyl thiazole orange: a new type of hybridization-sensitive fluorescent oligonucleotide for live-cell RNA imaging. *Org. Biomol.Chem*., *11*, 363–371.

(121) Kerr, C. E., Mitchell, C. D., Headrick, J., Eaton, B. E., and Netzel, T. L. (2000) Synthesis and photophysics of a 1-pyrenyl substituted 2'-deoxyuridine-5-carboxamidenucleoside: electron transfer products as CIS INDO/S excited states. *J. Phys. Chem. B 104*, 1637−1650.

(122) Netzel, T. L., Zhao, M., Nafisi, K., Headrick, J., Sigman, M. S., and Eaton, B. E. (1995) Photophysics of 2'-deoxyuridine (dU) nucleosides covalently substituted with either 1 -pyrenyl or 1 -pyrenoyl:observation of pyrene-to-nucleoside charge-transfer emission in 5-(1-Pyreny1)-dU. *J. Am. Chem. Soc. 117*, 9119–9128.

(123) Krim, J., Grinewald, C., Taourirte, M., and Engels. J. C. (2012) Efficient microwave-assisted synthesis, antibacterial activity and high fluorescence of 5-benzimidazolyl-2'-deoxyuridines. *Bioorg. Med. Chem. 20*, 480–486.

(124) Guo, P., Xu, X., Qiu, X., Zhou, Y., Yan, S., Wang, C., Lu, C., Ma, W., Weng, X., Zhang, X., and Zhou, X. (2013) Synthesis and spectroscopic properties of fluorescent 5-benzimidazolyl-2′-deoxyuridines 5-fdU probes obtained from o-phenylenediamine derivatives. *Org. Biomol. Chem. 11*, 1610–1613.

(125) Riedl, J., Pohl, R., Ernsting, N. P., Orság, P., Fojta, M., and Hocek, M. (2012) Labelling of nucleosides and oligonucleotides by solvatochromic 4-

aminophthalimide fluorophore for studying DNA−protein interactions. *Chem. Sci. 3*, 2797−2806.

(126) Riedl, J., Menova, P., Pohl, R., Orsag, P., Fojtac, and Hocek, M. (2012) GFP-like fluorophores as DNA labels for studying DNA−Protein interactions. *J. Org. Chem., 77*, 8287–8293.

(127) Venkatesan, N., Seo, Y. J., Bang, E. K., Park, S. M., Lee, Y. S., and Kim, B. H. Chemical Modification of Nucleic Acids toward Functional Nucleic Acid Systems. (2006) *Bull. Korean Chem. Soc. 27*, 613–630.

(128) Lee, II J., Kim, B. H. (2012) Monitoring i-motif transitions through the exciplex emission of a fluorescent probe incorporating two ^{Py}A units. *Chem. Commun, 48*, 2074–2076.

(129) Park, S. M., Nam, S.-J., Jeong, H. S., Kim, W. J., and Kim, B. H. (2011) The Effects of the 4-(4-Methylpiperazine)phenyl Group on Nucleosides and Oligonucleotides: Cellular Delivery, Detection, and Stability. *Chem.–Asian J. 6*, 487–492.

(130) Hawkins, M. E., Brand, L., and Michael, L. J. (2008) Fluorescent pteridine probes for nucleic acid analysis. *Methods Enzymol. 450*, 201–231.

(131) Hawkins, M. E. (2001) Fluorescent pteridine nucleoside analogs: a window on DNA interactions. *Cell. Biochem. Biophys., 34*, 257–281

(132) Hawkins, M. E., Pfleiderer, W., Mazumder, A., Pommier, Y. G., and Falls, F. M. (1995) Incorporation of a fluorescent guanosine analog into olignoucleotides and its application to a real time assay for the HIV-1 integrase 3′-Processing reaction. *Nucleic Acids Res. 23*, 2872–2880.

(133) Hawkins, M. E., Pfleiderer, W., Jungmann, O., and Balis, F. M. (2001) Synthesis and fluorescence characterization of pteridine adenosine nucleoside analogs for DNA incorporation. *Anal. Biochem. 298*, 231–240.

(134) Hawkins, M. E., Pfleiderer, W., Balis, F. M., Porter, D., and Knutson, J. R. (1997) Fluorescence properties of pteridine nucleoside analogs as monomers and incorporated into oligonucleotides. *Anal. Biochem 244*, 86–95.

(135) Parsons, J., and Hermann, T. (2007) Conformational flexibility of ribosomal decoding-site RNA monitored by fluorescent pteridine base analogues. *Tetrahedron 63*, 3548–3552.

(136) Matray, T. J., and Kool, E. T. (1999) A specific partner for abasic damage in DNA. *Nature 399*, 704–708.

(137) Teo, Y. N. and Kool, E. T. (2012) DNA-Multichromophore Systems. *Chem. Rev., 112*, 4221−4245.

(138) Koo, C.-K., Samain, F., Dai, N., and Kool, E. T. (2011) DNA-polyfluorophore chemosensors for environmentalremediation: vapor-phase identification of petroleum products in contaminated soil. *Chem. Sci.*, *2*, 1910–1917.

(139) Tan, S. S., Kim, S. J., and E. T. Kool, (2011) Differentiating between fluorescence-quenching metal ions with polyfluorophore sensors built on a DNA Backbone. *J. Am. Chem. Soc*., *133*, 2664–2671.

(140) Guo, J., Wang, S., Dai, N., Teo, Y. N., and Kool, E. T. (2011) Multispectral labeling of antibodies with polyfluorophores on a DNA backbone and application in cellular imaging. *Proc. Natl. Acad. Sci. U. S. A. 108*, 3493–3498.

(141) Coleman, R. S., and Madaras, M. L. (1998) Synthesis of a novel coumarin C-riboside as a photophysical probe of oligonucleotide dynamics. *J. Org. Chem. 63*, 5700–5703.

(142) Grigorenko, N. A.; and Leumann, C. J. (2008) Electron transfer through a stable phenanthrenyl pair in DNA. *Chem. Commun. 42*, 5417–5419.

(143) Kawai, M., Lee, M. J., Evans, K. O., and Nordlund, T. M. (2001) Temperature and base sequence dependence of 2-aminopurine fluorescence bands in single- and double-stranded oligodeoxynucleotides. *J. Fluoresc., 11*, 23–32.

(144) Greco, N. J., and Tor, Y. (2005) Simple fluorescent pyrimidine analogues detect the presence of DNA abasic sites. *J. Am. Chem. Soc.*, *127*, 10784–10785.

(145) Srivatsan, S. G., and Tor, Y. (2007) Fluorescent pyrimidine ribonucleotide: synthesis, enzymatic incorporation, and utilization. *J. Am. Chem. Soc. 129*, 2044−2053.

(146) Srivatsan, S. G., and Tor, Y. (2007) Using an emissive uridine analogue for assembling fluorescent HIV-1 TAR constructs. *Tetrahedron 63*, 3601–3607.

(147) Srivatsan, S. G., Greco, N. J., and Tor, Y. (2008) A highly emissive fluorescent nucleoside that signals the activity of toxic ribosome-inactivation proteins. *Angew. Chem., Int. Ed., 47*, 6661–6665.

(148) Xie, Y., Dix, A. V., and Tor, Y. (2009) Fluorescent ribonucleoside as a FRET acceptor for tryptophan in native proteins. *J. Am. Chem. Soc. 131*, 17605–17614.

(149) Shin, D., Sinkeldam, R. W., and Tor, Y. (2011) Emissive RNA Alphabet. *J. Am. Chem. Soc.133,* 14912–14915.

(150) Sinkeldam, R.W., Hopkins, P.A., and Tor, Y. (2012) Modified 6-Aza uridines: Highly emissive pH-sensitive fluorescent nucleosides. *ChemPhysChem 13,* 3350–3356.

(151) Pesnot, T. and Wagner, G. K. (2008) Novel derivatives of UDP-glucose: Concise synthesis and fluorescent properties. *Org. Biomol. Chem. 6,* 2884–2891.

(152) Gaied, N. B., Glasser, N., Ramalanjaona, N., Beltz, H., Wolff, P., Marquet, R., Burger, A., and Mely, Y. (2005) 8-vinyl-deoxyadenosine, an alternative fluorescent nucleoside analog to 2′-deoxyribosyl-2-aminopurine with improved properties. *Nucleic Acids Res. 33,* 1031–1039.

(153) Nadler, A., Strohmeier, J., and Diederichsen, U. (2011) 8-Vinyl-2'-deoxyguanosine as Fluorescent 2'-Deoxyguanosine Mimic for Investigating DNA Hybridization and Topology. *Angew. Chem.Int. Ed. 50,* 5392–5396.

(154) Holzberger, B., Strohmeier, J., Siegmund, V., Diederichsen, U., and Marx, A. (2012) Enzymatic synthesis of 8-vinyl- and 8-styryl-2'-deoxyguanosine modified DNA - novel fluorescent molecular probes. *Bioorg. Med. Chem. Lett. 22,* 3136–3139.

(155) Goodchild, J. (1990) Conjugates of oligonucleotides and modified oligonucleotides: a review of their synthesis and properties. *Bioconjugate Chem. 1,* 165–187.

(156) Verma, S., and Eckstein, F. (1998) Modified oligonucleotides: Synthesis and strategy for users. *Annu. Rev. Biochem. 67,* 99–134.

(157) Gait, M. J. (1984) *Oligonucleotide Synthesis: A Practical Approach*; Oxford University Press: Washington DC.

(158) Pitsch, S., Weiss, P. A., Jenny, L., Stutz, A., Wu, X. L. (2001) Reliable chemical synthesis of oligoribonucleotides (RNA) with 2′-*O*-[(Triisopropylsilyl)oxy]methyl(2′-*O*-tom)-protected phosphoramidites. *Helv. Chim. Acta 84,* 3773–3795.

(159) Micura, R. (2002) Small interfering RNAs and their chemical synthesis. *Angew. Chem., Int. Ed. 41,* 2265–2269.

(160) Scaringe, S. A., Wincott, F. E., and Caruthers, M. H. (1998) Novel RNA synthesis method using 5'-silyl-2'-orthoester protecting groups. *J. Am. Chem. Soc. 120,* 11820– 11821

(161) Scaringe. S. A. (2001) RNA oligonucleotide synthesis via 5'-silyl-2'-orthoester chemistry. *Methods 23*, 206–217.

(162) Marshall, W. S., and Kaiser, R. J. (2004) Recent advances in the high-speed solid phase synthesis of RNA. *Curr. Opin. Chem. Biol*. *8*, 222–229.

(163) Ludwig, J. A new route to nucleoside 5'-triphosphates. (1981) *Acta Biochim. Biophys. Acad. Sci. Hung. 16*, 131–133.

(164) Hirao, I., Harada, Y., Kimoto, M., Mitsui, T., Fujiwara, T., and Yokoyama, S. A. (2004) A two-unnatural-base-pair system toward the expansion of the genetic code**.** *J. Am. Chem. Soc. 126*, 13298–13305.

(165) Mitsui,T., Kimoto, M., Harada, Y., Yokoyama, S., and Hirao, I. (2005) An efficient unnatural base pair for a base-pair-expanded transcription system. *J. Am. Chem. Soc. 127*, 8652–8658.

(166) Rieder, R., Lang, K., Graber, D., and Micura, R. (2007) Ligand-induced folding of the adenosine deaminase A-riboswitch and implications on riboswitch translational control. *ChemBioChem 8*, 896–902.

(167) Agard, N. J., Prescher, J. A., and Bertozzi, C. R. (2004) A strain promoted [3+2] azide-alkyne cycloaddition for covalent modification of biomolecules in living systems. *J. Am. Soc. 126*, 15046–15047.

(168) Kohn, M., and Breinbauer, R. (2004) The Staudinger ligation: A gift to chemical biology. *Angew. Chem., Int. Ed 43*, 3106–3116.

(169) Salic, A., and Mitchison, T. J. (2008) A chemical method for fast and sensitive detection of DNA synthesis *in vivo*. *Proc. Natl. Acad. Sci. U.S.A. 105***,** 2415−2420.

(170) Jao, C. Y., and Salic, A. (2008) Exploring RNA transcription and turnover *in vivo* by using click chemistry. *Proc. Natl. Acad. Sci. U.S.A. 105*, 15779−15784.

(171) Weisbrod, S. H., and Marx, A. (2007) A nucleoside triphosphate for site-specific labelling of DNA by the Staudinger ligation. *Chem. Commun*. 1828−1830.

(172) Gramlich, P. M. E. Wirges, C. T. Manetto, A. and Carell, T. (2008) Postsynthetic DNA modification through the copper-catalyzed azide–alkyne cycloaddition reaction. *Angew. Chem. In. Ed*. **47,** 8350−8358.

(173) Jayaprakash, K. N., Peng, C. G., Butler, D., Varghese, J. P., Maier, M. A., Rajeev, K. G., and Manoharan, M. (2010) Non-Nucleoside Building Blocks forCopper-Assisted and Copper-Free ClickChemistry for the Efficient Synthesis of RNA Conjugates

(174) Šečkutė, J., Yang, J., and Devaraj, N. K. (2013) Rapid oligonucleotide-templated fluorogenic tetrazine ligations. *Nucleic Acids Research, 41,* e148.

(175) El-Sagheera, A. H.. and Tom B. (2010) New strategy for the synthesis of chemically modified RNA constructs exemplified by hairpin and hammerhead ribozymes. *Proc. Natl. Acad. Sci. U.S.A. 107,* 15329−157334.

(176) Rieder, U., and Luedtke, N. W. (2014) Alkene–Tetrazine Ligation for Imaging Cellular DNA. *Angew. Chem. Int. Ed., 53*, 9168–9172.

CHAPTER-2

Synthesis, Photophysical Characterization, and Enzymatic Incorporation of 5-Benzothiophene-Conjugated Fluorescent Uridine Analogue

2.1 Introduction

Microenvironment-sensitive fluorescent ribonucleoside analogues that report changes in nucleic acid confirmation during folding or the recognition process in the form of changes in basic photophysical properties have become very important analytical tools in investigating RNA structure and function.[1–6] As naturally occurring nucleobases are non fluorescent, several design principles were used to make them fluorescent. [7,8] Using naturally occurring fluorescent heterocycles and these design principles, several classes of base-modified fluorescent nucleobase analogues, like size-expanded base analogues, extended nucleobase analogues, polycyclic aromatic hydrocarbon, and isomorphic nucleobase analogues, have been developed.[9–11] Due to better photophysical properties of base-modified fluorescent nucleobase analogues, several of base-modified analogues were used in developing DNA as well as RNA bases based biophysical assays.[12–16] Notably, the majority of these analogues, except isomorphic bases, significantly deviate from the native structure of the nucleobases. An appealing feature of many of isomorphic analogues is that they closely resemble natural ribonucleosides and form stable Watson-Crick (WC) base pairs. Therefore, these modified isomorphic emissive ribonucleoside bases can be site-specifically placed in a target oligoribonucleotide in a non perturbing fashion and utilized in monitoring subtle conformational changes taking place around the point of investigation. In particular, the minimally perturbing nature and exquisite sensitivity of 2-aminopurine (2AP) to conformational changes have been widely used in designing several fluorescence- based assays to probe the structure, dynamics, and function of RNA molecules.[17,18] However, the emission maximum (~370 nm) in the near-UV region and low quantum yields when incorporated into nucleic acids substantially limit the utility of 2AP to *in vitro* systems only.[19–21]

Numerous base-modified ribonucleoside analogues with emission in the visible region and a high quantum yield have been developed, but only a few analogues have been effectively implemented in exploring the functions of RNA molecules.[6] In particular, only a very few structurally nonperturbing pyrimidine ribonucleoside analogues have shown promise as useful fluorescent probes.[22–28] In order to expand the repertoire of useful fluorescent pyrimidine ribonucleoside analogues, we sought to develop new fluorescent ribonucleoside analogues that (a) are structurally non invasive, (b) exhibit emission in the visible region, (c) display a reasonable quantum yield when incorporated into oligoribonucleotides, and (d) report changes in their surrounding environment via changes

in their photophysical properties. We have taken inspiration from a naturally occurring fluorescent amino acid, tryptophan, to construct an emissive pyrimidine ribonucleoside analogue. Tryptophan, an indole derivative, is reasonably emissive, and its emission properties are highly sensitive to its local environment.[29] Therefore, we hypothesize that the attachment of a bicyclic heterocycle such as benzo[*b*]thiophene moiety, in which nitrogen atom of indole is replaced by sulphur atom, on to a nucleobase may enhance the π-conjugation and impart better photophysical properties to the nucleobase.

Here, we report the synthesis, photophysical characterization, and enzymatic incorporation of a new microenvironment-sensitive fluorescent benzo[*b*]thiophene-conjugated uridine analogue **2** into RNA oligonucleotides. Interestingly, unlike 2AP the fluorescence quantum yield of **2** is not significantly compromised when placed within an ss RNA or a perfect complementary duplex.[30] Furthermore, using steady-state and time-resolved fluorescence spectroscopy techniques, we illustrate the ability of the fluorescently modified oligoribonucleotide in distinguishing between pyrimidines and purines upon hybridization to complementary and mismatched oligonucleotides.

2.2 Results and Discussions

2.2.1 Synthesis of Benzo[*b*]thiophene-Conjugated Uridine Analogue 2

Benzo[*b*]thiophene-conjugated uridine **2** has been synthesized by performing a palladium catalyzed cross-coupling reaction between the commercially available 5-iodouridine **1** and 2-tributylstannylbenzo[*b*]thiophene (Scheme1). The modified triphosphate substrate **3** required for *in vitro* transcription reactions has been synthesized by reacting ribonucleoside **2** with $POCl_3$, followed by reaction with bistributylammonium pyrophosphate in a one-pot two-step reaction. [31]

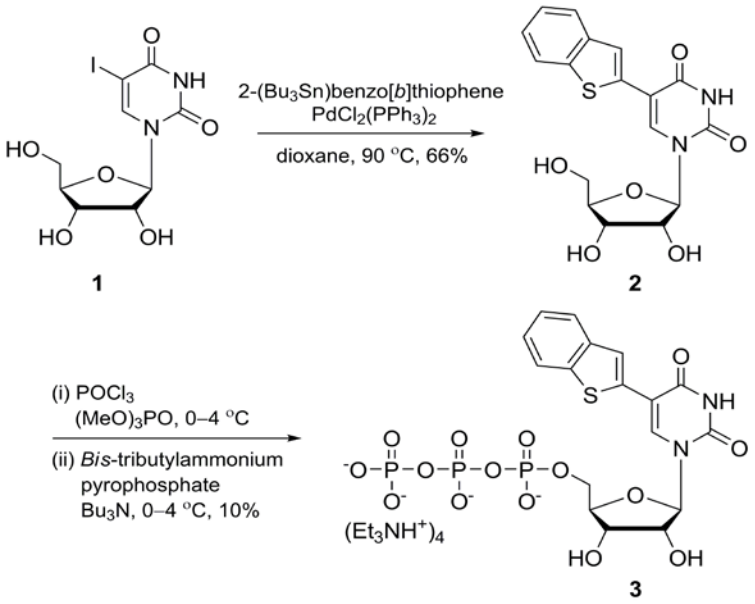

Scheme 1. Synthesis of benzo[*b*]thiophene-conjugated uridine **2** and its corresponding ribonucleoside triphosphate **3**.

2.2.2 Photophysical Properties of Benzo[*b*]thiophene-Conjugated Uridine Analogue 2

Before incorporating the benzo[*b*]thiophene-conjugated uridine analogue **2** into oligonucleotide, we want to know the responsiveness analogue **2** to its neighboring environment. For that we performed its primary photophysical studies like UV absorption, steady-state, and time-resolved fluorescence spectroscopic measurements in solvents of different polarity (Figure 2, Table 1). In the UV measurements, when the solvent polarity is progressively decreased from water to dioxane, the highest and the lowest absorption energy maxima are marginally get affected (Figure 2). In high polarity solvent, *i.e.* water **2** shows two absorption maxima at 274 nm and 318 nm corresponding nucleobase and benzo[*b*]thiophene moiety. Similarly in low polar solvent, *i.e.* dioxane **2** shows two absorption maxima at 276 nm and 322 nm corresponding nucleobase and benzo[*b*]thiophene moiety. Similarly, as solvent polarity decreases from water to dioxane; highest energy maximum shows hyperchromicity with small bathochromic shift *i.e.* increase in absorbance intensity with small shift in absorbance at longer wavelength in dioxane as compared to water. However, solvent polarity has a significant influence on both the emission maximum and intensity. When a solution of **2** in dioxane is excited at 322 nm, a strong fluorescence band is observed in the visible region (435 nm). As the solvent polarity is increased from dioxane to water, the ribonucleoside displays a marked

bathochromic shift (435 to 458 nm) and a nearly 2-fold fluorescence quenching (Figure 2, Table 1).

Table 1. Photophysical Properties of Fluorescent Ribonucleoside **2** in Various Solvents.

Solvent	λ_{max} [a] (nm)	λ_{em} (nm)	I_{rel} [b]	Φ [c]	τ_{ave} [c] (ns)	k_r/k_{nr}
Water	318	458	1.00	0.035	1.03	0.037
Methanol	321	446	1.69	0.047	0.60	0.049
Acetonitrile	321	443	1.31	0.034	0.49	0.036
Dioxane	322	435	2.09	0.060	0.45	0.064

[a] The absorption maximum, [b] Emission intensity relative to intensity in water. [c] standard deviation for Φ and τ_{ave} are ≤ 0.003 and 0.002 ns, respectively. k_r and k_{nr} are radiative and non radiative decay rate constants respectively.

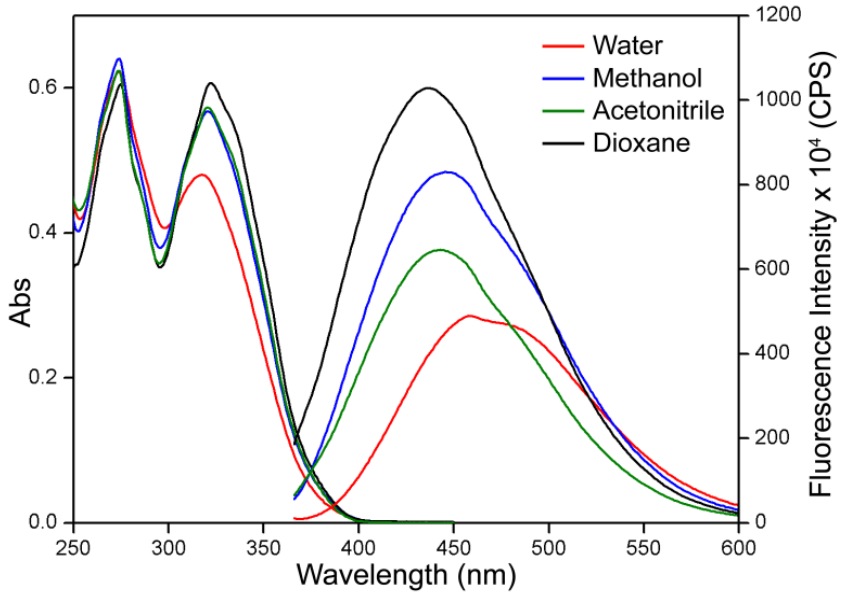

Figure 2. Absorption (50 μM) and emission (5 μM) spectra of ribonucleoside **2** in various solvents.

Time-resolved fluorescence measurements of **2** as a function of solvent polarity reveal distinct excited state decay profiles (Table 1, Figure 3). An aqueous solution of **2** shows the highest lifetime, and as the solvent polarity is decreased from water to dioxane a progressive decrease in lifetime is observed (Table 1). We then used the lifetimes and quantum yields to calculate the radiative (k_r) and nonradiative (k_{nr}) decay rate constants in different solvents (Table 1). The nearly 2-fold higher k_r/k_{nr} ratio in dioxane indicates that the radiative pathway is significantly favoured in dioxane as compared to water. Taken together, emission in the visible region, a reasonable quantum yield, and sensitivity to

changes in solvent polarity as exemplified by photophysical measurements confirm probe like character to the emissive ribonucleoside analogue **2**.

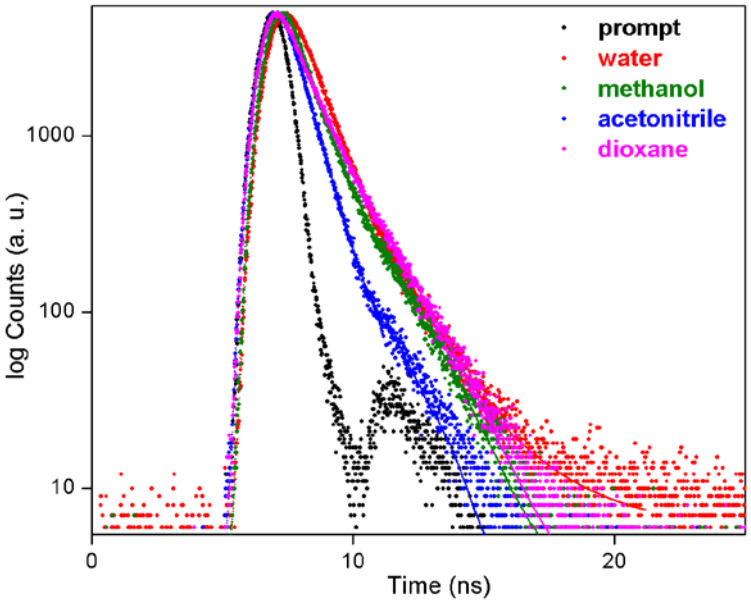

Figure 3. Excited state decay profile of ribonucleoside **2** (5 µM) in various solvents. Laser profile is shown in black (prompt). Curve fits are shown in solid lines.

2.2.3 Microscopic Solvent Polarity Parameters E_T(30) of Benzo[*b*]thiophene-Conjugated Uridine Analogue 2

The E_T(30) parameter is widely used for measuring empirically the polarity of many chromophores. When UV/vis absorption spectra of suitable chromophores are measured in solvents of different polarity, the position, intensity, and shape of their absorption are usually modified to a greater or lesser extent. This solvatochromism originates from the differential solvation of the ground and first excited state of the solute chromophore by means of nonspecific and specific intermolecular solute/solvent interactions, which stabilize ground and excited state to a different extent. However, solute/solvent interactions take place on a molecular-microscopic level, with mutually interacting individual solvent molecules surrounding the ions or molecules of the solute, which is dissolved in a more or less structured noncontinuous medium. Solvent molecules are characterized by molecular properties such as dipole moment, electronic polarizability, hydrogen-bond donor and hydrogen-bond acceptor capability, electron-pair donor and electron-pair acceptor capability, etc. According to the extent of these intermolecular solvent/solvent interactions, there exist highly structured solvents (*e.g.*, water) and less structured solvents (*e.g.*, hydrocarbons) [32].

The responsiveness of the ribonucleoside to changes in the solvent-polarity environment is also confirmed by plotting the Stokes shift in various solvents as a function of Reichardt's microscopic solvent polarity parameter, $E_T(30)$ (Figure 4).[33] A positive correlation between the Stokes shift and $E_T(30)$ further establishes the sensitiveness of the emissive ribonucleoside **2** to its surrounding environment.

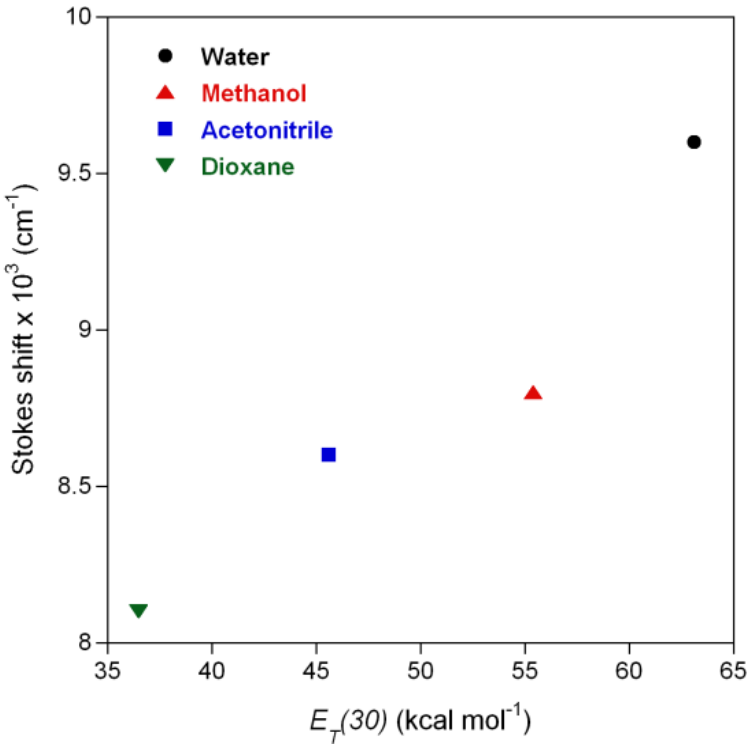

Figure 4. A plot of Stokes shift vs. $E_T(30)$ spectra of ribonucleoside **2** in various solvent.

2.2.4 Quenching Studies and Stern-Volmer plot of Benzo[*b*]thiophene-Conjugated Uridine Analogue 2

It is known that the fluorescence of emissive ribonucleoside get quenched due to the interaction like stacking, collisional interactions, electron transfer, hydrogen bonding with neighbouring bases. This quenching can be static or dynamic. To determine the effect of neighbouring bases on the fluorescence of ribonucleoside **2,** we performed its quenching studies in presence of different bases. These studies were performed with help of steady state fluorescence, by adding aliquots of different concentrated NMPs (UMP, GMP, AMP, and CMP) solution to ribonucleoside **2** solutions, where both solutions contained equal concentration of the ribonucleoside. By measuring the fluorescence intensity in the absence and in presence of quencher and putting in them into Stern-Volmer equation, the quenching constant (*Ksv*) values were determined. The ribonucleoside UMP and CMP did not show any quenching whereas GMP shows very marginal quenching with a K_{sv} of 24.9

± 2.4 μM^{-1}. Interestingly, AMP shows fluorescence enhancement with a very small negative K_{sv} of -8.7 ± 0.9 μM^{-1}. Taken together, collisional quenching of ribonucleosides fluorescence by NMPs is practically insignificant Therefore, diffusion controlled collisional interaction between the modified oligonucleotides does not significantly contribute to the observed fluorescence quenching of ribonucleoside **2** within oligoribonucleotides.

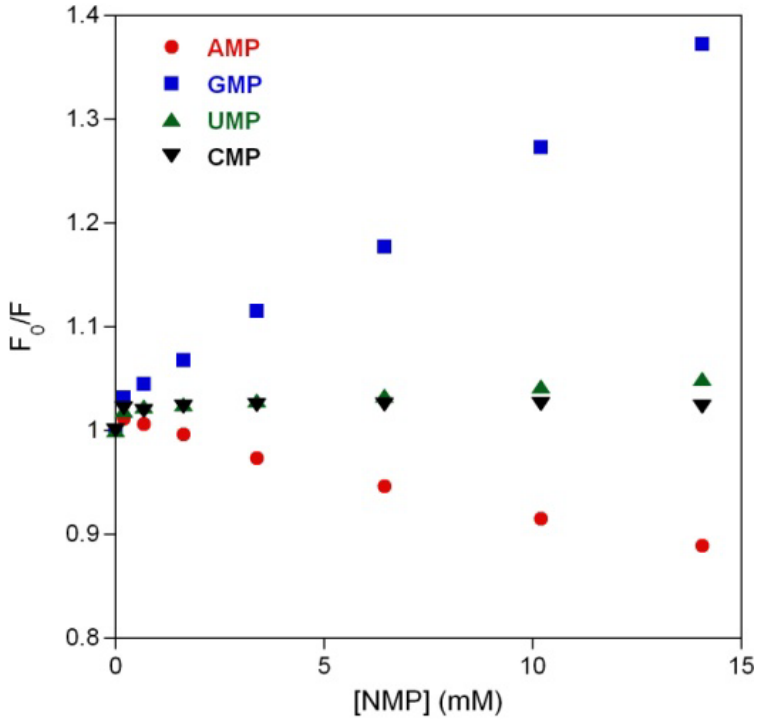

Figure 5. Steady-state Stern-Volmer plot for the titration of ribonucleoside **2** with NMPs.

2.2.5 Enzymatic Incorporation of Benzo[*b*]thiophene-Conjugated UTP Analogue 3

Modified ribonucleoside can be incorporated into oligonucleotides by solid phase synthesis or enzymatic incorporation method. By bearing in mind the advantages and disadvantage of both of these methods, we chose the enzymatic incorporation strategy to synthesize modified oligonucleotides as it does not involve elaborate protection-deprotection steps. [34–40] The efficacy of T7 RNA polymerase in incorporating the modified nucleoside triphosphate **3** into RNA transcripts was investigated by performing *in vitro* transcription reactions. A series of duplexes were assembled by annealing an 18-mer T7RNA polymerase consensus deoxyoligonucleotide promoter sequence to deoxyoligonucleotide templates (**T1-T5**, Figure 6). The templates were designed to possess one or two dA residues at different positions (*e.g.*, near the promoter region, away from the promoter region, and at multiple sites) to direct single or multiple incorporations

of **3.** In addition, all templates contained a unique dT residue at the 5'-end to direct the incorporation of a single adenosine at the 3'-end of each transcript. Therefore, successful transcription reactions performed in the presence of GTP, CTP, UTP/**3**, and α-^{32}P ATP would result in the formation of 3'-end ^{32}P-labeled RNA transcripts. The labeled oligoribonucleotide products could then be resolved by analytical denaturing polyacrylamide gel electrophoresis and imaged.

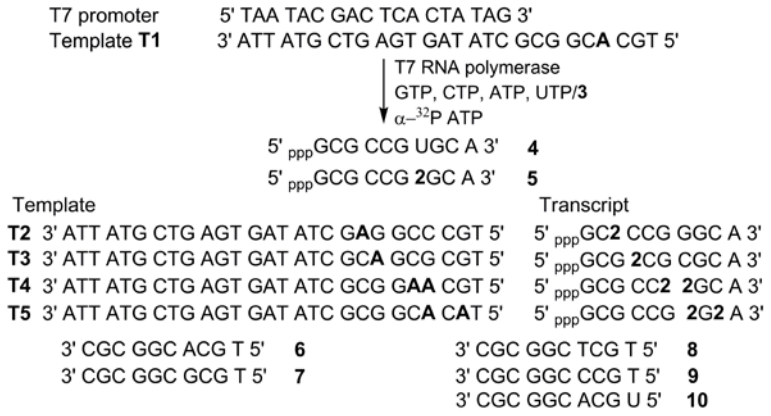

Figure 6. Enzymatic incorporation of ribonucleoside triphosphate **3**. Synthetic oligonucleotides (**6-10**) used in the study.

The transcription reaction in the presence of template **T1** containing a dA residue away from the promoter at the +7 position results in the formation of the 10-mer modified full-length oligoribonucleotide transcript **5** (Figure 7, lane 2).[41] Relative to natural UTP, **3** is incorporated into the transcript with an excellent efficiency of 85 ± 1%. The slower migration of transcript **5** clearly indicates the incorporation of a higher molecular weight modified ribonucleoside during the transcription reaction (Figure 7, compare lanes 1 and 2). Importantly, a control transcription in the absence of UTP and **3** did not yield any full-length oligoribonucleotide product, which clearly rules out the formation of full-length transcripts due to adventitious misincorporation (Figure 7, lane 3).

Interestingly, reaction in the presence of equimolar concentrations of UTP and **3** demonstrates that T7 RNA polymerase has an almost equal preference for UTP and unnatural nucleotide **3** (1:1.1, Figure 7, lane 4). When reactions are performed in the presence of templates **T2** and **T3** containing the dA residue near the promoter at +3 and +4 positions, the incorporation efficiency drops significantly (Figure 7, lanes 6 and 8). This is understandable as the efficiencies of transcription reactions are known to be significantly reduced by template sequences that lead to modifications near the promoter region.[42,43] In the presence of template **T4**, the RNA polymerase incorporates **3** in two successive

positions (+6 and +7) with reasonable efficiency (62 ± 1%, Figure 7, lane 10). However, for a reaction in the presence of template **T5**, which would direct the addition of a modified ribonucleoside in alternating positions (+7 and +9), the incorporation efficiency was found to be low (12 ± 3%, Figure 7, lane 12).

The yield obtained from transcription reaction in presence of template **T4** and **T5** is somewhat puzzling as transcription efficiency is higher with template **T4**, which would result in successive incorporation as compared to template **T5** (incorporation in alternating position). All transcription reactions reported in thesis has been performed in duplicate and results are reproducible. The yield of transcription reaction depends upon how efficiently modified triphosphate binds to T7 RNA polymerase, if modified triphosphate binds very weakly to the enzyme (low K_m), then it may not get incorporated at all. Alternatively, the modified nucleotide can get incorporated, but elongation of the modified nascent transcript may fail past the modification position due to steric hindrance and or due to unstable nascent RNA-DNA duplex. More detailed study with longer templates could provide better insight into the observed differences in transcription efficiency. Albeit certain limitations, our results with templates clearly demonstrate the utility of *in vitro* transcription reactions in generating fluorescently modified oligoribonucleotides.

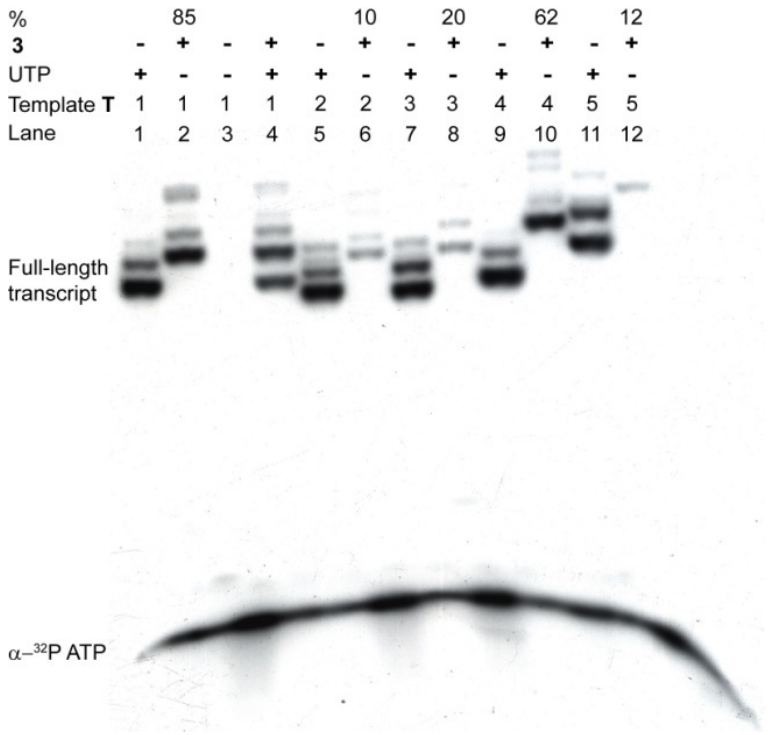

Figure 7. *In vitro* transcription reactions with templates **T1-T5** in the presence of UTP and modified UTP **3**. % incorporation of **3** is reported with respect to reaction in the presence of NTPs.

2.2.6 Charecterization of Benzo[*b*]thiophene Modified Oligoribonucleotide 5

*Mass analysis modified RNA transcript **5***: To confirm the presence of benzo[*b*]thiophene-conjugated uridine **2** in the transcript, a large-scale transcription reaction was performed with template **T1.** Modified transcript was purified by PAGE electrophoresis, the gel band corresponding modified oligonucleotide was UV shadowed, and proper band was cut, eluted in sodium acetate buffer and desalted using Sep-Pak classic C18 cartridge. The sample for the mass analysis was prepared by adding modified transcript **5** to a solution containing internal standard, citrate buffer and matrix 3-hydroxypiccolinic acid (3-HPA). The MALDI-TOF mass spectrum was calibrated relative to an internal standard. MALDI-TOF mass measurement of the PAGE purified transcript established the integrity of the modified full-length RNA (Figure 8).

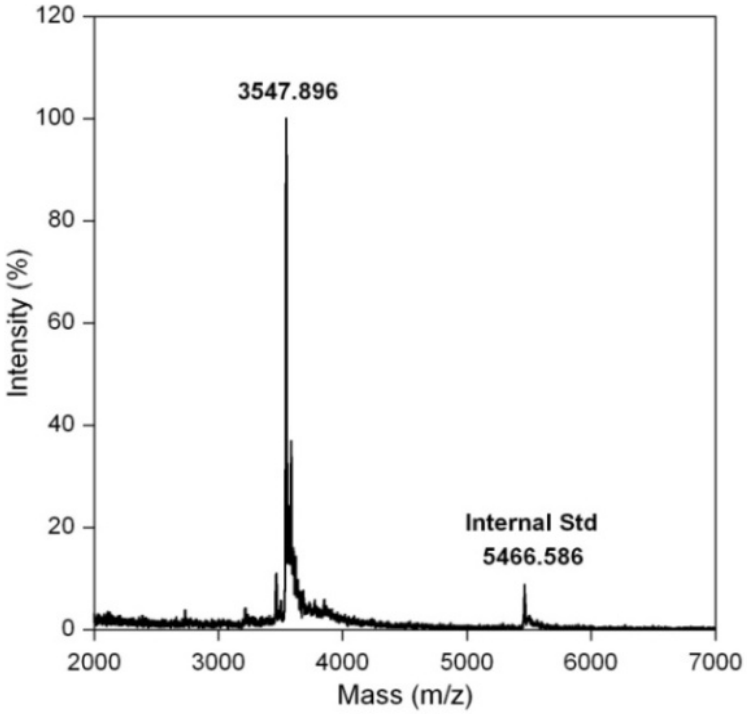

Figure 8. MALDI-TOF MS spectrum of the modified RNA transcript **5** calibrated relative to the +1 ion of an internal 18-mer DNA oligonucleotide standard (m/z: 5466.586). Calculated mass [M] = 3547.075; observed mass = 3547.896.

*Enzymatic digestion of the modified RNA transcript **5***: To further ascertain the presence of the intact benzo[*b*]thiophene modified nucleobase in the RNA transcript, enzymatic digestions of transcript **5** with snake venom phosphodiesterase I, calf intestine alkaline phosphatase, RNase A, and RNase T1 were performed. HPLC analysis of the resulting ribonucleoside mixture unambiguously revealed the presence of the modified nucleoside **4**

and verified the expected stoichiometry (Figure 9). Mass spectral analysis of individual HPLC fractions further confirmed the authenticity of the native and modified nucleosides present in the enzymatic digest. (Table 2)

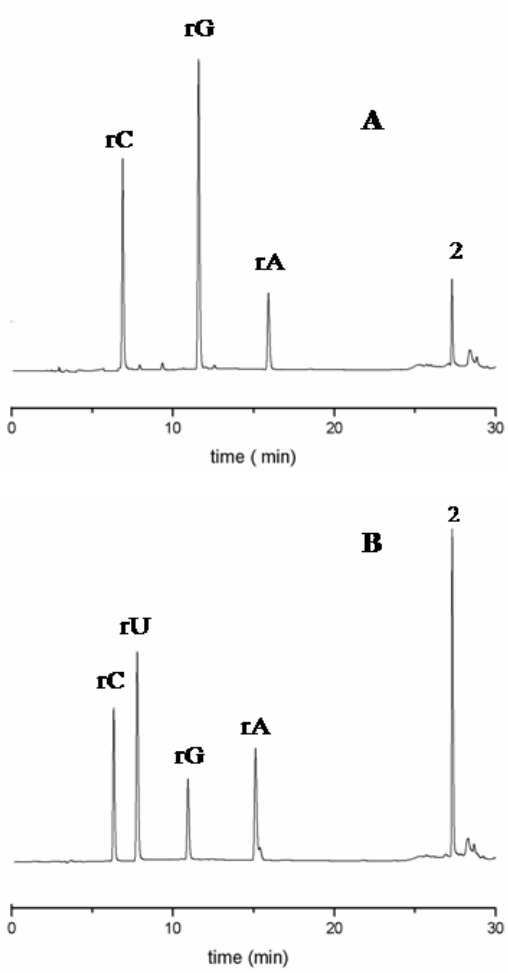

Figure 9. HPLC profile of enzymatic digestion of transcript **5** at 260 nm. (A) Digested RNA transcript **5** (B) Authentic nucleoside samples and modified nucleoside **2**.

Table 2. MALDI-TOF mass analysis of HPLC fractions of modified oligoribonucleotide **5** digest

HPLC fraction	Calculated mass for	Found
rC	$C_9H_{14}N_3O_5Na$ [M+Na^+]: 266.1	266.1
rG	$C_{10}H_{14}N_5O_5Na$ [M+ Na^+]: 306.1	306.1
rA	$C_{10}H_{14}N_5O_4Na$ [M+ Na^+]: 290.1	290.1
2	$C_{17}H_{16}N_2O_6SNa$ [M+ Na^+]: 399.1	399.1

2.2.7 Stability of Duplexes Made of Modified RNA Transcript 5

It has been observed that, when modified ribonucleoside was incorporated in oligonucleotide it can potentially perturb the native structure of oligoribonucleotides, which can lead to ineffective hybridization. The incorporation of **2** in oligoribonucleotide

5 can potentially perturb the native structure and hence, can result in ineffective hybridization. Thus the observed photophysical properties of duplex can be due to the mixture of single stranded RNA transcript as well as its duplex. To study the effect of incorporation of modified ribonucleoside **2**, on hybridization efficiency we performed thermal denaturation studies (T_m) and native gel mobility shift experiment with **2**-containing duplex and corresponding unmodified duplexes.

Thermal denaturation studies (T_m) *of duplexes made up of transcript **5***: Nucleic acid duplexes are held together by hydrophobic as well as stacking interactions between adjacent bases assisted by hydrogen bonding between opposite complementary base pairs. When we supply heat to these duplexes, enough thermal energy will be provided to break hydrogen bonding resulting in the separation of both strands, this is called thermal melting. The temperature at which half of the duplexes are denatured is called the melting temperature, which is dependent on the length, sequence and concentration of the nucleic acid as well as on its surroundings such as the salt concentration and p^H. Melting temperatures are often reported as a measure of the stability of nucleic acid duplexes. It is reported that when the modification is made on the nucleobase, the native hydrogen bonding pattern of nucleobase is get affected due perturbing nature of the modification. To study the effect of incorporation of modified ribonucleoside **2**, on hybridization efficiency we performed thermal denaturation studies (T_m). The thermal denaturation studies were performed by annealing the duplexes of modified transcript **5** and unmodified transcript **4** with control DNA **6**. The duplexes (**4•6** and **5•6**) were hybridized by heating a 1:1 mixture of the oligonucleotides at 90 °C for 3 min and cooling the solutions slowly to room temperature. Samples were placed in crushed ice for at least 30 min before analysis. The UV profiles of duplexes were recorded with increasing temperature. The UV profile shows the hyperchromicity. The T_m values calculated for duplexes **4•6** and **5•6** are 57.7 ± 0.9 °C and 54.4 ± 1.1 °C, respectively.(Figure 10) Thus Thermal denaturation studies with a 2-containing duplex and corresponding unmodified duplex show only marginal destabilization due to benzo[*b*]thiophene modification of uridine.

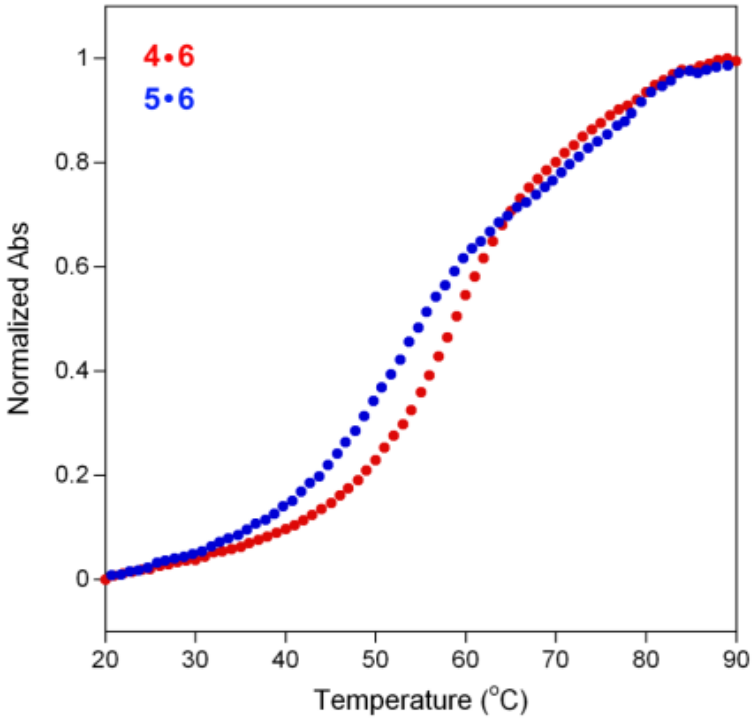

Figure 10. UV-thermal melting of control unmodified duplex **4•6** (red, 1 μM) and fluorescently-modified duplex **5•6** (blue, 1 μM).

*Native gel mobility shift experiment with modified duplexes of RNA transcript **5**:* Native gel retardation experiments performed to determine the hybridization efficiency with modified transcript with complementary and mismatch oligonucleotides. For native gel retardation experiment ^{32}P-labeled transcript **5**, was synthesized by a transcription reaction in the presence of template T1 and α-^{32}P ATP. The Radiolabeled transcript **5** was purified from PAGE by exposing the gel to X-ray sheet and appropriate band was excised, eluted in sodium acetate buffer and purified by Sep-Pak classic C18 cartridge. The duplexes of modified transcript were annealed by doping the radiolabelled transcript **5** with the non radiolabelled transcript **5** and custom oligonucleotides (**6–7**) under similar conditions used in the fluorescence experiments. These radiolabelled duplexes were run on 18% native PAGE. The radiolabelled products on gel was exposed to X-ray films, exposed films were developed and fixed. The gel shift experiments clearly revealed complete hybridization of the duplexes. (Figure 11).

Taken together, the thermal melting studies (T_m) and gel mobility shift experiment results clearly indicate that the benzo[*b*]thiophene moiety does not affect the hybridization efficiency. Hence, it can be concluded that the observed differences in the fluorescence properties of completely intact duplexes are completely due to differences in the microenvironment of the fluorescent ribonucleoside.

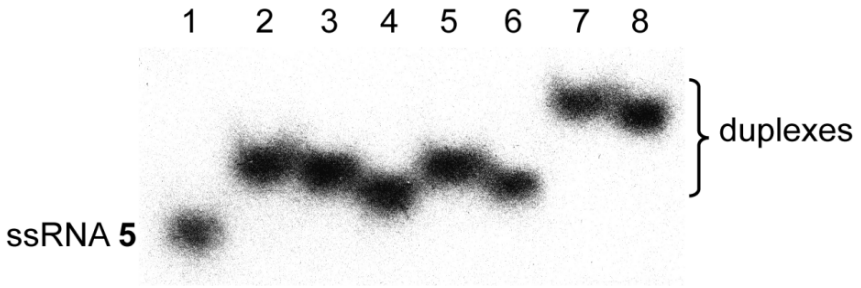

Figure 11. Gel mobility shift experiments to determine the hybridization efficiency of duplexes made of fluorescent oligoribonucleotide **5** and complementary and mismatched DNA and RNA. oligonucleotides. Lane 1, single stranded oligoribonucleotide **5**; Lanes 2–5 and 7, duplexes **5•6**, **5•8**, **5•7**, **5•9** and **5•10**, respectively. Lanes 6 and 8, duplexes made of **5** and complementary DNA and RNA oligonucleotides containing an abasic site opposite to the ribonucleoside **2**, respectively.

2.2.8 Photophysical Characterization of Benzo[*b*]thiophene Modified Transcript 5

Emissive nucleoside analogues when incorporated into oligonucleotides experience diverse interactions with neighboring bases such as stacking, hydrogen bonding, and collisional interactions, which can affect the photophysical properties of nucleosides[19–21]. In order to evaluate the effect of neighboring bases on the fluorescence of modified nucleoside **2**, we have photophysically characterized the modified transcript **5** and duplexes of **5**. These duplexes have been constructed by annealing transcript **5** with various complementary DNA and RNA oligonucleotides in which the modified nucleoside **2** has been placed opposite to its complementary and mismatch bases. Upon excitation at 320 nm, the modified oligoribonucleotide **5** and in which the modified nucleoside **2** has been placed opposite to its complementary and mismatch bases, in cacodylate buffer shows a slightly red shifted emission (482 nm) corresponding to a quantum yield of 0.010 ± 0.002, which is 2.7-fold lower than that for the free ribonucleoside. This fluorescence quenching accompanied by a small spectral shift is presumably due to the solvation effect and partial stacking of the fluorophore with neighboring bases. Surprisingly, perfect RNA-DNA (**5•6**) and RNA-RNA (**5•10**) duplexes display a small enhancement in fluorescence intensity (Figure12, Table 3). This observation is particularly interesting because most fluorescent nucleoside analogues (*e.g.*, 2AP, pyrroloC) exhibit progressive fluorescence quenching upon incorporation into ss-and ds-oligonucleotides due to stacking interactions with adjacent bases[19,44–46].

Interestingly, duplexes **5•8** and **5•9** in which the emissive ribonucleoside **2** is placed opposite to pyrimidines show an ~40 % increase in fluorescence intensity as compared to duplexes **5•6** and **5•7** containing **2** opposite to purines (Figure 13). The

possible explanation for observed fluorescence enhancement can be due to more exposure of benzothiophene moiety to solvent and less stacking in **5•8** and **5•9** as compared to **5•6** and **5•7**. In duplexes **5•6** and **5•7**, the modified uridine analogue forms a stable Watson-crick and wobble base pair with dA and dG, respectively, which results in better stacking of the fluorophore with adjacent bases which results in the reduced fluorescence intensity.

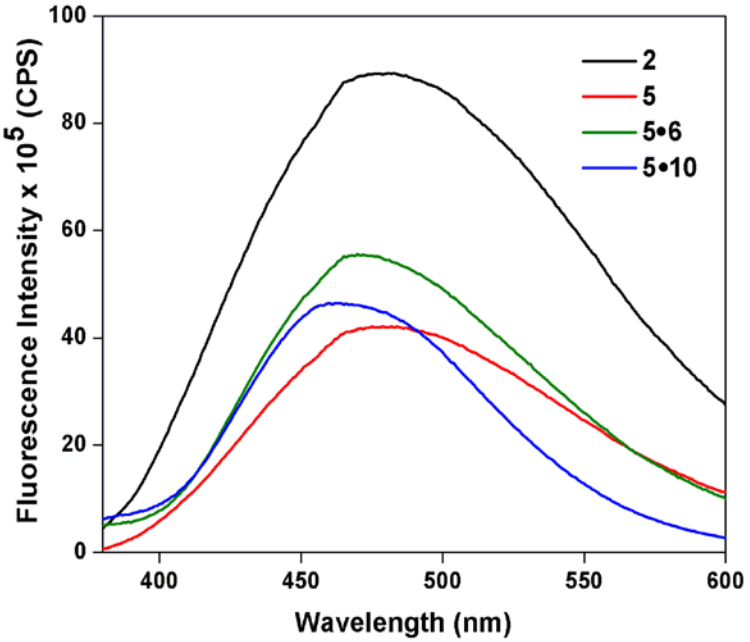

Figure 12. Emission spectra of **2**, **5**, and duplexes **5•6** and **5•10**.

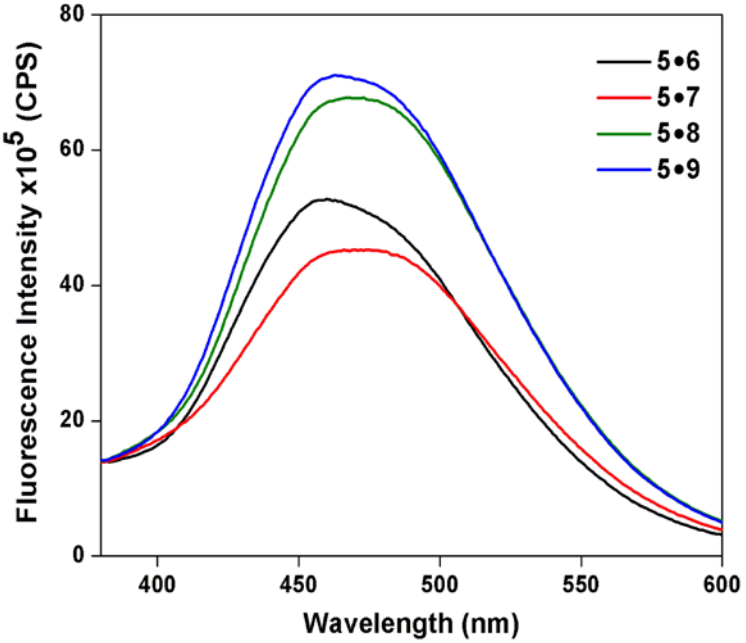

Figure 13. Emission spectra of duplexes containing modified nucleoside **2** opposite to purines and pyrimidines.

Table 3. Steady-state and time-resolved fluorescence spectroscopy measurements of benzo[*b*]thiophene-conjugated ribonucleoside **2** and oligoribonucleotide constructs.

Sample	λ_{em} (nm)	Φ	τ_1 (ns)	τ_2 (ns)	τ_{Ave} (ns)	k_r/k_{nr}
2	475	0.027 ± 0.0003	1.12	-	1.12 ± 0.004	0.028
5	482	0.010 ± 0.002	0.67 (0.77)	3.03 (0.23)	1.21 ± 0.005	0.010
5•6	470	0.011 ± 0.003	0.65 (0.86)	3.11 (0.14)	1.00 ± 0.03	0.011
5•7	488	ND	0.77 (0.76)	3.41 (0.24)	1.41 ± 0.03	ND
5•8	482	ND	0.72 (0.49)	4.15 (0.51)	2.46 ± 0.12	ND
5•9	476	ND	0.96 (0.60)	4.14 (0.40)	2.23 ± 0.05	ND
5•10	463	0.013 ± 0.002	0.63 (0.86)	3.13 (0.14)	0.98 ± 0.05	0.013

Relative amplitude is given in parenthesis. ND = not determined.

2.3 Conclusions

We have developed a new fluorescent uridine analogue based on a (benzo[*b*]thiophen-2-yl)pyrimidine core that has an emission maximum in the visible region and displays excellent solvatochromism. The corresponding triphosphate substrate is amenable to incorporation into oligoribonucleotides by transcription reactions. Interestingly, T7 RNA polymerase equally incorporates both natural UTP and modified UTP **3** into RNA oligonucleotides, a trait that can be utilized in the fluorescent labelling of RNA by a ribonucleoside salvage pathway.[17] The results reported here also demonstrate that polarity-sensitive fluorescent ribonucleoside analogue **2** can be used as a probe in investigating nucleic acid dynamics and the recognition process by monitoring changes in fluorescence properties such as fluorescence intensity, lifetime, and anisotropy.

2.4 Experimental Section

2.4.1 Materials

Unless otherwise mentioned, materials obtained from commercial suppliers were used without further purification. 5-iodouridine, 2-(tributylstannyl)benzo[*b*]thiophene and *bis*(triphenylphosphine)-palladium(II) chloride were obtained from Sigma-Aldrich. DNA oligonucleotides were either purchased from Integrated DNA Technologies, Inc. or from Sigma-Aldrich. Oligonucleotides were purified by gel electrophoresis under denaturing condition and desalted on Sep-Pak Classic C18 cartridges (Waters Corporation). Custom synthesized RNA oligonucleotides purchased from Dharmacon RNAi Technologies were

deprotected according to the supplier's procedure, PAGE-purified and desalted on Sep-Pak Classic C18 cartridges. T7 RNA polymerase, ribonuclease inhibitor (RiboLock) and NTPs were obtained from Fermentas Life Science. Radiolabeled α-^{32}P ATP (2000 Ci/mmol) was obtained from the Board of Radiation and Isotope Technology, Government of India. Chemicals for preparing buffer solutions were purchased from Sigma-Aldrich (BioUltra grade). Autoclaved water was used in all biochemical reactions and fluorescence measurements.

2.4.2 Instrumentation

NMR spectra were recorded on a 400 MHz Jeol ECS-400. All MALDI-MS measurements were recorded on an Applied Biosystems 4800 Plus MALDI TOF/TOF analyzer. Absorption spectra were recorded on a PerkinElmer, Lambda 45 UV-Vis spectrophotometer. UV-thermal melting analyses of oligonucleotides were performed on a Cary 300Bio UV-Vis spectrophotometer. Steady State and time-resolved fluorescence experiments were carried out in a micro fluorescence cuvette (Hellma, path length 1.0 cm) on a TCSPC instrument (Horiba Jobin Yvon, Fluorolog-3). Reversed-phase flash chromatographic (C18 Redi*SepRf* column) purifications were carried out using Teledyne ISCO, Combi Flash Rf.

2.4.3 Synthesis Benzo[*b*]thiophene-Conjugated Uridine 2

To a suspension of 5-iodouridine (0.200 g, 0.54 mmol, 1 equiv) and *bis*(triphenylphosphine)-palladium(II) chloride (0.007 g, 0.01 mmol, 0.02 equiv) in degassed anhydrous dioxane (15 ml) was added 2-(tributylstannyl)benzo[*b*]thiophene (0.571 g, 1.34 mmol, 2.5 equiv). The reaction mixture was heated at 90 °C for 2 hr, cooled, filtered through celite pad. Celite pad was washed with hot dioxane (3 x 10 ml). The solvent was evaporated and the residue was purified by flash chromatography using a C18 reverse phase column (C18 Redi*SepRf* 43 g column, 10–60% acetonitrile in water for 30 min) to afford the product as off-white solid (0.133 g, 66%). TLC (CH_2Cl_2:MeOH = 85:15) *Rf* = 0.53; ^{1}H NMR (400 MHz, d_6-DMSO): δ (ppm) 11.79 (br, 1H), 8.83 (s, 1H), 7.90 (d, *J* = 8.24 Hz, 1H), 7.79 (d, *J* = 6.80 Hz, 1H), 7.78 (s, 1H), 7.37–7.28 (m, 2H), 5.85 (d, *J* = 4.0 Hz, 1H), 5.54 (t, *J* = 4.4 Hz, 1H), 5.51 (d, *J* = 5.2 Hz, 1H), 5.12 (d, *J* = 5.6 Hz, 1H), 4.16 (dd, *J* = 9.2 Hz, *J* = 4.8 Hz, 1H), 4.10 (dd, *J* = 5.2 Hz, *J* = 10.4 Hz, 1 H), 3.96–3.94 (m, 1H), 3.84–3.80 (m, 1H), 3.70–3.67 (m, 1H); ^{13}C NMR (100 MHz, *d6*-DMSO): δ

(ppm) 161.4, 149.5, 139.1, 138.9, 137.6, 135.2, 124.4, 124.0, 123.1, 122.0, 119.0, 107.8, 89.0, 84.5, 74.4, 69.1, 60.0; MALDI-TOF MS (m/z): Calculated for $C_{17}H_{16}N_2O_6S$ [M] = 376.073, found $[M+K]^+$ = 414.931; λ_{max} (H_2O) = 274 and 318 nm, ε_{274} = 11760 $M^{-1}cm^{-1}$, ε_{318} = 9347 $M^{-1}cm^{-1}$, ε_{260} = 9040 $M^{-1}cm^{-1}$.

2.4.4 Benzo[*b*]thiophene-conjugated Uridine Triphosphate 3

To an ice cold solution of ribonucleoside **2** (0.090 g, 0.24 mmol, 1 equiv) in trimethyl phosphate (1 ml) was added freshly distilled $POCl_3$ (60 µL, 0.64 mmol, 2.7 equiv). The solution was stirred for 34 h at 0–4 °C. TLC revealed only partial conversion of the ribonucleoside into the product. A solution of *bis*-tributylammonium pyrophosphate (0.5 M in DMF, 2.7 ml, 5.7 equiv) and tributylamine (0.63 ml, 2.64 mmol, 11 equiv) was rapidly added under ice-cold condition. The reaction was quenched after 30 min with 1 M triethylammonium bicarbonate buffer (TEAB, pH 7.5, 18 ml) and was extracted with ethyl acetate (20 ml). The aqueous layer was evaporated and the residue was purified first on DEAE sephadex-A25 anion exchange column (10 mM–1M TEAB buffer, pH 7.5) followed by reverse-phase flash column chromatography (C18 Redi*SepRf*, 0–40% acetonitrile in 100 mM triethylammonium acetate buffer, pH 7.2, 40 min). Appropriate fractions were lyophilized to afford the desired triphosphate product **3** as a tetratriethylammonium salt (24 mg, 10%). ^{1}H NMR (400 MHz, D_2O): δ (ppm) 8.17 (s, 1H), 7.88 (d, *J* = 7.6 Hz, 1H), 7.86 (s, 1H), 7.74 (s, 1H), 7.40–7.31 (m, 2H), 5.92 (d, *J* = 2.8 Hz, 1H), 4.45 (br, 2H), 4.30–4.27 (m, 3H); ^{13}C NMR (100 MHz, D_2O): δ (ppm) 162.5, 150.2, 139.1, 138.9, 136.8, 133.1, 124.7, 124.6, 123.8, 121.9, 121, 109.4, 89.1, 83.4, 73.7, 69.8, 58.6; ^{31}P NMR (162 MHz, D_2O): δ (ppm) -8.87 (br, P_γ), -10.98 (br, P_α), -22.04 (br, P_β); MALDI-TOF MS negative mode (m/z): Calculated for $C_{17}H_{19}N_2O_{15}P_3S$ [M] = 615.972, found $[M-H]^-$ = 615.035.

2.4.5 Photophysical Characterization of Ribonucleoside 2

*Steady-state fluorescence of ribonucleoside **2** in various solvents:* Ribonucleoside **2** (5 µM) in water, methanol, acetonitrile and dioxane was excited at respective lowest energy absorption maximum with an excitation slit width of 4 nm and emission slit width of 6 nm, and the emission profile in each solvent was recorded. All solutions contained 0.5 % DMSO. Fluorescence experiments were performed in triplicate in a micro fluorescence cell (Hellma, path length 1.0 cm) on a Horiba Jobin Yvon, Fluorolog-3.

*Time-resolved fluorescence measurements of ribonucleoside **2** in various solvents:* Excited state lifetimes of **2** (5 μM) were determined under the same conditions as mentioned above using TCSPC instrument (Horiba Jobin Yvon, Fluorolog-3). Fluorescently modified ribonucleoside **2** was excited using 339 nm LED source (IBH, UK, NanoLED-339L) with a band pass of 6 nm and fluorescence signal at respective emission maximum was collected. Lifetime measurements were performed in duplicate and decay profiles were analyzed using IBH DAS6 analysis software. Fluorescence intensity decay profiles in all solvents were found to be biexponential with χ^2 (goodness of fit) values very close to unity.

2.4.6 Radiative and Non-radiative Decay Rate Constants

Radiative (k_r) and nonradiative decay (k_{nr}) rate constants of **2** in different solvents were determined from their respective quantum yield (Φ) and average lifetime (τ) using following equations.

$$k_r = \Phi/\tau$$

$$1/\tau = k_r + k_{nr}$$

2.4.7 Quantum Yield Determination

Quantum yield of ribonucleoside **2** in different solvents relative to 2-aminopurine standard was determined using the following equation (Du, H.; Fuh, R. A.; Li, J.; Corkan, A.; Lindsey, J. S. *Photochem. and Photobiol.*, **1998**, *68*, 141).

$$\Phi_{F(x)} = (A_s/A_x)\,(F_x/F_s)\,(n_x/n_s)^2\,\Phi_{F(s)}$$

Where s is the standard, x is the ribonucleoside, A is the absorbance at excitation wavelength, F is the area under the emission curve, *n* is the refractive index of the solvent and Φ_F is the quantum yield (Lavabre, D.; Fery-Forgues, S. *J. Chem. Educ.*, **1999**, *76*, 1260–1264).

2.4.8 Quenching Studies and Stern-Volmer Plot

Quenching of ribonucleoside fluorescence by NMPs was performed by adding aliquots of concentrated nucleotide solution (40 mM) to the ribonucleoside **2**, where both solutions contained equal concentration of the ribonucleoside (5 μM). All solutions were prepared in 20 mM cacodylate buffer containing 0.5% DMSO (100 mM NaCl, 0.5 mM EDTA, pH

7.1). The ribonucleoside was excited at 320 nm with an excitation slit width of 4 nm and emission slit width of 6 nm, and changes in fluorescence was monitored at the emission maximum, 475 nm. Stern-Volmer plot was obtained by plotting F_0/F vs. concentration of the quencher (NMPs) and was fit using the following equation.

$$F_0/F = 1 + K_{sv}[\text{NMPs}]$$

Where F_0 and F are the fluorescence intensities in the absence and presence of quenchers (NMPs) respectively, and K_{sv} is the quenching constant.

2.4.9 Enzymatic Incorporation of Ribonucleoside Triphosphate 3

Transcription reactions with α-^{32}P ATP: Promoter-template duplexes were assembled by heating a 1:1 concentration (final 5 μM) of deoxyoligonucleotide templates (**T1**–**T5**) and an 18-mer T7 RNA polymerase consensus promoter deoxyoligonucleotide sequence in TE buffer (10 mM Tris-HCl, 1 mM EDTA, 100 mM NaCl, pH 7.8) at 90 °C for 3 min and cooling the solution slowly to room temperature. The duplexes were then placed on crushed ice for 20 min and stored at -40 °C. Transcription reactions were performed in 40 mM Tris-HCl buffer (pH 7.9) containing 250 nM annealed templates, 10 mM $MgCl_2$, 10 mM NaCl, 10 mM dithiothreitol (DTT), 2 mM spermidine, 1 U/μL RNase inhibitor (RiboLock), 1 mM GTP, 1 mM CTP, 1 mM UTP and or 1 mM modified UTP **3**, 20 μM ATP, 5 μCi α-^{32}P ATP and 3 U/μL T7 RNA polymerase in a total volume of 20 μL. After 3.5 h at 37 °C, reactions were quenched by adding 20 μL of the loading buffer (7 M urea in 10 mM Tris-HCl, 100 mM EDTA, 0.05 % bromophenol blue, pH 8), heated to 75 °C for 3 min and cooled on an ice bath. The samples (4 μL) were loaded onto a sequencing 18% denaturing polyacrylamide gel. The products on the gel were exposed to X-ray film (1–2 h) and the exposed film was developed, fixed and dried. The bands were then quantified using the software (GeneTools from Syngene) to determine the relative transcription efficiencies. Percentage incorporation of modified ribonucleoside triphosphate **3** is reported with respect to transcription efficiency in the presence of natural NTPs. All reactions were performed in duplicate and the standard deviations were ± 6%.

Large-scale transcription reactions: Large-scale transcription reactions using template **T1** were performed in a 250 μL reaction volume under similar conditions to isolate oligoribonucleotides **4** and **5** for further characterization and fluorescence studies. The

reaction contained 2 mM GTP, 2 mM CTP, 2 mM ATP, 2 mM UTP or 2 mM modified UTP **3**, 20 mM $MgCl_2$, 0.4 U/μL RNase inhibitor (RiboLock), 300 nM annealed template and 800 units T7 RNA polymerase. After incubation for 12 h at 37 °C, the precipitated salt of pyrophosphate was removed by centrifugation. The reaction volume was reduced approximately to 1/3 by Speed Vac, and 50 μL of loading buffer was added. The mixture was heated at 75 °C for 3 min and cooled on the ice bath. The sample was loaded onto a preparative 20% denaturing polyacrylamide gel. The gel was UV shadowed; appropriate band was excised, extracted with 0.3 M sodium acetate and desalted using Sep-Pak classic C18 cartridge. Typical yields of the transcripts are 14–15 nmol. Transcript **4**, ε_{260} = 91000 $M^{-1}cm^{-1}$; transcript **5**, ε_{260} = 90340 $M^{-1}cm^{-1}$.

2.4.10 Charecterization of fluorescently modified transcript 5

*Mass analysis measurements of modified transcript **5***: Molecular weight of RNA transcript **5** was determined using Applied Biosystems 4800 Plus MALDI TOF/TOF analyzer. 1 μL of a ~150 μM stock solution of the transcript was combined with 1 μL of 100 mM ammonium citrate buffer (pH 9), 1 μL of a 100 μM DNA standard (18-mer) and 4 μL of saturated 3-hydroxypiccolinic acid solution. The samples were desalted with an ion exchange resin (*Dowex 50W-X8*, 100-200 mesh, ammonium form) and spotted on the MALDI plate, and were air dried. The resulting spectra were calibrated relative to an internal 18-mer DNA standard.

*Enzymatic digestion of modified transcript **5***: Approximately 4 nmol of the transcript **5** from the large scale transcription reaction was digested with snake venom phosphodiesterase I, calf intestine alkaline phosphatase and RNase A in 50 mM $MgCl_2$, 0.1 mM EDTA for 12 hr at 37^0C. The mixture was further treated with RNase T1 for 3 hr at 37 ^{o}C. The ribonucleoside mixture obtained was analyzed by reverse phase HPLC using Luna 5 micron C18 column (4.6 x 250 mm, 100 Å) at 260 nm and 320 nm.

2.4.11 Photophysical Characterization of Transcript 5

Steady-state fluorescence of benzo[b]thiophene-modified duplexes: Oligoribonucleotide **5** (10 μM) was annealed to custom DNA and RNA oligonucleotides (**6**−**10**, 11 μM) by heating a 1:1.1 mixture of the oligonucleotides in 20 mM cacodylate buffer (pH 7.1, 500 mM NaCl, 0.5 mM EDTA) at 90 °C for 3 min and cooling the samples slowly to room

temperature, followed by incubating the solutions in crushed ice. Samples were diluted to give a final concentration of 1 μM (with respect to **5**) in cacodylate buffer. Fluorescently modified duplex constructs were excited at 320 nm with an excitation slit width of 10 nm and emission slit width of 12 nm. Fluorescence experiments were performed at 18 °C in a micro fluorescence cell (Hellma, path length 1.0 cm) on a Horiba Jobin Yvon, Fluorolog-3.

Time-resolved fluorescence measurements of benzo[b]thiophene-modified duplexes: Lifetimes of the duplexes (2 μM) were determined under the same conditions as mentioned above using TCSPC instrument (Horiba Jobin Yvon, Fluorolog-3). Fluorescently modified oligoribonucleotides were excited using 339 nm LED source (IBH, UK, NanoLED-339L) with a band pass of 10 nm and fluorescence signal at respective emission maximum was collected. Experiments were performed in duplicate and decay profiles were analyzed using IBH DAS6 analysis software. Fluorescence intensity decay profiles for all oligonucleotide constructs were found to be biexponential with χ^2 (goodness of fit) values very close to unity.

2.4.12 Gel Mobility Shift Experiments using α^{32}P-Labeled Oligoribonucleotide 5

^{32}P-labeled oligoribonucleotide **5** was synthesized by transcription reaction using α-^{32}P ATP in the presence of template **T1**. Transcription reaction was performed in 40 mM Tris-HCl buffer (pH 7.9) containing 300 nM annealed template **T1**, 15 mM $MgCl_2$, 10 mM NaCl, 10 mM dithiothreitol (DTT), 2 mM spermidine, 0.4 U/μL RNase inhibitor (RiboLock), 0.4 mM GTP, 0.4 mM CTP, 1 mM modified UTP **3**, 40 μM ATP, 25 μCi α-^{32}P ATP and 3.2 U/μL T7 RNA polymerase in a total volume of 50 μL. After 6 h at 37 °C, reactions were quenched by adding 25 μL of the loading buffer, heated to 75 °C for 3 min and cooled on an ice bath. The sample was loaded onto a preparative 20% denaturing polyacrylamide gel. The radioactive band corresponding to the full-length RNA transcript **5** was excised and extracted with 0.3 M sodium acetate, and finally desalted using Sep-Pak classic C18 cartridge.

Non-radiolabelled transcript RNA **5** was doped with ^{32}P-labeled **5**, and was annealed to custom DNA and RNA oligonucleotides (**6**−**10**) under the same conditions used in the fluorescence experiments. To each sample was added 5 μL of non-denaturing loading buffer (10 mM Tris-HCl, pH 8, 500 mM NaCl, 30% sucrose, 10% glycerol, 0.05%

bromophenol blue), and samples (6 μL) were loaded onto an analytical 18% non-denaturing polyacrylamide gel containing 500 mM NaCl. The gel was electrophoresed in TBE buffer (90 mM Tris, 90 mM boric acid and 2 mM EDTA) containing 500 mM NaCl at ~20 °C (150 V). The buffer was recirculated using peristaltic pump. The products on the gel were exposed to X-ray film (3 h), and the exposed film was developed, fixed and dried.

2.5 References

(1) Rist, M. J., and Marino, J. P. (2002) Fluorescent nucleotide base analogues as probes of nucleic acid structure, dynamics and interactions. *Curr. Org. Chem*., *6*, 775–793.

(2) Wilson, G. M. (2005) RNA folding and RNA-Protein binding analysed by fluorescence anisotropy and resonance transfer. *Rev. Fluoresc*, 223–243.

(3) Asseline, U. (2006) Development and application of fluorescent oligonucleotides. *Curr. Org. Chem. 10*, 491−518.

(4) Shi, X., and Herschlag, D. (2009) Fluorescence Polarization Anisotropy to Measure RNA Dynamics *Methods Enzymol. 469*, 288–302.

(5) Sinkeldam, R. W., Greco, N. J., and Tor, Y. (2010) Fluorescent analogues of biomolecular building blocks: Design, Properties, and Applications. *Chem. Rev. 110*, 2579–2619.

(6) Srivatsan, S. G., and Sawant, A. A. (2011) Fluorescent ribonucleoside analogues as probes for investigating RNA structure and function. *Pure Appl. Chem. 83*, 213–232.

(7) Daniels, M., and Hauswirth, W. (1971) Fluorescence of the Purine and Pyrimidine Bases of the Nucleic Acids in Neutral Aqueous Solution at 300°K. *Science*, *171*, 675–677.

(8) Peacourt, J.-M, L; Peon, J; and Kohler, B. (2000) Ultrafast internal conversion of electronically excited RNA and DNA nucleosides in water. *J. Am. Chem. Soc.*, *122*, 9348–9349.

(9) Hawkins, M. E. (2000) Fluorescent pteridine probes for nucleic acid Analysis. *Methods Enzymol.* 2008, *450*, 201–231.\

(10) Wilson J. N., and Kool. E. T. (2006) Fluorescent DNA base replacements: reporters and sensors for biological systems. *Org. Biomol. Chem.*, *4*, 4265–4274. Ranasinghe

(11) , R., T. and Brown T. (2005) Fluorescence based strategies for genetic analysis. *Chem. Commun., 2005*, 5487–5502.

(12) Thoresen L. H., Jiao, G.-S., Haaland,W. C., Metzker M. L. and Burgess K. (2003) Rigid, conjugated, fluoresceinated thymidine triphosphates: Syntheses and polymerase mediated incorporation into DNA analogues. *Chem. Eur. J.*, *9*, 4603–4610.

(13) Greco, N. J. and Tor, Y. (2005) Simple fluorescent pyrimidine analogues detect the presence of DNA abasic sites. *J. Am. Chem. Soc.*, *127*, 10784–10785.

(14) Teo, Y. N.; Wilson J. N. and Kool, E. T. (2009) Polyfluorophores on a DNA backbone: A multicolor set of labels excited at one wavelength. *J. Am. Chem. Soc.*, *131*, 3923–3933.

(15) Shandrick, S.; Zhao, Q.; Han, Q.; Ayida, B. K.; Takahashi, M.; Winters, G. C.; Simonsen, K. B.; Vourloumis, D. and Hermann, T. (2004) Monitoring molecular recognition of the ribosomal decoding site. .*Angew. Chem.*, 2004, 116, 3239– 3244

(16) Jeong, H. S., Kang, S., Lee, J. Y. and Kim, B. H. (2009) Probing specific RNA bulge conformations by modified fluorescent nucleosides. *Org. Biomol. Chem.*, *7*, 921–925.

(17) Xia, T. (2008) Taking fento second snapshots of RNA conformational dynamics and complexity. *Curr. Opin. Chem. Biol.*, *12*, 604–611.

(18) Hall, K. B. (2009) 2-aminopurine as a probe of RNA conformational transitions *Methods Enzymol.* 2009, *469*, 269–285.

(19) Ward, D. C., Reich, E., and Stryer, L. (1969) Fluorescence studies of nucleotides and polynucleotides. I. Formycin, 2-aminopurine riboside, 2, 6-diaminopurine riboside, and their derivatives. *J. Biol. Chem.*, *244*, 1228–1237.

(20) Kawai, M., Lee, M. J., Evans, K. O., and Nordlund, T. M. (2001) Temperature and base sequence dependence of 2-aminopurine fluorescence bands in single- and double-stranded oligodeoxynucleotides. *J. Fluoresc.*, *11*, 23–32.

(21) Rachofsky, E. L., Osman, R,. and Ross, J. B. A. (2001) Probing structure and dynamics of DNA with 2-Aminopurine: Effects of local environment on fluorescence. *Biochemistry, 40*, 946–956.

(22) Parsons, J., and Hermann, T. (2007) Conformational flexibility of ribosomal decoding-site RNA monitored by fluorescent pteridine base analogues. *Tetrahedron*, *63*, 3548–3552.

(23) Srivatsan, S. G., Greco, N. J., and Tor, Y. (2008) A highly emissive fluorescent nucleoside that signals the activity of toxic ribosome-inactivation proteins. *Angew. Chem., Int. Ed., 47*, 6661–6665.

(24) Zhang, C.-M., Liu, C., Christian, T., Gamper, H.; Rozenski, J., Pan, D., Randolph, J. B., Wickstrom, E., Cooperman, B. S., and Hou, Y.-M. (2008) Pyrrolo-C as a molecular probe for monitoring conformations of the tRNA 3' end. *RNA, 14*, 2245–2253.

(25) Jeong, H. S., Kang, S., Lee, J. Y., and Kim, B. H. (2009) Probing specific RNA bulge conformations by modified fluorescent nucleosides. *Org. Biomol. Chem., 7*, 921–925.

(26) Xie, Y., Maxson, T., and Tor, Y. (2010) Fluorescent ribonucleoside as a FRET Acceptor for tryptophan in native proteins. *J. Am. Chem. Soc., 132*, 11896–11897.

(27) Peacock, H., Maydanovych, O., and Beal, P. A. (2010) N^2-Modified 2-aminopurine ribonucleosides as minor-groove-modulating adenosine replacements in duplex RNA. *Org. Lett., 12*, 1044–1047.

(28) Wahba, A. S., Esmaeili, A., Damha, M. J., and Hudson, R. H. E. (2010) A single-label phenylpyrrolocytidine provides a molecular beacon-like response reporting HIV-1 RT RNase H activity. *Nucleic Acids Res., 38*, 1048–1056.

(29) Lakowicz, J. R. (2006*) Principles of Fluorescence Spectroscopy, 3rd ed.*, Springer, New York.

(30) Up to a 100-fold reduction in quantum yield is observed when 2AP is incorporated into oligonucleotides. See ref 19.

(31) Moffatt, J. G. (1964) General synthesis of nucleoside 5'-triphosphates. *Can. J. Chem., 42*, 599–604.

(32) Reichardt, C. (2008) Pyridinium-*N*-phenolate betaine dyes as empirical indicators of solvent polarity: Some new findings. *Pure Appl. Chem., 80*, 1415–1432.

(33) Reichardt, C. (1994) Solvatochromic dyes as solvent polarity indicators. *Chem. Rev., 94*, 2319–2358.

(34) Enzymatic ligation has also been employed to synthesize labeled RNAs. Höbartner, C., Rieder, R., Kreutz, C., Puffer, B., Lang, K., Polonskaia, A., Serganov, A., and Micura, R. (2005) Syntheses of RNAs with up to 100 nucleotides containing site-specific 2'-methylseleno labels for use in X-ray crystallography *J. Am. Chem. Soc., 127*, 12035–12045.

(35) Reider, R., Lang, K., Graber, D., and Micura, R.; (2007) Ligand-induced folding of the adenosine deaminase A-riboswitch and implications on riboswitch translational control. *ChemBioChem, 8,* 896-902.

(36) Huang, F., Wang, G., Coleman, T., and Li, N. (2003) Synthesis of adenosine derivatives as transcription initiators and preparation of 5' fluorescein- and biotin-labeled RNA through one-step *in vitro* transcription. *RNA, 9*, 1562–1570.

(37) Fiammengo, R., Musilek, K., and Jäschke, A. (2005) Efficient Preparation of Organic Substrate-RNA Conjugates via *in Vitro* Transcription. *J. Am. Chem. Soc., 127*, 9271–9276.

(38) Kimoto, M., Mitsui, T., Harada, Y., and Sato, A. (2007) Fluorescent probing for RNA molecules by an unnatural base-pair system. *Nucleic Acids Res., 35*, 5360–5369.

(39) Srivatsan, S. G., and Tor, Y. (2009) Enzymatic incorporation of emissive pyrimidine ribonucleotides. *Chem.–Asian J., 4*, 419–427.

(40) Stengel, G., Urban, M., Purse, B. W., and Kuchta, R. D. (2010) Incorporation of the fluorescent ribonucleotide analogue tCTP by T7 RNA polymerase. *Anal. Chem., 82*, 1082–1089.

(41) Transcription reactions are known to produce trace amounts of N+1 and N+2 products due to random incorporation of noncoded nucleotides. Milligan, J. F., and Uhlenbeck, O. C. (1989) Synthesis of small RNAs using T7 RNA polymerase. *Methods Enzymol., 180*, 51–62.

(42) Milligan, J. F., Groebe, D. R., Witherell, G. W. and Uhlenbeck, O. C. (1987) Oligoribonucleotide synthesis using T7 RNA polymerase and synthetic DNA templates. *Nucleic Acids Res., 15*, 8783–8798.

(43) Srivatsan, S. G., and Tor, Y. (2007) Fluorescent pyrimidine ribonucleotide: Synthesis, enzymatic incorporation, and utilization. *J. Am. Chem. Soc., 129*, 2044–2053.

(44) Berry, D. A., Jung, K.-Y., Wise, D. S., Sercel, A. D., Pearson, W. H., Mackie, H., Randolph, J. B., and Somers, R. L. (2004) Pyrrolo-dC and pyrrolo-C: fluorescent *analogues* of cytidine and 2'-deoxycytidine for the study of oligonucleotides. *Tetrahedron Lett., 45*, 2457–2461.

(45) Tinsley, R. A., and Walter, N. J. (2006) Pyrrolo-C as a fluorescent probe for monitoring RNA secondary structure formation. *RNA, 12*, 522–529.

(46) Omumi, A., Beach, D. G., Baker, M., Gabryelski, W., and Manderville, R. A. (2011) Exploring RNA transcription and turnover *in vivo* by using click chemistry. *J. Am. Chem. Soc.*, *133*, 42–50.

2.6 Appendix-I. Characterization Data of Synthesized Compounds

2.6.1 ^{1}H NMR spectrum of compound **2**

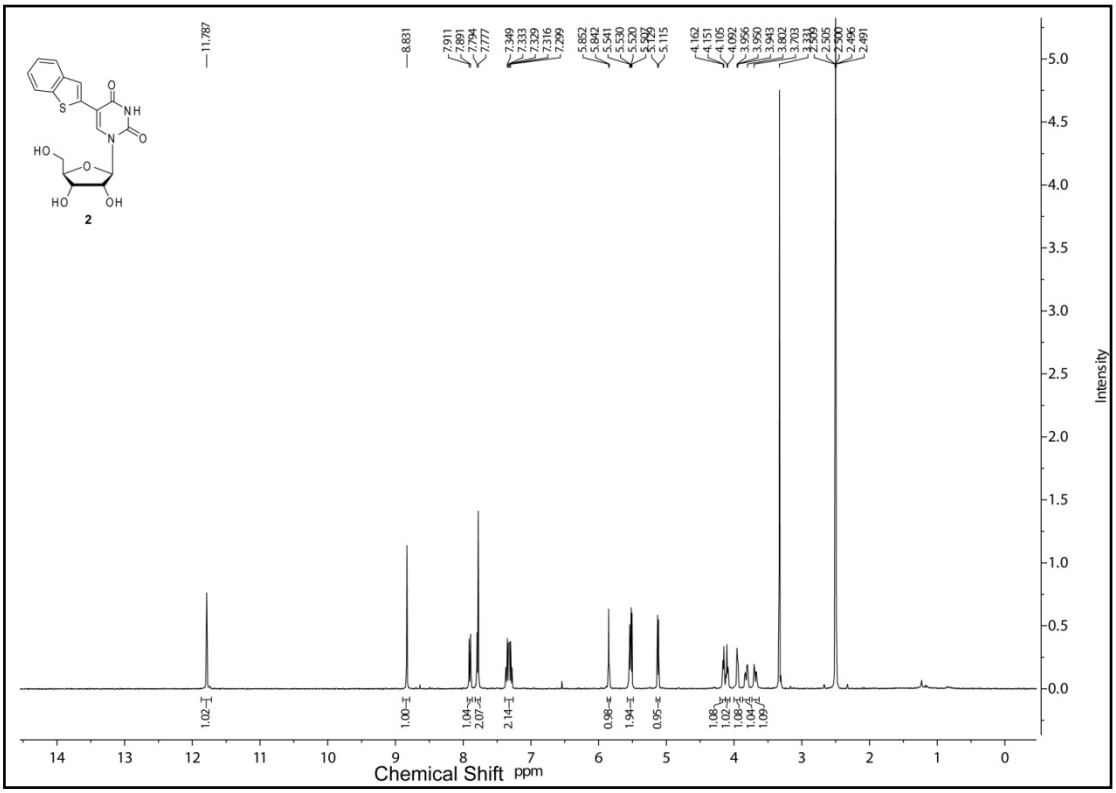

2.6.2 ^{13}C NMR spectrum of compound **2**

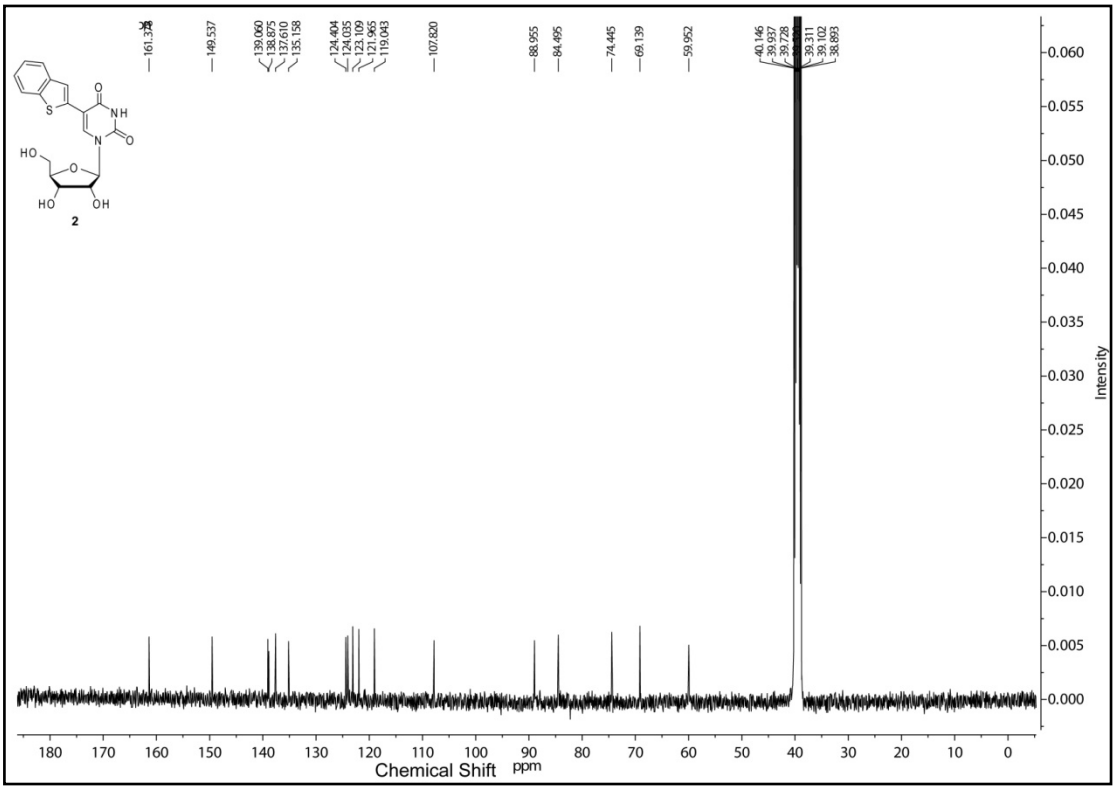

2.6.3 ^{1}H NMR spectrum of compound **3**

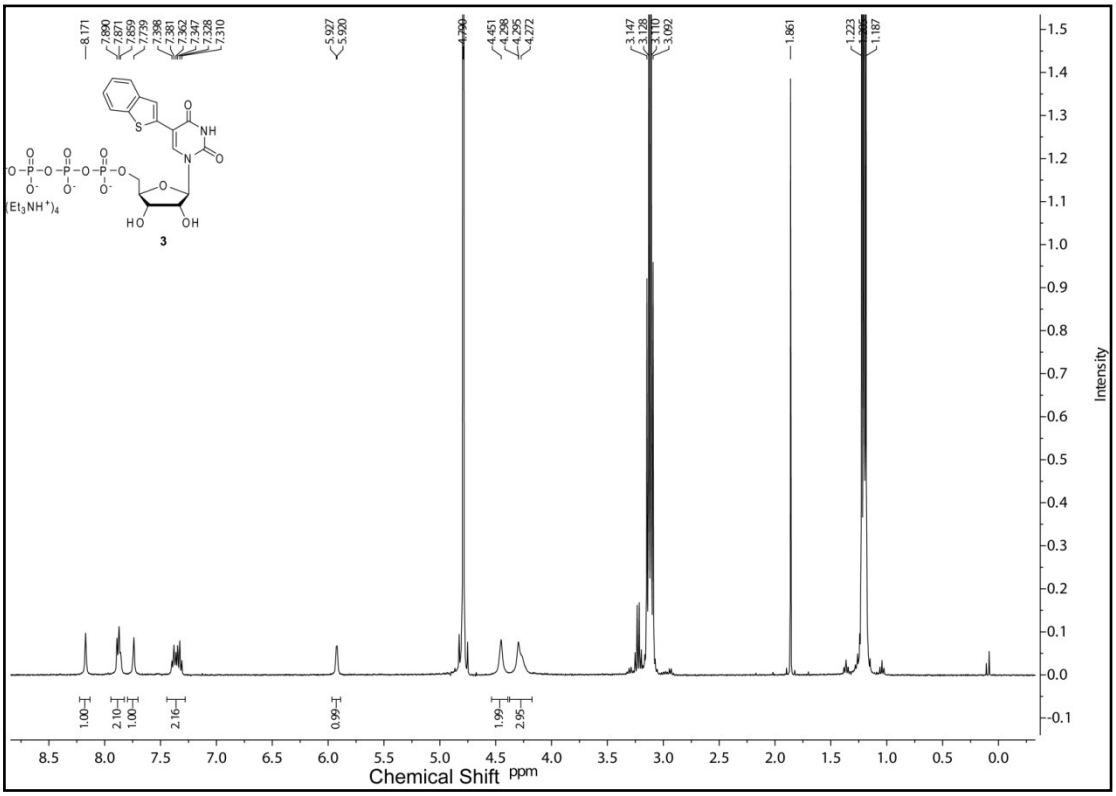

2.6.4 ^{13}C NMR spectrum of compound **3**

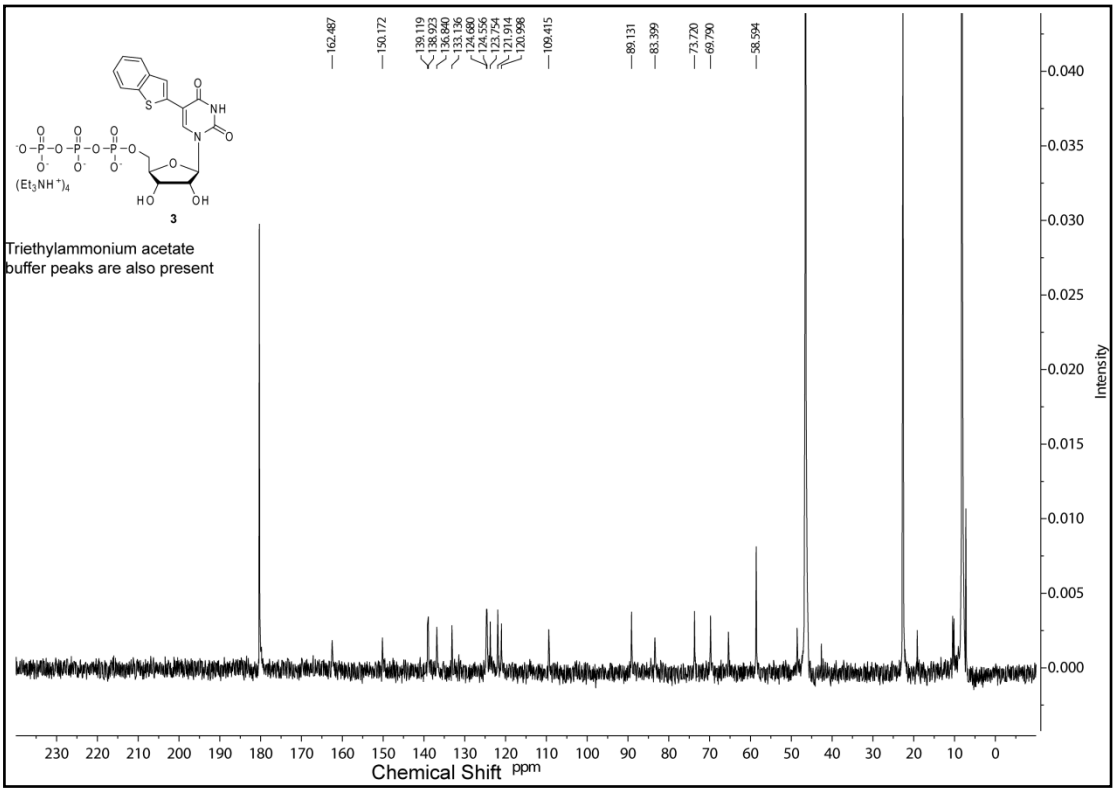

2.6.5 ^{31}P NMR spectrum of compound **3**

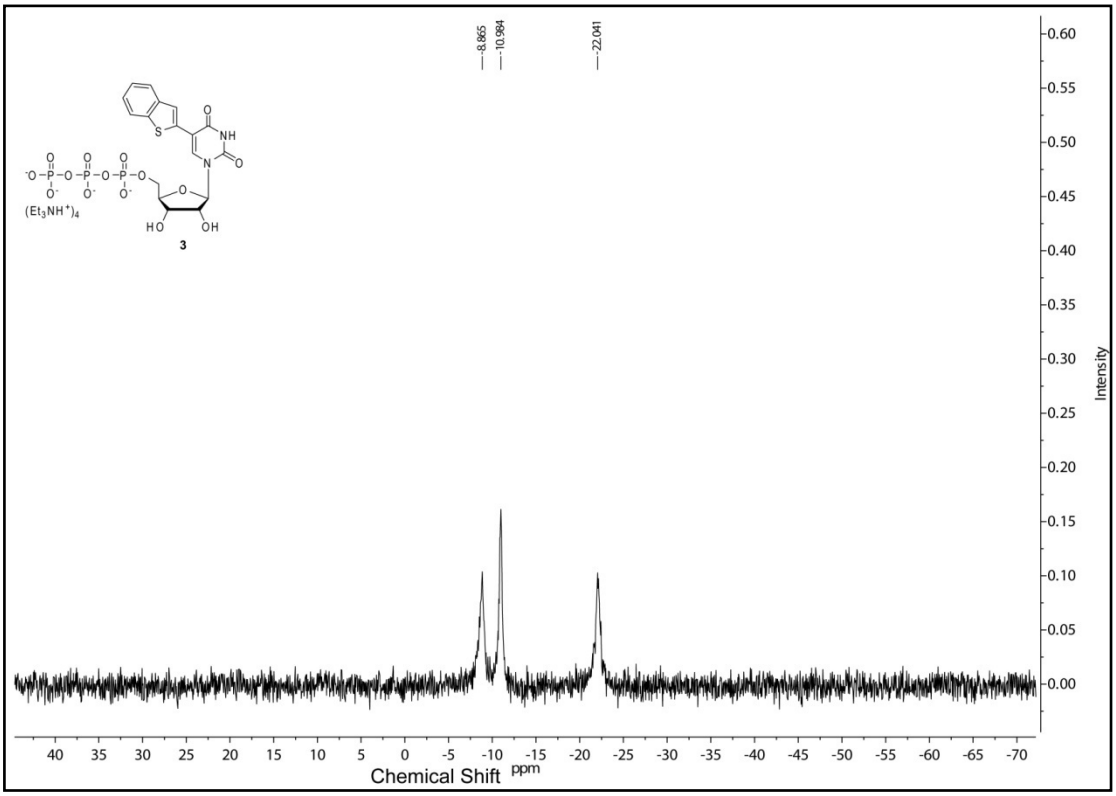

2.6.6 MALDI TOF Mass spectrum of oligonucleotide **5** HPLC digest

(A) MALDI-TOF mass spectrum of ribonucleoside Cytidine

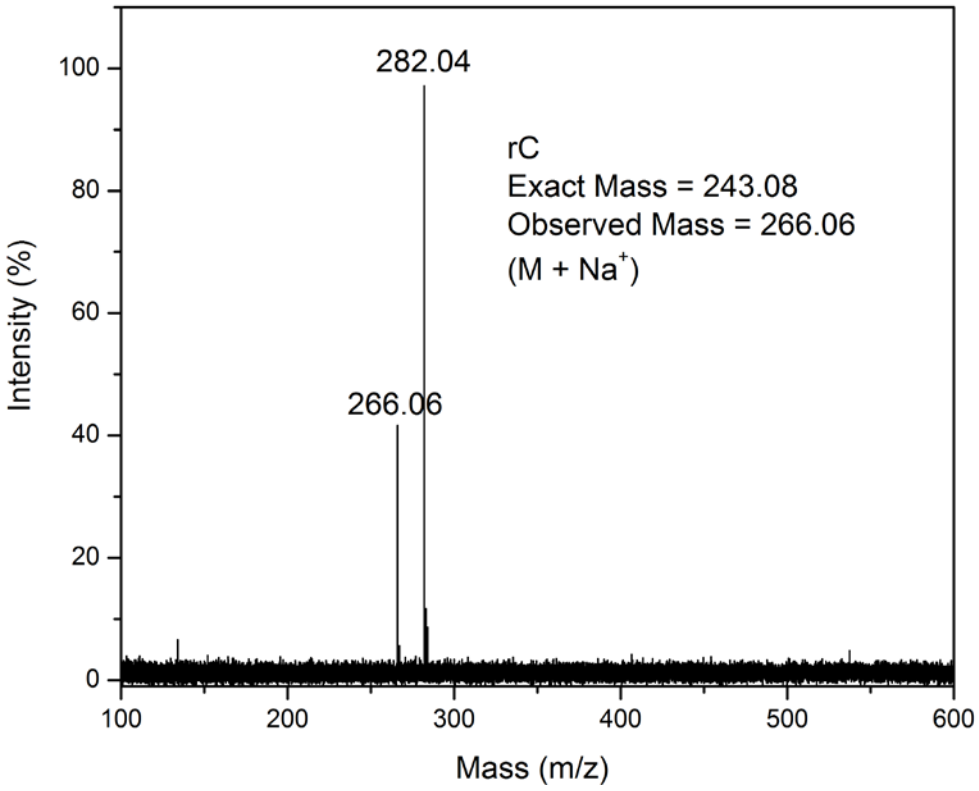

(B) MALDI-TOF mass spectrum of ribonucleoside Guanosine

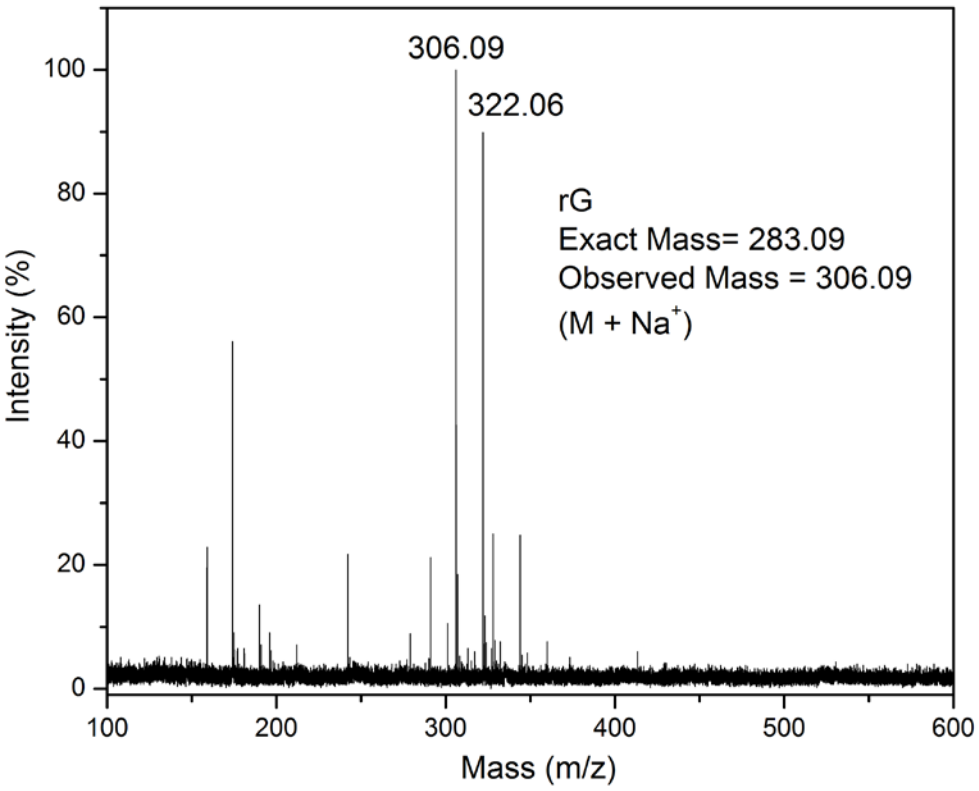

(C) MALDI-TOF mass spectrum of ribonucleoside Adenosine

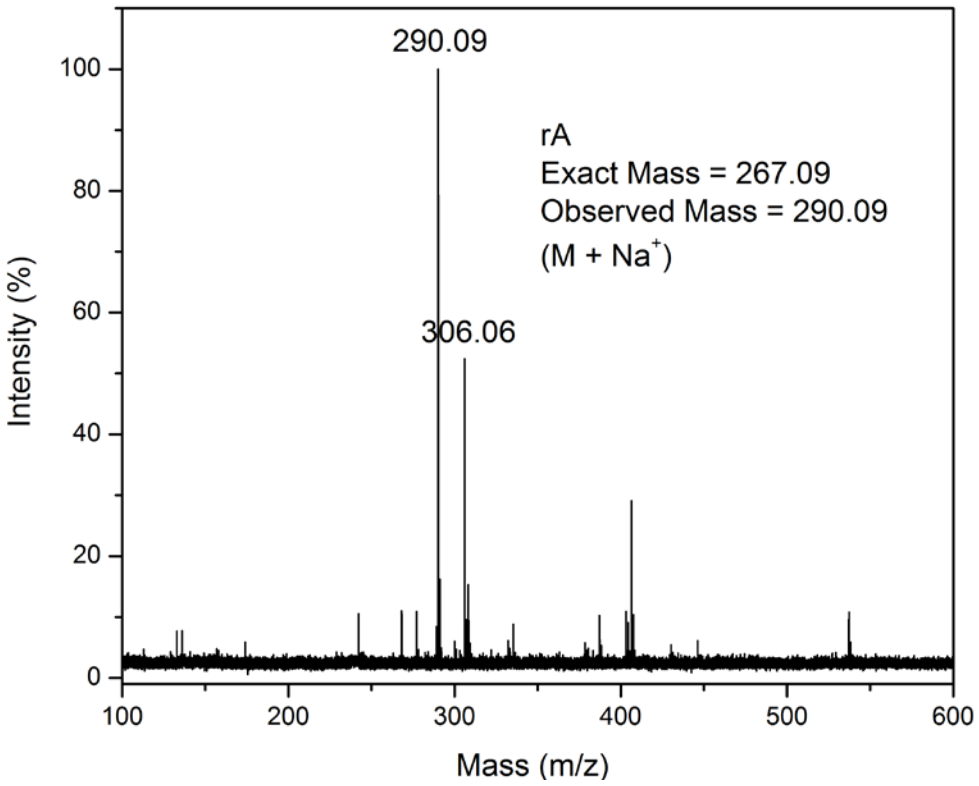

(D) MALDI-TOF mass spectrum of ribonucleoside **2**

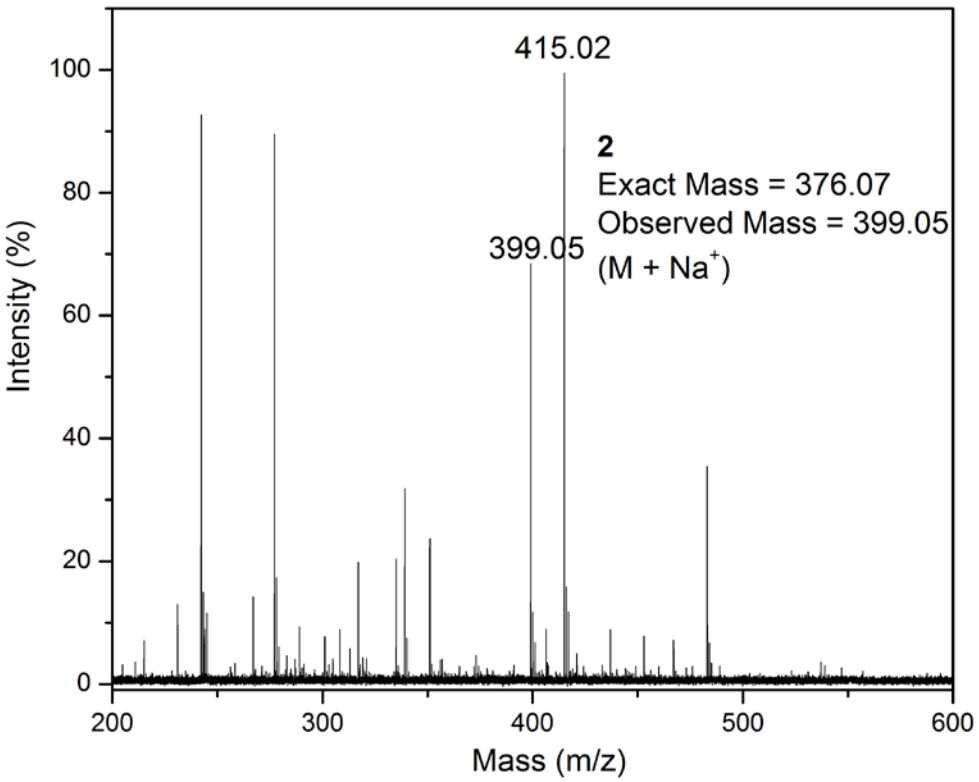

CHAPTER-3

5-Benzothiophene-Modified Uridine Analogue as a Fluorescence Probe for Studying Oligonucleotide Dynamics in a Model Cell-Like Compartment

3.1 Introduction

Nucleic acids carry out their functions by interacting with nucleic acids, proteins, and small-molecule metabolites, and during such processes, they often undergo significant conformational changes. Numerous biophysical tools have been developed to investigate these conformational changes and hence the dynamics and binding properties of nucleic acids *in vitro*.[1−10] Biophysical probes, in particular, fluorescent nucleoside analogues that closely resemble natural nucleosides and photophysically report conformational changes, have been instrumental in studying the dynamics and function of various nucleic acid motifs.[11−17] Some examples include (a) the detection of single nucleotide polymorphism (SNP)[18−23] and DNA and RNA lesions,[24−27] (b) monitoring of nucleic acid structural dynamics,[28−30] (c) the determination of binding affinities of therapeutically relevant nucleic acid−protein and nucleic acid−small molecule complexes,[31−35] and (d) the analysis of the electron-transfer process in nucleic acids.[36,37] However, the excitation maximum in the UV region and low quantum yields when incorporated into oligonucleotides have substantially limited the applications of the majority of fluorescent nucleoside analogues to *in vitro* systems only.[14] Interestingly, comparative studies in aqueous buffers and in membrane models, mimicking the physical properties and crowding that exist in a cellular environment, indicate that the structure, dynamics, activity, and recognition properties of biological macromolecules depend on the environment in which they are present.[38−42] Therefore, a fundamental understanding of the behavior of oligonucleotides in a model cellular milieu could provide new insights into nucleic acid folding and recognition properties, which may have implications for the discovery of drugs and diagnostic tools.

In general, water encapsulated in RM of amphiphilic surfactants, which resembles confined water in biological systems, has been used as a very good experimental model for studying the structure, dynamics, and function of biopolymers in a cell-like compartment.[43−52] One of the well characterized RM-forming surfactants, AOT (aerosol OT, dioctyl sodium sulfosuccinate), has the ability to solubilise substantial amounts of water in various nonpolar solvents.[53,54] RM formed by a ternary mixture of water/AOT/apolar solvent consists of nanometer-sized water droplets or water pools surrounded by surfactant molecules in such a way that the polar head groups are oriented toward the surface of the water pool and nonpolar tails are projected out toward the organic bulk phase (Figure 1). It has been well documented that the size of the aqueous micellar core increases linearly with w_0 (w_0 = [water]/[AOT]),[55] resulting in variations in the physical properties of the entrapped water such as dynamics,[56,57] polarity,[58,59]

viscosity,[60] and proton-transfer efficiency.[61,62] Attempts have been made to investigate the folding process of nucleic acids of varying masses (30−2700 kDa) in RM.[63−69] UV absorption, fluorescence, and circular dichroism (CD) measurements revealed that nucleic acids in RM are condensed. Goto and co-workers utilized the slower hybridization rates of DNA in RM to detect the presence of mismatched base pairs in DNA duplexes.[70] More recently, Flynn and Workman compared the conformational flexibility of two functionally important hairpin RNA motifs, HIV TAR and U4 snRNA, by NMR in RM and aqueous buffer.[71] Their results indicated that confinement restricted the conformational flexibility of both RNA motifs. On the basis of these reports, we envisioned that the photophysical characterization of oligonucleotides labeled with an environment-sensitive fluorescent nucleoside analogue probe in AOT RM would provide an alternative approach to study the structural dynamics and functions of oligonucleotides in a model cell-like confined environment. Such an endeavor would expand the scope of applications of fluorescent nucleoside analogue probes in general.

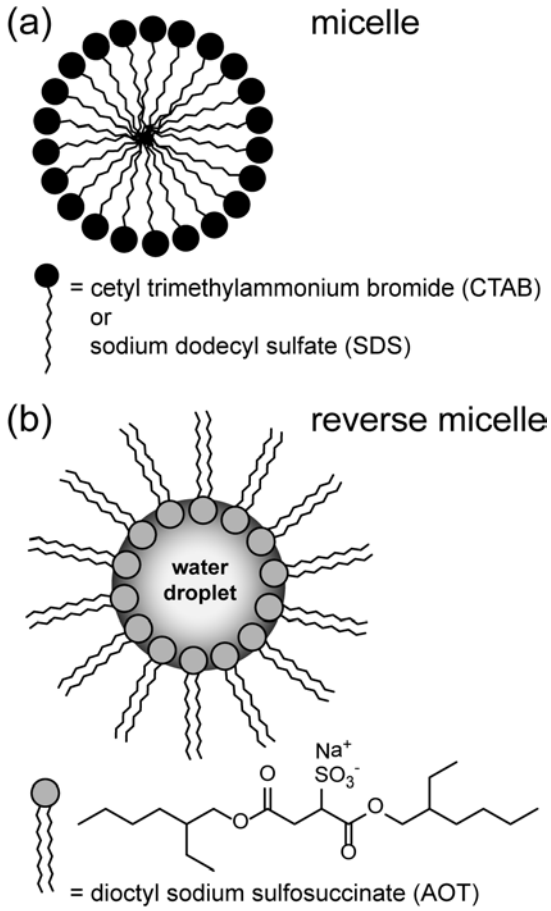

Figure 1. Schematic representation of (a) micelle and (b) reverse micelle.

In this context, we envisaged that the responsiveness of benzothiophene-modified ribonucleoside **1** to changes in its environment and minimally perturbing nature could be aptly utilized in studying the properties of oligonucleotides in RM. Here, we describe the photophysical properties of emissive ribonucleoside **1** in micelles and AOT RM as a function of surfactant concentration and water loading, respectively. Rewardingly, the ribonucleoside analogue reports the environment of these surfactant assemblies via changes in its fluorescence properties such as emission maximum, quantum yield, lifetime, and anisotropy. Furthermore, the photophysical characterization of the nucleoside analogue incorporated into oligonucleotides illustrates the potential of the emissive nucleoside as an efficient probe for studying the structural dynamics and function of nucleic acids in RM.

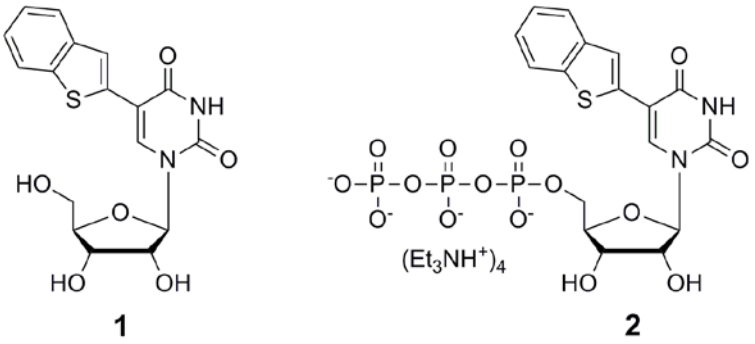

Figure 2. Structure of 5-benzothiophene-conjugated uridine **1** and corresponding triphosphate **2**.[72]

3.2 Results and Discussion

3.2.1 Photophysical Properties of Ribonucleoside 1 in Solvents of Different Polarity and Viscosity

Preliminary photophysical characterizations in solvents of different polarity and viscosity indicated that nucleoside analogue **1** could be utilized in studying the polarity and viscosity changes that occur in micellar systems.[72,75] The ribonucleoside analogue showed two distinct absorption maxima (Chapter 2, Figure 2), which were marginally affected by changes in solvent polarity (Table 1). However, the fluorescence properties of nucleoside **1** were found to be affected significantly by solvent polarity change while a solution of nucleoside in water, when excited at its lowest-energy maximum, displayed emission in the visible region (λ_{em} = 462 nm) with a quantum yield of 3.5% and a lifetime of 1.07 ns, a solution of nucleoside in dioxane displayed a blue-shifted emission (λ_{em} = 435 nm) with an enhanced quantum yield of 6.0% and a shorter lifetime of 0.45 ns.[72]

In the benzothiophene modified uridine analogue **1**, the fluorophore *i.e.* benzothiophene moiety is attached nucleobase by rotatable aryl-aryl single bond. When benzothiophene moiety rotates around single bond, the co-planarity between nucleobase and benzothiophene get disturbed which results in changes in the fluorescence properties of the nucleoside. When the benzothiophene moiety and nucleobase are coplanar, the fluorescence is highest whereas when co-planarity get disturbed, it is least. To know the effect of rotation, around single bond on the fluorescence of ribonucleoside **1,** we carried out its fluorescence studies in the solvents of different viscosities having almost similar polarities. When we excited a solution of nucleoside **1** in ethylene glycol ($\eta_{25°C}$ = 16.1 cP) showed a blue-shifted emission maximum corresponding to a nearly 3-fold enhancement in fluorescent intensity as compared to that in water ($\eta_{25°C}$ = 0.9 cP,). When measured in a more viscous solvent, glycerol ($\eta_{25°C}$ = 934 cP), a further enhancement in fluorescence intensity was observed with no apparent change in the emission maximum because the polarities of ethylene glycol and glycerol are similar (Figure 3, Table 1). Furthermore, as the solvent viscosity was increased, the nucleoside exhibited a longer lifetime and greater anisotropy as a result of the rigidification of the chromophore in a viscous solvent compared to the same parameters in a less-viscous solvent (Table 1, Figure 4).

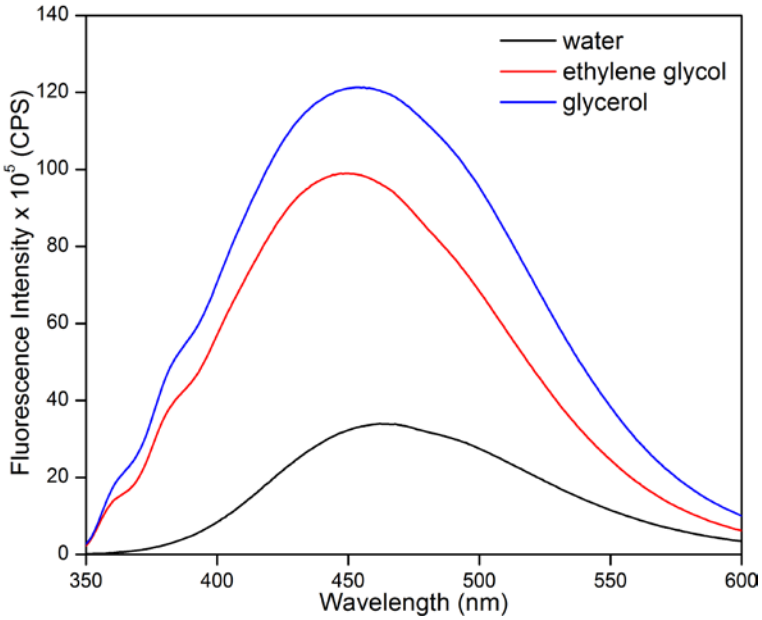

Figure 3. Emission spectra of ribonucleoside **1** (5 μM) in solvents of different viscosity. The ribonucleoside was excited at 318 nm (water) and 322 nm (ethylene glycol and glycerol).

Table 1. Photophysical properties of ribonucleoside **1** in different solvents.[72,75,76]

solvent	$E_T(30)^{77f}$ (kcal mol^{-1})	λ_{max1} (nm)	λ_{max2} (nm)	λ_{em} (nm)	Φ^a	$\tau_{ave}{}^a$ (ns)	$r^{a,b}$
water	63.1	274	318	462	0.035	1.07	0.037
methanol	55.4	274	321	446	0.047	0.60	-
dioxane	36.0	275	322	435	0.060	0.45	-
ethylene glycol	53.8	275	322	450	0.103	1.68	0.167
glycerol	57.0	275	322	454	0.139	2.02	0.308

[a] Standard deviations for quantum yield (Φ), average lifetime (τ_{av}) and anisotropy (r) are ≤0.003, 0.02 ns, and 0.005, respectively. [b] r values reported here are blank uncorrected.

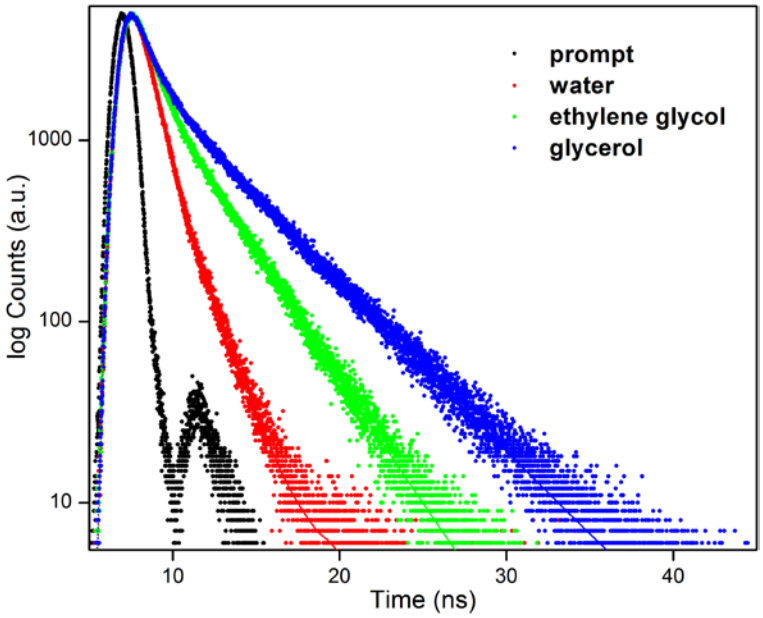

Figure 4. Excited-state decay profile of ribonucleoside **1** in solvents of different viscosity. Laser profile is shown in black (prompt). Curve fits are shown in solid lines.

The solvent dipolar relaxation process can affect the emission maximum of a polar fluorophore upon excitation at the red edge of the absorption band.[78,79] The dipolar relaxation process can be studied by performing a red-edge excitation shift (REES) experiment in which the fluorophore excited at the red edge of the absorption band results in the shift of the emission maximum to longer wavelengths. Typically, the REES effect is observed when a fluorophore is in a motionally restricted environment (*e.g.*, viscous solvents, micelles, liposomes, and proteins) in which the rate of solvent relaxation is comparable to the lifetime of the fluorophore.[78–83] Hence, REES can be used as a marker for probing the dynamics of a solvent and the environment of a fluorophore. To study the dependence of the emission maximum on the excitation wavelength, we examined the emission profile of ribonucleoside **1** in glycerol. Upon increasing the excitation

wavelength from 310 nm to the red edge of the absorption spectrum (380 nm), we observed a discernible red shift (10 nm) in the emission maximum, which resembles the solvent-relaxed emission profile in water (Figure 5). This result indicates that ribonucleoside **1**, which exhibits a solvent dipolar relaxation process, can be potentially used as a probe to study the dynamics and polarity of its immediate environment in a motionally restricted medium.

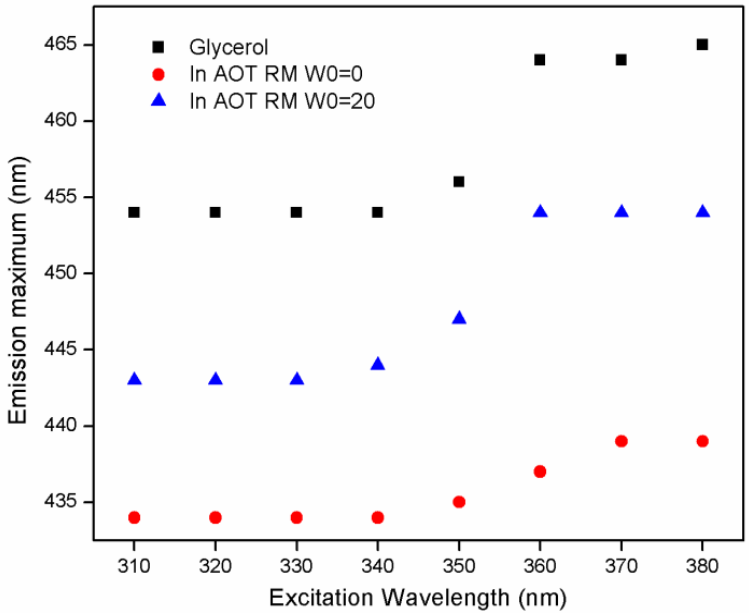

Figure 5. Dependence of emission maximum of ribonucleoside **1** (5 μM) as a function of excitation wavelength in glycerol and AOT RM (w_0 = 0 and 20) at 24 ºC

3.2.2 Fluorescence Properties of Ribonucleoside 1 in Anionic and Cationic Micelles

Surfactants such as SDS and CTAB in aqueous solutions form micellar aggregates above a certain concentration called the critical micelle concentration (cmc, Figure 1). The physical properties (*e.g.*, polarity and viscosity) of surfactant solutions above and below the cmc are significantly different, and hence fluorescent probes that interact with specific domains of micelles have been utilized in understanding the morphology and aggregation mechanism and determining the physical properties of micelles.[84–88] Pyrene and its derivatives, prodan and coumarin dyes, are some of the commonly used probes in the determination of the cmc of surfactant solutions.[84–88] Consequently, these studies prompted us to evaluate the usefulness of benzothiophene conjugated uridine **1** in monitoring the aggregation process of the surfactant solutions. The emission spectrum of **1** has been recorded in aqueous solutions of anionic (SDS) and cationic (CTAB) surfactants. The nucleoside in an aqueous solution containing SDS at a concentration well below its

cmc shows an emission band similar to that in water (Figure 6a). As the concentration of SDS is increased, there is a significant increase in fluorescence intensity, which saturates at high concentrations of the surfactant. A similar trend is also observed when the fluorescence of nucleoside **1** is measured in aqueous solutions containing increasing concentration of CTAB (Figure 7a). A plot of intensity at λ_{em} = 465 nm as a function of surfactant concentration gave a typical sigmoidal profile for both surfactants (Figures 6b and 7b). The cmc of SDS (9.3 ± 0.2 mM) and CTAB (0.96 ± 0.01 mM) determined from these plots have been found to be in reasonable agreement with the literature reports (8.0−8.5 and 0.92−1.1 mM, respectively).[73,89]

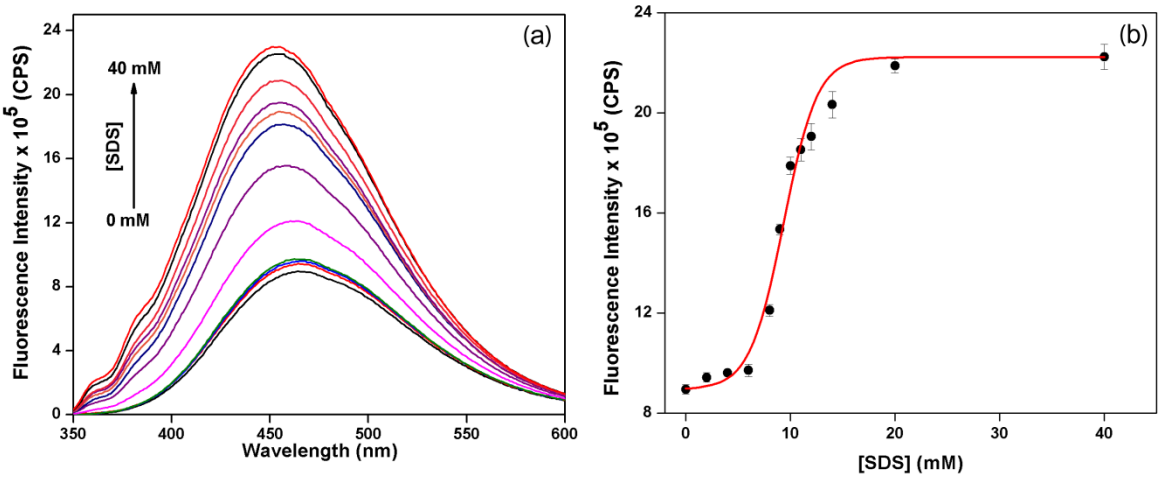

Figure 6. (a) Emission spectra of aqueous solutions of ribonucleoside **1** (5 μM) containing increasing concentration of SDS. (b) A plot of fluorescence intensity of **1** at 465 nm as a function of SDS concentration.[75]

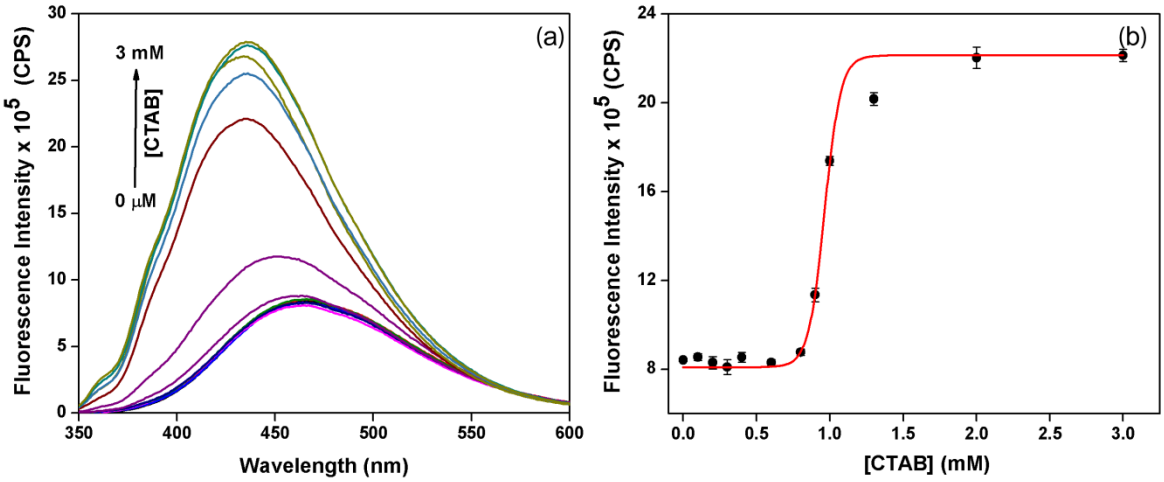

Figure 7. (a) Emission spectra of aqueous solutions of ribonucleoside **1** (5 μM) containing increasing concentrations of CTAB. (b) A plot of fluorescence intensity of **1** at 465 nm as a function of CTAB concentration.[75]

A significant increase in fluorescence intensity accompanied by a small spectral shift toward the blue region upon increasing the concentration of the surfactant above the cmc can be explained as follows. At low surfactant concentrations, the emissive nucleoside is solubilized in a more-polar, less-viscous aqueous medium and hence shows quenched emission. This observation is in agreement with the behavior of the nucleoside in solvents of different polarity and viscosity (Table 1). Upon increasing the concentration of the surfactants to above the respective cmc values, the nucleoside gets solubilized in less polar, more-rigid micellar aggregates, resulting in an enhancement of the fluorescence intensity. Excited-state decay kinetics analysis indicates that the environment around the fluorophore is distinctly different at surfactants concentration below and above respective cmc values (Table 2, Figure 8).

Table 2. Excited-state lifetime and fluorescence anisotropy of ribonucleoside **1** (5 μM) in SDS and CTAB.[75]

surfactant	[surfactant] (mM)	$\tau_{ave}{}^{a}$ (ns)	$r^{a,b}$
SDS	4.0	1.16	0.038
	9.0	1.72	0.055
	20.0	2.03	0.067
CTAB	0.4	1.21	0.040
	1.0	1.93	0.090
	3.0	2.15	0.109

[a]Standard deviations for the average lifetime (τ_{ave}) and anisotropy (r) are ≤0.02 ns and 0.002, respectively. [b]r values reported here are blank uncorrected.

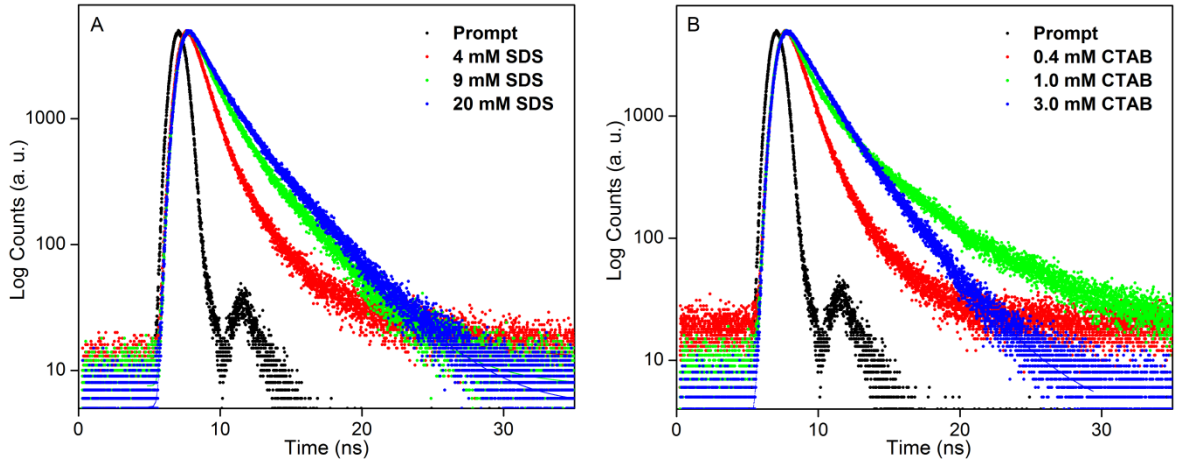

Figure 8. Excited-state decay profile of aqueous solutions of ribonucleoside **1** (5 μM) in various concentrations of SDS (A) and CTAB (B). Laser profile is shown in black (prompt). Curve fits are shown in solid lines.

Furthermore, a higher fluorescence anisotropy at a surfactant concentration above the cmc as compared to that of an aqueous solution containing a low surfactant concentration indicates that benzothiophene-conjugated uracil is rigidified by the incorporation of the nucleoside within the micellar aggregates (Table 2). On the basis of the above results, it is likely that the benzothiophene-conjugated base is embedded in the hydrocarbon continuum and its hydrophilic sugar moiety is anchored on the micellar surface. Earlier studies have also predicted similar type of interactions with micelles when using probes made of hydrophilic and hydrophobic moieties.[84,90]

3.2.3 Fluorescence Properties of Ribonucleoside 1 in AOT RM

The encapsulated water in RM is characterized by a "bound" water close to the interface, which is involved in the hydration of the head groups and counterions, and "free" bulk water in the inner region (Figure 1b).[91] At low water content ($w_0 < 8$), there are fewer water molecules to form a well-defined water pool because most of the water molecules interact with head groups and counterions, forming a domain of structured water that has significantly reduced motion compared to bulk water.[91] As the water-surfactant ratio is increased, a free water pool that exhibits variations in physical parameters (*e.g.*, polarity, viscosity, and water motion) starts to emerge.[92,93] Typically, an increase in the size of the surfactant-entrapped water pool results in a decrease in the microviscosity and an increase in the micropolarity of the solubilized water.[58−60] Extensive solvation dynamics studies using ultrafast time resolved spectroscopy also reveal that the motion of water in RM is significantly slower as compared to that in bulk water.[94−99]

Several techniques, in particular, fluorescence-based methods, have been utilized in investigating the dynamics, polarity, viscosity, and acid−base reactivity of the confined water as a function of w_0 values.[54,56−60,100] Most of these methods utilize environment-sensitive fluorescent probes, which have an affinity of one or more of the micellar domains such as the water pool, surfactant interface, or hydrocarbon continuum. While 1,8-anilinonaphthalene sulfonate (**3**), pyrenesulfonicacid (**4**), 1-aminonaphthylene-4-sulfonic acid (**5**), rhodamine B (**6**), auramine O (**7**), and pyranine (**8**) are solubilized in the aqueous micellar core, amphiphilic pyrene, indole, and tryptophan derivatives are localized in the surfactant interface.[59] Interestingly, depending on the water loading, prodan has been shown to be present in the inner water pool, AOT interface, and nonpolar solvent phase.[59,83]Although extensively utilized in several fluorescence assays, these

probes are relatively large. Hence, when introduced site-specifically (*e.g.*, site of interaction) into target oligonucleotides, they are likely to perturb the native structure of oligonucleotides. Because benzothiophene-modified ribonucleoside **1** is structurally minimally invasive,[72] we decided to evaluate the efficacy of the ribonucleoside to sense the environment of AOT RM as a function of w_0.[101]

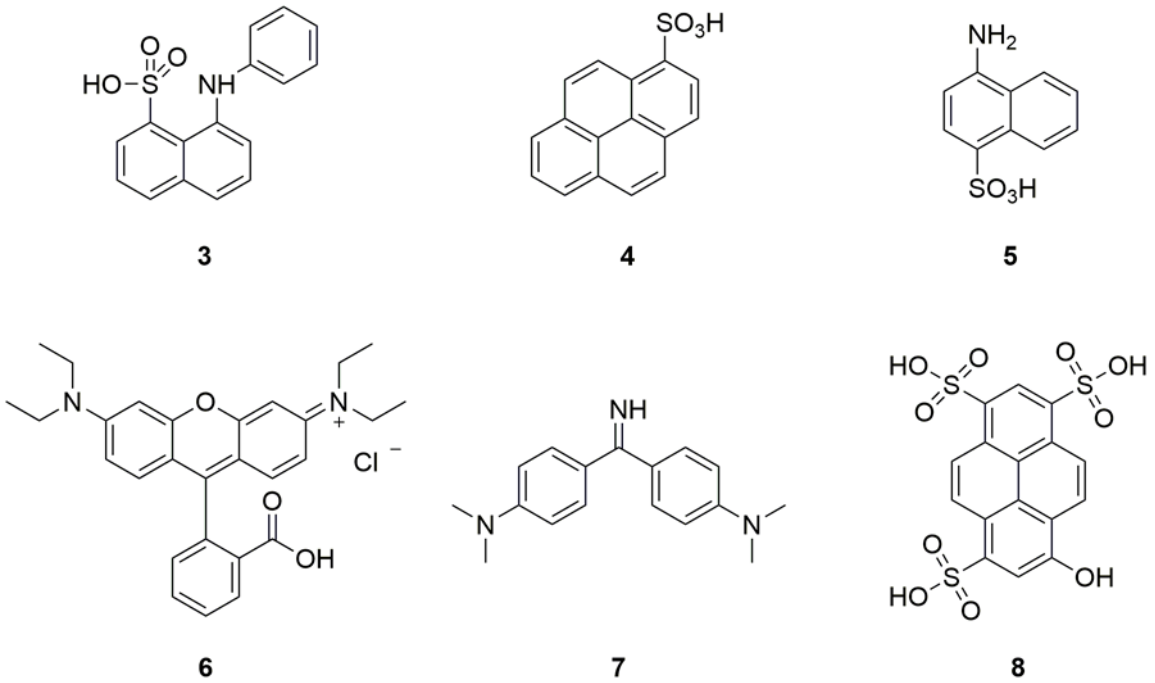

Figure 9. Different environment sensitive fluorescent probes used to study confined environment in RM.

Stock solutions of AOT RM in heptane with increasing w_0 values are prepared by adding appropriate amounts of the stock solutions in water such that the concentration of nucleoside **1** is maintained at 5 μM.[75,102–104] At low w_0 values (0.7−1.4), the nucleoside shows an intense blue-shifted emission band (λ_{em} = 432 nm) as compared to the free nucleoside in water (λ_{em} = 462 nm, Figure 10). When samples with increasing w_0 values are excited, the nucleoside exhibits significant quenching in fluorescence intensity and a red-shifted emission maximum, which starts to saturate around w_0 = 22 (Figure 10). The emission maximum near the saturation point (~443 nm) is close to the emission maximum of the free nucleoside in methanol (Table 1). Earlier studies using fluorescent dyes that have been used to probe the polarity of AOT RM have also revealed an environment similar to that of methanol in the micellar core.[105,106] The excited-state decay kinetics of nucleoside **1** has been analyzed by time-resolved fluorescence spectroscopy at varying w_0

values. Upon increasing the water loading, the lifetime decreases progressively and levels off at w_0 = 22, which is consistent with the above steady-state fluorescence data (Figure 10, Table 3). Similarly, fluorescence anisotropy measurements indicate that the water pool in RM is very viscous as compared to the free water (Table 3).

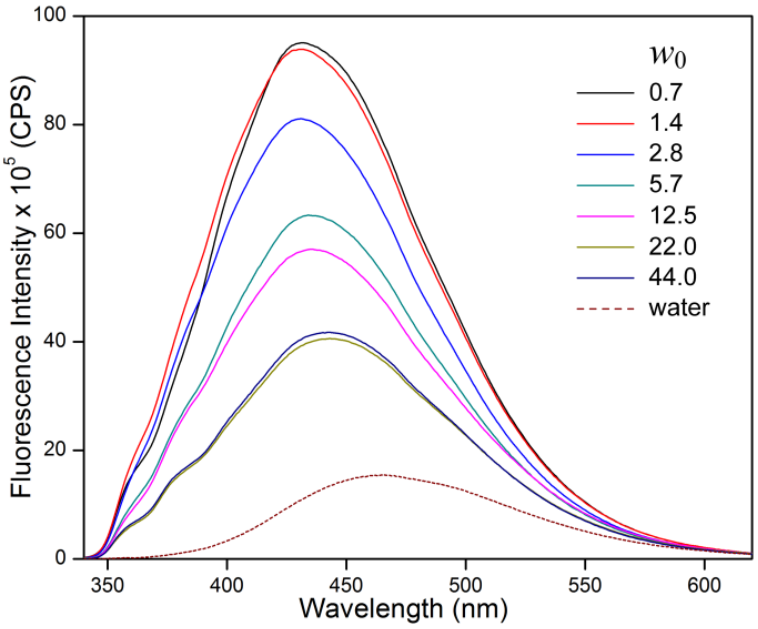

Figure 10. Emission spectra of ribonucleoside **1** (5 μM) in AOT RM as a function of w_0.

The ability of an emissive nucleoside to report the environment of the water pool in RM will depend on the partitioning of the nucleoside in a specific domain at a given w_0 value. On the basis of the above photophysical characterizations, the location of the charge-neutral nucleoside analogue in RM can be predicted. At low water content, a well-defined water pool does not exist, and hence it is likely that the nucleoside resides at the AOT−water interface, which is rigid and less polar. As a result, the nucleoside shows high intensity and a blue-shifted emission maximum. However, as the water content in RM is increased the nucleoside percolates from a more-rigid, less-polar environment to a less-rigid, more-polar water pool. This notion is supported by the fact that the nucleoside exhibits fluorescence quenching, a red-shifted emission maximum, and reduced anisotropy upon increasing the water/AOT molar ratio. Upon performing REES experiments in AOT RM, ribonucleoside **1** exhibits a significant red shifted emission maximum (11 nm) at w_0 = 20 as compared to that at w_0 = 0 (Figure 5). This observation indicates the heterogeneity in the fluorophore−solvent interactions in the confined environment. Because ribonucleoside **1** can report the environment in RM in the form of changes in fluorescence properties such as the fluorescence intensity, emission maximum, lifetime, and anisotropy, we decided to

study the photophysical behavior of oligonucleotides labeled with the emissive nucleoside in RM.

Table 3. Excited-state life time and fluorescence anisotropy of ribonucleoside **1** in AOT RM at different w_0 values.

w_0	τ_{Ave} [a] (ns)	$r^{a,b}$
0.7	1.26	nd
1.4	1.08	nd
2.8	1.01	0.186
5.7	0.68	0.176
12.5	0.46	0.143
22.0	0.46	0.148
44.0	0.51	0.125
In water	1.07	0.037

[a] Standard deviations for average lifetime (τ_{ave}) and anisotropy (r) at different w_0 values are ≤ 0.07 ns and 0.004, respectively. nd = not determined. [b] r values reported are blank uncorrected.

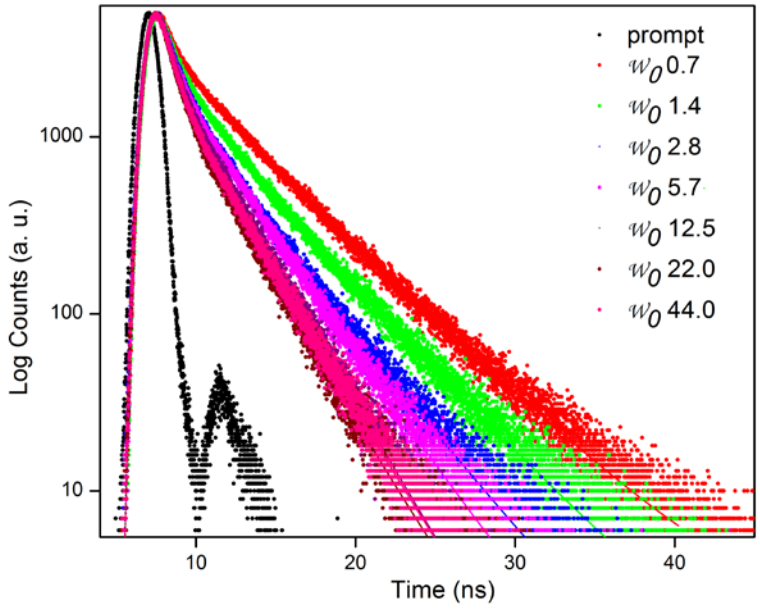

Figure 11. Excited-state decay profile of ribonucleoside **1** in AOT RM at different w_0 values. Laser profile is shown in black (prompt). Curve fits are shown in solid lines.

3.2.4 Dynamic Light Scattering Studies of Ribonucleoside 1 in AOT RM at w_0 = 20

To study the effect of encapsulation of modified ribonucleoside **1** on the size of reverse micelles, we performed dynamic light scattering studies of reverse micelles at w_0 = 20, in presence and absence of modified ribonucleoside **1**. The size of RM found in absence of modified ribonucleoside **1** was 10.7 ± 0.1 nm and in presence of it 11.7 ± 0.1 nm. This observed value in absence of modified ribonucleoside **1** of RM is in good agreement with

literature values[103,104]. From this observation, we can conclude the encapsulation of modified ribonucleoside **1** in RM slightly affect the size of by 1 nm. (Figure 12)

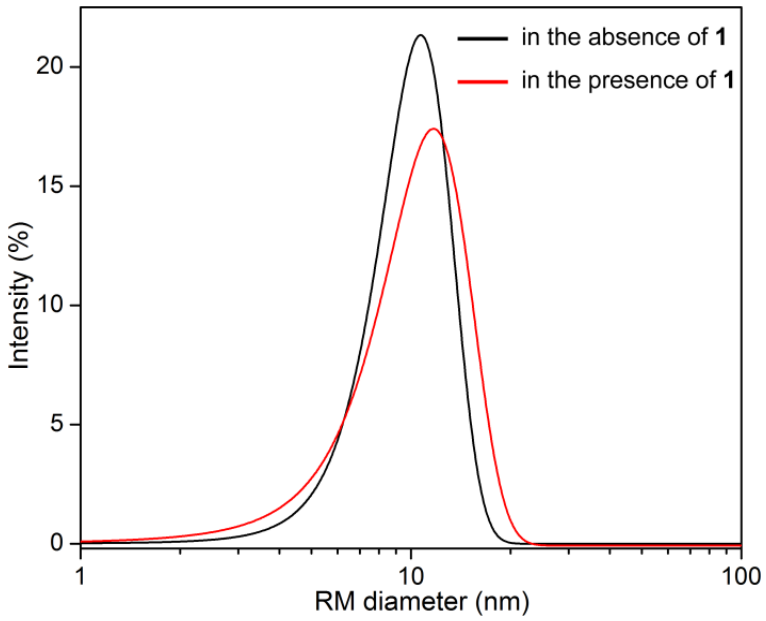

Figure 12. DLS profile of AOT RM at w_0 = 20 in the absence and presence of ribonucleoside **1** at 24 ºC.

3.2.5 Fluorescence Properties of Oligonucleotides 9 Labeled with Ribonucleoside 1 in AOT RM

The amicability of benzothiophene-modified UTP **2** to enzymatic incorporation allowed the easy synthesis of RNA oligonucleotide **9** containing fluorescent label **1** by *in vitro* transcription reactions (Figure 13).[75,107–112] The effect of benzothiophene modification on the hybridization efficiency of oligoribonucleotide **9** was evaluated by performing UV-thermal denaturation and native-gel retardation experiments. The results revealed that the modified oligoribonucleotide formed stable duplexes with complementary oligonucleotides with only a minor reduction in thermal melting temperatures.[72]

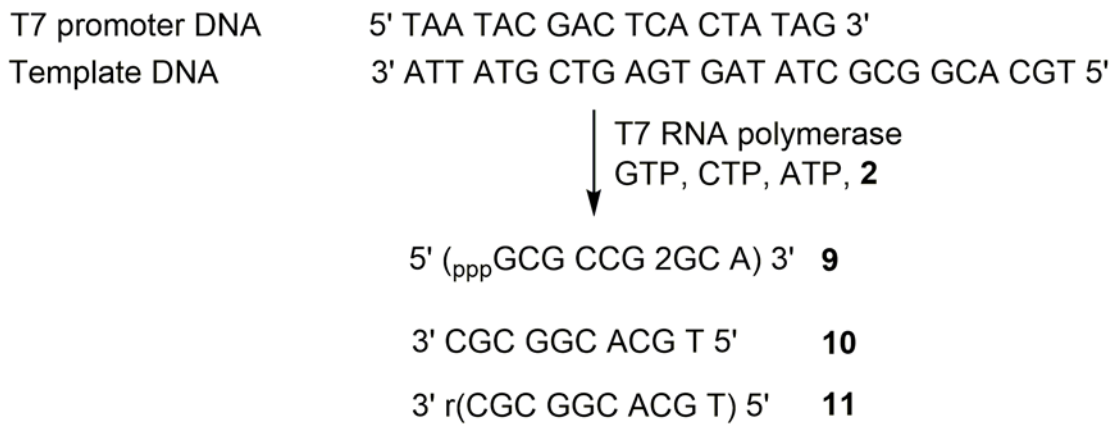

Figure 13. Synthesis of fluorescently modified RNA oligonucleotide **9** by *in vitro* transcription reaction in the presence of modified UTP **2** and T7 RNA polymerase.[75] Sequence of complementary DNA and RNA oligonucleotides **10** and **11**, respectively, used in this study.

The conformational flexibility and hybridization rates of oligonucleotides have been studied by NMR and UV absorption spectroscopy, respectively, in AOT RM at w_0 = 20.[70,71] Hence, we studied the photophysical behavior of fluorescent RNA oligonucleotide **9** and corresponding complementary RNA·DNA (**9•10**) and RNA·RNA (**9•11**) duplexes in AOT RM at w_0 = 20. Appropriate amounts of the oligonucleotide stock solutions in cacodylate buffer (pH 7.6) were added to AOT RM such that the concentration of the oligonucleotides and w_0 value were maintained at 2 μM and 20, respectively. Upon excitation, RNA oligonucleotide **9** in RM displayed a slightly red-shifted, quenched emission band as compared to the free nucleoside in RM (Figure 14, Figure 15 Table 4). Interestingly, duplexes **9•10** and **9•11** exhibited discernible enhancements in fluorescence intensity as compared to single-stranded oligoribonucleotide **9**. This observation is uncommon because most of the fluorescent nucleoside analogues, when incorporated into single- and double-stranded oligonucleotides, show significant quenching in fluorescence intensity in aqueous buffers.[14] Consequently, the fluorescence properties of oligonucleotides were also evaluated under similar conditions in aqueous cacodylate buffer. Both single-stranded oligonucleotide and duplexes showed significant fluorescence quenching (4- to 5-fold) in aqueous buffer as compared to that in AOT RM (Table 4, Figure 15). The excited-state lifetime measurements reveal a longer lifetime for oligonucleotides in RM as compared to that in aqueous buffer (Table 4, Figure 16). Furthermore, anisotropy measurements indicate that the motion of the emissive oligonucleotides is considerably retarded in AOT RM as opposed to that in aqueous buffer (Table 4).

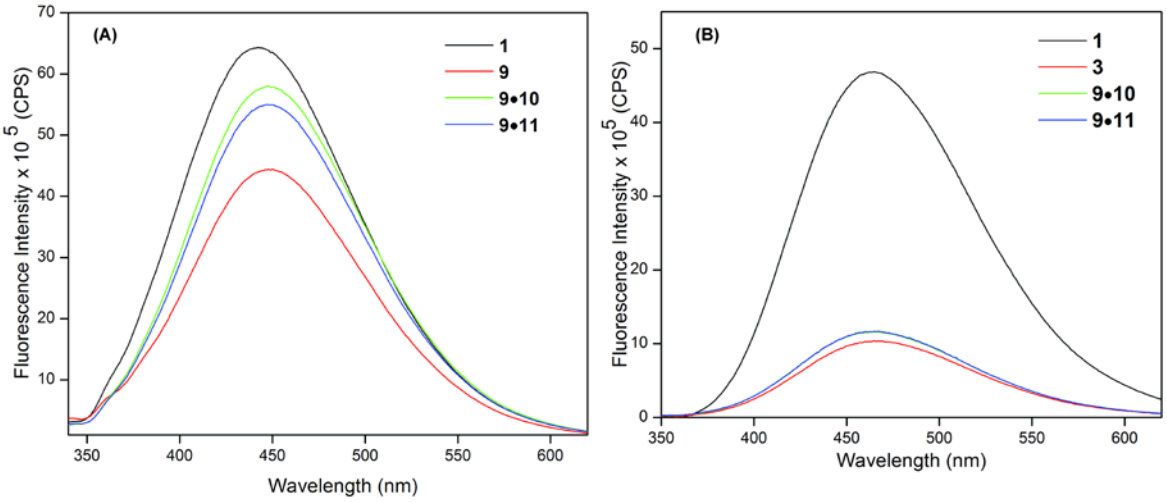

Figure 14. Emission spectra of nucleoside **1**, oligoribonucleotide **9** and duplexes of **9** (2 μM) in (A) AOT RM and (B) aqueous buffer.

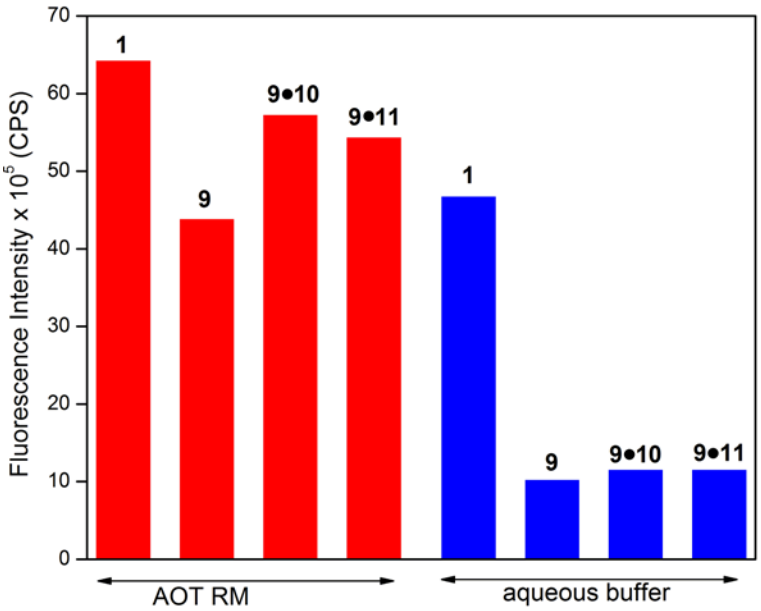

Figure 15. Emission intensity of nucleoside **1**, oligoribonucleotide **9** and duplexes of **9** (2 μM) in AOT RM and aqueous buffer at respective emission maximum. [75]

Table 4. Fluorescence properties of **9** and duplexes made of **9** in AOT RM and aqueous buffer.[75]

	sample	λ_{em} (nm)	τ_{ave} [a] (ns)	$r^{a.b}$
AOT RM	**1**	442	1.46	0.137
	9	450	1.67	0.171
	9•10	448	1.61	0.174
	9•11	447	1.65	0.174
aqueous buffer	**1**	465	1.14	0.040
	9	465	1.27	0.101
	9•10	465	1.27	0.101
	9•11	465	1.22	0.105

[a] Standard deviations for average lifetime (τ_{av}) and anisotropy (r) are ≤ 0.05 ns, and 0.003, respectively. [b] r values reported are blank uncorrected.

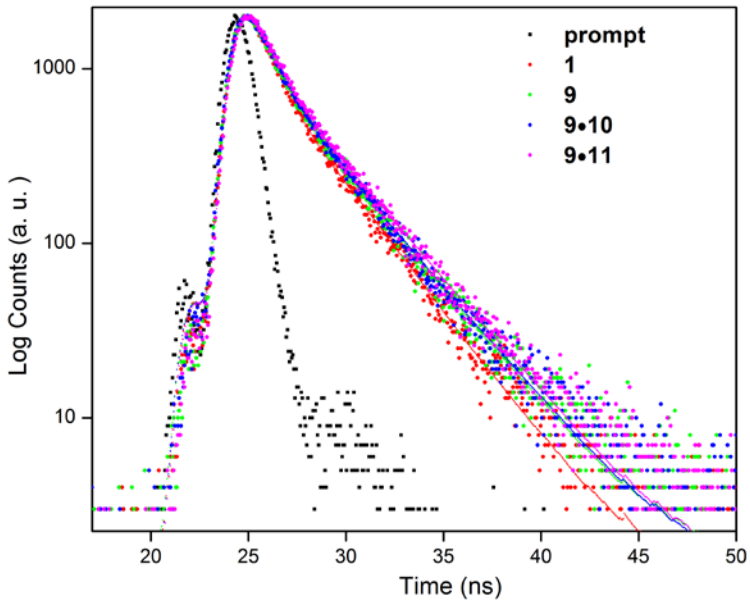

Figure 16. Excited-state decay profile of oligoribonucleotide **9** and duplexes of **9** in AOT RM containing 20 mM cacodylate buffer (pH 7.6, 50 mM NaCl, 0.5 mM EDTA). Laser profile is shown in black (prompt). Curve fits are shown in solid lines.

3.2.6 Thermal Melting and Circular Dichroism Analysis of Oligonucleotide 9 and its Perfect Complementary Duplexes

To confirm whether the observed photophysical properties of fluorescently modified oligonucleotide duplexes in AOT RM are due to intact duplexes, we performed UV-thermal melting and circular dichroism (CD) analyses. UV-thermal melting analysis revealed that modified oligoribonucleotide **9** formed stable duplexes with complementary oligonucleotides **10** (45.8 ± 1.0 °C) and **11** (60.5 ± 0.8 °C) in aqueous cacodylate buffer under the conditions used for fluorescence studies (Figure 17). However, a similar analysis could not be performed in AOT RM because the structure of micelles is very sensitive to temperature.[104,113] Therefore, we performed CD analysis of oligonucleotide duplexes **9•10** and **9•11** in aqueous buffer and AOT RM. The CD spectrum of RNA−DNA duplex **9•10** in aqueous cacodylate buffer displays a positive band centered at 281nm and a negative band at 251 nm, with a crossover at 263 nm. Although duplex **9•10** in AOT RM (w_0 = 20) exhibits no shift in the positive band, it shows a noticeable shift in the negative band to 230 nm. However, RNA−RNA duplex **9•11** displays similar CD profiles in both aqueous buffer and AOT RM, with positive and negative bands at around 274 and 234 nm, respectively (Figure 18). Hence, we believe that the differences in the fluorescence properties of the oligonucleotides in aqueous buffer and RM could be due to the retarded motion and a slight change in the conformation (especially in RNA−DNA duplex) of the intact oligonucleotide duplexes in AOT RM. Moreover, the higher fluorescence intensity,

lifetime, and anisotropy exhibited by fluorescent oligonucleotides in RM are consistent with the environment of the inner core of the water pool in RM, which is less polar and less mobile as compared to those of bulk water. Taken together, these results demonstrate that emissive nucleoside analogue **1** incorporated into oligonucleotides, which can sense the environment of the water pool in RM, can be used to study the dynamics, conformation and recognition properties of nucleic acids in a model biological compartment.

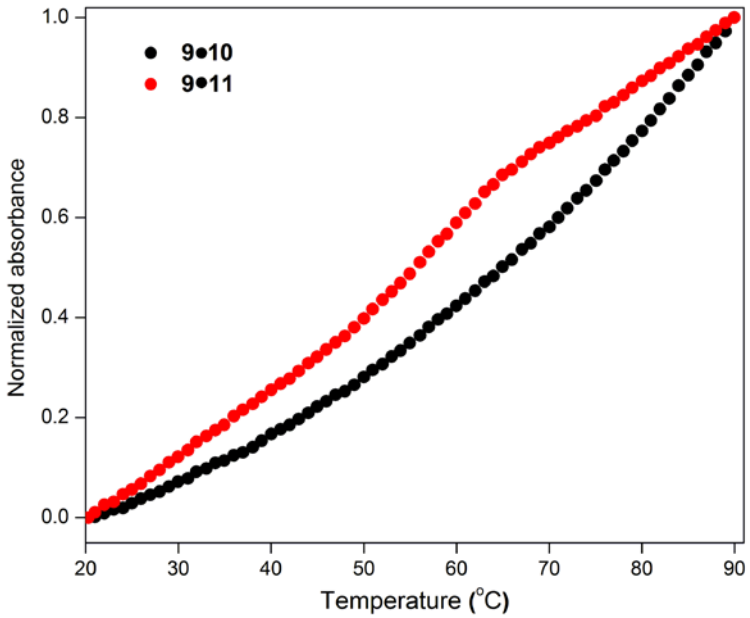

Figure 17. UV thermal melting profile of oligonucleotide duplexes **9•10** and **9•11** in aqueous buffer.

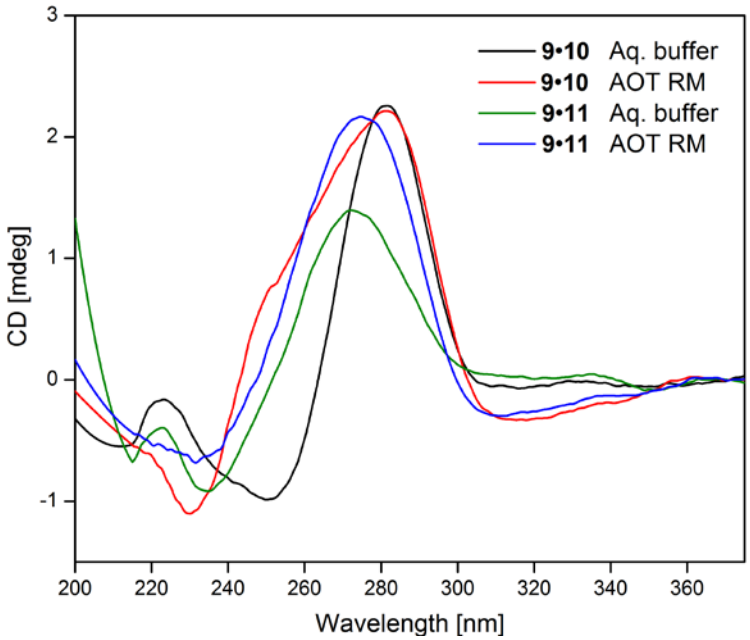

Figure 18. CD profile of oligonucleotide duplexes **9•10** and **9•11** in aqueous buffer and AOT RM (w_0 = 20) at 24 ºC.

3.3 Conclusions

We have introduced an environment-sensitive fluorescent nucleoside analogue probe, based on the 5-(benzo[*b*]-thiophen-2-yl)pyrimidine core, that reports the environment of micelles and RM via changes in its fluorescence properties. The photophysical characterization of the uridine analogue incorporated into oligonucleotides indicate that the motion of oligonucleotides is considerably retarded in RM as compared to that in aqueous buffer, which is in agreement with the environment of the encapsulated water pool in RM. Taken together, emission in the visible region with a reasonable quantum yield, sensitivity to changes in polarity and viscosity, and the ability to report the environment of micelles adequately bestow a probe-like attribute to emissive nucleoside **1**. These favorable properties of the nucleoside can be potentially utilized in studying the structural dynamics and recognition properties of oligonucleotides in a cell-like confined environment. Efforts to implement this nucleoside analogue in investigating the recognition properties of therapeutically relevant nucleic acid motifs in RM are currently in progress.

3.4 Experimental Section

3.4.1 Materials

Cetyltrimethylammonium bromide (CTAB) and dioctyl sodium sulfosuccinate (AOT) were obtained from Sigma-Aldrich. AOT was dried under vacuum for 48 h before use. Sodium dodecyl sulfate (SDS) and n-heptane (HPLC grade) were obtained from SRL India Limited and RANKEM India, respectively. Benzothiophene-modified RNA oligonucleotide **9** was prepared by *in vitro* transcription reactions according to our earlier report.[72] Synthetic oligonucleotides **10** and **11** purchased from Integrated DNA Technologies, Inc. and Dharmacon RNAi Technologies were purified by polyacrylamide gel electrophoresis (PAGE) under denaturing conditions. Millipore water or autoclaved water was used in all spectroscopic measurements.

3.4.2 Instruments

Absorption spectra were recorded on PerkinElmer, Lambda 45, and Shimadzu UV-2600 UV−vis spectrophotometers. Steady-state fluorescence experiments were carried out in a microfluorescence cuvette (Hellma, path length 1.0 cm) on either a Fluorolog-3 (Horiba Jobin Yvon) or Fluoromax-4 spectrophotometer (Horiba Jobin Yvon). Time resolved

fluorescence experiments were performed on a TCSPC instrument (Horiba Jobin Yvon, Fluorolog-3).

3.4.3 Fluorescence Properties of Ribonucleoside 1 in Anionic and Cationic Micelles

Steady-State Fluorescence Measurements: Aqueous solutions of various concentrations of surfactants (SDS and CTAB) containing ribonucleoside **1** (5 μM) and DMSO (0.5 %) were excited at 318 nm. The excitation and emission slit widths were maintained at 2 and 6nm, respectively. A spectral blank in the absence of emissive ribonucleoside at a respective surfactant concentration was subtracted from each sample spectrum. Fluorescence experiments were performed in triplicate in a microfluorescence cell at 24 °C. Plots of fluorescent intensity at 465 nm versus surfactant concentration were fitted using a sigmoid function of the Boltzmann type (Origin Pro 8.5.1, eq 1) to determine the cmc values of SDS and CTAB.[73,74] For all plots, the χ^2(goodness of fit) values were very close to unity.

$$y = (A_1 - A_2)/\{1 + \exp[(x - x_0)/\Delta x]\} + A_2 \qquad (1)$$

Where y is the fluorescence intensity at 465 nm, x is the surfactant concentration, x_0 is the center of the sigmoid (cmc), Δx is the slope factor, A_1 is the upper limit of fluorescence intensity, and A_2 is the fluorescence intensity in the absence of surfactant.

Steady-State Fluorescence Anisotropy Measurements: Steady-state fluorescence anisotropy measurements in various solvents were performed on a Fluoromax-4 spectrophotometer (Horiba Jobin Yvon) at 24 °C. Samples (5 μM) were excited at 318 nm, and the emission intensity was collected at the respective emission maximum. The anisotropy value (r) was determined by analyzing the data using software provided with the instrument. Anisotropy measurements were performed in triplicate, and each value reported in this study is an average of 10 successive measurements for each sample.

Time-Resolved Fluorescence Measurements: Excited-state decay kinetics analysis of aqueous solutions of ribonucleoside **1** (5 μM) at varying surfactant concentrations was performed on the TCSPC instrument. The samples were excited using a 339nm diode laser source (IBH, UK, NanoLED-339L) with a band pass of 10 nm, and the fluorescence signal at the respective emission maximum was collected. Lifetime measurements were

performed in triplicate, and decay profiles were analyzed using IBH DAS6 analysis software. The χ^2 (goodness of fit) values were found to be very close to unity for all decay profiles.

3.4.4 Fluorescence Properties of Ribonucleoside 1 in AOT RM

AOT RM in n-heptane with increasing w_0 values were prepared by adding appropriate volumes of the nucleoside stock solutions in water such that the concentrations of nucleoside **1** and AOT were maintained at 5 μM and 200 mM, respectively. The samples were prepared in glass vials, sonicated for ~20 s, and then equilibrated for 30 min before fluorescence measurements were carried out.

Steady-State Fluorescence Measurements: Samples were excited at 322 nm with an excitation slit width of 3 nm and an emission slit width of 5 nm. A spectral blank at respective w_0 value in the absence of ribonucleoside was subtracted from each sample spectrum. Fluorescence experiments were performed in triplicate in a microfluorescence cell at 24 °C.

Time-Resolved Fluorescence Measurements: Excited-state decay kinetics analysis of ribonucleoside **1** (5 μM) in AOT RM as a function of w_0 was performed by exciting the samples using 339 nm diode laser source (IBH, UK, NanoLED-339L) with a band pass of 6 nm. The fluorescence signal at the emission maximum was collected. Lifetime measurements were performed in triplicate, and decay profiles were analyzed using IBH DAS6 analysis software. Fluorescence intensity decay profiles at different w_0 values were found to be triexponential with χ^2 (goodness of fit) values very close to unity.

3.4.5 Synthesis of Modified Oligoribonucleotide 9

Modified oligoribonucleotide **9** was synthesized by transcription reaction. A large-scale transcription reactions using template **T1** were performed in a 250 μL reaction volume. The reaction contained 2 mM GTP, 2 mM CTP, 2 mM ATP, and 2 mM modified UTP **2**, 20 mM $MgCl_2$, 0.4 U/μL RNase inhibitor (RiboLock), 300 nM annealed template and 800 units T7 RNA polymerase. After incubation for 12 h at 37 °C, the precipitated salt of pyrophosphate was removed by centrifugation. The reaction volume was reduced approximately to 1/3 by Speed Vac, and 50 μL of loading buffer was added. The mixture was heated at 75 °C for 3 min and cooled on the ice bath. The sample was loaded onto a

preparative 20% denaturing polyacrylamide gel. The gel was UV shadowed; appropriate band was excised, extracted with 0.3 M sodium acetate and desalted using Sep-Pak classic C18 cartridge. Transcript **9**, ε_{260} = 90340 $M^{-1}cm^{-1}$.

3.4.6 Fluorescence Properties of Oligoribonucleotide 9 and Duplexes Made of 9 in AOT RM

Stock solutions of **9** and duplexes **9•10** and **9•11** (28 μM) were prepared by annealing a 1:1 mixture of the respective oligonucleotides in 20 mM cacodylate buffer (pH 7.6, 50 mM NaCl, 0.5 mM EDTA) at 90 °C for 3 min and cooling the samples slowly to room temperature. The samples were stored at ~4 °C overnight before use. An appropriate volume of the oligonucleotide stock was added to the AOT RM in heptane such that the w_0 value and concentration of the oligonucleotide and AOT were maintained at 20, 2 μM and 200 mM, respectively. The samples were sonicated for nearly 5 s and then equilibrated for 30 min. Steady-state fluorescence measurements were performed in duplicate (24 °C) by exciting the samples at 322 nm with excitation and emission slit widths of 3 and 8 nm, respectively. A spectral blank of AOT RM at w_0 = 20 in the absence of oligonucleotides was subtracted from each sample spectrum. Time-resolved fluorescence measurements were performed by exciting the samples using 320 nm diode laser source (IBH, UK, NanoLED-320L) with a band pass of 2 nm, and the fluorescence signal was collected at the respective emission maximum. The decay profiles were analyzed using IBH DAS6 analysis software. The χ^2 (goodness of fit) values were found to be very close to unity for all decay profiles. The fluorescence properties of **9** and duplexes **9•10** and **9•11** (2 μM) were also evaluated in aqueous buffer (20 mM cacodylate, pH 7.6, 50mM NaCl, 0.5 mM EDTA) under similar conditions by following the above procedure.

3.5 References

(1) Asseline, U. (2006) Development and applications of fluorescent oligonucleotides. *Curr.Org. Chem.* , *10*, 491−518.

(2) Martí, A. A., Jockusch, S., Stevens, N., Ju, J., and Turro, N. J. (2007) Fluorescent hybridization probes for sensitive and selective DNA and RNA detection. *Acc. Chem. Res.*, *40*, 402−409.

(3) Hall, K. B. (2008) RNA in motion. *Curr. Opin. Chem. Biol.*, *12*, 612−618.

(4) Piton, N., Mu, Y., Stock, G., Prisner, T. F., Schiemann, O., and Engels, J. W. (2007) Base-specific spin-labeling of RNA for structure determination. *Nucleic Acids Res., 35*, 3128−3143.

(5) Aitken, C. E., Petrov, A., and Puglisi, J. D. (2010) Single ribosome dynamics and the mechanism of translation. *Annu. Rev. Biophys., 39*, 491−513.

(6) Bardaro, M. F., Jr., and Varani, G. (2012) Examining the relationship between RNA function and motion using nuclear magnetic resonance. *WIREs RNA, 3*, 122−132.

(7) Nguyen, P., and Qin, P. Z. (2012) RNA dynamics: Perspectives from spin labels. *WIREs RNA, 3*, 62−72.

(8) Ogle, J. M., Carter, A. P., and Ramakrishnan, V. (2003) Insights into the decoding mechanism from recent ribosome structures. *Trends Biochem.Sci., 28*, 259−266.

(9) Korostelev, A., Trakhanov, S., Laurberg, M., and Noller, H. F. (2006) Crystal structure of a 70S ribosome tRNA complex reveals functional interactions and rearrangements. *Cell, 126*, 1065−1077.

(10) Serganov, A., and Patel, D. J. (2012) Molecular recognition and function of riboswitches. *Curr. Opin. Struct. Biol., 22*, 279−286.

(11) Ranasinghe, R. T., and Brown, T. (2005) Fluorescence based strategies for genetic analysis. *Chem. Commun.*, 5487−5502.

(12) Shi, X., and Herschlag, D. (2009) Fluorescence polarization anisotropy to measure RNA dynamics. *Methods Enzymol., 469*, 287−302.

(13) Wilson, J. N., and Kool, E. T. (2006) Fluorescent DNA base replacements: Reporters and sensors for biological systems. *Org. Biomol. Chem., 4*, 4265−4274.

(14) Sinkeldam, R. W., Greco, N. J., and Tor, Y. (2010) Fluorescent analogs of biomolecular building blocks: Design, properties, and applications. *Chem. Rev., 110*, 2579−2619.

(15) Wilhelmsson, L. M. (2010) Fluorescent nucleic acid base analogues. *Q. Rev. Biophy., 43*, 159−183.

(16) Srivatsan, S. G., and Sawant, A. A. (2011) Fluorescent ribonucleoside analogues as probes for investigating RNA structure and function. *Pure Appl. Chem., 83*, 213−232.

(17) Phelps, K., Morris, A., and Beal, P. A. (2012) Novel modifications in RNA. *ACS Chem. Biol., 7*, 100−109.

(18) Okamoto, A., Saito, Y., and Saito, I. (2005) Design of base-discriminating fluorescent nucleosides. *J. Photochem. Photobiol.C, 6*, 108−122.

(19) Mayer-Enthart, E., and Wagenknecht, H.-A. (2006) Structure-sensitive and self-assembled helical pyrene array based on DNA architecture. *Angew.Chem., Int. Ed., 45*, 3372−3375.

(20) Tainaka, K., Tanaka, K., Ikeda, S., Nishiza, K.-I., Unzai, T., Fujiwara, Y., Saito, I., and Okamoto, A. (2007) PRODAN-Conjugated DNA: Synthesis and photochemical properties. J. *Am. Chem. Soc., 129*, 4776−4784.

(21) Xiao, Q., Ranasinghe, R. T., Tang, A. M. P., Brown, T. (2007) Naphthalenyl- and anthracenyl-ethynyl dT analogues as base discriminating fluorescent nucleosides and intramolecular energy transfer donors in oligonucleotide Probes. *Tetrahedron, 63*, 3483−3490.

(22) Srivatsan, S. G., Weizman, H., and Tor, Y. (2008) A Highly fluorescent nucleoside analog based on Thieno[3,4-d]pyrimidine senses mismatched pairing. *Org. Biomol. Chem., 6*, 1334−1338.

(23) Gardarsson, H., Kale, A. S., and Sigurdsson, S. T. (2011) Structure−function relationships of phenoxazine nucleosides for identification of mismatches in duplex DNA by fluorescence spectroscopy. *ChemBioChem, 12*, 567−575.

(24) Shipova, E., and Gates, K. S. (2005) A fluorimetric assay for the spontaneous release of an N7-alkylguanine residue from duplex DNA. *Bioorg. Med. Chem. Lett., 15*, 2111−2113.

(25) Greco, N. J., Sinkeldam, R. W., and Tor, Y. (2009) An emissive C analog distinguishes between G, 8-oxoG, and T. *Org. Lett., 11*, 1115−1118.

(26) Srivatsan, S. G., Greco, N. J., and Tor, Y. (2008) A highly emissive fluorescent nucleoside that signals the activity of toxic ribosome- inactivating proteins. *Angew. Chem., Int. Ed., 47*, 6661−6665.

(27) Hirose, W., Sato, K., and Matsuda, A. (2010) Selective detection of 5-formyl-2′-deoxyuridine, an oxidative lesion of thymidine, in DNA by a fluorogenic reagent. *Angew.Chem., Int. Ed., 49*, 8392−8394.

(28) Parsons, J., Castaldi, M. P., Dutta, S., Dibrov, S. M., Wyles, D.L., and Hermann, T. (2009) Conformational inhibition of the hepatitis C virus internal ribosome entry site RNA. *Nat. Chem. Biol., 5*, 823−825.

(29) Nadler, A., Strohmeier, J., and Diederichsen, U. (2011) 8-Vinyl-2′-deoxyguanosine as a fluorescent 2′-deoxyguanosine mimic for investigating DNA hybridization and topology. *Angew.Chem, Int.Ed., 50*, 5392−5396.

(30) Lee, J., II, and Kim, B. H. (2012) Monitoring i-motif transitions through the exciplex emission of a fluorescent probe incorporating two PyA units. *Chem. Commun., 48*, 2074−2076.

(31) Rieder, R., Lang, K., Graber, D., and Micura, R. (2007) Ligand-induced folding of the adenosine deaminase A-riboswitch and implications on riboswitch translational control. *ChemBioChem., 8*, 896−902.

(32) Xie, Y., Dix, A. V., and Tor, Y. (2009) FRET Enabled real time detection of RNA-small molecule binding. *J. Am. Chem. Soc., 131*, 17605−17614.

(33) Wahba, A. S., Esmaeili, A., Damha, M. J., Hudson, R. H. E. (2010) A single-label phenyl pyrrolocytidine provides a molecular beacon-like response reporting HIV-1 RT RNase H activity. *Nucleic Acids Res., 38*, 1048−1056.

(34) Riedl, J., Pohl, R., Ernsting, N. P., Orsaág, P., Fojta, M., and Hocek, M. (2012) Labelling of nucleosides and oligonucleotides by solvatochromic 4-aminophthalimide fluorophore for studying DNA−Protein interactions. *Chem. Sci., 3*, 2797−2806.

(35) Pawar, M. G., Nuthanakanti, A., and Srivatsan, S. G. (2013) Heavy atom containing fluorescent ribonucleoside analog probe for the fluorescence detection of RNA-Ligand binding. *Bioconjugate Chem., 24*, 1367−1377.

(36) Kelley, S. O., and Barton, J. K. (1999) Electron transfer between bases in double helical DNA. *Science, 283*, 375−381.

(37) Grigorenko, N. A., and Leumann, C. J. (2008) Electron transfer through a stable phenanthrenyl pair in DNA. *Chem. Commun.*, 5417−5419.

(38) Murphy, L. D., and Zimmerman, S. B. (1994) Macromolecular crowding effects on the interaction of DNA with escherichia coli DNA-binding proteins: A model for bacterial nucleoid stabilization. *Biochim. Biophys. Acta, 1219*, 277−284.

(39) Ellis, R. J. (2001) Macromolecular crowding: An important but neglected aspect of the intracellular environment. *Curr.Opin.Struct.Biol., 11*, 114−119.

(40) Flynn, P. F. (2004) Multidimensional multinuclear solution NMR studies of encapsulated macromolecules. *Prog. Nucl. Magn. Reson. Spectrosc., 45*, 31−51.

(41) Snoussi, K., and Halle, B. (2005) Protein self-association induced by macromolecular crowding: A quantitative analysis by magnetic relaxation dispersion. *Biophys. J., 88*, 2855−2866.

(42) Minton, A. P. (2005) Influence of macromolecular crowding upon the stability and state of association of proteins: predictions and observations. *J. Pharm. Sci., 94*, 1668−1675.

(43) Luisi, P. L., Giomini, M., Pileni, M. P., and Robinson, B. H. (1988) Reverse micelles as hosts for proteins and small molecules. *Biochim. Biophys. Acta, 947*, 209 −246.

(44) Bru, R., Sanchez-Ferrer, A., and García-Carmona, F. (1995) Kinetic models in reverse micelles. *Biochem. J., 310*, 721−739.

(45) Levinger, N. E. (2002) Water in confinement. *Science, 298*, 1722−1723.

(46) Effects of crowding and confinement on the structure and activity of biomacromolecules, especially proteins, have been studied in RM. Visser, A. J. W. G., and Fendler, J. H. (1982) Reduction of reversed micelle entrapped cytochrome C and cytochrome C3 by electrons generated by pulse radiolysis or by pyrene photoionization. *J. Phys. Chem., 86*, 947−950. See also refs 47−52.

(47) Shastry, M. C. R., and Eftink, M. R. (1996) Reversible thermal unfolding of ribonuclease T1 in reverse micelles. *Biochemistry, 35*, 4094−4101.

(48) Das, P. K., and Chaudhuri, A. (2000) On the origin of unchanged lipase activity profile in cationic reverse micelles. *Langmuir, 1*6, 76−80.

(49) Uskova, M. A., Borst, J.-W., Hink, M. A., van Hoek, A., Schots, A., Klyachko, N. L., and Visser, A. J. W. G. (2000) Fluorescence dynamics of green fluorescent protein in AOT reversed micelles. *Biophys. Chem., 87*, 73−84.

(50) Airoldi, M., Boicelli, C. A., Gennaro, G., Giomini, M., Giuliani,A. M., Giustini, M., and Scibetta, L. (2002) Different factors affecting PolyAT conformation in microemulsions: effects of variable P_0 and KCl concentration. *Phys. Chem. Chem. Phys., 4*, 3859−3864.

(51) Shi, Z., Peterson, R. W., Wand, A. J. (2005) New reverse micelle surfactant systems optimized for high-Resolution NMR spectroscopy of encapsulated proteins. *Langmuir, 21*, 10632−10637.

(52) Van Horn, W. D., Ogilvie, M. E., and Flynn, P. F. (2009) Reverse micelle encapsulation as a model for intracellular crowding. *J. Am. Chem. Soc., 131*, 8030− 8039.

(53) De, T. K., and Maitra, (1995) A. solution behaviour of aerosol OT in nonpolar solvents. *Adv. Colloid Interface Sci., 59,* 95−193.

(54) Silber, J. J., Biasutti, A., Abuin, E., and Lissi, E. (1999) Interactions of small molecules with reverse micelles. *Adv. Colloid Interface Sci., 82,*189−252.

(55) Fletcher, P. D. I., Howe, A. M., Robinson, B. H. (1987) The kinetics of solubilisate exchange between water droplets of a water-in-oil microemulsion. *J. Chem. Soc., Faraday Trans. 1, 83,* 985−1006.

(56) Nandi, N., Bhattacharyya, K., and Bagchi, B. (2000) Dielectric relaxation and solvation dynamics of water in complex chemical and biological systems. *Chem. Rev., 100,* 2013−2045.

(57) Levinger, N. E., and Swafford, L. A. (2009) Ultrafast dynamics in reverse micelles. *Annu.Rev. Phys. Chem., 60,* 385−406.

(58) Correa, N. M., Biasutti, M. A., and Silber, J. J. (1995) Micropolarity of reverse micelles of aerosol-OT in n-Hexane. *J. Colloid Interface Sci., 172,* 71−76.

(59) Karukstis, K. K., Frazier, A. A., Martula, D. S., and Whiles, J. A. (1996) Characterization of the microenvironments in AOT reverse micelles using multidimensional spectral analysis. *J. Phys. Chem., 100,* 11133−11138.

(60) Hasegawa, M., Sugimura, T., Suzaki, Y., and Shindo, Y. (1994) Microviscosity in water pool of aerosol-OT reversed micelle determined with viscosity-sensitive fluorescence Probe, auramine O, and fluorescence depolarization of xanthene dyes.

(61) Politi, M. J., and Chaimovich, H. (1986) Water activity in reversed sodiumbis(2-ethylhexyl) sulfosuccinate micelles. *J. Phys. Chem., 90,*282−287.

(62) Mukherjee, T. K., Panda, D., and Datta, A. (2005) Excited-state proton transfer of 2-(2′ -Pyridyl)benzimidazole in microemulsions: Selective enhancement and slow dynamics in aerosol OT reverse micelles with an aqueous Core. *J. Phys. Chem. B, 109,* 18895−18901.

(63) Luisi, P. L., and Magid, L. J. (1986) Solubilization of enzymes and nucleic acids in hydrocarbon micellar solutions. *CRC Crit. Rev. Biochem., 20,* 409−474.

(64) Ijiro, K., Okahata, Y. (1992) A DNA-Lipid complex soluble in organic solvents. *J. Chem. Soc., Chem. Commun.,* 1339−1341.

(65) Melnikov, S. M., and Lindman, B. (1999) Solubilization of DNA-cationic lipid complexes in hydrophobic solvents. A single-molecule visualization by fluorescence microscopy. *Langmuir, 15*, 1923−1928.

(66) Budker, V. G., Slattum, P. M., Monahan, S. D., and Wolff, J. A. (2002) Entrapment and condensation of DNA in neutral reverse micelles. *Biophy. J., 82*, 1570−1579.

(67) Shaw, A. K., Sarkar, R., and Pal, S. K. (2005) Direct observation of DNA condensation in a nano-cage by Using a molecular ruler. *Chem.Phys. Lett., 408*, 366 −370.

(68) Sarkar, R., and Pal, S. K. (2006) Ligand−DNA interaction in a nanocage of reverse micelle. *Biopolymers, 83*, 675−686.

(69) Nezhad, E. H., Ghorbani, M., Zeinalkhani, M., and Heidari, A. (2013) DNA encapsulation in an anionic reverse micellar solution of dioctyl sodium sulfosuccinate. *Phys. Chem., 3*, 7−10.

(70) Park, L.-C., Maruyama, T., and Goto, M. (2003) DNA hybridization in reverse micelles and its application to mutation detection. *Analyst, 128*, 161−165.

(71) Workman, H., and Flynn, P. F. (2009) Stabilization of RNA oligomers through reverse micelle encapsulation. *J. Am. Chem. Soc., 131*, 3806−3807.

(72) Pawar, M. G., and Srivatsan, S. G. (2011) Synthesis, photophysical characterization, and enzymatic incorporation of a microenvironment sensitive fluorescent uridine analog. *Org. Lett., 13*, 1114−1117.

(73) Bahri, M. A., Hoebeke, M., Grammenos, A., Delanaye, L., Vandewalle, N., and Seret, A. (2006) Investigation of SDS, DTAB and CTAB micelle microviscosities by electron spin resonance. *Colloids Surf., A, 290*, 206−212.

(74) Aguiar, J., Carpena, P., Molina-Bolívar, J. A., and Carnero Ruiz, C. (2003) On the determination of the critical micelle concentration by the pyrene 1:3 ratio method. *J. Colloid Interface Sci., 258*, 116−122.

(75) See the Experimental Section for details.

(76) Tanpure, A. A., Pawar, M. G., and Srivatsan, S. G. (2013) Fluorescent nucleoside analogs: probes for investigating nucleic acid structure and function. *Isr. J. Chem., 53*, 366−378.

(77) Reichardt, C. (1994) Solvatochromic dyes as solvent polarity indicators. *Chem. Rev., 94*, 2319−2358.

(78) Demchenko, A. P. (1982) On the nanosecond mobility in proteins: Edge excitation fluorescence red shift of protein-bound 2-(p-toluidinylnaphthalene)-6-sulfonate. *Biophys.Chem., 15,* 101−109.

(79) Lakowicz, J. R., and Keating-Nakamoto, S. (1984) Red-edge excitation of fluorescence and dynamic properties of proteins and membranes. *Biochemistry, 23,* 3013−3021.

(80) Macgregor, R. B., and Weber, G. (1986) Estimation of the polarity of the protein interior by optical spectroscopy. *Nature, 319,* 70−73.

(81) Chattopadhyay, A., and Mukherjee, S. (1993) Fluorophore environments in mebrane-bound probes: A red edge excitation shift study. *Biochemistry, 32,* 3804−38 11.

(82) Dennison, S. M., Guharay, J., and Sengupta, P. K. (1999) Excited-state intramolecular proton transfer (ESIPT) and charge transfer (CT) fluorescence probe for model membranes. *Spectrochim. Acta A, 55,* 1127−1132.

(83) Sengupta, B., Guharay, J., and Sengupta, P. K. (2000) Characterization of the fluorescence emission properties of prodan in different reverse micellar environments. *Spectrochim. Acta A, 56,* 1433−1441.

(84) Kalyanasundaram, K., and Thomas, J. K. (1977) Solvent-dependent fluorescence of pyrene-3-carboxaldehyde and its applications in the estimation of polarity at micelle-water interfaces. *J. Phys. Chem., 81,* 2176−2180.

(85) Ananthapadmanabhan, K. P., Goddard, E. D., Turro, N. J., and Kuo, P. L. (1985) Fluorescence probes for critical micelle concentration. *Langmuir, 1,* 352−355.

(86) Karukstis, K. K., Suljak, S. W., Waller, P. J., Whiles, J. A., and Thompson, E. H. Z. (1996) Fluorescence analysis of single and mixed micelle systems of SDS and DTAB. *J. Phys. Chem., 100,* 11125−11132.

(87) Shirota, H., Tamoto, Y., and Segawa, H. (2004) Dynamic fluorescence probing of the microenvironment of sodium dodecyl sulfate micelle solutions: Surfactant concentration dependence and solvent isotope effect. *J. Phys. Chem. A, 108,* 3244−3252.

(88) Chaudhuri, A., Haldar, S., and Chattopadhyay, A. (2009) Organization and dynamics in micellar structural transition monitored by pyrene fluorescence. *Biochem.Biophys. Res. Commun., 390,* 728−732.

(89) Mohr, A., Talbiersky, P., Korth, H.-G., Sustmann, R., Boese, R., Bläser, D., and Rehage, H. (2007) A new pyrene-based fluorescent probe for the determination of critical micelle concentrations. *J. Phys. Chem. B, 111*, 12985−12992.

(90) Fendler, J. H., Fendler, E. J., Infante, G. A., Shih, P.-S., and Patterson, L. K. (1975) Absorption and proton magnetic resonance spectroscopic investigation of the environment of acetophenone and benzophenone in aqueous micellar solutions. *J. Am. Chem. Soc., 97*, 89−95.

(91) Zinsli, P. E. (1979) Inhomogeneous interior of aerosol OT microemulsions probed by fluorescence and polarization decay. *J.Phys. Chem., 83*, 3223−3231.

(92) Wong, M., Thomas, J. K., and Gratzel, M. (1976) Fluorescence probing of inverted micelles. The state of solubilized water clusters in alkane/diisooctyl sulfosuccinate (aerosol OT) solution. *J. Am. Chem. Soc., 98*, 2391−2397.

(93) Fulton, J. L., Blitz, J. P., Tingey, J. M., and Smith, R. D. (1989) Reverse micelle and microemulsion phases in super critical xenon and ethane: Light scattering and spectroscopic probe studies. *J. Phys. Chem., 93*, 4198−4204.

(94) Even at w_0 value as high as 40 the properties of the water pool are discernibly different than those of the continuous aqueous solution. See ref 92.

(95) Zhang, J., and Bright, F. V. (1991) Nanosecond reorganization of water within the interior of reversed micelles revealed by frequency-domain fluorescence spectroscopy. *J. Phys. Chem., 95*, 7900−7907.

(96) Onori, G., and Santucci, A. (1993) IR investigations of water structure in aerosol OT reverse micellar aggregates. *J. Phys. Chem., 97*, 5430−5434.

(97) Sarkar, N., Das, K., Datta, A., Das, S., and Bhattacharyya, K. (1996) Solvation dynamics of coumarin 480 in reverse micelles. Slow relaxation of water molecules. *J. Phys. Chem., 100*, 10523−10527.

(98) Das, S., Datta, A., and Bhattacharyya, K. (1997) Deuterium isotope effect on 4-aminophthalimide in neat water and reverse micelles. *J. Phys.Chem. A, 101*, 3299−3304.

(99) Riter, R. E., Undiks, E. P., and Levinger, N. E. (1998) Impact of counterion on water motion in aerosol OT reverse micelles. *J. Am. Chem. Soc., 120*, 6062−6067.

(100) Behera, G. B., Mishra, B. K., Behera, P. K., and Panda, M. (1999) Fluorescent probes for structural and distance effect studies in micelles, reversed micelles and microemulsions. *Adv. Colloid Interface Sci., 82,* 1−42.

(101) 2-Aminopurine, a fluorescent analog of adenine, has been used as a donor to construct FRET pairs in RM. Ghatak, C., Rao, V. G., Mandal, S., Pramanik, R., Sarkar, S., Verma, P. K., and Sarkar, N. (2012) Förster resonance energy transfer among a structural isomer of adenine and various coumarins inside a nanosized reverse micelle. *Spectrochim. Acta A, 89,* 67−73.

(102) The size of AOT RM in the absence and presence of nucleoside **1** determined by using dynamic light scattering (DLS) is in good agreement with literature reports (Figure 16). See also refs 103and 104.

(103) Riter, R. E., Kimmel, J. R., Undiks, E. P., and Levinger, N. E. (1997) Novel reverse micelles partitioning non aqueous polar solvents in a hydrocarbon continuous phase. *J. Phys. Chem. B, 101*, 8292−8297.

(104) Mitra, R. K., Sinha, S. S., and Pal, S. K. (2008) Temperature-dependent solvation dynamics of water in sodium bis(2-ethylhexyl)-sulfosuccinate/isooctane reverse micelles. *Langmuir, 24*, 49−56.

(105) Belletete, M., Lachapelle, M., and Durocher, G. (1990) Polarity of AOT micellar interfaces: Use of the preferential solvation concepts in the evaluation of the effective dielectric constants. *J. Phys. Chem., 94*, 5337−5341.

(106) Hazra, P., and Sarkar, N. (2001) Intramolecular charge transfer processes and solvation dynamics of coumarin 490 in reverse micelles. *Chem.Phy. Lett., 342*, 303−311.

(107) Enzymatic methods have been effectively used to synthesize fluorescently modified oligonucleotides. Lang, K., Rieder, R., and Micura, R. (2007) Ligand-Induced Folding of the thiM TPP Riboswitch Investigated by a Structure-Based Fluorescence Spectroscopic Approach. *NucleicAcids Res., 35*, 5370−5378. See refs 108−112.

(108) Srivatsan, S. G., and Tor, Y. (2009) Enzymatic incorporation of emissive pyrimidine ribonucleotides. *Chem. Asian J., 4*, 419−427.

(109) Kimoto, M., Mitsui, T., Yokoyama, S., and Hirao, I. (2010) A unique fluorescent base analogue for the expansion of the genetic alphabet. *J. Am. Chem. Soc., 132*, 4988−4989.

(110) Tanpure, A. A., and Srivatsan, S. G. (2011) A microenvironment-sensitive fluorescent pyrimidine ribonucleoside analogue: Synthesis, enzymatic incorporation, and fluorescence detection of a DNA abasic Site. *Chem–Eur. J., 17,* 12820−12827.

(111) Riedl, J., Menova, P., Pohl, R., Orsag, P., Fojta, M., and Hocek, M. (2012) GFP-like fluorophores as DNA labels for studying DNA−Protein interactions. *J. Org. Chem., 77*, 8287−8293.

(112) Holzberger, B., Strohmeier, J., Siegmund, V., Diederichsen, U., and Marx, A. (2012) Enzymatic synthesis of 8-vinyl- and 8-styryl-2′ -deoxyguanosine modified DNA−Novel fluorescent molecular probes. *Bioorg. Med. Chem. Lett., 22*, 3136−3139.

(113) Mitra, R. K., and Paul, B. K. (2005) Effect of NaCl and temperature on the water solubilization behavior of AOT/nonionics mixed reverse micellar systems stabilized in IPM oil. *Colloids Surf. A, 255*,165−180.

CHAPTER-4

A Double Duty Ribonucleoside Analogue Probe Based on a 5-(selenophen-2-yl)pyrimidine Core for the Fluorescence Detection of RNA-Ligand Binding

4.1 Introduction

Ribonucleic acid participates in a multitude of essential cellular processes including catalysis, and maintenance and regulation of genetic information by interacting with proteins, nucleic acids, and small molecule metabolites. Despite limited chemical diversity as compared to proteins, RNA expands its functional repertoire by utilizing its intrinsic conformational dynamics and by adopting diverse secondary and tertiary structures.[1−4] Several techniques such as fluorescence, electrophoresis, nuclear magnetic resonance, electron paramagnetic resonance, to name a few, have been very useful in advancing our understanding of the structure, dynamics, and recognition properties of nucleic acids.[5−9] In parallel, high-resolution X-ray structures of a significant number of functional RNA motifs have provided better insights into the relationship between RNA structure and function at the molecular level.[10,11]

Needless to say, several of the biophysical tools require appropriately labeled nucleic acid reporters.[12−14] In this context, oligonucleotides (ONs) labeled with fluorescent nucleoside Analogues that signal changes in their local environment via changes in their fluorescence properties−quantum yield, emission maximum, lifetime, and anisotropy −have been very useful in devising several nucleic acid-based bioanalytical and discovery assays.[15−26] Similarly, 3-D structure determination of nucleic acids by X-ray crystallography has greatly relied on heavy atom derivatization of nucleic acids for phase determination. Conventionally, the anomalous scattering from a bromine or iodine atom of brominated or iodinated nucleic acids is used in determining the structures by single-wavelength anomalous dispersion (SAD) phasing or by multiwavelength anomalous dispersion (MAD) phasing techniques.[27,28] Subsequently, the superior anomalous scattering property of selenium atom that has been extensively exploited in protein X-ray crystallography has also been extended to nucleic acid X ray crystallography.[29,30] Huang, Egli, and co-workers for the first time used Se-MAD phasing technique to report the X-ray structure of selenium-modified DNA and RNA oligonucleotides obtained via phosphoroselenoate backbone modification and 2′-methylselenouridine modification, respectively.[31−34] Later, methods have been developed to introduce selenium atom into oligonucleotides by using native nucleosides with 2′-methylseleno group or by replacing the base oxygen atoms withselenium.[35−37] These heavy atom derivatization methodologies have been successfully utilized in the X-ray structure determination of nucleic acids, and nucleic acid−protein and nucleic acid−small molecule complexes.[31−34,38−42]

The amount of information and fundamental knowledge we have gained on the structure and function of certain nucleic acid motifs through these experiments is arguably undeniable. Nevertheless, the rate at which new functional RNAs are being discovered, and since the current knowledge on the structure-function relationship of RNA is limited, it is essential to develop robust tools to understand how RNA structure complements its function. Toward this endeavour, it is highly desirable to develop a label compatible with two complementing biophysical techniques, one that would provide information on the dynamics and recognition properties in real time and the other on the 3D structure of nucleic acids. For example, incorporating a conformation-sensitive fluorescent nucleoside analogue probe, containing an anomalous scattering atom (*e.g.*, selenium), into nucleic acids would allow the analysis of structure−function relationship by both fluorescence and X-ray crystallography techniques. Literature reports indicate that minimally perturbing fluorescent nucleoside analogue probes can be assembled by attaching or fusing heterocyclic rings onto nucleobases.[15,43−48] In particular, Tor and co-workers have developed fluorescent nucleoside analogues by conjugating furan at the 5-position of uracil, and have utilized them in devising assays to detect the presence of DNA abasic sites and the binding of aminoglycoside antibiotics to RNA.[49,50] Drawing inspiration from these reports, we hypothesized that the conjugation of a selenophene moiety at the 5-position of uracil would generate a minimally perturbing emissive nucleobase analogue, which could serve as a fluorescence probe as well as an anomalous scattering label for the phase determination in X-ray crystallography. Here, we describe the synthesis and photophysical characterization of a new emissive uridine analogue **2**, based on a (selenophen-2-yl)pyrimidine core. Notably, the selenophene-conjugated uridine analogue displays emission in the visible region and very good fluorescence solvatochromism. Furthermore, as a proof of responsiveness of the nucleoside to RNA conformational changes, we have enzymatically labeled a therapeutically important RNA motif, ribosomal decoding site (A-site), with the emissive nucleoside **2**, and have developed a fluorescence binding assay to effectively monitor the binding of aminoglycoside antibiotics to the bacterial A-site.

4.2 Results and Discussion

4.2.1 Synthesis of Selenophene-Modified Uridine Analogue 2

The selenophene-modified uridine analogue **2** has been synthesized by reacting 5-iodouridine **1** with 2-(tri-n-butylstannyl)selenophene under typical Stille cross coupling reaction conditions using a palladium catalyst, $Pd(PPh_3)_2Cl_2$ (Scheme 1).

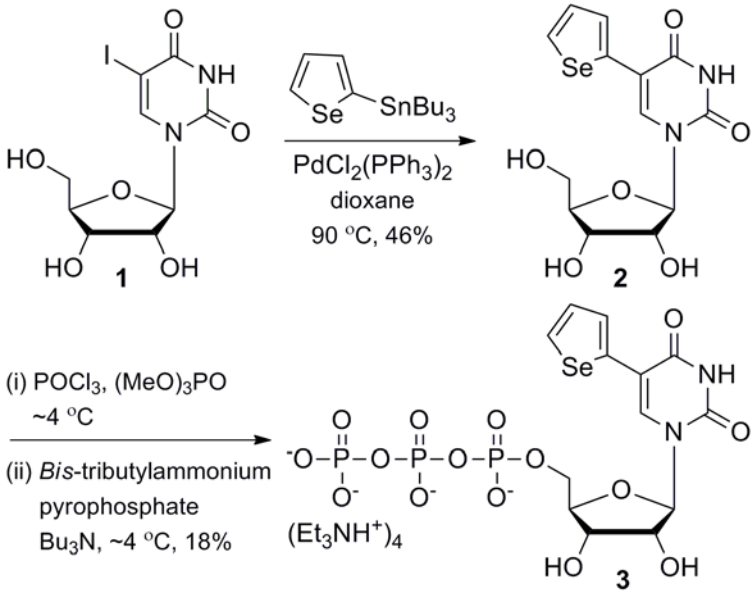

Scheme 1. Synthesis of selenophene-modified uridine analog **2** and corresponding triphosphate **3**.[55] 2-(tributylstannyl)selenophene was synthesized by following a literature report.[51]

4.2.2 Photophysical Properties of Selenophene-Modified Uridine Analogue 2

Many fluorescence probes that have been used to study the structure and function of nucleic acids photophysically respond to changes in their surrounding environment (*e.g.*, polarity and viscosity).[15] The ground-state electronic spectrum of nucleoside **2** in various solvents shows two major absorption maxima, which is not significantly affected by solvent polarity changes (Figure 1, Table 1). However, fluorescence properties such as quantum yield, emission maximum, and excited-state lifetime are significantly affected by polarity changes. In water, the nucleoside has an emission band centered around 454 nm, which significantly blue shifts (17 nm) and also shows a hyperchromic effect (~2-fold) as the solvent polarity is decreased from water to dioxane (Figure 1, Table 1). The time-resolved fluorescence spectroscopy analysis reveals a longer lifetime in water, which decreases in less polar solvents (Table 1, Figure 2). A positive correlation is obtained when the Stokes shift in different solvents is plotted as a function of $E_T(30)$, Reichardt's

microscopic solvent polarity parameter, which further indicates that the nucleoside **2** is sensitive to its microenvironment (Figure 3).[56]

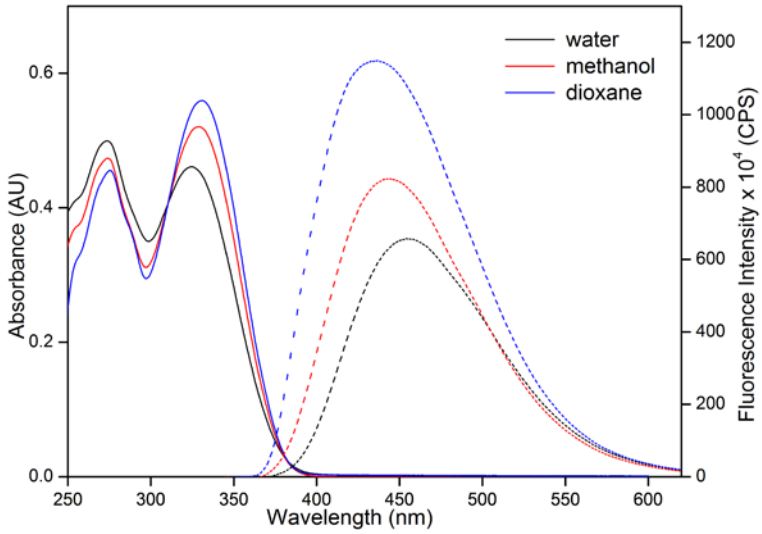

Figure 1. Absorption (solid line, 50 μM) and emission (dashed line, 5 μM) spectra of nucleoside **2** in different solvents.[55]

Table 1. Photophysical properties of **2** in different solvents.[55]

solvent	λ_{max} [a] (nm)	λ_{em} (nm)	I_{rel} [b]	Φ [c]	τ_{av} [c] (ns)
water	325	454	1.00	0.014	0.40
methanol	329	445	1.25	0.015	0.23
dioxane	331	437	1.75	0.025	0.27

[a] The lowest energy maximum is given. [b] Fluorescence intensity with respect to intensity in water. [c]Standard deviations for quantum yield (Φ) and average lifetime (τ_{av}) are ≤0.001 and 0.01 ns, respectively.

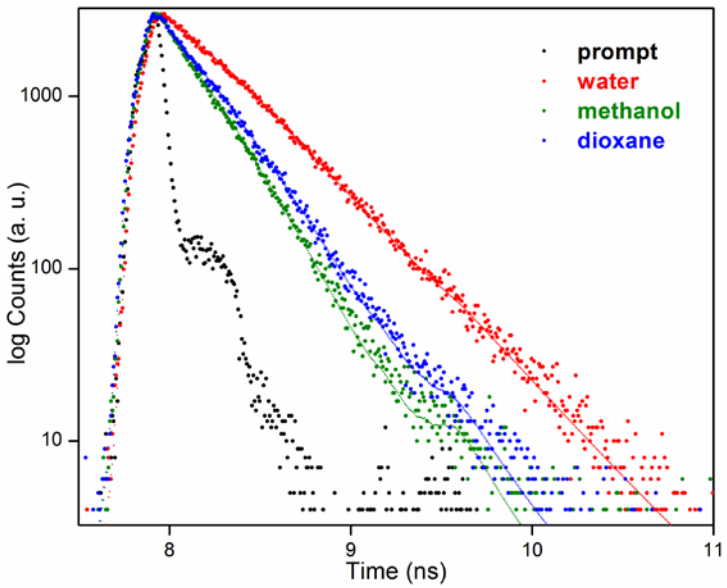

Figure 2. Excited state decay profile of ribonucleoside **2** in various solvents. Laser profile is shown in black (prompt). Curve fits are shown in solid lines.

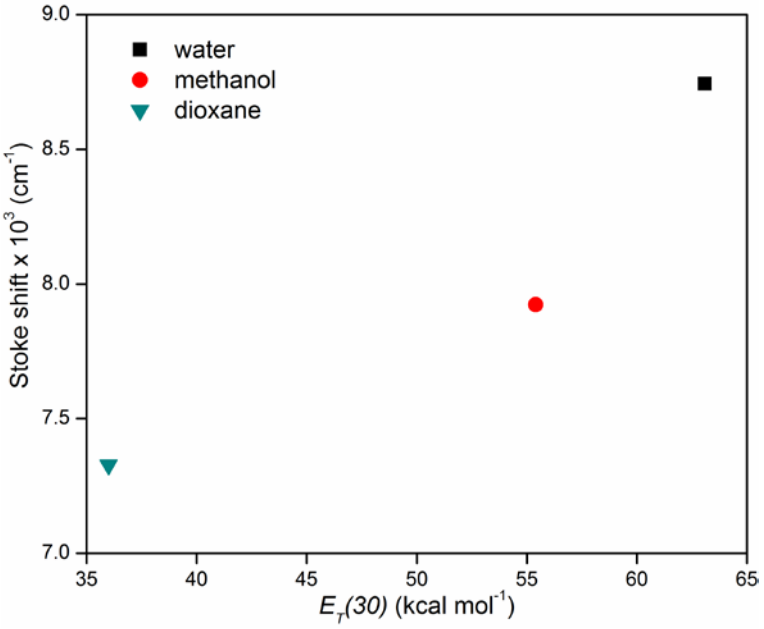

Figure 3. A plot of Stokes shift *vs.* E_T(30) value.

The conformation of selenophene moiety with respect to pyrimidine ring connected by a rotatable aryl−aryl bond can affect the effective conjugation and, hence, the fluorescence properties of the emissive nucleoside. The conformation of such extended nucleoside analogues, when incorporated into ONs, can be affected by subtle changes in interaction with neighbouring bases during a folding or recognition process.[57] In order to evaluate if nucleoside **2** could be utilized as a conformation-sensitive probe, further photophysical characterization has been carried out in solvents of similar polarity but different viscosity. Upon excitation, the nucleoside in glycerol shows a nearly 2-fold enhancement in fluorescence intensity with no apparent change in the emission maximum as compared to in a less viscous medium, ethylene glycol (Figure 4, Table 2). Furthermore, excited-state decay kinetics and fluorescence anisotropy analysis indicate a longer lifetime and a higher anisotropy value in glycerol than in ethylene glycol due to rigidification of the fluorophore in a more viscous medium (Table 2, Figure 5). This dual-sensitivity of the nucleoside to polarity and viscosity changes, which bestows probe-like character to the nucleoside, encouraged us to incorporate the fluorescent nucleoside **2** into RNA ONs.

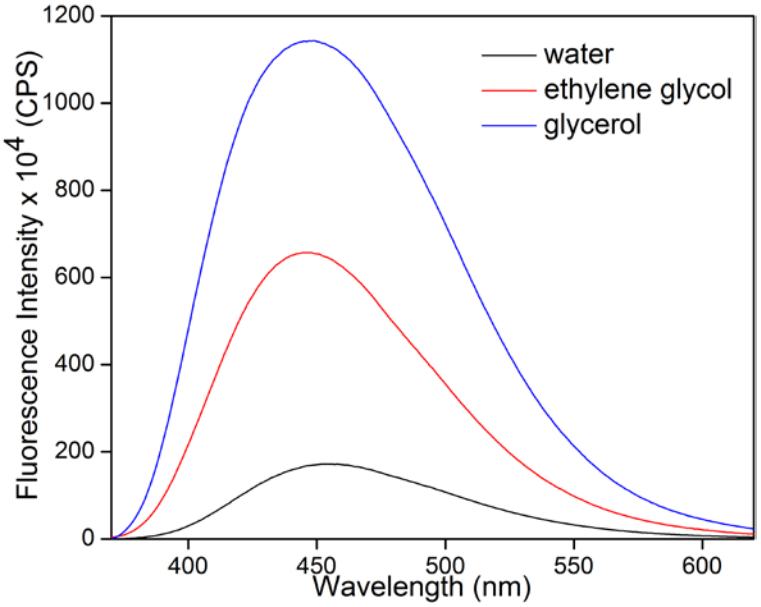

Figure 4. Emission spectra of nucleoside **2** (5 μM) in solvents of different viscosity.[55]

Table 2. Photophysical properties of ribonucleoside **2** in solvents of different viscosity.

Solvent[a]	λ_{max}[b] (nm)	λ_{em} (nm)	I_{rel}[c]	Φ[d]	τ_{ave}[d] (ns)	k_r/k_{nr}	r[d]
water	325	454	1.0	0.014	0.40	0.014	0.102
ethylene glycol	331	446	3.8	0.037	0.54	0.038	0.249
glycerol	331	447	6.7	0.087	0.98	0.095	0.355

[a]Viscosity ($\eta_{25°C}$) of ethylene glycol and glycerol is 16.1 cP and 934 cP, respectively. [b]The lowest energy maximum is given. [c] Relative emission intensity with respect to intensity in water. [d] Standard deviations for quantum yield (Φ), average lifetime (τ_{av}) and anisotropy (r) are ≤0.002, 0.04 ns and 0.008, respectively. Ratio of radiative (k_r) to nonradiative decay (k_{nr}) rate constants are also given.

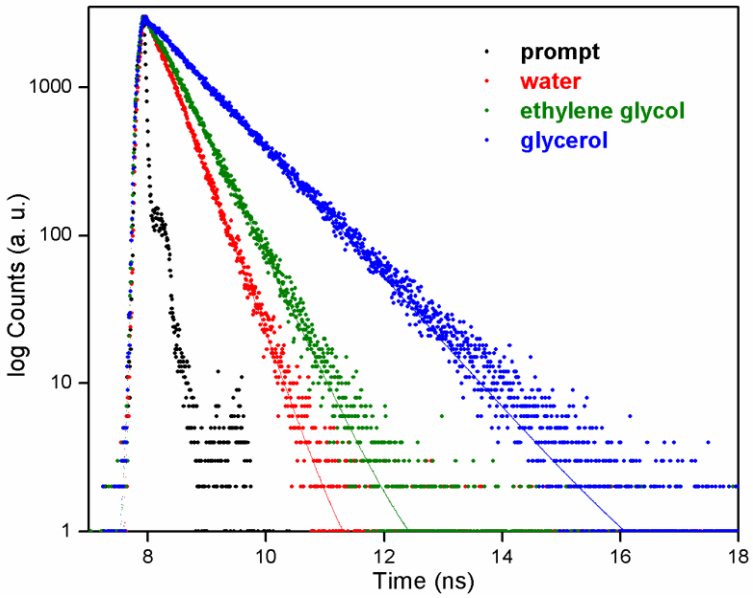

Figure 5. Excited state decay profile of ribonucleoside **2** in various viscosity solvents. Laser profile is shown in black (prompt). Curve fits are shown in solid lines.

4.2.3 Enzymatic Incorporation of Selenophene-Modified UTP Analogue 3

Modified RNA ONs can be obtained by solid phase chemical synthesis and by enzymatic methods using RNA polymerases and ligases.[49, 58–61] Here, we have adopted *in vitro* transcription reactions in the presence of T7 RNA polymerase, similar to Tor's report, [49] to incorporate the selenophene modification into RNA ONs. Selenophene-modified UTP **3** necessary for transcription reactions has been prepared in two steps by treating nucleoside **2** with $POCl_3$ and then with bistributylammonium pyrophosphate (Scheme 1).[49,62] Transcription reactions have been carried out in the presence of a series of promoter-template DNA duplexes constructed by hybridizing a promoter DNA sequence with DNA templates **T1**−**T5** (Figure 6). The templates contain one or two dA residues to facilitate single or double incorporations of the monophosphate of **3** into RNA transcripts. In addition, all templates contain a dT residue at the 5′-end to guide the incorporation of a unique adenosine residue at the 3′-end of each transcript. Therefore, in a transcription reaction (in the presence of GTP, CTP, **3**, and α-^{32}P ATP), if T7 RNA polymerase accepts and incorporates the modification then the full-length modified RNA product would contain a α-^{32}Plabeled adenosine at the 3′-end, which could be resolved on a polyacrylamide gel and phosphorimaged. However, abortive sequences resulting from failed transcription reactions would not carry the radiolabel, and hence, would remain undetected in this reaction setup.

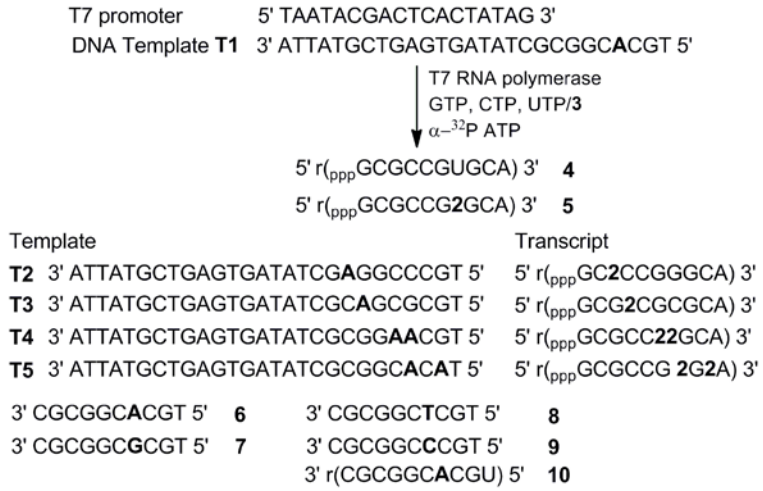

Figure 6. Synthesis of selenophene-modified fluorescent RNA ONs by *in vitro* transcription reactions in the presence of DNA templates **T1**–**T5**. cDNA (**6**–**9**) and cRNA (**10**) ONs used in this study.[55]

A transcription reaction carried out in the presence of template **T1** and triphosphate **3** afforded the full-length RNA ON **5** containing selenophene-modified uridine at the +7

position in a very good yield (Figure 7, lane 2). In addition to the full-length product, trace amounts of random nontemplated incorporation products (N+1 and N+2) are also formed. Such nontemplated incorporation products are known to form in trace amounts in *in vitro* transcription reactions.[63] Absence of bands corresponding to full-length transcripts in a control reaction performed in the absence of UTP and **3** rules out any adventitious misincorporation (Figure 7, lane 3). Interestingly, RNA polymerase incorporates the modified UTP better as compared to the natural UTP in a reaction containing equimolar concentrations of **3** and UTP (Figure 7, lane 4). Reactions in the presence of templates **T2** and **T3** result in the formation of transcripts containing the modification near the promoter region (+3 and +4 positions, respectively) in lower yields (Figure 7, lanes 6 and 8), whereas, when reactions are performed in the presence of templates **T4** and **T5**, the polymerase produces doubly modified transcripts in good yields (Figure 7, lanes 10 and 12).

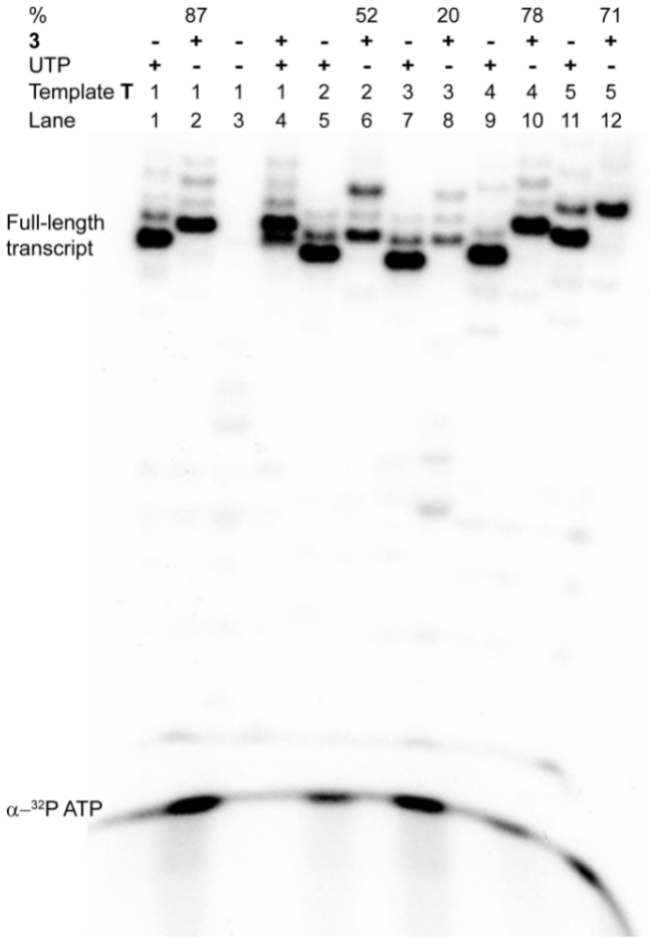

Figure 7. PAGE of transcription products from *in vitro* transcription reactions with DNA templates **T1**−**T5** in the presence of UTP and modified UTP **3** under denaturing conditions. % incorporation of **3** into the full-length oligoribonucleotide product is reported with respect to the amount of full-length product formed in the presence of natural UTP.[55]

4.2.4 Charecterization of Selenophene-Modified Oligoribonucleotide 5

*Mass analysis of modified RNA transcript **5*:** The fluorescently modified oligoribonucleotide 5 was isolated by gel electrophoresis from large scale transcription reaction in presence of template **T1** for further chemical and photophysical characterization. To confirm the presence of fluorescently modified ribonucleotide **3** in modified oligoribonucleotide **5**, we performed MALDI-TOF mass analysis. MALDI-TOF mass analysis gave the mass corresponding to the full-length modified oligoribonucleotide product **5** (Figure 8).

The sample for the MALDI-TOF mass analysis was prepared by the known procedure. 1 μL of a ~ 150 μM stock solution of the transcript **5** was combined with 1 μL of 100 mM ammonium citrate buffer (pH 9), 1 μL of a 150 μM DNA standard (18-mer) and 4 μL of saturated 3-hydroxypiccolinic acid solution. The sample were desalted with an ion exchange resin (Dowex 50W-X8, 100-200 mesh, ammonium form) and spotted on the MALDI plate, and was air dried. The resulting spectrum was calibrated relative to an internal 18-mer DNA standard.

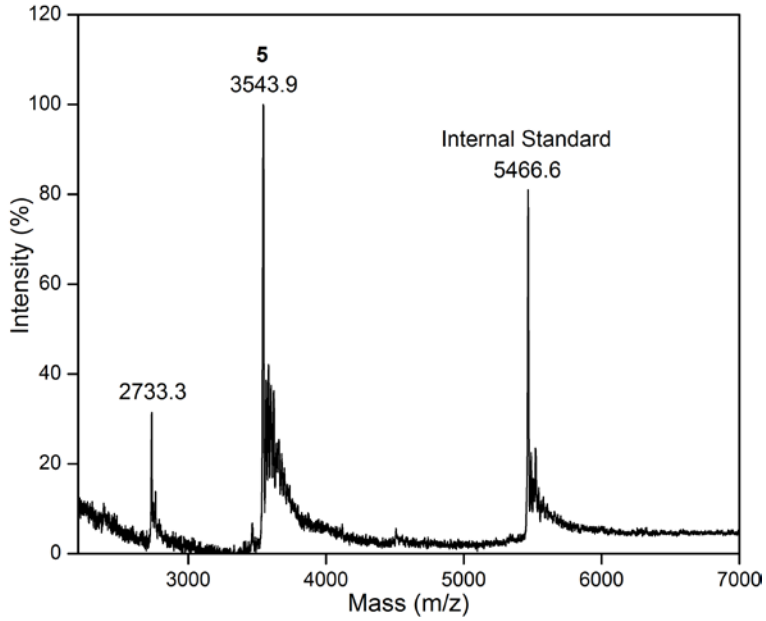

Figure 8. MALDI-TOF MS spectrum of selenophene-modified oligoribonucleotide **5.** Calcd. Mass for oligonucleotide **5**: 3543.9 [M]; found: 3543.9.

*Enzymatic digestion of the modified RNA transcript **5***: To further ascertain the presence of fluorescently modified ribonucleotide **3** in modified transcript **5** enzymatic digestion of modified transcript was done. Enzymatic digestion was performed in the presence of cocktail different RNase enzymes. This cocktail consists of snake venom

phosphodiesterase I, calf intestine alkaline phosphatase, RNase A, and RNase T1. In this cocktail, Snake venom phosphodiesterase I act as an exonucleotidase, by stepwise removal of 5'-mononucleotide units from the end that bears a free hydroxyl group, calf intestine alkaline phosphatase removes of phosphate groups from the 5' end of RNA strand, RNase A cleaves the phosphodiester bond between the 5'-ribose of a nucleotide and the phosphate group attached to the 3'-ribose of an adjacent nucleotide, RNase T1 is an endoribonuclease that specifically degrades single-stranded RNA at G residues. The action of all these enzymes on modified transcript results in mixture of free ribonucleoside. This mixture of free ribonucleoside was resolved on the HPLC and their retention time was confirmed with authentic ribonucleosides. The HPLC profile of the authentic ribonucleoside samples and ribonucleosides product obtained from enzymatic digestion of **5** clearly ascertains the presence of selenophene modified nucleoside in the transcript product (Figure 9). Further the HPLC fractions of digest were collected and analysed by mass spectroscopy. The observed mass of HPLC fraction also gives us surety for presence of modified ribonucleoside in transcript. (Table 3)

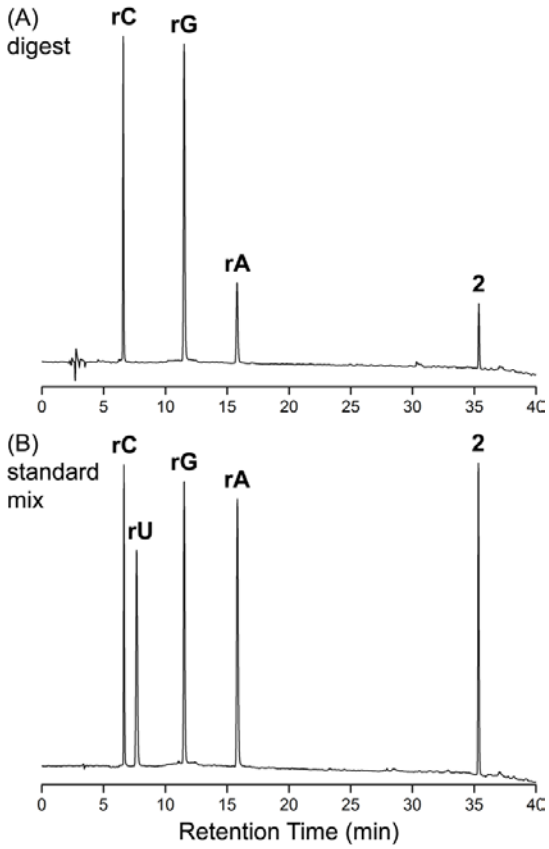

Figure 9. RP-HPLC chromatogram of ribonucleoside products obtained from an enzymatic digestion reaction of transcript **5** at 260 nm. (A) Digested transcript **5**, (B) ribonucleoside mix containing authentic samples (rC, rU, rG, rA and **2**).

Table 3. MALDI-TOF mass analysis of HPLC fractions of modified oligoribonucleotide **5** digest

HPLC fraction	Calculated mass for	Found
rC	$C_9H_{13}N_3O_5K$ [M+K$^+$]: 282.0	281.9
rG	$C_{10}H_{13}N_5O_5K$ [M+K$^+$]: 322.1	322.0
rA	$C_{10}H_{13}N_5O_4K$ [M+K$^+$]: 306.1	306.0
2	$C_{13}H_{14}N_2O_6SeK$ [M+K$^+$]: 412.9	413.2

4.2.5 Stability of Duplexes Made of Modified RNA Transcript 5

It has been observed that, when modified ribonucleoside was incorporated in oligonucleotide it can potentially perturb the native structure of oligoribonucleotides, which can lead to ineffective hybridization. Thus the observed photophysical properties of duplex can be due to the mixture of single stranded RNA transcript as well as its duplex. Although the selenophene moiety attached at the 5-position of uracil is reasonably small, its incorporation can potentially affect the native structure of oligoribonucleotides and their ability to form stable duplexes. To study the effect of incorporation of selenophene modified uridine analogue **2** on the duplex stability, we performed thermal melting (T_m) analysis of its duplexes. The T_m values of control unmodified duplex **4•6** and fluorescently-modified duplex **5•6** is 60.5 ± 1.9 ºC and 57.3 ± 1.7 ºC, respectively, and T_m values of control unmodified duplex **4•10** and fluorescently-modified duplex **5•10** is 74.4 ± 0.8 ºC and 71.4 ± 1.9 ºC, respectively. Small differences in *Tm* values (ΔT_m = ~3 °C) between control unmodified (**4•6** and **4•10**) and modified (**5•6** and **5•10**) duplexes indicate that the modification has only a minor impact on the duplex stability (Figure 6 and Figure 10).

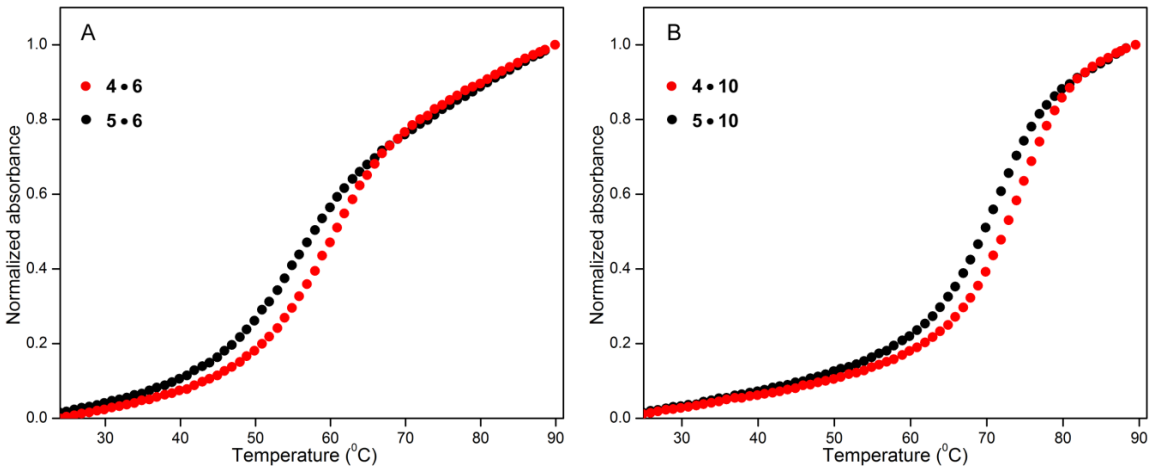

Figure 10. (A) UV-thermal melting profile of control unmodified (**4•6**) and fluorescently-modified (**5•6**) RNA-DNA duplexes (1 μM). (B) UV-thermal melting profile of control unmodified (**4•10**) and fluorescently-modified (**5•10**) RNA-RNA duplexes (1 μM).

Collectively, these results highlight that *in vitro* transcription reaction catalyzed T7 RNA polymerase can be used as a viable method to incorporate the minimally perturbing fluorescent selenophene-modified nucleoside into RNA ONs.

4.2.6 Selenophene-Modified Uridine Analogue in Different Base Environment

It is observed that the photophysical properties of the majority fluorescent nucleoside analogues, when incorporated into ONs, are affected by various mechanisms, which often involve neighbouring nucleobases.[57,64−68] Hence, the photophysical behaviour of fluorescent nucleoside **2** in different base environments has been studied by steady-state and time-resolved fluorescence spectroscopic techniques using transcript **5** and duplexes made by hybridizing **5** with complementary DNA and RNA ONs (**6**−**10**, Figure 6). The duplexes have been designed in such a fashion that the selenophene-modified ribonucleoside **2** has been positioned opposite to complementary or mismatched bases. When excited at 330 nm, a solution of single stranded oligoribonucleotide **5** in cacodylate buffer displays an emission band similar to that of the free nucleoside **2** (Figure 11 A and B). RNA−DNA duplex **5•6** and RNA−RNA duplex **5•10** in which the ribonucleoside **2** is placed opposite the complementary bases, dA and A, respectively, show emission profiles analogous to the single stranded oligoribonucleotide **5**. Interestingly, **2** placed opposite the pyrimidine bases in duplexes **5•8** and **5•9** shows a nearly **2** fold enhancement in fluorescence intensity as compared to duplexes **5•6** and **5•7** in which **2** is placed opposite the purines (Figure 11A and B). This observation is noteworthy because, baring a few examples,[48,69−71] the majority of fluorescent nucleoside analogue probes when incorporated into single stranded and double stranded ONs display sequential quenching in fluorescence intensity due to stacking of the chromophore with flanking bases and/or electron transfer process.[64−66,72]

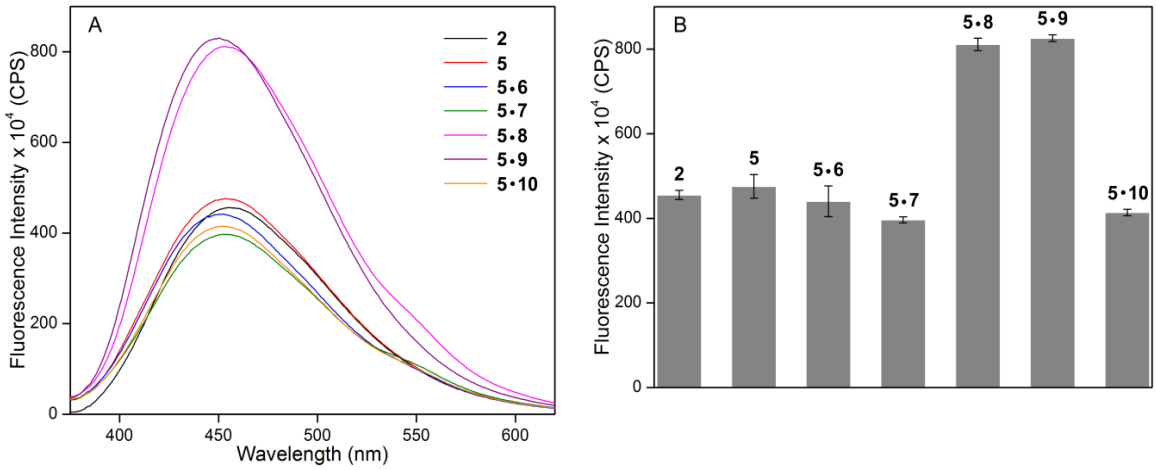

Figure 11. (A) Emission spectra (1 µM) of nucleoside **2**, ON **5**, and duplexes made by hybridizing **5** with complementary (**6** and **10**) and mismatched (**7**–**9**) ONs. (B) Fluorescence intensity of **5** and duplexes made of **5** at 452 nm.[55]

Although the exact morphology of emissive nucleoside in these duplexes is unknown, the enhancement in fluorescence intensity exhibited by **2** when placed opposite the pyrimidines can possibly be due to the following reasons. It is likely in duplexes **5•6** and **5•7** that the fluorescent uridine analogue is locked due to the formation of a stable Watson−Crick and a wobble base pair with dA and dG residues, respectively. This would favor the nonradiative decay pathway due to electron transfer process between nucleoside **2** and neighbouring bases.[72] However, in duplexes **5•8** and **5•9** the emissive nucleoside is opposite the mismatched bases dT and dC, respectively, and hence is not constrained by H-bonding interactions. This could reduce the electron transfer between the selenophene-modified base and neighbouring bases. The relative conformation of the selenophene moiety and uracil ring, which could be affected by interactions with neighbouring bases, could also contribute to the overall photophysical behaviour of the nucleoside in different base environments.[57] Excited-state decay kinetics show longer lifetimes for **5•8** and **5•9** as compared to **5•6** and **5•7**, which further suggest that the microenvironment of emissive nucleoside in this set of duplexes is distinctly different (Figure 12, Table 4).

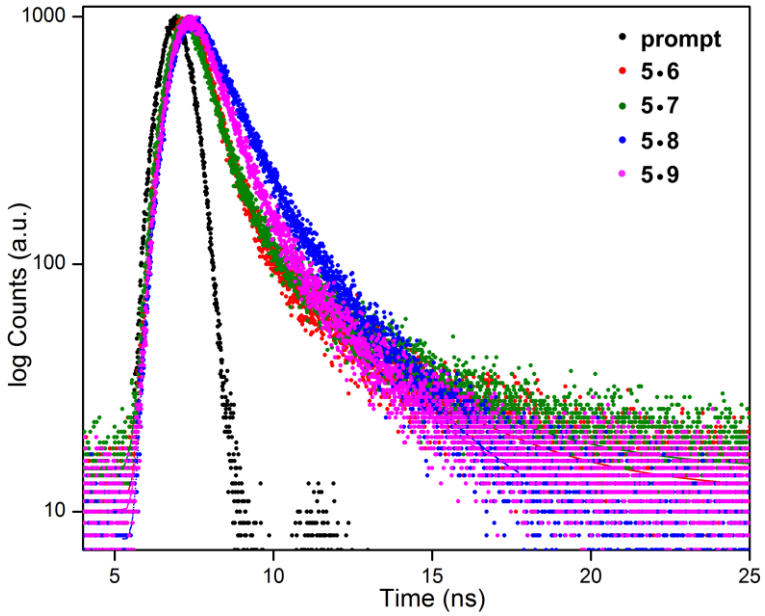

Figure 12. Excited state decay profile of modified duplexes **5•6**, **5•7**, **5•8** and **5•9**. Laser profile is shown in black (prompt) and curve fits are shown in solid lines.

Table 4. Photophysical properties of oligonucleotide constructs containing ribonucleoside **2**

Sample	λ_{em}	τ_1 [a] (ns)	τ_2 [a] (ns)	τ_{ave} [b] (ns)
5•6	452	0.54 (0.92)	3.21 (0.08)	0.74
5•7	452	0.51 (0.92)	3.21 (0.08)	0.73
5•8	453	0.99 (0.77)	2.61 (0.23)	1.37
5•9	450	0.78 (0.86)	2.57 (0.14)	1.04

[a] Relative amplitude is given in parenthesis. [b] Standard deviations for τ_{ave} (lifetime) is $\leq$ 0.03 ns.

Taken together, these observations clearly indicate that the fluorescence properties of nucleoside **2** are affected by base pair substitution. Such environment sensitive fluorescent nucleoside analogue that report subtle alterations in their neighbouring base environment during a recognition event have been utilized in devising assays to study the dynamics, structure, and binding properties of nucleic acids.[15–17]

4.2.7 Fluorescence Detection of Aminoglycoside Antibiotics Binding to A-Site RNA

To explore the usefulness of selenophene-modified uridine **2** in investigating the recognition property of RNA, we have chosen a therapeutically important and well-studied RNA motif, bacterial ribosomal decoding site (A-site), as a test system.[73,74] The A-site RNA maintains the high fidelity of protein translation process by monitoring correct mRNA codon and tRNA anticodon base pairing.[75] An important component of the decoding center is a small loop present in the 16S rRNA, which contains flexible adenine residues A1492 and A1493 (Figure 13A). Naturally occurring aminoglycoside antibiotics

(*e.g.*, paromomycin and neomycin,) bind to this region of the bacterial 16S rRNA and fix A1492 and A1493 in a conformation similar to the one induced by cognate tRNA binding to the A-site (Figure 14).[76,77] This reduces the ability of bacterial A-site to discriminate between the correct and incorrect codon−anticodon pairs resulting in mistranslation.

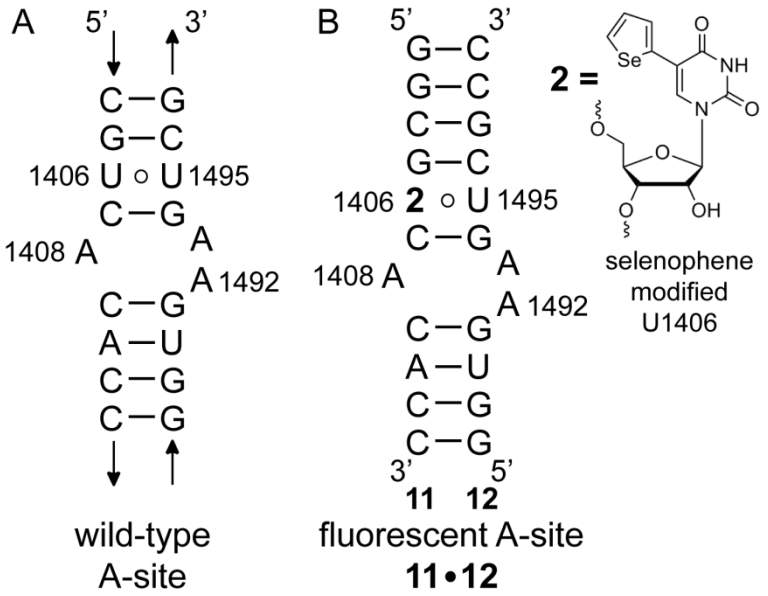

Figure 13. (A) Secondary structure of the bacterial A-site motif that binds to aminoglycoside antibiotics. (B) Selenophene-modified fluorescent A-site model construct **11•12** used in this study.[55]

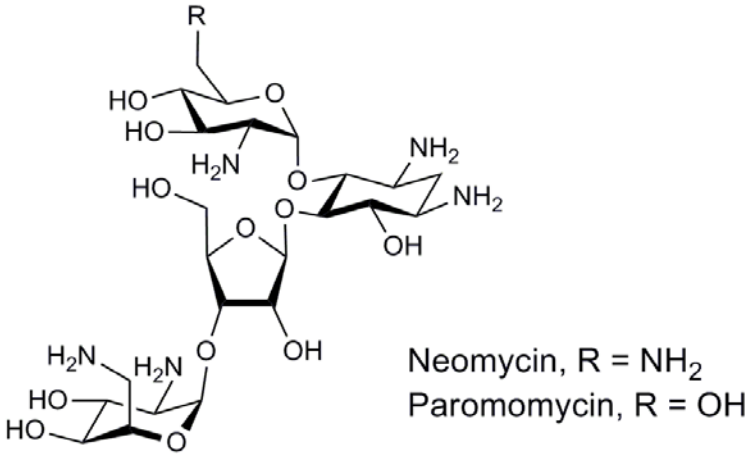

Figure 14. Structure of paromomycin and neomycin.

Based on the structures of aminoglycosides complexed with A-site,[78,79] fluorescent A-site RNA surrogates have been constructed by replacing A1492 or A1493 or U1406 residues with fluorescent nucleoside analogues.[49,53,80−84] These constructs have been used in determining the binding constants and thermodynamic parameters of A-site−aminoglycoside complexes by monitoring the changes in the fluorescence properties. Although reasonably sensitive, the fluorescence response of some of these analogues (*e.g.*,

2-aminopurine (2-AP)) is aminoglycoside-specific.[49,53,83,84] Therefore, robust assays that are amicable to discovery platforms for the identification of new bacterial-specific RNA binders are highly desired to counter the ever increasing number of antibiotic-resistant strains.

Encouraged by crystal structures showing evidence for further stabilization of A-site–aminoglycoside complexes through direct and water-bridged H-bonds to the non-canonical U1406◦U1495 pair,[78,79] we decided to replace one of the uridine residues (U1406) with selenophene-modified uridine analogue **2** to generate a fluorescent A-site RNA construct. To synthesize the fluorescent A-site construct by *in vitro* transcription reactions, we chose a short RNA duplex (**11•12**) that essentially represents the aminoglycosides binding domain of the wild type A-site (Figure 13). [49,53, 81−84]

4.2.8 Synthesis and Characterization of Selenophene-Modified Fluorescent A-Site transcript 11

Oligoribonucleotide **11** containing emissive ribonucleoside **2** at U1406 was synthesized by large-scale transcription reactions in the presence of triphosphate **3**. The integrity of the modified full-length transcript was confirmed by mass analysis (Figure 15).

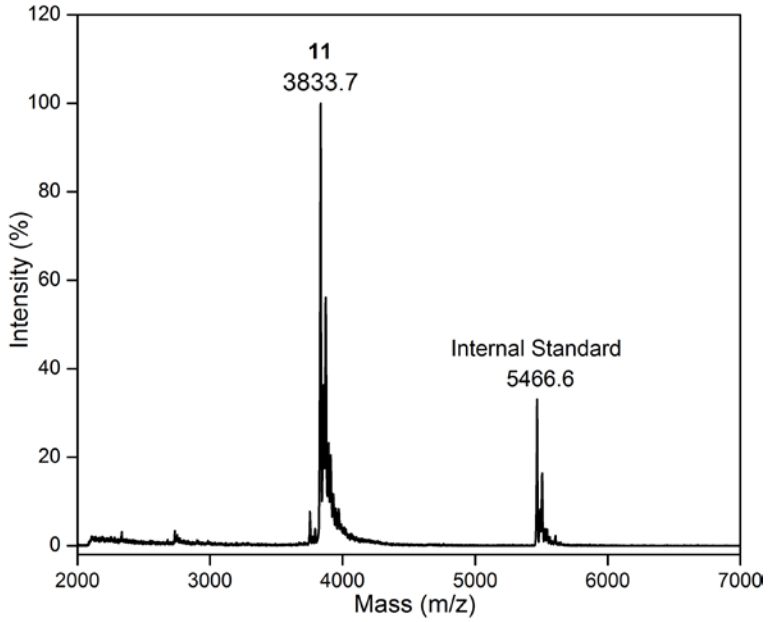

Figure 15. MALDI-TOF MS spectrum of selenophene-modified oligoribonucleotide **11**. Calcd. Mass for oligonucleotide **11**: 3833.1 [M]; found: 3833.7.

4.2.9 Synthesis of Selenophene-Modified Fluorescent A-Site construct 11•12

The fluorescent A-site construct was assembled by hybridizing **11** with a custom synthesized counter strand **12** in HEPES buffer. The A-site construct was excited at 330 nm and changes in fluorescence intensity upon titration with aminoglycosides were recorded at its emission maximum 452 nm. Titration of paromomycin to **11•12** resulted in an increase in fluorescence intensity, which corresponded to a nearly 2-fold at the saturation concentration of the aminoglycoside (Figure 16A). An EC_{50} value (concentration required for 50% response) of 7.57 ± 0.10 μM for the titration of paromomycin to A-site was found to be in good agreement with earlier literature reports (Figure 16B).[53,81−84]

2-AP, a widely used fluorescent adenosine analogue, has been previously employed in constructing A-site RNA motifs by replacing either A1492 or A1493 residues.[53,83,84] While 2-AP modified A-site constructs photophysically report the binding of paromomycin, they fail to signal the binding of neomycin (Figure 19).[49,53,83,84] This observation is particularly intriguing because the structures of A-site complexed with paromomycin and neomycin closely resemble each other.[78,79] To test if selenophene-modified uridine **2** could photophysically report the binding of neomycin to A-site, duplex **11•12** was titrated with neomycin B. Rewardingly, the emissive nucleoside signaled the binding of neomycin to A-site construct with enhancement in fluorescence intensity, which corresponded to a comparable EC_{50} value of 3.13 ± 0.17 μM (Figure 17A and B).[49] Importantly, control titrations performed by titrating single stranded ON **11** with either paromomycin or neomycin resulted in minor changes in fluorescence intensity (Figure 18). This indicates that the increase in fluorescence intensity exhibited by nucleoside **2** is due to cognate binding of aminoglycosides to A-site construct **11•12**. A furan-modified fluorescent A-site RNA construct developed by Tor's group also signals the binding of paromomycin and neomycin with enhancement in fluorescence intensity.[49] However, the EC_{50} values for the binding of paromomycin and neomycin to A-site (11.5 μM and 5.0 μM, respectively) determined by using furan modified A-site were found to be higher than the literature reports.[49,53,81−84] On the other hand, selenophene-modified nucleoside **2** reports the binding of aminoglycoside antibiotics to bacterial decoding site with EC_{50} values closer to literature reports.

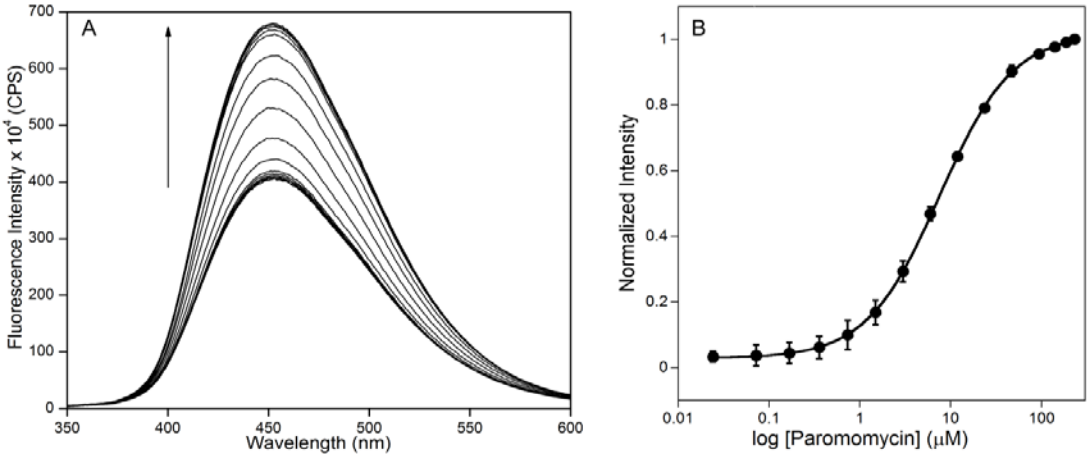

Figure 16. (A) Emission spectra for the titration of A-site construct **11•12** with paromomycin. (B) Curve fit for the titration of A-site with paromomycin. Normalized fluorescence intensity at λ_{em}= 452 nm is plotted against log [aminoglycoside]. Hill coefficient (n) = 1.1.[55]

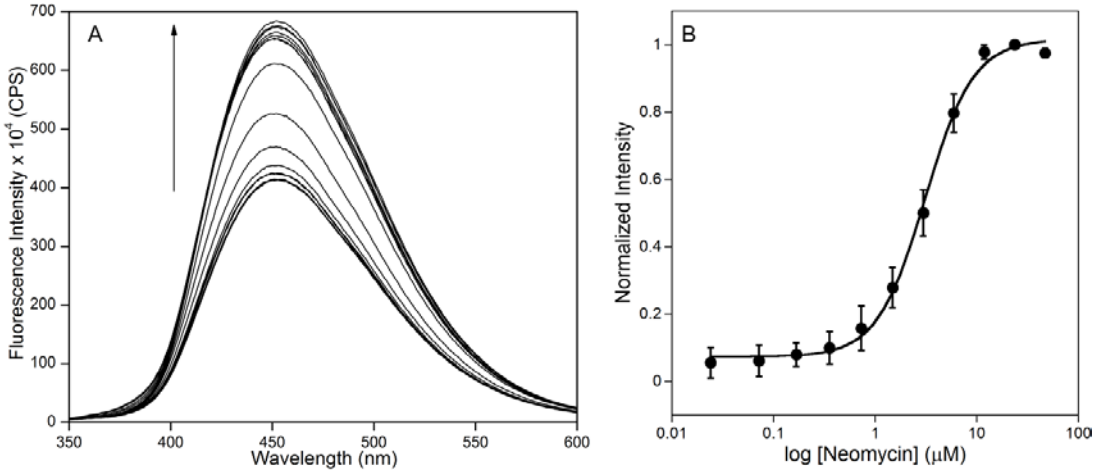

Figure 17. (A) Emission spectra for the titration of A-site construct **11•12** with neomycin. (B) Curve fit for the titration of A-site with neomycin. Normalized fluorescence intensity at λ_{em}= 452 nm is plotted against log [aminoglycoside]. Hill coefficient (n) = 1.8.[55]

Taken together, these results clearly demonstrate that the selenophene-modified nucleoside **2** is a useful probe in detecting RNA−ligand interactions, in this case A-site−aminoglycoside complexes, which cannot be effectively monitored by 2-AP, a most commonly used probe for studying RNA−ligand interactions. Importantly, this heavy-atom-containing nucleoside has a clear advantage over many other fluorescence probes as it can be used to investigate the nucleic acid structure and function in real time by fluorescence as well as in solid state by X-ray crystallography.

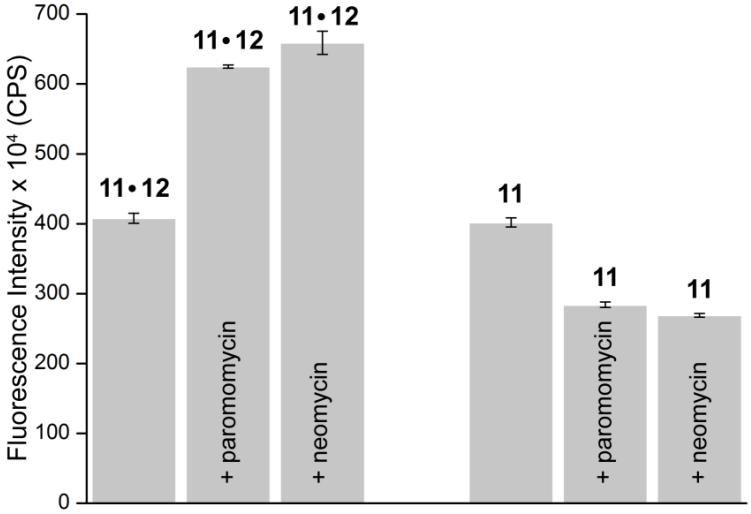

Figure 18. Fluorescence intensity of selenophene-modified A-site duplex **11•12** and single stranded oligoribonucleotide **11** in the absence and presence of paromomycin (~23 μM) and neomycin (~12 μM). Concentration of aminoglycosides has been taken such that it was nearly 3 times the respectively EC_{50} values. While addition of aminoglycosides to fluorescent A-site duplex **11•12** shows increase in intensity, addition of aminoglycosides to single stranded **11** shows slight reduction in intensity.

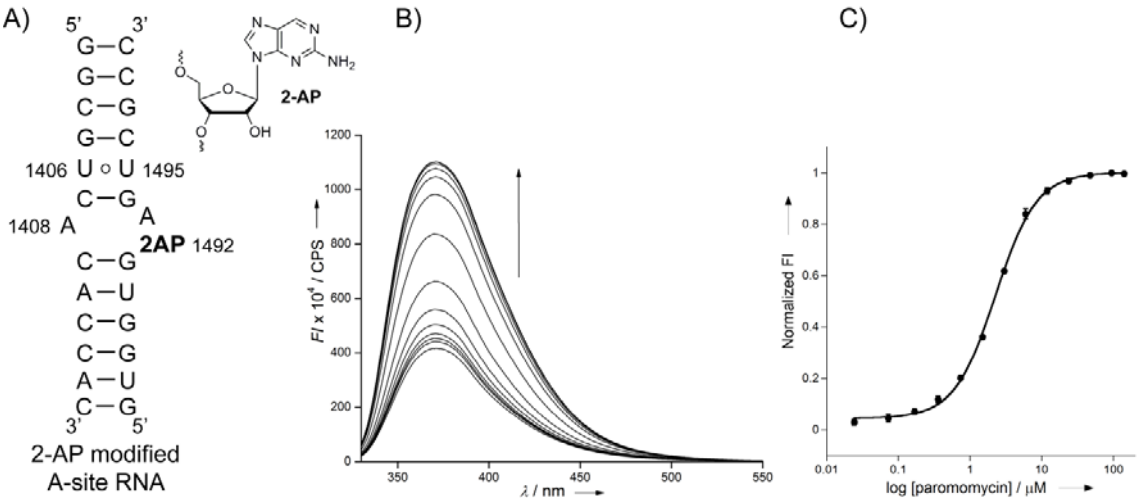

Figure 19. (A) Secondary structure of 2-AP-modified A-site RNA construct. Structure of 2-AP is also shown. (B) Representative fluorescence spectra for the titration of the above A-site construct with paromomycin. Fluorescence intensity (FI) increases with increasing concentrations of paromomycin. (C) Curve fit for the titration of A-site with paromomycin. Normalized FI at λ_{em}= 370 nm is plotted against log [paromomycin]. An EC_{50} value of 2.27 ± 0.07 μM was obtained for the titration of paromomycin to 2-AP-modified A-site, which is in good agreement with earlier literature reports.[2,3] The fluorescence response is significantly weaker when neomycin is titrated with 2-AP-modified A-site RNA to determine a reliable EC_{50} value.

4.3 Conclusions

We have developed a new ribonucleoside analogue probe **2** by appending selenophene moiety at the 5-position of uridine. The emissive nucleoside exhibits favourable photophysical properties such as sensitivity to changes in its microenvironment and conformation. The amicability of modified ribonucleotide to enzymatic incorporation has allowed the easy synthesis of a selenophene-modified fluorescent A-site RNA construct by transcription reaction. Our results demonstrate that the selenophene-modified uridine incorporated into the decoding site can effectively signal the binding of aminoglycoside antibiotics to the bacterial A-site. Taken together, this heavy-atom containing fluorescent label is a unique and useful combination wherein its dual properties can be utilized to study the dynamics, structure, and recognition properties of nucleic acids by two mutually exclusive but complementing techniques, namely, fluorescence and X-ray crystallography. We strongly believe that this simple approach of assembling a "two-in-one" probe would provide new opportunities to study the structure−function relationship of biomacromolecules.

As fluorescently modified nucleoside **2** does undergo minute fluorescence quenching after incorporation into oligonucleotides, and it possesses selenium heavy atom which is very well used for obtaining the crystals of biomolecules. We want further explore the anomalous scattering properties of selenium atom by incorporating the modified nucleoside **2** into biologically relevant DNA and RNA molecules.

For this purpose we have chosen biologically important internal ribosome entry site (IRES), which is present in pathogenic viruses. In eukaryotes, protein synthesis initiates primarily by a mechanism that requires a modified nucleotide 'cap' on the mRNA and also proteins that recruit and position the ribosome. Many pathogenic viruses use an alternative, cap-independent mechanism that substitutes RNA structure for the cap and many proteins. The RNAs driving this process are called internal ribosome-entry sites (IRESs) and some are able to bind the ribosome directly using a specific 3D RNA structure. In order to study IRES binding mechanism to we have incorporated nucleoside **2** into IRES RNA by solid phase synthesis. The structural and binding studies are under progress.

4.4 Experimental Section

4.4.1 Materials

5-Iodouridine, selenophene, tributyltin chloride, and bis(triphenylphosphine)-palladium(II) chloride were obtained from Sigma-Aldrich. $POCl_3$ was purchased from Acros Organics, and was distilled before use. Paromomycin and neomycin were purchased from Sigma-Aldrich. Synthetic DNA ONs were either purchased from Integrated DNA Technologies, Inc., or from Sigma-Aldrich. ONs were purified by polyacrylamide gel electrophoresis (PAGE) under denaturing conditions, and desalted on Sep-Pak Classic C18 cartridges (Waters Corporation). Custom synthesized oligoribonucleotides purchased from Dharmacon RNAi Technologies were deprotected according to the supplier's instructions, PAGE purified, and desalted on Sep-Pak Classic C18 cartridges. T7 RNA polymerase, ribonuclease inhibitor (RiboLock), RNase A, RNase T1, and NTPs were obtained from Fermentas Life Science. Calf intestinal alkaline phosphatase was purchased from Invitrogen. Snake venom phosphodiesterase I was purchased from Sigma-Aldrich. Radiolabeled α-^{32}P ATP (2000 Ci/mmol) was obtained from the Board of Radiation and Isotope Technology, Government of India. Chemicals for preparing buffer solutions were purchased from Sigma-Aldrich (BioUltra grade). Autoclaved water was used in all biochemical reactions and fluorescence measurements.

4.4.2 Instrumentation

NMR spectra were recorded on a 400 MHz Jeol ECS-400. All mass measurements were recorded on an Applied Biosystems 4800 Plus MALDI TOF/TOF analyser and Water Synapt G2 High Definition mass spectrometer. Absorption spectra were recorded on a PerkinElmer, Lambda 45 UV−vis spectrophotometer. UV-thermal melting analysis was performed on a Cary 300Bio UV−vis spectrophotometer. Steady state fluorescence experiments were performed on a Fluoromax-4 spectrophotometer (Horiba Jobin Yvon) and time-resolved fluorescence experiments were carried on a TCSPC instrument (Horiba Jobin Yvon, Fluorolog-3, and Horiba Jobin Yvon, IBH, USA) in a microfluorescence cuvette (Hellma, path length 1.0 cm). Reversed-phase (RP) flash chromatography (C18 Redi*Sep*Rf column) purifications were carried out using Teledyne ISCO, Combi Flash Rf. Agilent technologies HPLC (1260 infinity) was used for RP-HPLC analysis. Phosphorimages were recorded on a Typhoon Trio+, GE-Healthcare.

4.4.3 Synthesis of Selenophene-Modified Uridine Analogue 2

To a suspension of 5-iodouridine (0.250 g, 0.68 mmol, 1.00 equiv) and bis(triphenylphosphine)-palladium(II) chloride (0.024 g, 0.034 mmol, 0.05 equiv) in degassed anhydrous dioxane (7.5 mL) was added 2-(tributylstannyl)selenophene[51] (0.425 g, 1.01 mmol, 1.5 equiv). The reaction mixture was heated at 90°C for 2 h and was cooled to RT. The reaction mixture was then filtered through a celite pad and washed with hot dioxane (3 × 10 mL). The filtrate was concentrated and precipitated with petroleum ether. The precipitated crude product was purified by flash chromatography using a C18 RP column (C18 Redi*Sep*Rf 43 g column, 10−55% acetonitrile in water for 35 min) to afford the product as a white solid (0.115 g, 46%). TLC ($CHCl_3$:MeOH = 80:20) *Rf* = 0.63; ^{1}H NMR (400 MHz, d_6-DMSO): δ = 11.81 (s, 1H), 8.80 (s, 1H), 8.08 (d, *J* = 5.6 Hz, 1H), 7.60 (d, *J* = 3.6 Hz, 1H), 7.28 (dd, J= 5.6 Hz, *J* = 4.0 Hz, 1H), 5.84 (d, *J* = 3.6 Hz, 1H), 5.51−5.49 (m, 2H), 5.11 (d, *J* =5.2 Hz, 1H), 4.13 (dd, *J* = 9.2 Hz, J= 4.8 Hz, 1H), 4.07 (dd, *J* = 10.4 Hz, *J* = 5.2 Hz, 1H), 3.93−3.92 (m, 1H), 3.81−3.76 (m, 1H), 3.68−3.63 (m, 1H) ppm; ^{13}C NMR (100 MHz, d_6-DMSO): δ = 161.8, 149.4, 137.6, 134.5, 131.7, 128.6, 122.8, 109.9, 88.9, 84.6, 74.4, 69.2, 60.0 ppm; HRMS: m/z Calcd. For $C_{13}H_{14}N_2O_6SeNa$ $[M+Na]^+$: 396.9915; found: 396.9873; λ_{max} (H_2O) = 273 and 325 nm, ε_{273}= 9990 $M^{-1}cm^{-1}$, ε_{325}= 9221$M^{-1}cm^{-1}$, ε_{260} = 8576 $M^{-1}cm^{-1}$.

4.4.4 Synthesis of Selenophene-Conjugated Uridine Triphosphate Analogue 3

To an ice-cold solution of ribonucleoside **2** (0.070 g, 0.19 mmol, 1 equiv) in trimethyl phosphate (1 mL) was added freshly distilled $POCl_3$ (45µL, 0.48 mmol, 2.5 equiv). The solution was stirred for 29 h at ∼4 °C. TLC revealed only partial conversion of the ribonucleoside to the monophosphorylated nucleoside intermediate. A solution of bis-tributylammonium pyrophosphate[52] (0.5 M in DMF, 2 mL, 5.3 equiv) and tributylamine (0.5 mL, 2.12 mmol, 11.3 equiv) was rapidly added under ice-cold conditions. The reaction was quenched after 30 min with 1 M triethylammonium bicarbonate buffer (TEAB, pH 7.5, 15 mL) and was extracted with ethyl acetate (20 mL). The aqueous layer was evaporated and the residue was purified first on DEAE sephadex-A25 anion exchange column (10 mM to 1 M TEAB buffer, pH 7.5) followed by RP flash column chromatography (C18 Redi*Sep*Rf, 0−40% acetonitrile in 50 mM triethylammonium acetate buffer, pH 7.2, 40 min). Appropriate fractions were lyophilized to afford the desired triphosphate product **3** as a tetratriethylammonium salt (34 mg, 18%). ^{1}H NMR (400 MHz, D_2O): δ = 8.17 (s, 1H), 8.10 (d, *J* = 5.6, 1H), 7.71 (d, *J* = 3.2, 1H), 7.36 (dd, *J*

= 5.2 Hz, *J* = 4.0 Hz, 1H), 5.98 (d, *J* = 4.8, 1H), 4.45−4.44 (m, 2H), 4.28−4.25 (m, 3H) ppm;^{13}C NMR (100 MHz, D_2O): δ = 163.2, 150.7, 135.9, 134.5, 132.3, 129.7, 125.7, 112.0, 88.6, 83.7, 73.9, 69.9, 65.4 ppm; ^{31}P NMR (162 MHz, D_2O): δ = −6.94 (d, *J* = 15.2 Hz),−11.63 (d, *J* = 16.0 Hz),−22.54 (t, *J* = 15.6 Hz) ppm; HRMS: m/z Calcd. for $C_{13}H_{17}N_2O_{15}P_3Se$ [M]: 613.9007, found: 612.8951 $[M-H]^-$.

4.4.5 Photophysical Characterization of Ribonucleoside 2 in Various Solvents

Absorption Spectroscopy: Absorption spectra of selenophene-modified ribonucleoside **2** (50 μM) was recorded in water, methanol, and dioxane. All solutions contained 5% DMSO. All experiments were performed in triplicate in a micro cuvette (Hellma, path length 1.0 cm) on a Perkin Elmer, Lambda 45 UV−vis spectrophotometer.

Steady-State Fluorescence: Steady-state fluorescence of ribonucleoside **2** (5 μM) was recorded by exciting at respective lowest energy absorption maximum with an excitation slit width of 6 nm and emission slit width of 9 nm. All solutions contained 0.5% DMSO. Fluorescence experiments were performed in triplicate in a microfluorescence cell (Hellma, path length 1.0 cm).

Time-Resolved Fluorescence Measurements: Excited-state lifetimes of **2** (250 μM) were determined using TCSPC instrument. Fluorescently modified ribonucleoside **2** was excited using 375 nm diode laser source (IBH, UK, NanoLED-375L) with a band-pass of 10 nm and fluorescence signal at respective emission maximum was collected. Lifetime measurements were performed in duplicate and decay profiles were analysed using IBH DAS6 analysis software. Fluorescence intensity decay profiles in all solvents were found to be biexponential with χ^2 (goodness of fit) values very close to unity.

4.4.6 Enzymatic Incorporation of Ribonucleoside Triphosphate 3

Transcription Reactions in the Presence of α-^{32}P ATP: Promoter-template duplexes were assembled by heating a 1:1 concentration (final 5 μM) of DNA ON templates (**T1**−**T5**) and an 18-mer T7 RNA polymerase consensus promoter DNA ON sequence in TE buffer (10 mM Tris-HCl, 1 mM EDTA, 100 mM NaCl, pH 7.8) at 90°C for 3 min and cooling the solution slowly to RT. The duplexes were then placed on crushed ice for 30 min and stored at −40 °C. Transcription reactions were performed in 40 mM Tris-HCl buffer (pH 7.9) containing 250 nM promoter-template duplexes, 10 mM $MgCl_2$, 10 mM NaCl, 10

mM dithiothreitol (DTT), 2 mM spermidine, 1 U/μL RNase inhibitor (RiboLock), 1 mM GTP, 1 mM CTP, 1 mM UTP, and or 1 mM modified UTP **3**, 20 μM ATP, 5μCi α-^{32} ATP, and 3 U/μL T7 RNA polymerase in a total volume of 20 μL. After 3.5 h at 37 °C, reactions were quenched by adding 20μL of the loading buffer (7 M urea in 10 mM Tris-HCl, 100 mM EDTA, 0.05% bromophenol blue, pH 8), heated to 75°C for 3 min, and cooled on an ice bath. The samples (4 μL) were loaded onto a sequencing 18% denaturing polyacrylamide gel and run at a constant power of 11 W for nearly 4 h. The gel was phosphorimaged and the bands were then quantified using the software (GeneTools from Syngene). Percentage incorporation of triphosphate **3** into full-length transcripts was calculated by comparing the transcription efficiency in the presence of natural NTPs. All reactions were performed in duplicate and errors in yields were ± 2%.

4.4.7 Large-Scale Synthesis of Oligoribonucleotides 4, 5, and 11 by Transcription Reactions

Large-scale transcription reactions using template **T1** were performed in a 250 μL reaction volume under similar conditions as mentioned above to isolate control unmodified (**4**) and modified (**5**) oligoribonucleotides. Reactions were performed in the presence of 2 mM GTP, 2 mM CTP, 2 mM ATP, 2 mM UTP, or 2 mM modified UTP3, 20 mM $MgCl_2$, 0.4 U/μL RNase inhibitor (RiboLock), 300 nM annealed promoter-template DNA duplex, and 800 units T7 RNA polymerase. After incubation for 12 h at 37 °C, the precipitated salt of pyrophosphate was removed by centrifugation and the reaction volume was reduced approximately to 1/3 by SpeedVac, and 50μL of loading buffer was added. The mixture was heated at 75°C for 3 min and cooled on an ice bath. The sample was loaded onto a preparative denaturing polyacrylamide gel (20%) and was electrophoresed under denaturing conditions. The gel was UV shadowed and the appropriate band was excised. The oligoribonucleotide was extracted with 0.3 M sodium acetate and desalted using SepPak classic C18 cartridge. Selenophene-modified A-site oligoribonucleotide **11** was synthesized by following the above procedure using a DNA template sequence 5′ GGTGTGACGCCTATAGTGAGTCGTATTA 3′. Large scale transcription reactions under these conditions gave nearly 10−16 nmol of the oligoribonucleotide products. Transcript **4**, ε_{260} = 91,000 $M^{-1}cm^{-1}$; transcript **5**, ε_{260} = 91,800 $M^{-1}cm^{-1}$, transcript **11**, ε_{260} = 100500 $M^{-1}cm^{-1}$.

4.4.8 Enzymatic Digestion of Modified Oligoribonucleotide 5

3.5 nmol of the modified transcript **5** was treated with snake venom phosphodiesterase I (0.01 U), calf intestinal alkaline phosphatase (10μL, 1 U/μL), and RNase A (0.25μg) in a total volume of 100μL in 50 mM Tris-HCl buffer (pH 8.5, 40 mM $MgCl_2$, 0.1 mM EDTA) for 12 h at 37 °C. RNase T1 (0.2 U/ μL) was then added to the above reaction solution and was incubated for another 4 h at 37 °C. The ribonucleoside mixture obtained from the digest was analysed by RP-HPLC using Eclipse plus C18 column (250 × 4.6 mm, 5 μm) at 260 nm. Mobile phase A: 50 mM triethylammonium acetate buffer (pH 7.5), mobile phase B: acetonitrile. Flow rate: 1 mL/min. Gradient: 0−10% B (10 min), 10−100% B (20 min), and 100% B (10 min). The fractions corresponding to individual ribonucleosides were collected and analysed by mass spectroscopy.

4.4.9 Photophysical Characterization of Oligoribonucleotide 5 and Duplexes of 5

Steady-State Fluorescence: Oligoribonucleotide **5** (10 μM) was annealed to custom DNA and RNA ONs (**6−10**, 11 μM) by heating ONs in 20 mM cacodylate buffer (pH 7.1, 500 mM NaCl, 0.5 mM EDTA) at 90 °C for 3 min and cooling the samples slowly to room temperature, followed by incubating the solutions in crushed ice. Samples were diluted to give a final concentration of 1 μM (with respect to **5**) in cacodylate buffer. Fluorescently modified duplex constructs were excited at 330 nm with an excitation slit width of 10 nm and emission slit width of 12 nm. Fluorescence experiments were performed in duplicate in a microfluorescence cell.

4.4.10 Fluorescence Binding Assay

*Fluorescently Modified A-Site RNA Construct **11•12**:*For binding experiments, A-site construct (4 μM) **11•12** was formed by heating a 1:1 mixture of RNA ONs in HEPES buffer (20 mM HEPES, 100 mM NaCl, 0.5 mM EDTA, pH 7.5) at 75 °C for 5 min. The sample was cooled to RT and placed on crushed ice for ~ 4 h. The samples were brought to RT before fluorescence experiments were performed.

Binding of Aminoglycosides to a Model Selenophene Modified A-Site RNA ***11•12*** :Aliquots (1 μL) of increasing concentrations of the aminoglycoside stock was added to a microfluorescence cuvette containing 200 μL of A-site construct **11•12** (4 μM) in the above HEPES buffer. The fluorescence spectrum after each addition of the aminoglycoside was recorded by exciting at 330 nm with excitation and emission slit widths of 6 and 8 nm, respectively. The aminoglycoside was added till fluorescence saturation was observed. The change in volume over the entire titration was ≤ 8%. A spectral blank of the HEPES buffer in the absence of RNA and aminoglycoside was subtracted from all titrations. All fluorescence titrations were performed in triplicate. Normalized fluorescence intensity (FN) versus log of aminoglycoside (AG) concentration plots were fitted using eq 1 (KaleidaGraph) to determine the EC_{50} values for the binding of aminoglycosides to A-site construct.[53,54]

$$F_N = \frac{F_i - F_0}{F_s - F_0}$$

Fi is the fluorescence intensity at each titration point. F_0 and *Fs* are the fluorescence intensity in the absence of aminoglycoside and at saturation, respectively. n is the Hill coefficient or degree of cooperativity associated with the binding.

$$F_N = F_0 + \frac{F_S[AG]^n}{[EC_{50}]^n + [AG]^n} \qquad (1)$$

4.5 References

(1) Hermann, T., and Patel, D. J. (2000) RNA bulges as architectural and recognition motifs. *Structure 8*, R47−R54.

(2) Leulliot, N., and Varani, G. (2001) Current topics in RNA Protein recognition: control of specificity and biological function through induced fit and conformational capture. *Biochemistry 40,* 7947−7956.

(3) Al-Hashimi, H. M., and Walter, N. G. (2008) RNA dynamics: it is about time. *Curr.Opin.Struct.Biol. 18*, 321−329.

(4) Aitken, C. E., Petrov, A., and Puglisi, J. D. (2010) Single ribosome dynamics and the mechanism of translation. *Annu. Rev. Biophys. 39*, 491−513.

(5) Ranasinghe, R. T., and Brown, T. (2005) Fluorescence based strategies for genetic analysis. *Chem. Commun.*, 5487−5502.

(6) Asseline, U. (2006) Development and application of fluorescent oligonucleotides. *Curr.Org. Chem. 10,* 491−518.

(7) Martí, A. A., Jockusch, S., Stevens, N., Ju, J., and Turro, N. J. (2007) Fluorescent hybridization probes for sensitive and selective DNA and RNA detection. *Acc. Chem. Res. 4*, 402−409.

(8) Bardaro, M. F., Jr., and Varani, G. (2012) Examining the relationship between RNA function and motion using nuclear magnetic resonance. *WIREs RNA 3*, 122−132.

(9) Nguyen, P., and Qin, P. Z. (2012) RNA dynamics: perspectives from spin labels. *WIREs RNA 3*, 62−72.

(10) Holbrook, S. R. (2008) Structural principles from large RNAs. *Annu. Rev. Biophys.37*, 45−464.

(11) Serganov, A., and Patel, D. J. (2012) Molecular recognition and function of riboswitches. *Curr.Opin.Struct.Biol. 22*, 279−286.

(12) Weisbrod, S. H., and Marx, A. (2008) Novel strategies for the site-specific covalent labelling of nucleic acids. *Chem. Commun*., 5675−5685.

(13) Wachowius, F., and Höbartner, C. (2010) Chemical RNA modifications for studies of RNA structure and dynamics. *ChemBioChem 11*, 469−480.

(14) Khakshoor, O., and Kool, E. T. (2011) Chemistry of nucleic acids: impacts in multiple fields.*Chem. Commun. 47*, 7018−7024.

(15) Sinkeldam, R. W., Greco, N. J., and Tor, Y. (2010) Fluorescent analogues of biomolecular building blocks: design, properties, and applications. *Chem. Rev. 110*, 2579−2619.

(16) Wilhelmsson, L. M. (2010) Fluorescent nucleic acid base analogueues. *Quart. Rev. Biophy. 43*, 159−183.

(17) Srivatsan, S. G., and Sawant, A. A. (2011) Fluorescent ribonucleoside analogueues as probes for investigating RNA structure and Function. *Pure Appl. Chem. 83*, 213−232.

(18) Phelps, K., Morris, A., and Beal, P. A. (2012) Novel modifications in RNA. *ACS Chem. Biol. 7*, 100−109.

(19) Teo, Y. N., and Kool, E. T. (2012) DNA-multichromophore systems. *Chem. Rev.112*, 4221−4245.

(20) Förster, U., Lommel, K., Sauter, D., Grünewald, C., Engels, J. W., and Wachtveitl, J. (2010) 2-(1-Ethynylpyrene)-adenosine as a folding probe for RNA–pyrene in or out. *ChemBioChem 11*, 664−672.

(21) Peacock, H., Maydanovych, O., and Beal, P. A. (2010) N^2-modified 2-aminopurine ribonucleosides as minor-groove-modulating adenosine replacements in duplex RNA. *Org. Lett. 12*, 1044−1047.

(22) Kimoto, M., Mitsui, T., Yokoyama, S., and Hirao, I. (2010) A unique fluorescent base analogue for the expansion of the genetic alphabet. *J. Am. Chem. Soc. 132*, 4988−4989.

(23) Nadler, A., Strohmeier, J., and Diederichsen, U. (2011) 8-Vinyl-2′-deoxyguanosine as a fluorescent 2′-deoxyguanosine mimic for investigating DNA hybridization and topology. *Angew. Chem., Int. Ed. 50*, 5392−5396.

(24) Ehrenschwender, T., and Wagenknecht, H.-A. (2011) 4,4-Difluoro-4-bora-3a,4a-diaza-s-indacene as a bright fluorescent label for DNA. *J. Org. Chem. 76*, 2301−2304.

(25) Lee, J., II., and Kim, B. H. (2012) Monitoring i-motif transitions through the exciplex emission of a fluorescent probe incorporating two PyA units. *Chem. Commun. 48*, 2074−2076.

(26) Wojciechowski, F., Lietard, J., and Leumann, C. J. (2012) 2-Pyrenyl-DNA: synthesis, pairing, and fluorescence properties. *Org. Lett. 14*, 5176−5179.

(27) Halogenated ONs are light sensitive and undergo dehalogenation when exposed to X−ray radiation, which cause failures in phasing; Ennifar, E., Carpentier, P., Ferrer, J.-L., Walter, P., and Dumas, P. (2002) X-ray-induced debromination of nucleic acids at the Br K absorption edge and implications for MAD Phasing. *Acta Crystallogr. D58*, 1262−1268.

(28) Dibrov, S., Mclean, J., and Hermann, T. (2011) Structure of an RNA dimer of a regulatory element from human thymidylate synthase mRNA. *Acta Crystallogr. D67*, 97−104.

(29) Egli, M., and Pallan, P. S. (2007) Insights from crystallographic studies into the structural and pairing properties of nucleic acid analogues and chemically modified DNA and RNA oligonucleotides. *Annu. Rev. Biophys. Biomol. Struct. 36*, 281−305.

(30) Sheng, J., and Huang, Z. (2010) Selenium derivatization of nucleic acids for X-Ray crystal-structure and function studies. *Chem. Biodivers. 7*, 753−785.

(31) Du, Q., Carrasco, N., Teplova, M., Wilds, C. J., Egli, M., and Huang, Z. (2002) Internal derivatization of oligonucleotides with selenium for X-ray crystallography using MAD. *J. Am. Chem. Soc. 124*, 24−25.

(32) Wilds, C. J., Pattanayek, R., Pan, C., Wawrzak, Z., and Egli, M.(2002) Selenium-assisted nucleic acid crystallography: use of phosphoroselenoates for MAD phasing of a DNA structure. *J. Am.Chem. Soc. 124*, 14910−14916.

(33) Teplova, M., Wilds, C. J., Wawrzak, Z., Tereshko, V., Du, Q., Carrasco, N., Huang, Z., and Egli, M. (2002) Covalent incorporation of selenium into oligonucleotides for X-ray crystal structure determination via MAD: proof of principle. *Biochimie 84*, 849−858.

(34) Carrasco, N., Caton-Williams, J., Brandt, G., Wang, S., and Huang, Z. (2006) Efficient enzymatic synthesis of phosphoroselenoate RNA by using adenosine 5′-(α-P-seleno)triphosphate. *Angew. Chem., Int. Ed. 45*, 94−97.

(35) Höbartner, C., and Micura, R. (2004) Synthesis of selenium modified oligoribonucleotides and their enzymatic ligation leading to an U6 SnRNA stem-loop segment. *J. Am. Chem. Soc. 126*, 1141−1149.

(36) Salon, J., Sheng, J., Jiang, J., Chen, G., Caton-Williams, J., andHuang, Z. (2007) Oxygen replacement with selenium at the thymidine4-position for the Se base pairing and crystal structure studies. *J. Am. Chem. Soc. 129*, 4862−4863.

(37) Caton-Williams, J., and Huang, Z. (2008) Synthesis and DNA polymerase incorporation of colored 4-selenothymidine triphosphate for polymerase recognition and DNA visualization. *Angew. Chem., Int. Ed. 47*, 1723−1725.

(38) Serganov, A., Keiper, S., Malinina, L., Tereshko,V., Skripkin, E.,Höbartner, C., Polonskaia, A., Phan, A. T., Wombacher, R., Micura, R., Dauter, Z., Jäschke, A., and Patel, D. J. (2005) Structural basis for Diels-Alder ribozyme-catalyzed carbon-carbon bond formation. *Nat. Struct. Mol. Biol. 12*, 218−224.

(39) Freisz, S., Lang, K., Micura, R., Dumas, P., and Ennifar, E.(2008) Binding of aminoglycoside antibiotics to the duplex form of the HIV-1 genomic RNA dimerization initiation site. *Angew. Chem., Int. Ed. 47*, 4110−4113.

(40) Salon, J., Jiang, J., Sheng, J., Gerlits, O. O., and Huang, Z. (2008) Derivatization of DNAs with selenium at 6-position of guanine for function and crystal structure studies. *Nucleic Acids Res. 36*, 7009−7018.

(41) Olieric, V., Rieder, U., Lang, K., Serganov, A., Schulze-Briese, C., Micura, R., Dumas, P., and Ennifar, E. (2009) A fast selenium derivatization strategy for crystallization and phasing of RNA structures. *RNA 15*, 707−715.

(42) Sun, H., Sheng, J., Hassan, A. E. A., Jiang, S., Gan, J., and Huang,Z. (2012) Novel RNA base pair with higher specificity using single selenium atom. *Nucleic Acids Res. 40*, 5171−5179.

(43) Wahba, A. S., Esmaeili, A., Damha, M. J., and Hudson, R. H. E. (2010) A single-label phenyl pyrrolocytidine provides a molecular beacon-like response reporting HIV-1 RT RNase H activity. *Nucleic Acids Res. 38*, 1048−1056.

(44) Shin, D., Sinkeldam, R. W., and Tor, Y. (2011) Emissive RNA alphabet. *J. Am. Chem. Soc. 133*, 14912−14915.

(45) Tanpure, A. A., and Srivatsan, S. G. (2011) A microenvironment-sensitive fluorescent pyrimidine ribonucleoside analogue: synthesis, enzymatic incorporation, and fluorescence detection of a DNA abasic site. *Chem.–Eur. J. 17*, 12820−12827.

(46) Pawar, M. G., and Srivatsan, S. G. (2011) Synthesis, photophysical characterization, and enzymatic incorporation of a microenvironment-sensitive fluorescent uridine analogue. *Org. Lett. 13*, 1114−1117.

(47) Riedl, J., Pohl, R., Ernsting, N. P., Orsá g , P., Fojta, M., and Hocek, M. (2012) Labelling of nucleosides and oligonucleotides by solvatochromic 4-aminophthalimide fluorophore for studying DNA−protein interactions. *Chem. Sci. 3*, 2797−2806.

(48) Tanpure, A. A., and Srivatsan, S. G. (2012) Synthesis and photophysical characterisation of a fluorescent nucleoside analogue that signals the presence of an abasic site in RNA. *ChemBioChem 13*, 2392−2399.

(49) Srivatsan, S. G., and Tor, Y. (2007) Fluorescent pyrimidine ribonucleotide: synthesis, enzymatic incorporation, and utilization. *J. Am. Chem. Soc. 129*, 2044−2053.

(50) Greco, N. J., and Tor, Y. (2005) Simple fluorescent pyrimidine analogues detect the presence of DNA Abasic sites. *J. Am. Chem. Soc. 127*, 10784−10785.

(51) Tributyl(2-selenophene)stannane was prepared by following a literature report. Instead of performing the reaction in dry THF, it was performed in dry diethyl ether at nearly−70°C. Yang, R., Tian, R., Yan, J., Zhang, Y., Yang, J., Hou, Q., Yang, W., Zhang, C., and Cao, Y. (2005) Deep-red electroluminescent polymers: synthesis and characterization of new low-band-gap conjugated copolymers for light emitting diodes and photovoltaic devices. *Macromolecules 38*, 244−253.

(52) Moffatt, J. G. (1964) A general synthesis of nucleoside 5′ triphosphates. *Can. J. Chem. 42*, 599−604.

(53) Shandrick, S., Zhao, Q., Han, Q., Ayida, B. K., Takahashi, M., Winters, G. C., Simonsen, K. B., Vourloumis, D., and Hermann, T. (2004) Monitoring molecular recognition of the ribosomal decoding site. *Angew. Chem., Int. Ed. 43*, 3177−3182.

(54) Tam, V. K., Kwong, D., and Tor, Y. (2007) Fluorescent HIV-1 dimerization initiation site: design, properties, and use for ligand discovery. *J. Am. Chem. Soc. 129*, 3257−3266.

(55) See Experimental section for details.

(56) Reichardt, C. (1994) Solvatochromic dyes as solvent polarity indicators. *Chem. Rev. 94*, 2319−2358.

(57) Fluorescence properties of fluorophores containing a molecular rotor element are affected by molecular crowing effects and viscosity. Sinkeldam, R. W., Wheat, A. J., Boyaci, H., and Tor, Y. (2011) Emissive nucleosides as molecular rotors. *ChemPhysChem 12*, 567−570.

(58) Rieder, R., Lang, K., Graber, D., and Micura, R. (2007) Ligand induced folding of the adenosine deaminase A-riboswitch and implications on riboswitch translational control. *ChemBioChem 8*, 896−902.

(59) Hikida, Y., Kimoto, M., Yokoyama, S., and Hirao, I. (2010) Site specific fluorescent probing of RNA molecules by unnatural base-pair transcription for local structural conformation analysis. *Nat. Protoc. 5*, 1312−1323.

(60) Kimoto, M., Mitsui, T., Harada, Y., Sato, A., Yokoyama, S., and Hirao, I. (2007) Fluorescent probing for RNA molecules by an unnatural base-pair system. *Nucleic Acids Res. 35*, 5360−5369.

(61) Rao, H., Tanpure, A. A., Sawant, A. A., and Srivatsan, S. G. (2012) Enzymatic incorporation of an azide-modified UTP analogue into oligoribonucleotides for post-transcriptional chemical functionalization. *Nat. Protoc. 7*, 1097−1112.

(62) Ludwig, J. (1981) A new route to nucleoside 5′-triphosphates. *Acta Biochim. Biophys. Acad. Sci. Hung. 16*, 131−133.

(63) Milligan, J. F., and Uhlenbeck, O. C. (1989) Synthesis of small RNAs using T7 RNA polymerase. *Methods Enzymol.180*,51−62.

(64) Ward, D. C., Reich, E., and Stryer, L. (1969) Fluorescence studies of nucleotides and polynucleotides. *J. Biol. Chem. 244*, 1228−1237.

(65) Rachofsky, E. L., Osman, R., and Ross, J. B. A. (2001) Probing structure and dynamics of DNA with 2-aminopurine: effects of local environment on fluorescence. *Biochemistry 40*, 946−956.

(66) Jean, J. M., and Hall, K. B. (2001) 2-Aminopurine fluorescence quenching and lifetimes: role of base stacking. *Proc. Natl. Acad. Sci. U.S.A. 98*, 37−41.

(67) Seidel, C. A. M., Schulz, A., and Sauer, M. H. M. (1996) Nucleobase-specific quenching of fluorescent dyes. 1. Nucleobase one electron redox potentials and their correlation with static and dynamic quenching efficiencies. *J. Phys. Chem. 100*, 5541−5553.

(68) Kelley, S. O., and Barton, J. K. (1999) Electron transfer between bases in double helical DNA. *Science 283*, 375−381.

(69) Sandin, P., Borjesson, K., Li, H., Martensson, J., Brown, T., Wilhelmsson, L. M., and Albinsson, B. (2008) Characterization and use of an unprecedentedly bright and structurally non-perturbing fluorescent DNA base analogue. *Nucleic Acids Res. 36*, 157−167.

(70) Dierckx, A., Diné r, P., El-Sagheer, A. H., Joshi, D. K., Brown, T., Grøtli, M., and Wilhelmsson, L. M. (2011) Characterization of photophysical and base-mimicking properties of a novel fluorescent adenine analogueue in DNA. *Nucleic Acids Res. 39*, 4513−4524.

(71) Gardarsson, H., Kale, A. S., and Sigurdsson, S. T. (2011) Structure−function relationships of phenoxazine nucleosides for identification of mismatches in duplex DNA by fluorescence spectroscopy. *ChemBioChem 12*, 567−575.

(72) Among the nucleobases, purines (especially guanine) quench the fluorescence of many probes including 2-AP by photoinduced electron transfer process. See ref 67.

(73) Bacterial A-site is one of the oldest and important RNA targets for the discovery of new antibiotics; Gallego, J., and Varani, G. (2001) Targeting RNA with small-molecule drugs: therapeutic promise and chemical challenges. *Acc. Chem. Res. 34*, 836−843.

(74) Hermann, T., and Tor, Y. (2005) RNA as a target for small molecule therapeutics. *Expert Opin. Ther. Pat. 15*, 49−62.

(75) Ogle, J. M., Carter, A. P., and Ramakrishnan, V. (2003) Insights into the decoding mechanism from recent ribosome structures. *Trends Biochem.Sci. 28*, 259−266.

(76) Moazed, D., and Noller, H. F. (1987) Interaction of antibiotics with functional sites in 16S ribosomal RNA. *Nature 327*, 389−394.

(77) Carter, A. P., Clemons, W. M., Brodersen, D. E., MorganWarren, R. J., Wimberly, B. T., and Ramakrishnan, V. (2000) Functional insights from the structure of the 30S ribosomal subunit and its interactions with antibiotics. *Nature 407*, 340−348.

(78) Fourmy, D., Recht, M. I., Blanchard, S. C., and Puglisi, J. D.(1996) Structure of the A-site of Escherichia coli 16S ribosomal RNA complexed with an aminoglycoside antibiotic. *Science 274*, 1367−1371.

(79) Vicens, Q., and Westhof, E. (2001) Crystal structure of paromomycin docked into the eubacterial ribosomal decoding A-site. *Structure 9*, 647−658.

(80) Kaul, M., Barbieri, C. M., and Pilch, D. S. (2006) Aminoglycoside-induced reduction in nucleotide mobility at the ribosomal RNA A-Site as a potentially key determinant of antibacterial activity. *J. Am. Chem. Soc. 128*, 1261−1271.

(81) Parsons, J., and Hermann, T. (2007) Conformational flexibility of ribosomal decoding-site RNA monitored by fluorescent pteridines base analogueues. *Tetrahedron 63*, 3548−3552.

(82) Xie, Y., Dix, A. V., and Tor, Y. (2009) FRET enabled real time detection of RNA-small molecule binding. *J. Am. Chem. Soc. 131*, 17605−17614.

(83) Kaul, M., Barbieri, C. M., and Pilch, D. S. (2004) Fluorescence based approach for detecting and characterizing antibiotic-induced conformational changes in ribosomal RNA: comparing aminoglycoside binding to prokaryotic and eukaryotic ribosomal RNA sequences. *J. Am. Chem. Soc. 126*, 3447−3453.

(84) Barbieri, C. M., Kaul, M., and Pilch, D. S. (2007) Use of 2-aminopurine as a fluorescent tool for characterizing antibiotic recognition of the bacterial rRNA A-site. *Tetrahedron 63*, 3567−3574.

4.6 Appendix-II. Characterization data of synthesized compounds

4.6.1 ^{1}H NMR spectrum of compound **2**

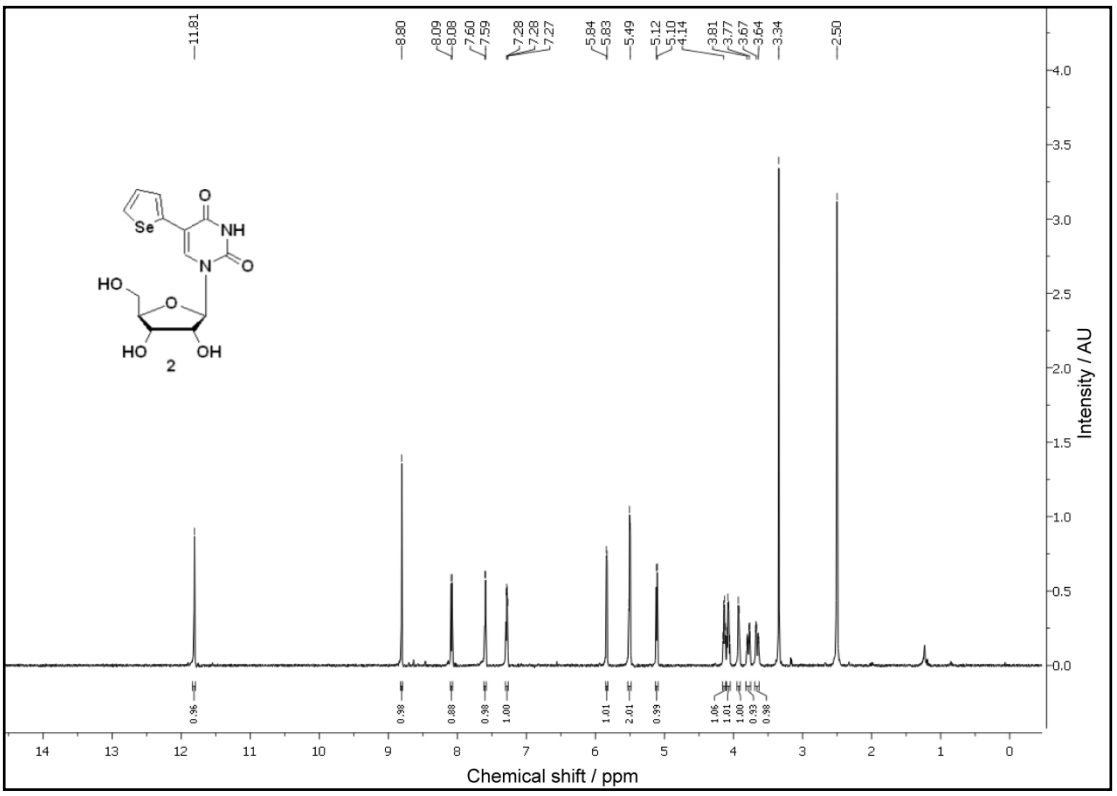

4.6.2 ^{13}C NMR spectrum of compound **2**

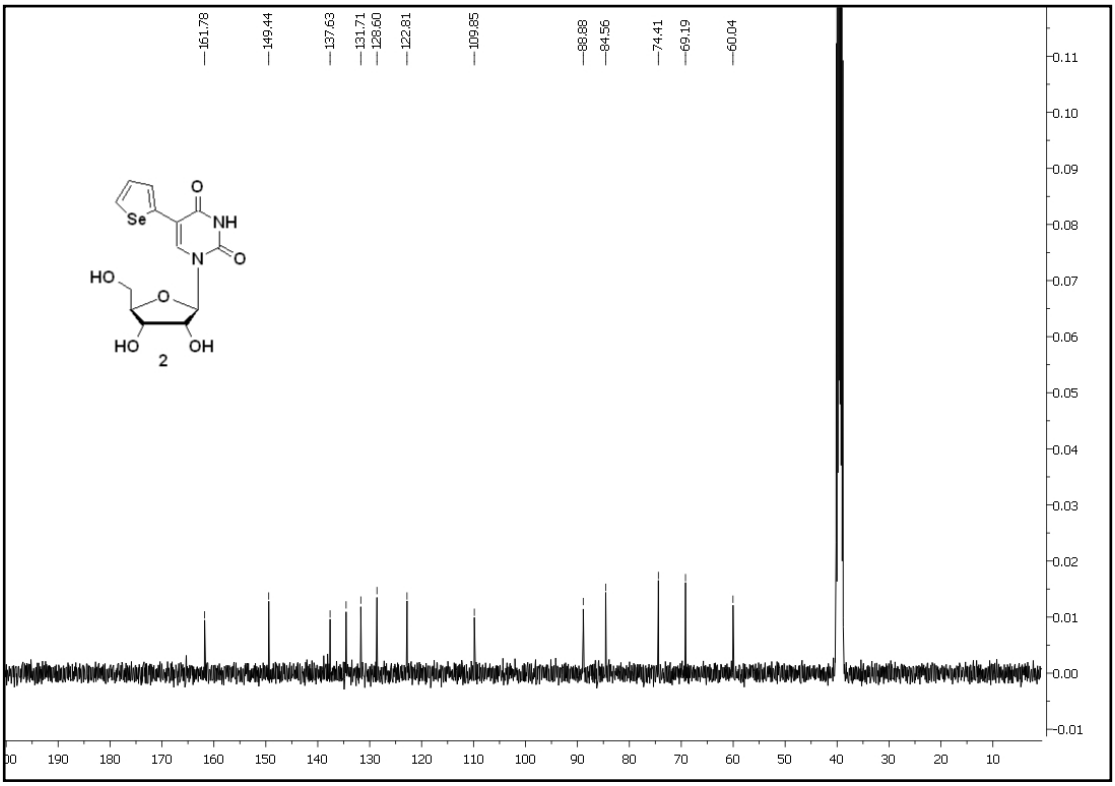

4.6.3 ^{1}H NMR spectrum of compound **3**

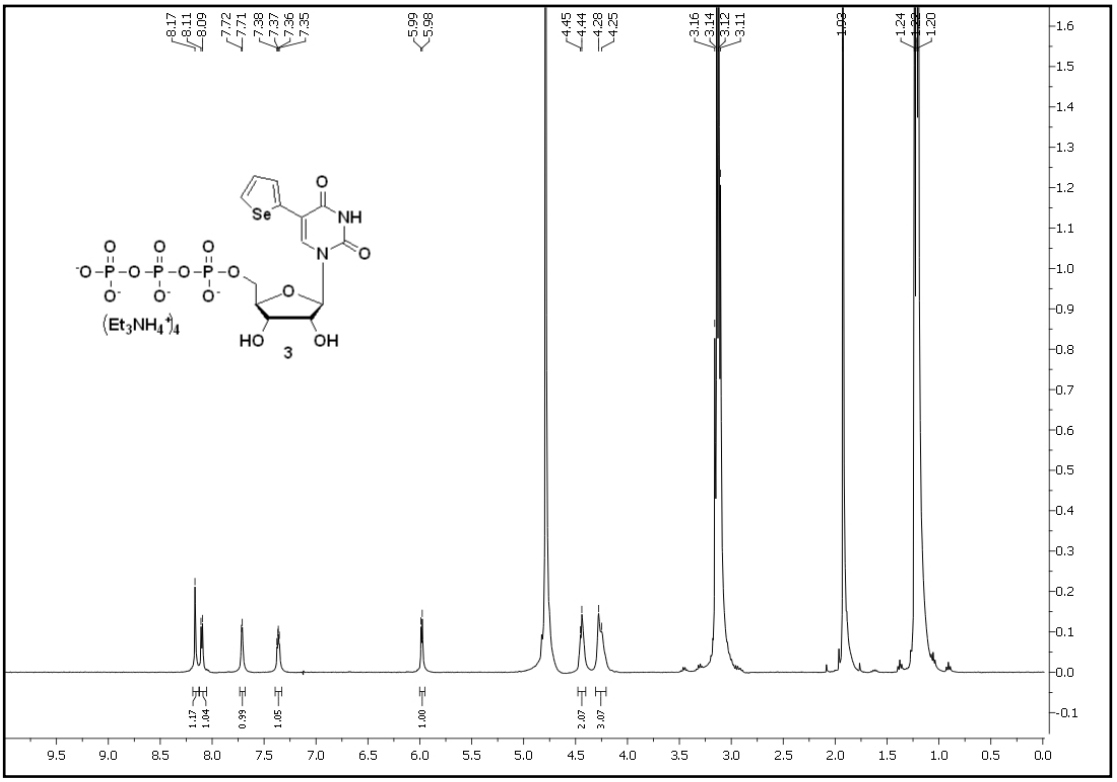

4.6.4 ^{13} C NMR spectrum of compound **3**

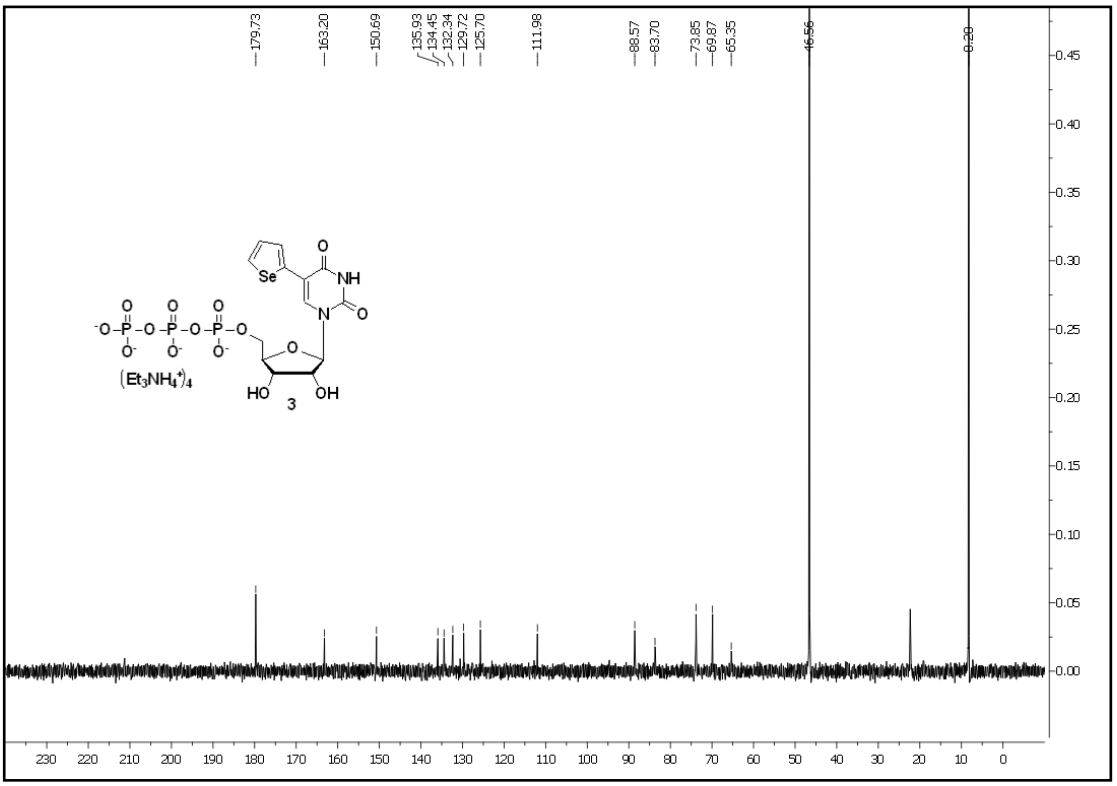

4.6.5 ^{31}P NMR spectrum of compound **3**

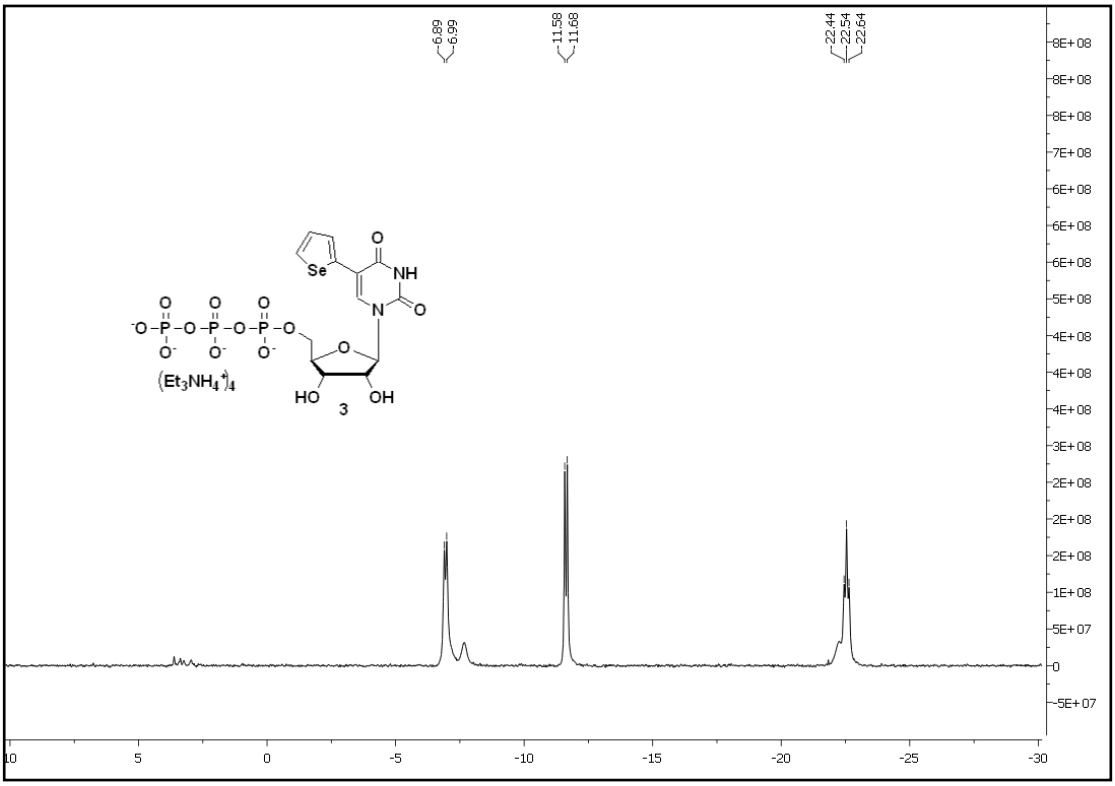

4.6.6 MALDI TOF Mass spectra of oligonucleotide **5** HPLC digests

(A) MALDI-TOF mass spectrum of ribonucleoside Cytidine

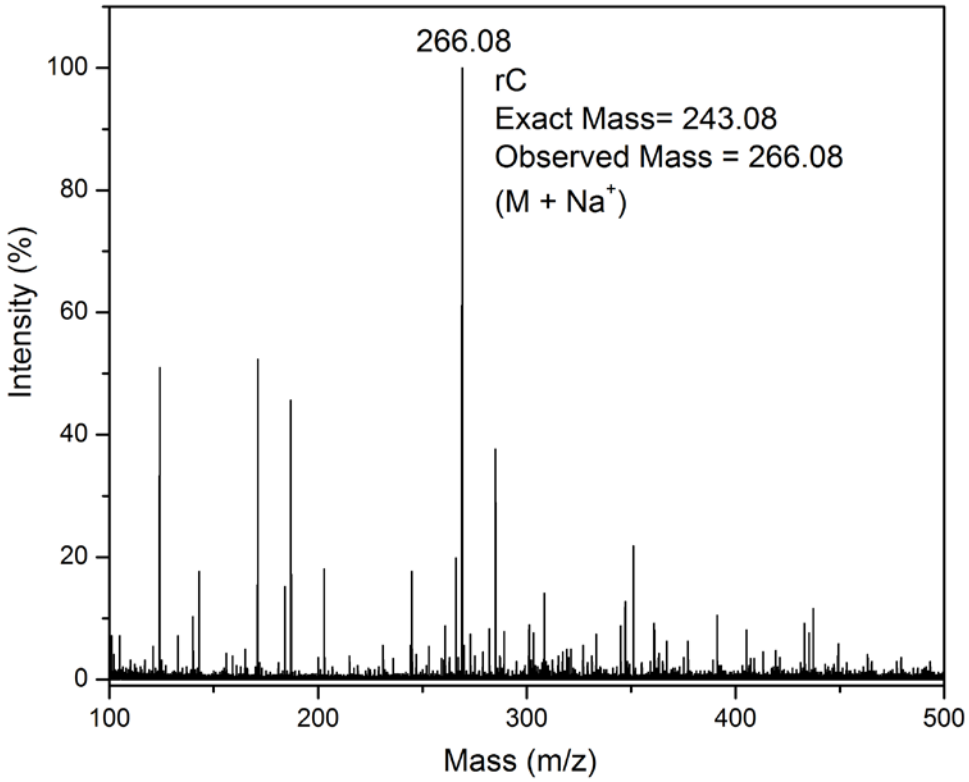

(B) MALDI-TOF mass spectrum of ribonucleoside Guanosine

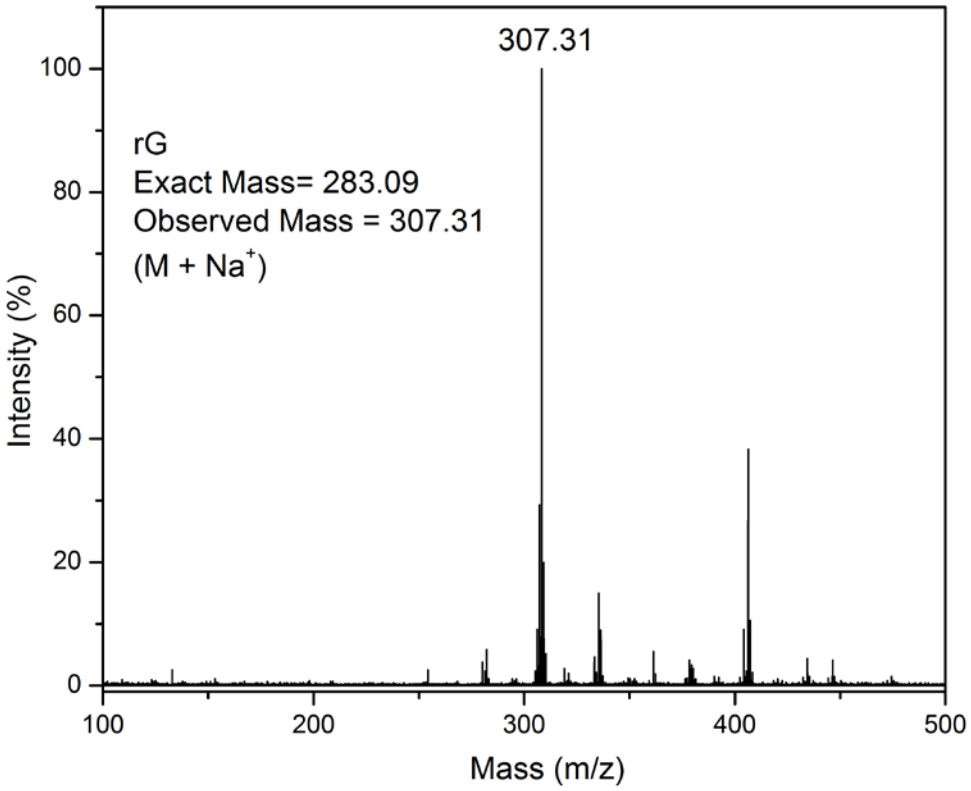

(C) MALDI-TOF mass spectrum of ribonucleoside Adenosine

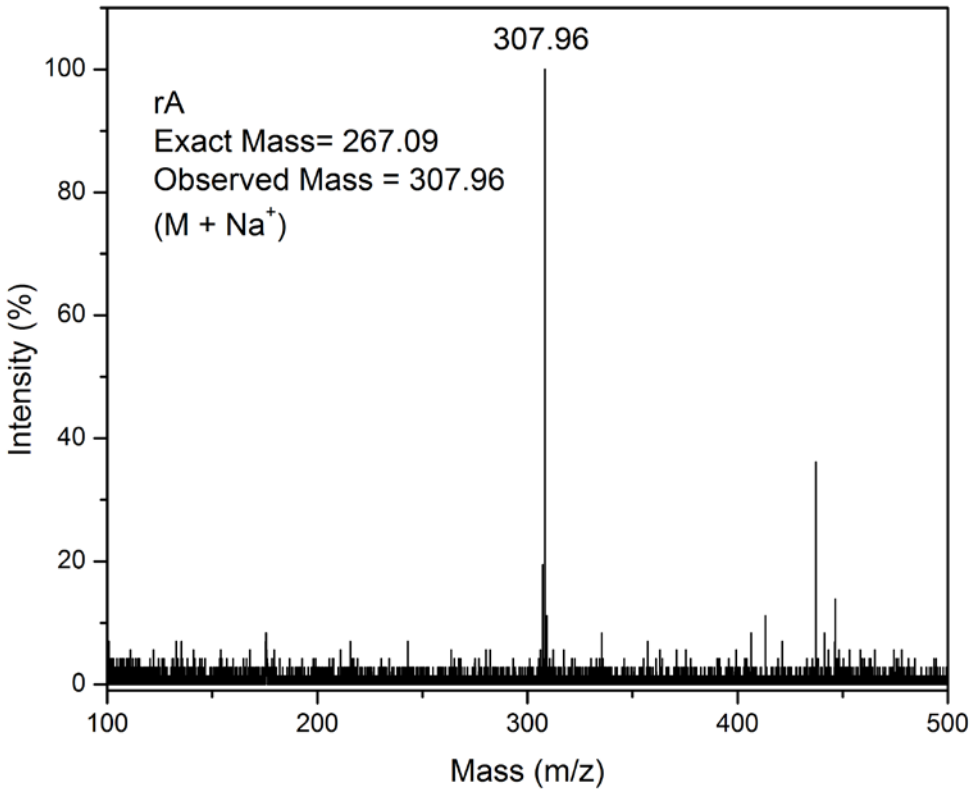

(D) MALDI-TOF mass spectrum of ribonucleoside **2**